Quileute Natural Resources

Quillayute River Project

Geomorphic Assessment and Action Plan

VOLUME II: APPENDICES

September 2020

TETRA TECH

APPENDIX A – QUILLAYUTE RIVER TOPOBATHYMETRIC LIDAR TECHNICAL DATA REPORT

(Prepared by: Quantum Spatial)

Quillayute River Project
Geomorphic Assessment and Action Plan
Quillayute River Topobathymetric LiDAR Technical Data Report

Appendix A

(Prepared by: Quantum Spatial, Inc.)

Submitted to:

Quileute Natural Resources
401 Main Street
La Push, WA 98350

Submitted by:

19803 North Creek Parkway
Bothell, WA 98011
Tel 425.482.7600 | Fax 425.482.7652
www.tetratech.com

September 2020

December 6, 2019

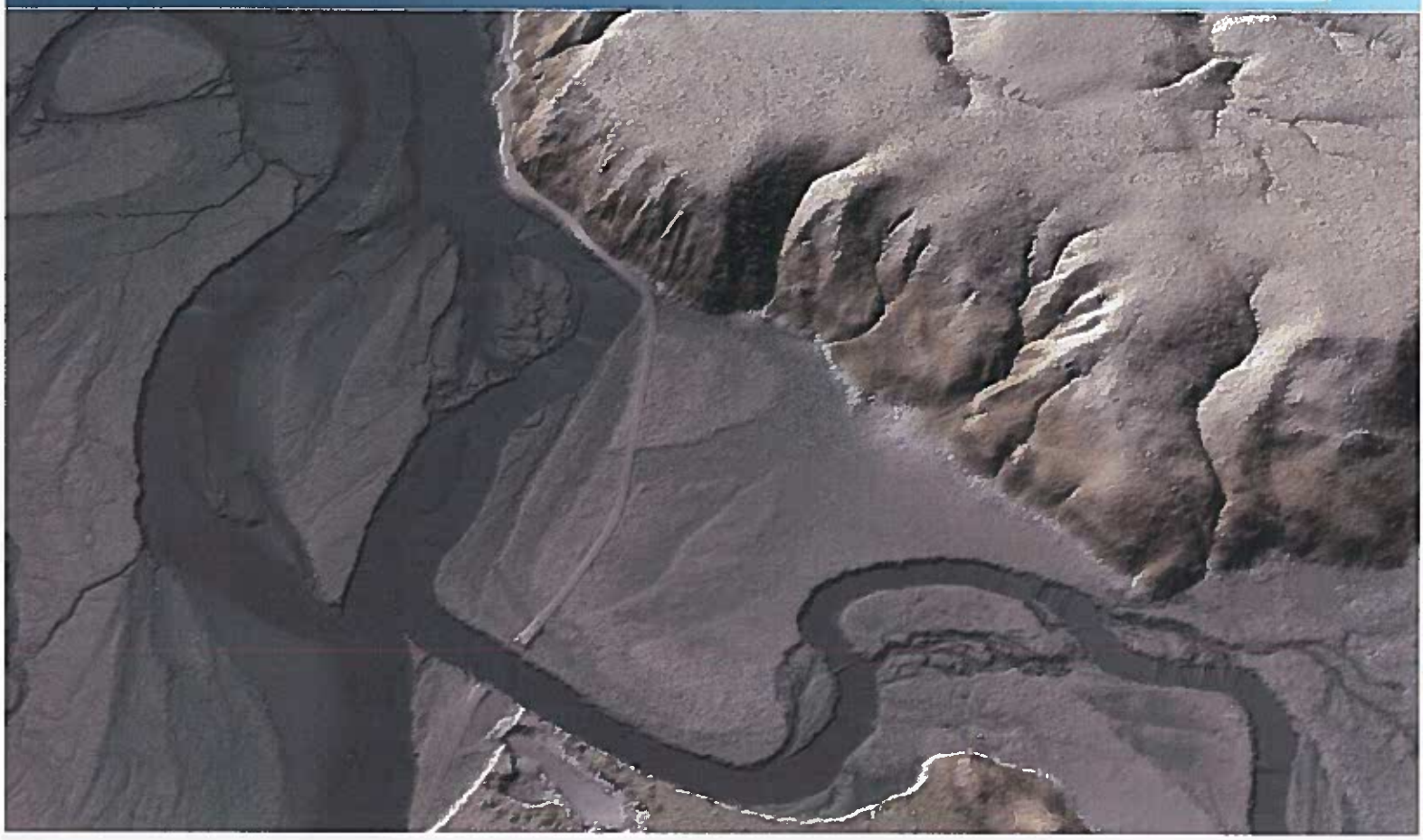

Quillayute River, Washington

Topobathymetric LiDAR Technical Data Report

Prepared For:

TETRA TECH

Chris James
Tetra Tech, Inc.
19803 N. Creek Pkwy
Bothell, WA 98011
PH: 425-482-7622

Prepared By:

QSI Corvallis
1100 NE Circle Blvd, Ste. 126
Corvallis, OR 97330
PH: 541-752-1204

Table of Contents

Introduction 1
Deliverable Products 2
Acquisition 4
Planning 4
Turbidity Measurements and Secchi Depth Readings 4
Airborne LiDAR Survey 8
Ground Survey 10
Base Stations 10
Ground Survey Points (GSPs) 11
Processing 13
Topobathymetric LiDAR Data 13
Bathymetric Refraction 15
LiDAR Derived Products 15
Topobathymetric DEMs 15
Intensity Images 15
Feature Extraction 16
Water's edge breaklines 16
Results & Discussion 17
Bathymetric LiDAR 17
LiDAR Point Density 17
First Return Point Density 17
Bathymetric and Ground Classified Point Densities 18
LiDAR Accuracy Assessments 20
LiDAR Non-Vegetated Vertical Accuracy 20
LiDAR Bathymetric Vertical Accuracies 23
LiDAR Relative Vertical Accuracy 25
LiDAR Horizontal Accuracy 26
Certifications 27
Glossary 28
Appendix A - Accuracy Controls 29

Cover Photo: A view looking west over the Quillayute River. Image was generated from the LiDAR bare earth model and colored by elevation.

INTRODUCTION

This photo taken by QSI acquisition staff shows a view of the Quillayute River site in Washington.

In August 2019, Quantum Spatial (QSI) was contracted by Tetra Tech Inc. to collect topobathymetric Light Detection and Ranging (LiDAR) data in the summer of 2019 for the Quillayute River site in Washington. The Quillayute River area of interest contains roughly 7.0 miles of the Quillayute River and the outflow delta into the Pacific Ocean. Traditional near-infrared (NIR) LiDAR was fully integrated with green wavelength return data (bathymetric) LiDAR in order to provide a seamless topobathymetric LiDAR dataset. Data were collected to aid Tetra Tech Inc. in assessing tsunami risk mapping for a local elementary school within the study area and to support mapping of safety zones.

This report accompanies the delivered topobathymetric LiDAR data, and documents contract specifications, data acquisition procedures, processing methods, and analysis of the final dataset including LiDAR accuracy and density. Acquisition dates and acreage are shown in Table 1, a complete list of contracted deliverables provided to Tetra Tech Inc. is shown in Table 2, and the project extent is shown in Figure 1.

Table 1: Acquisition dates, acreage, and data types collected on the Quillayute River site

Project Site	Contracted Acres	Buffered Acres	Acquisition Dates	Data Type
Quillayute River, WA	7,625	8,318	09/02/2019 & 10/01/2019	Topobathymetric LiDAR

Deliverable Products

Table 2: Products delivered to Tetra Tech Inc. for the Quillayute River site

Quillayute River, WA Topobathymetric LiDAR Products Projection: Washington State Plane North Horizontal Datum: NAD83 (2011, defined as NAD83) Vertical Datum: NAVD88 (GEOID12B) Units: US Survey Feet	
Topobathymetric LiDAR	
Points	LAS v 1.4 • All Classified Returns
Rasters	3.0 Foot ESRI Grids • Combined Topobathymetric Digital Surface Model (DSM) • Highest Hit Digital Elevation Model (DEM) 1.5 Foot GeoTiffs • Green Sensor Intensity Images • NIR Sensor Intensity Images
Vectors	Shapefiles (*.shp) • Survey Boundary • LiDAR Tile Index • Ground Survey Shapes • Bathymetric Coverage Shape • Water's Edge Breaklines

**The data were created in NAD83 (2011), but for GIS purposes are defined as NAD83 as per contract requirements.*

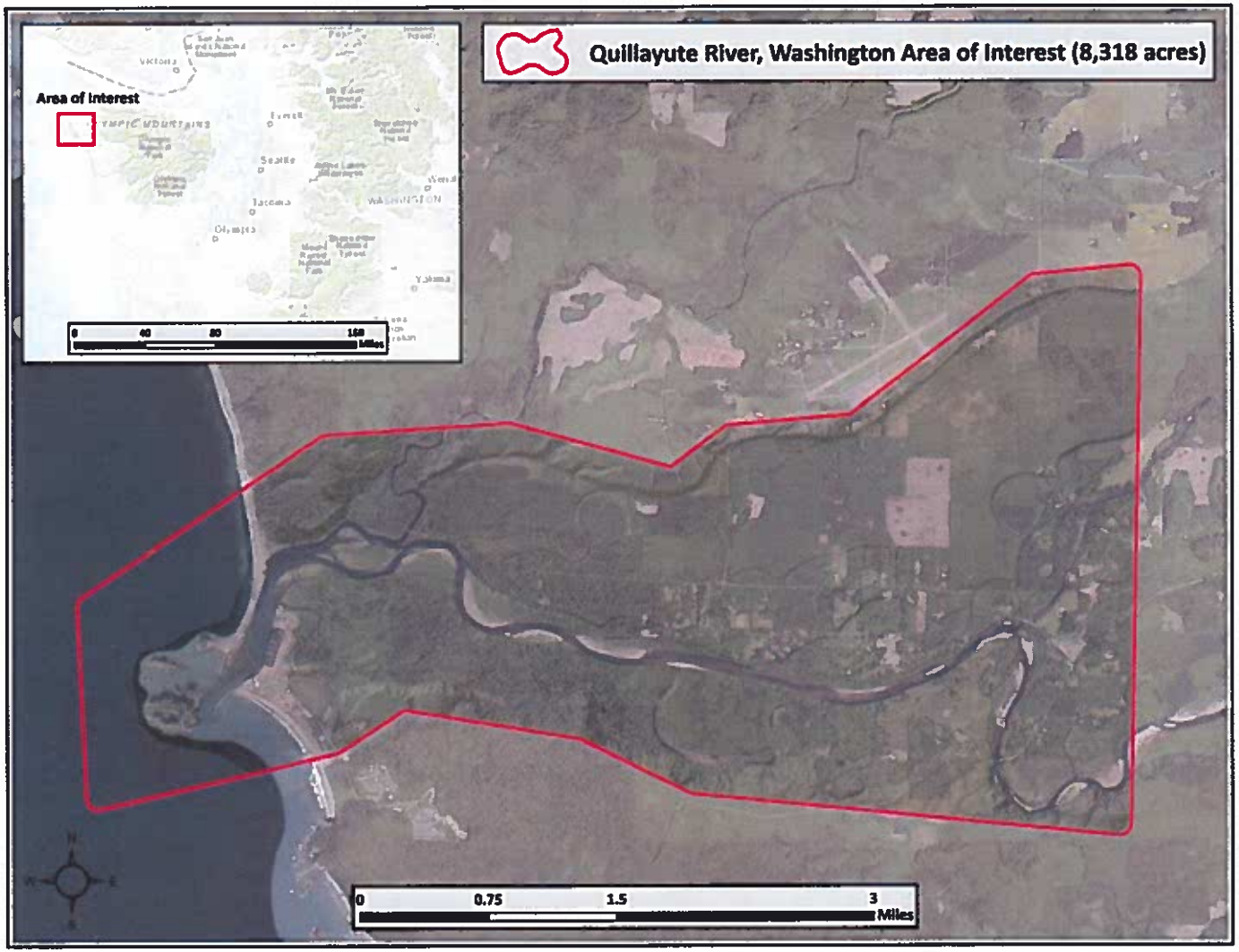

Figure 1: Location map of the Quillayute River site in Washington State

QSI's ground acquisition equipment set up within the Quillayute River LiDAR study area.

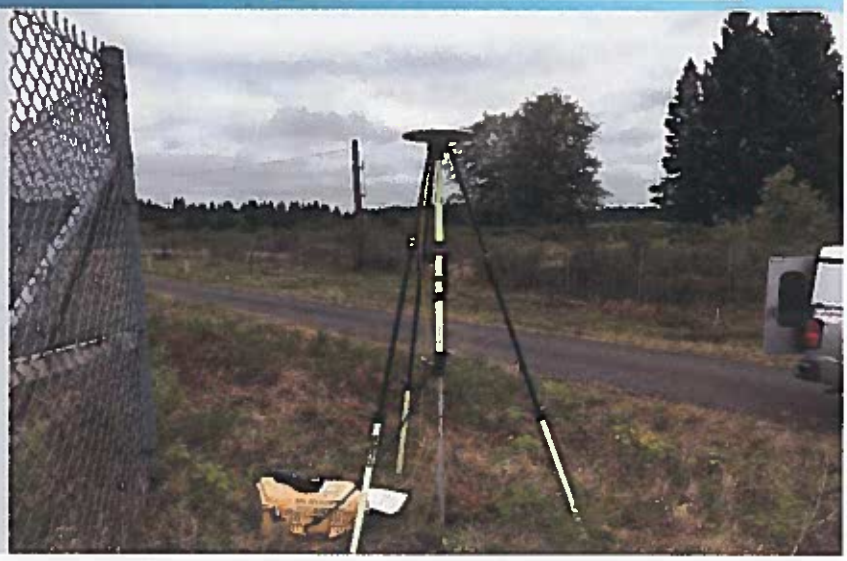

Planning

In preparation for data collection, QSI reviewed the project area and developed a specialized flight plan to ensure complete coverage of the Quillayute River LiDAR study area at the target combined point density of ≥16 points/m^2. Acquisition parameters including orientation relative to terrain, flight altitude, pulse rate, scan angle, and ground speed were adapted to optimize flight paths and flight times while meeting all contract specifications.

Factors such as satellite constellation availability and weather windows must be considered during the planning stage. Any weather hazards or conditions affecting the flight were continuously monitored due to their potential impact on the daily success of airborne and ground operations. In addition, logistical considerations including private property access, potential air space restrictions, river gage height and tide conditions (Figure 3 through Figure 2), and water clarity were reviewed.

Turbidity Measurements and Secchi Depth Readings

In order to assess water clarity conditions prior to and during LiDAR and digital imagery collection, QSI collected turbidity measurements prior to airborne acquisition. Readings were collected at six locations throughout the project site between August 28 and August 30, 2019. The table below provides turbidity results per site on each day of data collection.

Table 3: Water Clarity Observations collected for the Quillayute River Project Area

Water Clarity Observations							
Date	**Location**	**Longitude**	**Latitude**	**Turbidity Read 1**	**Turbidity Read 2**	**Turbidity Read 3**	**LiDAR Mapped Depth (ft)**
08/28/19	East end of AOI	-124.542194	47.914667	0.30	0.26	0.36	3.02
08/28/19	West end of AOI	-124.63836	47.915467	0.41	0.24	0.41	4.44
08/28/19	East end of AOI	-124.643616	47.910986	0.34	0.28	0.40	1.73
08/29/19	East end of AOI	-124.636773	47.910455	0.13	0.21	0.40	8.46
08/30/19	West end of AOI	-124.63836	47.915467	1.30	1.61	1.33	4.44
08/30/19	East end of AOI	-124.643616	47.910986	1.47	2.20	2.13	1.73

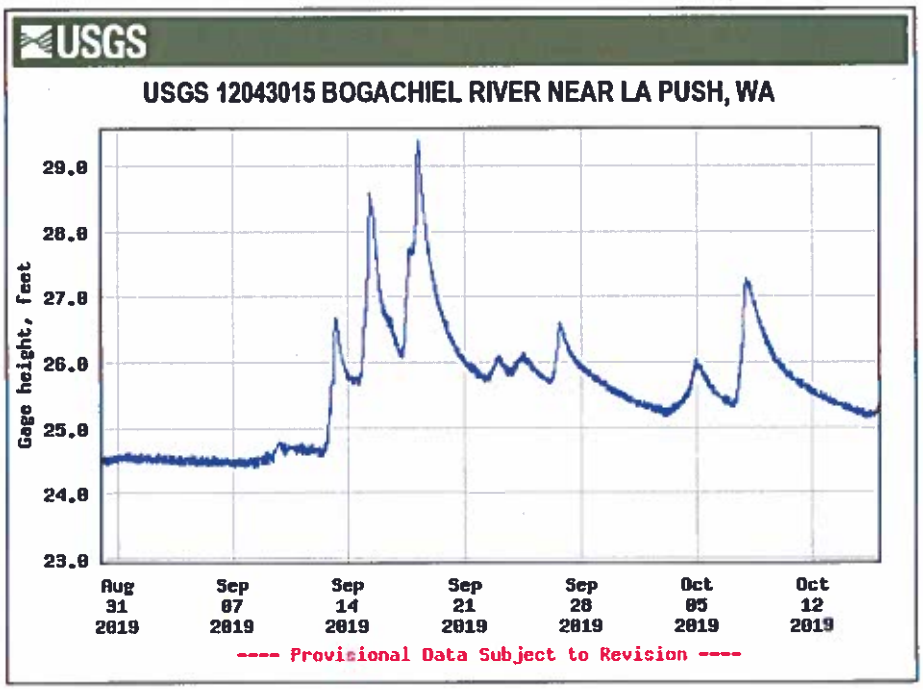

Figure 2: USGS Station 12043015 gage height along the Bogachiel at the time of LiDAR acquisition.

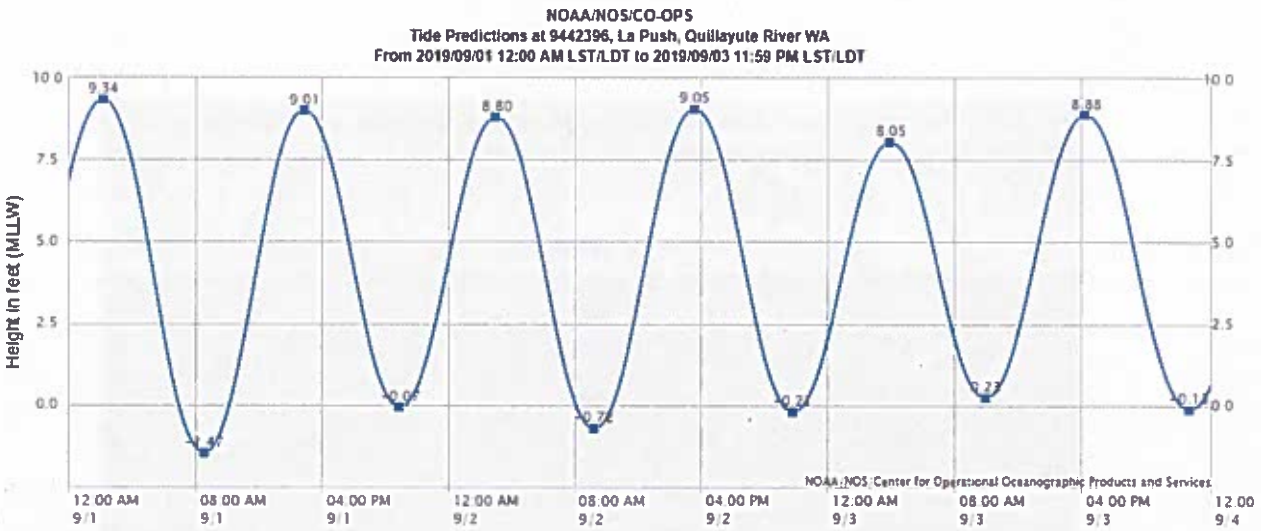

Note: The interval is High/Low; the solid blue line depicts a curve fit between the high and low values and approximates the segments between.
Disclaimer: These data are based upon the latest information available as of the date of your request, and may differ from the published tide tables.

Figure 3: NOAA Station 9442396 tide levels predictions for La Push, WA at the time of LiDAR acquisition.

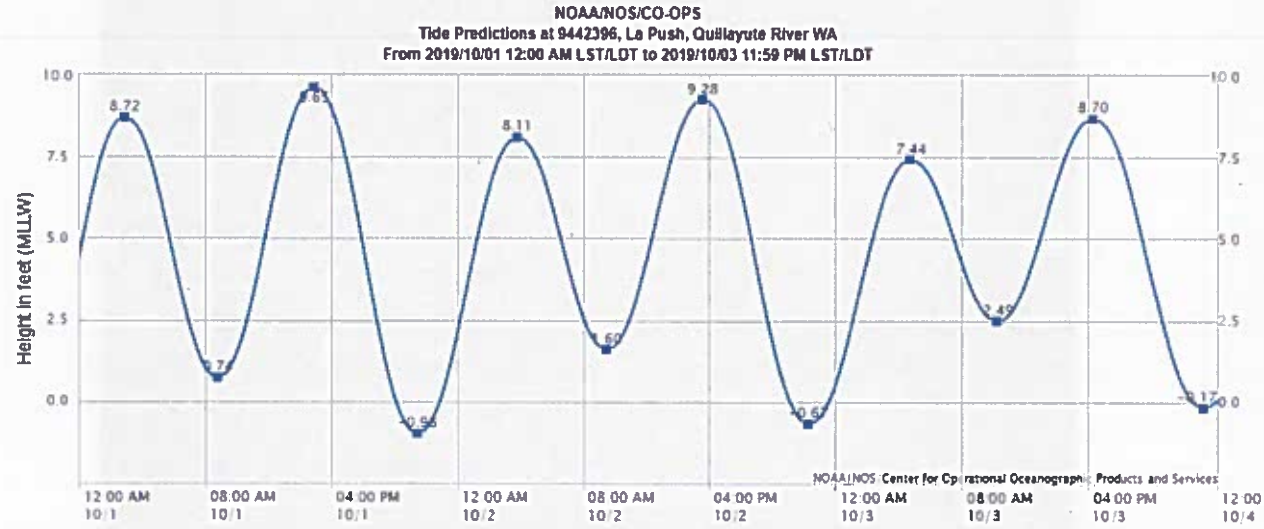

Note: The interval is High/Low; the solid blue line depicts a curve fit between the high and low values and approximates the segments between.
Disclaimer: These data are based upon the latest information available as of the date of your request, and may differ from the published tide tables.

Figure 4: NOAA Station 9442396 tide levels predictions for La Push, WA at the time of LiDAR acquisition.

The above images show water clarity conditions at two different sites on the Quillayute River at the time of the LIDAR Acquisition.

Airborne LiDAR Survey

The LiDAR survey was accomplished using a Riegl VQ-880-GII laser system mounted in a Cessna Caravan. The Riegl VQ-880-GII boasts a higher repetition pulse rate (up to 750 kHz), higher scanning speed, small laser footprint, and wide field of view which allows for seamless collection of high-resolution data of both topographic and bathymetric surfaces. The green wavelength (λ=532 nm) laser is capable of collecting high resolution topography data, as well as penetrating the water surface with minimal spectral absorption by water. The Riegl VQ-880-GII contains an integrated NIR laser (λ=1064 nm) that adds additional topography data and aids in water surface modeling. The recorded waveform enables range measurements for all discernible targets for a given pulse. The typical number of returns digitized from a single pulse range from 1 to 14 for the Quillayute River project area. It is not uncommon for some types of surfaces (e.g., dense vegetation or water) to return fewer pulses to the LiDAR sensor than the laser originally emitted. The discrepancy between first return and overall delivered density will vary depending on terrain, land cover, and the prevalence of water bodies. All discernible laser returns were processed for the output dataset. Table 4 summarizes the settings used to yield an average pulse density of ≥16 pulses/m^2 over the Quillayute River project area.

Table 4: LiDAR specifications and survey settings

LiDAR Survey Settings & Specifications		
Acquisition Dates	09/02/2019, 10/01/2019	09/02/2019, 10/01/2019
Wave Length	NIR	Green
Aircraft Used	Cessna Caravan	Cessna Caravan
Sensor	Riegl	Riegl
Laser	VG-880-GII-IR	VG-880-GII
Maximum Returns	Unlimited	Unlimited
Resolution/Density	Average 16 pulses/m^2	Average 16 pulses/m^2
Nominal Pulse Spacing	0.25 m	0.25 m
Survey Altitude (AGL)	400 m	400 m
Survey speed	140 knots	140 knots
Field of View	40°	40°
Mirror Scan Rate	Uniform Point Spacing	80 Lines per second
Target Pulse Rate	300 kHz	200 kHz
Pulse Length	3.0 ns	1.5 ns
Laser Pulse Footprint Diameter	8.0 cm	28.0 cm
Central Wavelength	1064 nm	532 nm
Pulse Mode	MTA (multiple times around)	MTA (multiple times around)
Beam Divergence	0.2 mrad	0.7 mrad
Swath Width	291 m	291 m
Swath Overlap	60 %	60%
Intensity	16-bit	16-bit
Accuracy	$RMSE_z \leq 10$ cm	$RMSE_z \leq 10$ cm

All areas were surveyed with an opposing flight line side-lap of ≥50% (≥100% overlap) in order to reduce laser shadowing and increase surface laser painting. To accurately solve for laser point position (geographic coordinates x, y and z), the positional coordinates of the airborne sensor and the attitude of the aircraft were recorded continuously throughout the LiDAR data collection mission. Position of the aircraft was measured twice per second (2 Hz) by an onboard differential GPS unit, and aircraft attitude was measured 200 times per second (200 Hz) as pitch, roll and yaw (heading) from an onboard inertial measurement unit (IMU). To allow for post-processing correction and calibration, aircraft and sensor position and attitude data are indexed by GPS time.

QSIs Cessna Caravan

Ground Survey

Ground control surveys, including monumentation and ground survey points (GSPs), were conducted to support the airborne acquisition. Ground control data were used to geospatially correct the aircraft positional coordinate data and to perform quality assurance checks on final LiDAR data.

QSI Established Monument

Base Stations

Base stations were used for collection of ground survey points using real time kinematic (RTK), post-processed kinematic (PPK), and fast static (FS) survey techniques.

Monument locations were selected with consideration for satellite visibility, field crew safety, and optimal location for GSP coverage. QSI established one new monument for the Quillayute River LiDAR project (Table 5, Figure 6). New monumentation was set using 5/8" x 30" rebar topped with stamped 2 ½ " aluminum caps. QSI's professional land surveyor, Evon Silvia (WAPLS#53957) oversaw and certified the ground survey.

Table 5: Monument position for the Quillayute River Topobathymetric LiDAR acquisition. Coordinates are on the NAD83 (2011) datum, epoch 2010.00

Monument ID	Latitude	Longitude	Ellipsoid (meters)
QUILL_01	47° 55' 58.50354"	-124° 33' 39.74789"	32.711

QSI utilized static Global Navigation Satellite System (GNSS) data collected at 1 Hz recording frequency for each base station. During post-processing, the static GNSS data were triangulated with nearby Continuously Operating Reference Stations (CORS) using the Online Positioning User Service (OPUS[1]) for precise positioning. Multiple independent sessions over the same monument were processed to confirm antenna height measurements and to refine position accuracy.

Monuments were established according to the national standard for geodetic control networks, as specified in the Federal Geographic Data Committee (FGDC) Geospatial Positioning Accuracy Standards for geodetic networks.[2] This standard provides guidelines for classification of monument quality at the 95% confidence interval as a basis for comparing the quality of one control network to another. The monument rating for this project is shown in Table 6.

[1] OPUS is a free service provided by the National Geodetic Survey to process corrected monument positions. http://www.ngs.noaa.gov/OPUS/.

[2] Federal Geographic Data Committee, Geospatial Positioning Accuracy Standards (FGDC-STD-007.2-1998). Part 2: Standards for Geodetic Networks, Table 2.1, page 2-3. http://www.fgdc.gov/standards/projects/FGDC-standards-projects/accuracy/part2/chapter2

Table 6: Federal Geographic Data Committee monument rating for network accuracy

Direction	Rating
1.96 * St Dev $_{NE}$:	0.020 m
1.96 * St Dev $_{z}$:	0.020 m

For the Quillayute River LiDAR project, the monument coordinates contributed no more than 2.8 cm of positional error to the geolocation of the final ground survey points and LiDAR, with 95% confidence.

Ground Survey Points (GSPs)

Ground survey points were collected using real time kinematic (RTK), post-processed kinematic (PPK), and fast-static (FS) survey techniques. For RTK surveys, a roving receiver receives corrections from a nearby base station or Real-Time Network (RTN) via radio or cellular network, enabling rapid collection of points with relative errors less than 1.5 cm horizontal and 2.0 cm vertical. PPK and FS surveys compute these corrections during post-processing to achieve comparable accuracy. RTK and PPK surveys record data while stationary for at least five seconds, calculating the position using at least three one-second epochs. FS surveys record observations for up to fifteen minutes on each GSP in order to support longer baselines. All GSP measurements were made during periods with a Position Dilution of Precision (PDOP) of ≤ 3.0 with at least six satellites in view of the stationary and roving receivers. See Table 7 for QSI ground survey equipment information.

GSPs were collected in areas where good satellite visibility was achieved on paved roads and other hard surfaces such as gravel or packed dirt roads. GSP measurements were not taken on highly reflective surfaces such as center line stripes or lane markings on roads due to the increased noise seen in the laser returns over these surfaces. GSPs were collected within as many flightlines as possible; however, the distribution of GSPs depended on ground access constraints and monument locations and may not be equitably distributed throughout the study area (Figure 6).

Table 7: QSI ground survey equipment identification

Receiver Model	Antenna	OPUS Antenna ID	Use
Trimble R7 GNSS	Zephyr GNSS Geodetic Model 2 RoHS	TRM57971.00	Static
Trimble R8	Integrated Antenna	TRM_R8_GNSS	Rover

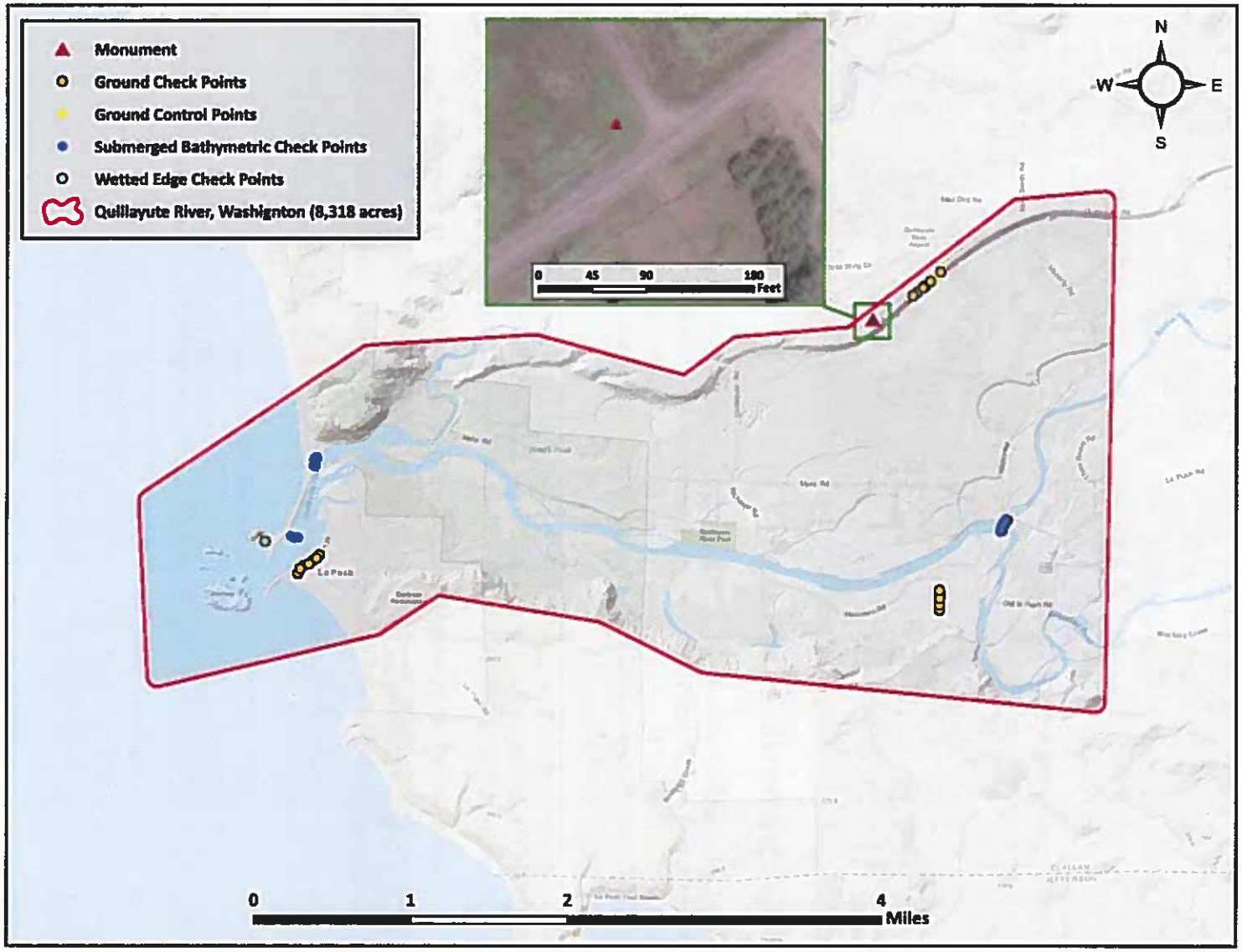

Figure 5: Ground survey location map

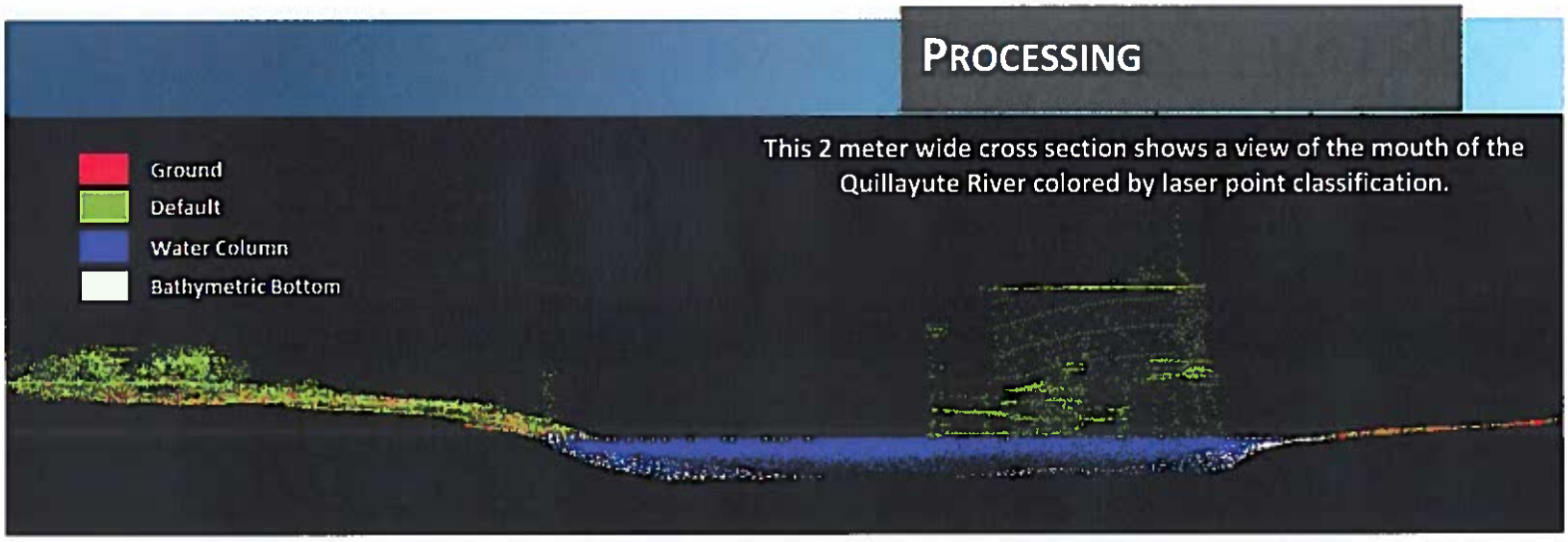

Topobathymetric LiDAR Data

Upon completion of data acquisition, QSI processing staff initiated a suite of automated and manual techniques to process the data into the requested deliverables. Processing tasks included GPS control computations, smoothed best estimate trajectory (SBET) calculations, kinematic corrections, calculation of laser point position, sensor and data calibration for optimal relative and absolute accuracy, and LiDAR point classification (Table 8).

QSI refracted water column points using QSI's proprietary LAS processing software, Las Monkey. The resulting point cloud data were classified using both manual and automated techniques. Processing methodologies were tailored for the landscape. Brief descriptions of these tasks are shown in Table 9.

Table 8: ASPRS LAS classification standards applied to the Quillayute River dataset

Classification Number	Classification Name	Classification Description
1	Default/Unclassified	Laser returns that are not included in the ground class, composed of vegetation and anthropogenic features
2	Ground	Laser returns that are determined to be ground using automated and manual cleaning algorithms
9	Water	Laser returns that are determined to be water using automated and manual cleaning algorithms
40	Bathymetric Bottom	Refracted Riegl sensor returns that fall within the water's edge breakline which characterize the submerged topography.
41	Water Surface	Green laser returns that are determined to be water surface points using automated and manual cleaning algorithms.
45	Water Column	Refracted Riegl sensor returns that are determined to be water using automated and manual cleaning algorithms.

Table 9: LiDAR processing workflow

LiDAR Processing Step	Software Used
Resolve kinematic corrections for aircraft position data using kinematic aircraft GPS and static ground GPS data. Develop a smoothed best estimate of trajectory (SBET) file that blends post-processed aircraft position with sensor head position and attitude recorded throughout the survey.	POSPac MMS v.8.3
Calculate laser point position by associating SBET position to each laser point return time, scan angle, intensity, etc. Create raw laser point cloud data for the entire survey in *.las (ASPRS v. 1.4) format. Convert data to orthometric elevations by applying a geoid correction.	RiProcess v1.8.5 TerraMatch v.19
Import raw laser points into manageable blocks to perform manual relative accuracy calibration and filter erroneous points. Classify ground points for individual flight lines.	TerraScan v.19
Using ground classified points per each flight line, test the relative accuracy. Perform automated line-to-line calibrations for system attitude parameters (pitch, roll, heading), mirror flex (scale) and GPS/IMU drift. Calculate calibrations on ground classified points from paired flight lines and apply results to all points in a flight line. Use every flight line for relative accuracy calibration.	TerraMatch v.19 RiProcess v1.8.5
Apply refraction correction to all subsurface returns.	Las Monkey 2.4.3 (QSI proprietary software)
Classify resulting data to ground and other client designated ASPRS classifications (Table 8). Assess statistical absolute accuracy via direct comparisons of ground classified points to ground control survey data.	TerraScan v.19 TerraModeler v.19
Generate bare earth models as triangulated surfaces. Generate highest hit models as a surface expression of all classified points. Export all surface models as ESRI GRID format at a 3.0 foot pixel resolution.	Las Product Creator 3.0 (QSI proprietary software) ArcMap v. 10.3.1
Export intensity images as GeoTIFFs at a 1.5 foot pixel resolution.	Las Product Creator 3.0 (QSI proprietary software)

Bathymetric Refraction

The water surface models used for refraction are generated using elevation information derived from the NIR channel to inform where the green water surface level is located, and then water surface points are classified for both the forward and reverse look directions of the green scanner. Points are filtered and edited to obtain the most accurate representation of the water surface and are used to create a water surface model for each flight line and look direction. Water surface classification and modeling is processed on each flight line to accommodate water level changes due to tide and temporal changes in water surface. Each look direction (forward and reverse) are modeled separately to correctly model short duration time dependent surface changes (e.g. waves) that change between the times that each look direction records a unique location. The water surface model created is raster based with an associated surface normal vector to obtain the most accurate angle of incidence during refraction.

LiDAR Derived Products

Because hydrographic laser scanners penetrate the water surface to map submerged topography, this affects how the data should be processed and presented in derived products from the LiDAR point cloud. The following discusses certain derived products that vary from the traditional (NIR) specification and delivery format.

Topobathymetric DEMs

Bathymetric bottom returns can be limited by depth, water clarity, and bottom surface reflectivity. Water clarity and turbidity affects the depth penetration capability of the green wavelength laser with returning laser energy diminishing by scattering throughout the water column. Additionally, the bottom surface must be reflective enough to return remaining laser energy back to the sensor at a detectable level. Although the predicted depth penetration range of the Riegl VQ-880-G sensor is 1.5 Secchi depths on brightly reflective surfaces, it is not unexpected to have no bathymetric bottom returns in turbid or non-reflective areas.

As a result, creating digital elevation models (DEMs) presents a challenge with respect to interpolation of areas with no returns. Traditional DEMs are "unclipped", meaning areas lacking ground returns are interpolated from neighboring ground returns (or breaklines in the case of hydro-flattening), with the assumption that the interpolation is close to reality. In bathymetric modeling, these assumptions are prone to error because a lack of bathymetric returns can indicate a change in elevation that the laser can no longer map due to increased depths. The resulting void areas may suggest greater depths, rather than similar elevations from neighboring bathymetric bottom returns. Therefore, QSI created a water polygon with bathymetric coverage to delineate areas with successfully mapped bathymetry. This shapefile was used to control the extent of the delivered clipped topobathymetric model to avoid false triangulation (interpolation from TIN'ing) across areas in the water with no bathymetric returns.

Intensity Images

In traditional NIR LiDAR, intensity images are often made using first return information. For bathymetric LiDAR however, it is most often the last returns that capture features of interest below the water's surface. Therefore, a first return intensity image would display intensity information of the water's surface, obscuring the features of interest below.

With bathymetric LiDAR a more detailed and informative intensity image can be created by using all or selected point classes, rather than relying on return number alone. If intensity information of the

bathymetry is the primary goal, water surface and water column points can be excluded. However, water surface and water column points often contain potentially useful information about turbidity and submerged but unclassified features such as vegetation. For the Quillayute River project, QSI created one set of intensity images from NIR laser first returns, as well as one set of intensity images from green laser returns. Green laser intensity images were created using first returns over terrestrial areas only, as well as all water column and bathymetric bottom points in order to display more detail in intensity values.

Feature Extraction

Water's Edge Breaklines

Waters boundary break lines were identified and vectors where produced using a combination of manual and automated processes. Once polygons were developed the initial ground classified points falling within water polygons were reclassified as water points to omit them from the final ground model. Elevations were then obtained from the filtered LiDAR returns to create the final breaklines. Lakes were assigned a consistent elevation for an entire polygon while rivers were assigned consistent elevations on opposing banks and smoothed to ensure downstream flow through the entire river channel.

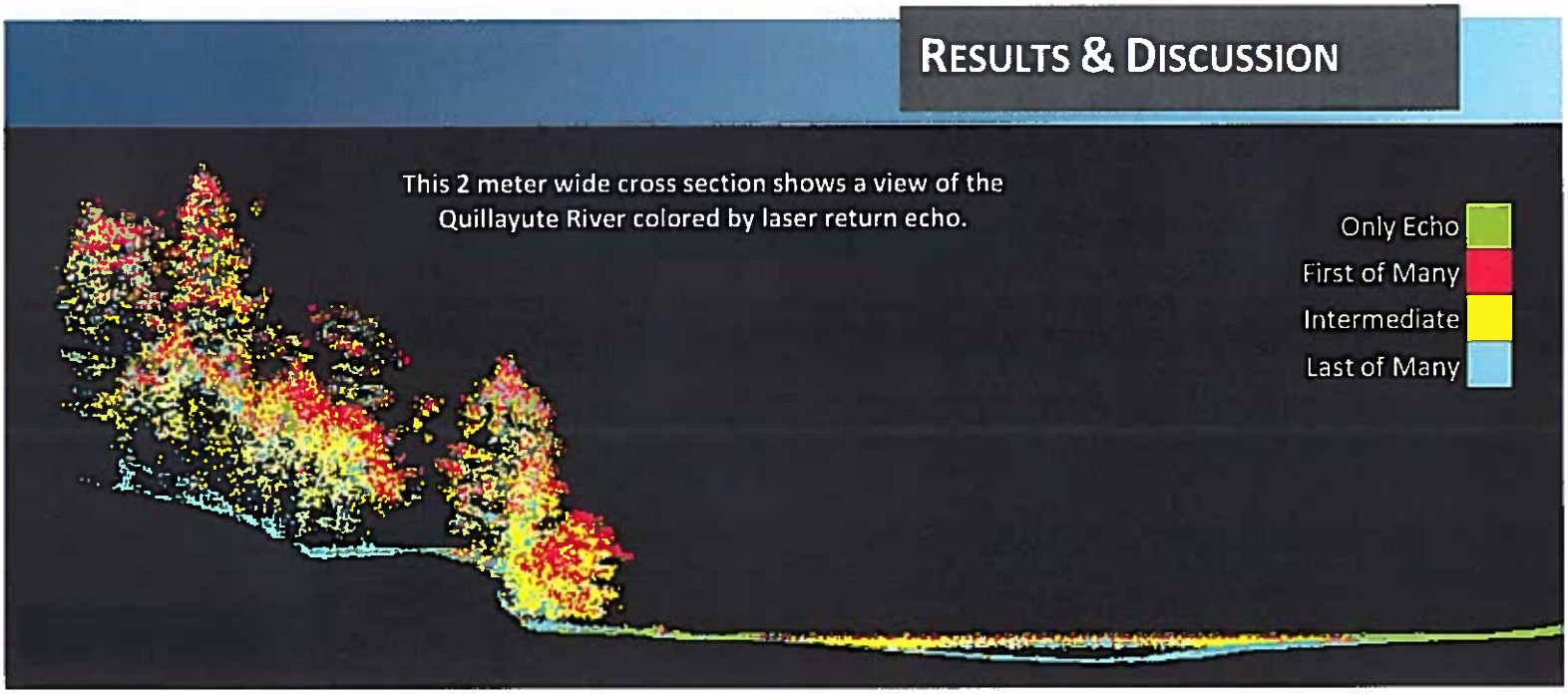

Bathymetric LiDAR

An underlying principle for collecting hydrographic LiDAR data is to survey near-shore areas that can be difficult to collect with other methods, such as multi-beam sonar, particularly over large areas. In order to determine the capability and effectiveness of the bathymetric LiDAR, several parameters were considered; below the water surface, bathymetric return density, and spatial accuracy.

LiDAR Point Density

First Return Point Density

The acquisition parameters were designed to acquire an average first-return density of 16 points/m^2. First return density describes the density of pulses emitted from the laser that return at least one echo to the system. Multiple returns from a single pulse were not considered in first return density analysis. Some types of surfaces (e.g., breaks in terrain, water and steep slopes) may have returned fewer pulses than originally emitted by the laser.

First returns typically reflect off the highest feature on the landscape within the footprint of the pulse. In forested or urban areas, the highest feature could be a tree, building or power line, while in areas of unobstructed ground, the first return will be the only echo and represents the bare earth surface.

The average first-return density of the Quillayute River LiDAR project was 1.79 points/ft^2 (19.30 points/m^2) (Table 10). The statistical and spatial distributions of all first return densities per 100 m x 100 m cell are portrayed in Figure 6.

Bathymetric and Ground Classified Point Densities

The density of ground classified LiDAR returns, and bathymetric bottom returns were also analyzed for this project. Terrain character, land cover, and ground surface reflectivity all influenced the density of ground surface returns. In vegetated areas, fewer pulses may have penetrated the canopy, resulting in lower ground density. Similarly, the density of bathymetric bottom returns was influenced by turbidity, depth, and bottom surface reflectivity. In turbid areas, fewer pulses may have penetrated the water surface, resulting in lower bathymetric density.

The ground and bathymetric bottom classified density of LiDAR data for the Quillayute River project was 0.30 points/ft^2 (3.26 points/m^2) (Table 10). The statistical and spatial distributions ground classified and bathymetric bottom return densities per 100 m x 100 m cell are portrayed in Figure 7.

Additionally, for the Quillayute River project, density values of only bathymetric bottom returns were calculated for areas containing at least one bathymetric bottom return. Areas lacking bathymetric returns were not considered in calculating an average density value. Within the successfully mapped area, a bathymetric bottom return density of 0.54 points/ft^2 (5.88 points/m^2) was achieved.

Table 10: Average LiDAR point densities

Density Type	Point Density
First Returns	1.79 points/ft^2 19.30 points/m^2
Ground and Bathymetric Bottom Classified Returns	0.30 points/ft^2 3.26 points/m^2
Bathymetric Bottom Classified Returns	0.54 points/ft^2 5.88 points/m^2

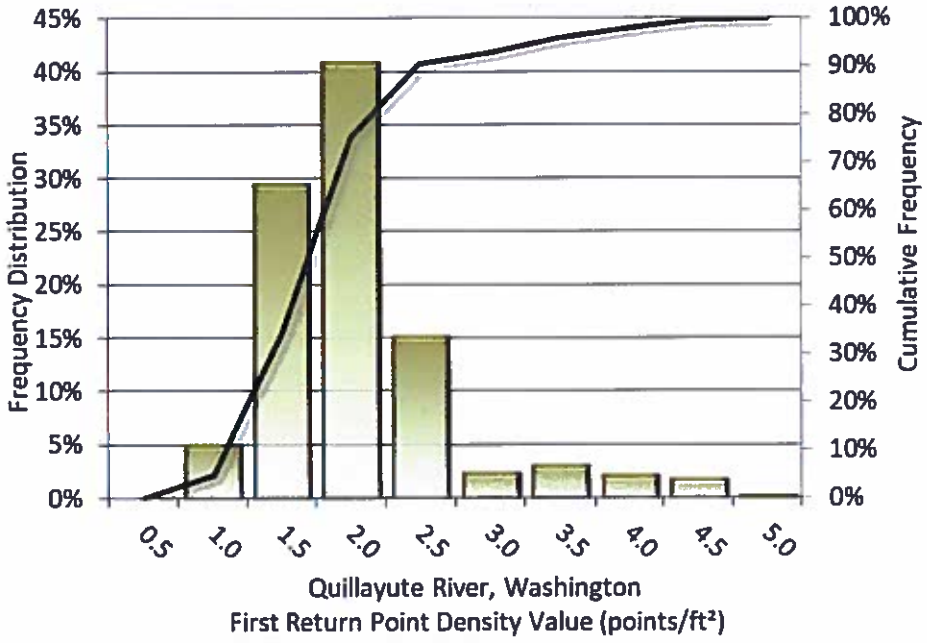

Figure 6: Frequency distribution of first return densities per 100 x 100 m cell

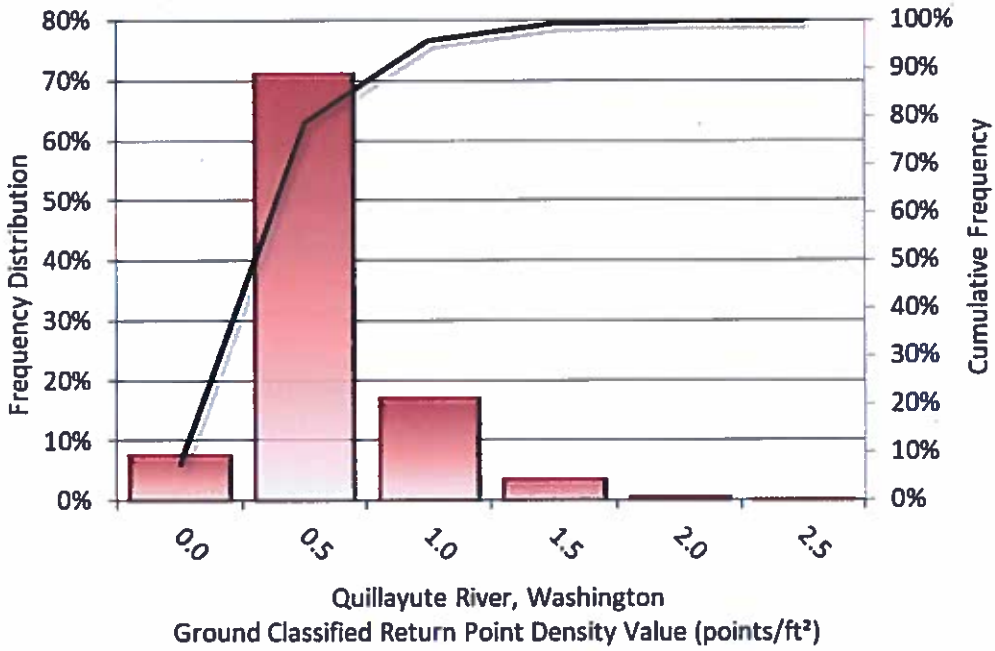

Figure 7: Frequency distribution of ground and bathymetric bottom classified return densities per 100 x 100 m cell

LiDAR Accuracy Assessments

The accuracy of the LiDAR data collection can be described in terms of absolute accuracy (the consistency of the data with external data sources) and relative accuracy (the consistency of the dataset with itself). See Appendix A for further information on sources of error and operational measures used to improve relative accuracy.

LiDAR Non-Vegetated Vertical Accuracy

Absolute accuracy was assessed using Non-vegetated Vertical Accuracy (NVA) reporting designed to meet guidelines presented in the FGDC National Standard for Spatial Data Accuracy[3]. NVA compares known ground check point data that were withheld from the calibration and post-processing of the LiDAR point cloud to the triangulated surface generated by the unclassified LiDAR point cloud as well as the derived gridded bare earth DEM. NVA is a measure of the accuracy of LiDAR point data in open areas where the LiDAR system has a high probability of measuring the ground surface and is evaluated at the 95% confidence interval (1.96 * RMSE), as shown in Table 11.

The mean and standard deviation (sigma σ) of divergence of the ground surface model from ground check point coordinates are also considered during accuracy assessment. These statistics assume the error for x, y and z is normally distributed, and therefore the skew and kurtosis of distributions are also considered when evaluating error statistics. For the Quillayute River survey, 20 ground check points were withheld from the calibration and post-processing of the LiDAR point cloud, with resulting non-vegetated vertical accuracy of 0.120 feet (0.037 meters) as compared to the unclassified LAS, and 0.118 feet (0.036 meters) against the bare earth DEM, with 95% confidence (Figure 8 and Figure 9).

QSI also assessed absolute accuracy using 96 ground control points. Although these points were used in the calibration and post-processing of the LiDAR point cloud, they still provide a good indication of the overall accuracy of the LiDAR dataset, and therefore have been provided in Table 11 and Figure 10.

[3] Federal Geographic Data Committee, ASPRS POSITIONAL ACCURACY STANDARDS FOR DIGITAL GEOSPATIAL DATA EDITION 1, Version 1.0, NOVEMBER 2014. http://www.asprs.org/PAD-Division/ASPRS-POSITIONAL-ACCURACY-STANDARDS-FOR-DIGITAL-GEOSPATIAL-DATA.html.

Table 11: Absolute accuracy results

Absolute Vertical Accuracy			
	NVA, as compared to Unclassified LAS	NVA, as compared to Bare Earth DEM	Ground Control Points
Sample	20 points	20 points	96 points
95% Confidence (1.96*RMSE)	0.120 ft 0.037 m	0.118 ft 0.036 m	0.144 ft 0.044 m
Average	-0.011 ft -0.004 m	0.012 ft 0.004 m	-0.028 ft -0.008 m
Median	-0.018 ft -0.006 m	-0.004 ft -0.001 m	-0.021 ft -0.007 m
RMSE	0.061 ft 0.019 m	0.060 ft 0.018 m	0.074 ft 0.022 m
Standard Deviation (1σ)	0.062 ft 0.019 m	0.060 ft 0.018 m	0.069 ft 0.021 m

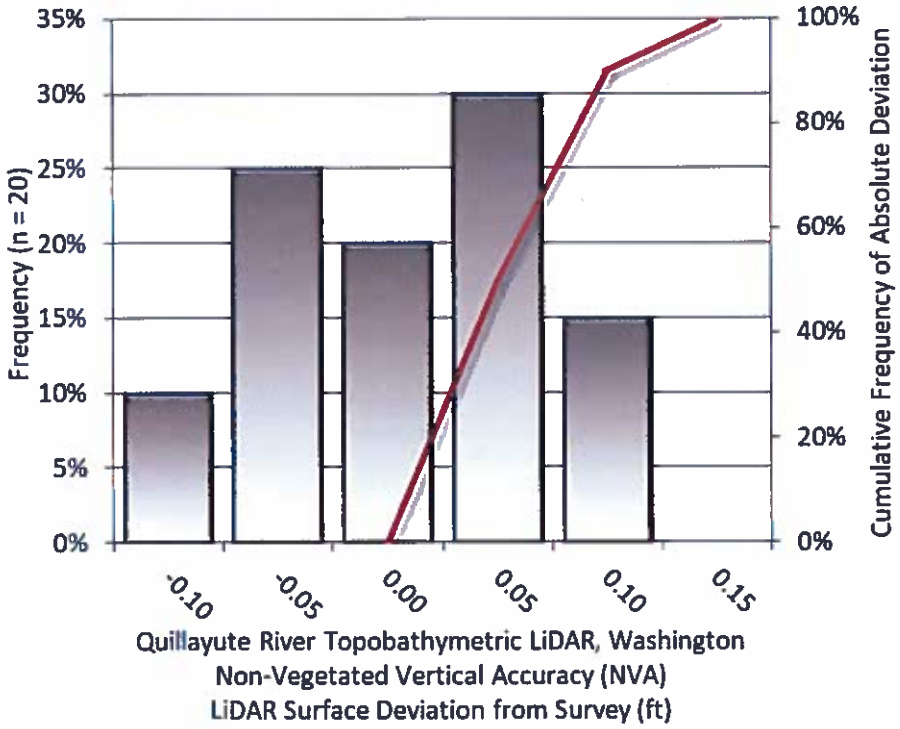

Figure 8: Frequency histogram for unclassified LAS deviation from ground check point values

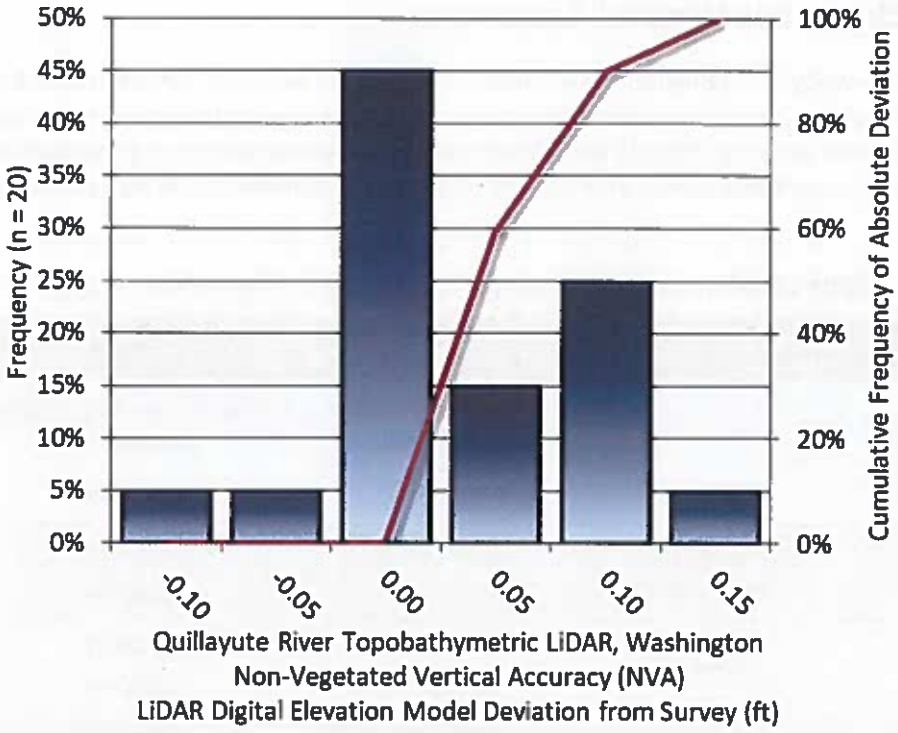

Figure 9: Frequency histogram for LiDAR bare earth DEM deviation from ground check point values

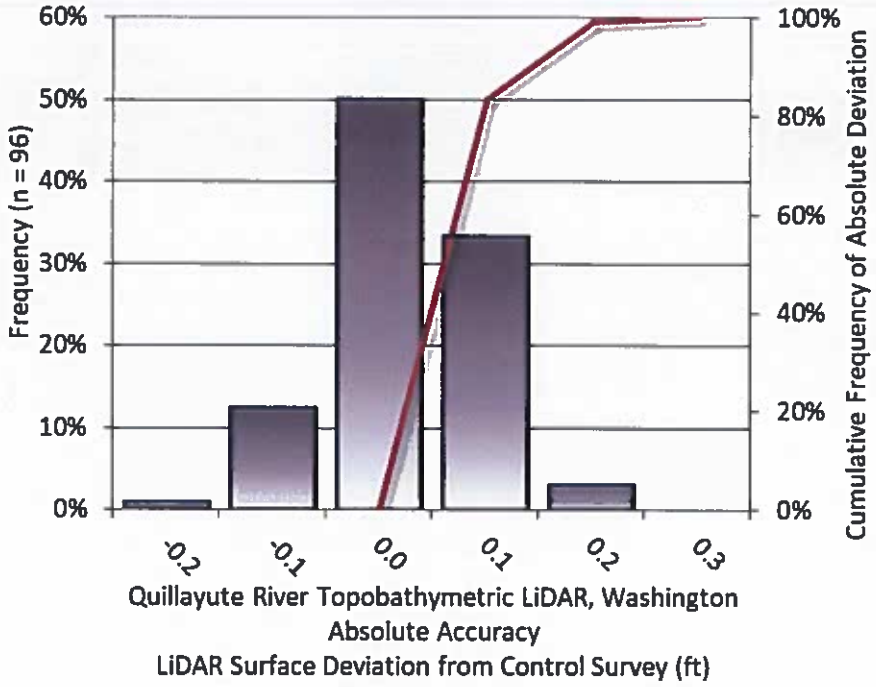

Figure 10: Frequency histogram for LiDAR surface deviation ground control point values

LiDAR Bathymetric Vertical Accuracies

Bathymetric (submerged or along the water's edge) check points were also collected in order to assess the submerged surface vertical accuracy. Assessment of 73 submerged bathymetric check points resulted in a vertical accuracy of 0.391 feet (0.119 meters), while assessment of 18 wetted edge check points resulted in a vertical accuracy of 0.227 feet (0.069 meters), evaluated at 95% confidence interval (Table 12).

Table 12: Bathymetric Vertical Accuracy for the Quillayute River Project

Bathymetric Vertical Accuracy (VVA)		
	Submerged Bathymetric Check Points	**Wetted Edge Bathymetric Check Points**
Sample	73 points	18 points
95% Confidence (1.96*RMSE)	0.391 ft 0.119 m	0.227 ft 0.069 m
Average Dz	-0.132 ft -0.040 m	-0.046 ft -0.011 m
Median	-0.151 ft -0.046 m	-0.036 ft -0.011 m
RMSE	0.200 ft 0.061 m	0.116 ft 0.035 m
Standard Deviation (1σ)	0.150 ft 0.046 m	0.109 ft 0.033 m

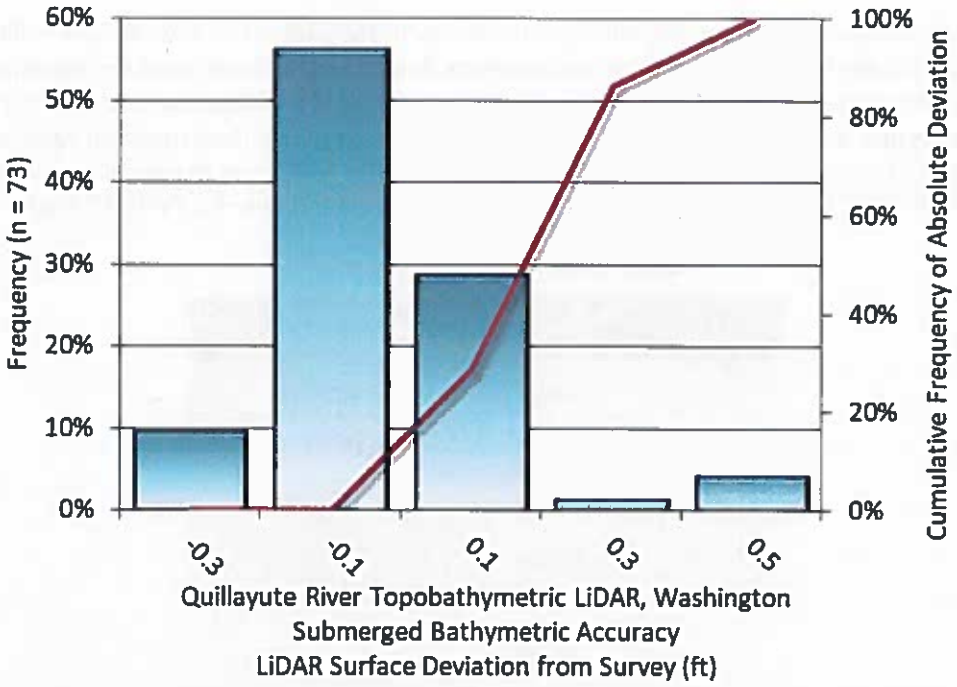

Figure 11: Frequency histogram for LiDAR surface deviation from submerged check point values

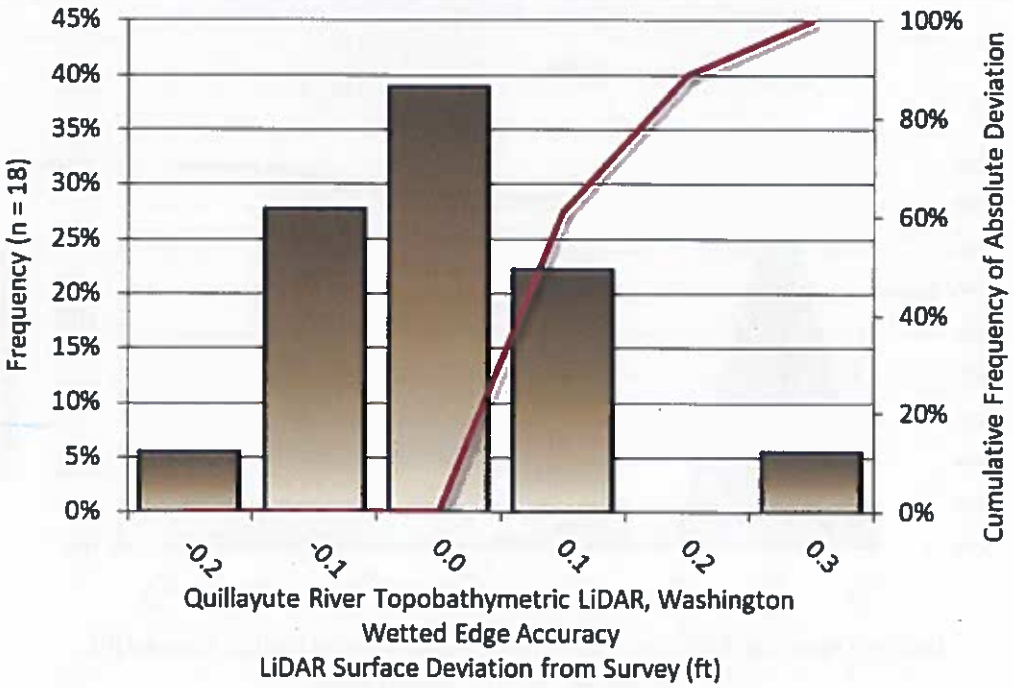

Figure 12: Frequency histogram for LiDAR surface deviation from wetted edge check point values

LiDAR Relative Vertical Accuracy

Relative vertical accuracy refers to the internal consistency of the data set as a whole: the ability to place an object in the same location given multiple flight lines, GPS conditions, and aircraft attitudes. When the LiDAR system is well calibrated, the swath-to-swath vertical divergence is low (<0.10 meters). The relative vertical accuracy was computed by comparing the ground surface model of each individual flight line with its neighbors in overlapping regions. The average (mean) line to line relative vertical accuracy for the Quillayute River LiDAR project was 0.105 feet (0.032 meters) (Table 13, Figure 13).

Table 13: Relative accuracy results

Relative Accuracy	
Sample	104 surfaces
Average	0.105 ft 0.032 m
Median	0.108 ft 0.033 m
RMSE	0.208 ft 0.063 m
Standard Deviation (1σ)	0.140 ft 0.043 m
1.96σ	0.274 ft 0.083 m

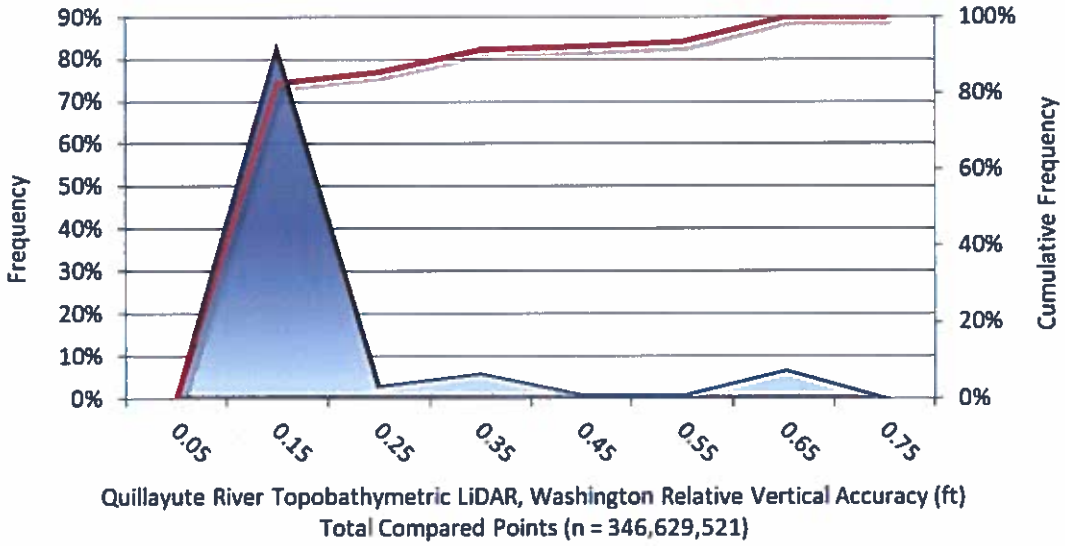

Figure 13: Frequency plot for relative vertical accuracy between flight lines

LiDAR Horizontal Accuracy

LiDAR horizontal accuracy is a function of Global navigation Satellite System (GNSS) derived positional error, flying altitude, and INS derived attitude error. The obtained RMSE, value is multiplied by a conversion factor of 1.7308 to yield the horizontal component of the National Standards for Spatial Data Accuracy (NSSDA) reporting standard where a theoretical point will fall within the obtained radius 95 percent of the time. Using a flying altitude of 400 meters, an IMU error of 0.002 decimal degrees, and a GNSS positional error of 0.015 meters, compiled to meet (0.002 feet, 0.001 meters) horizontal accuracy at the 95% confidence level.

CERTIFICATIONS

Quantum Spatial, Inc. provided LiDAR services for the Quillayute River project as described in this report.

I, Steve Miller, have reviewed the attached report for completeness and hereby state that it is a complete and accurate report of this project.

Dec 6, 2019

Steve Miller
Project Manager
Quantum Spatial, Inc.

I, Evon P. Silvia, PLS, being duly registered as a Professional Land Surveyor in and by the state of Washington, hereby certify that the methodologies, static GNSS occupations used during airborne flights, and ground survey point collection were performed using commonly accepted Standard Practices. Field work conducted for this report was conducted between August 28 and October 1, 2019.

Accuracy statistics shown in the Accuracy Section of this Report have been reviewed by me and found to meet the "National Standard for Spatial Data Accuracy".

Dec 6, 2019

Evon P. Silvia, PLS
Quantum Spatial, Inc.
Corvallis, OR 9733

GLOSSARY

1-sigma (σ) Absolute Deviation: Value for which the data are within one standard deviation (approximately 68th percentile) of a normally distributed data set.

1.96 * RMSE Absolute Deviation: Value for which the data are within two standard deviations (approximately 95th percentile) of a normally distributed data set, based on the FGDC standards for Non-vegetated Vertical Accuracy (FVA) reporting.

Accuracy: The statistical comparison between known (surveyed) points and laser points. Typically measured as the standard deviation (sigma σ) and root mean square error (RMSE).

> **Absolute Accuracy:** The vertical accuracy of LiDAR data is described as the mean and standard deviation (sigma σ) of divergence of LiDAR point coordinates from ground survey point coordinates. To provide a sense of the model predictive power of the dataset, the root mean square error (RMSE) for vertical accuracy is also provided. These statistics assume the error distributions for x, y and z are normally distributed, and thus we also consider the skew and kurtosis of distributions when evaluating error statistics.
>
> **Relative Accuracy:** Relative accuracy refers to the internal consistency of the data set; i.e., the ability to place a laser point in the same location over multiple flight lines, GPS conditions and aircraft attitudes. Affected by system attitude offsets, scale and GPS/IMU drift, internal consistency is measured as the divergence between points from different flight lines within an overlapping area. Divergence is most apparent when flight lines are opposing. When the LiDAR system is well calibrated, the line-to-line divergence is low (<10 cm).
>
> **Root Mean Square Error (RMSE):** A statistic used to approximate the difference between real-world points and the LiDAR points. It is calculated by squaring all the values, then taking the average of the squares and taking the square root of the average.

Data Density: A common measure of LiDAR resolution, measured as points per square meter.

Digital Elevation Model (DEM): File or database made from surveyed points, containing elevation points over a contiguous area. Digital terrain models (DTM) and digital surface models (DSM) are types of DEMs. DTMs consist solely of the bare earth surface (ground points), while DSMs include information about all surfaces, including vegetation and man-made structures.

Intensity Values: The peak power ratio of the laser return to the emitted laser, calculated as a function of surface reflectivity.

Nadir: A single point or locus of points on the surface of the earth directly below a sensor as it progresses along its flight line.

Overlap: The area shared between flight lines, typically measured in percent. 100% overlap is essential to ensure complete coverage and reduce laser shadows.

Pulse Rate (PR): The rate at which laser pulses are emitted from the sensor; typically measured in thousands of pulses per second (kHz).

Pulse Returns: For every laser pulse emitted, the number of wave forms (i.e., echoes) reflected back to the sensor. Portions of the wave form that return first are the highest element in multi-tiered surfaces such as vegetation. Portions of the wave form that return last are the lowest element in multi-tiered surfaces.

Real-Time Kinematic (RTK) Survey: A type of surveying conducted with a GPS base station deployed over a known monument with a radio connection to a GPS rover. Both the base station and rover receive differential GPS data and the baseline correction is solved between the two. This type of ground survey is accurate to 1.5 cm or less.

Post-Processed Kinematic (PPK) Survey: GPS surveying is conducted with a GPS rover collecting concurrently with a GPS base station set up over a known monument. Differential corrections and precisions for the GNSS baselines are computed and applied after the fact during processing. This type of ground survey is accurate to 1.5 cm or less.

Scan Angle: The angle from nadir to the edge of the scan, measured in degrees. Laser point accuracy typically decreases as scan angles increase.

Native LiDAR Density: The number of pulses emitted by the LiDAR system, commonly expressed as pulses per square meter.

Relative Accuracy Calibration Methodology:

Manual System Calibration: Calibration procedures for each mission require solving geometric relationships that relate measured swath-to-swath deviations to misalignments of system attitude parameters. Corrected scale, pitch, roll and heading offsets were calculated and applied to resolve misalignments. The raw divergence between lines was computed after the manual calibration was completed and reported for each survey area.

Automated Attitude Calibration: All data were tested and calibrated using TerraMatch automated sampling routines. Ground points were classified for each individual flight line and used for line-to-line testing. System misalignment offsets (pitch, roll and heading) and scale were solved for each individual mission and applied to respective mission datasets. The data from each mission were then blended when imported together to form the entire area of interest.

Automated Z Calibration: Ground points per line were used to calculate the vertical divergence between lines caused by vertical GPS drift. Automated Z calibration was the final step employed for relative accuracy calibration.

LiDAR accuracy error sources and solutions:

Type of Error	Source	Post Processing Solution
GPS (Static/Kinematic)	Long Base Lines	None
	Poor Satellite Constellation	None
	Poor Antenna Visibility	Reduce Visibility Mask
Relative Accuracy	Poor System Calibration	Recalibrate IMU and sensor offsets/settings
	Inaccurate System	None
Laser Noise	Poor Laser Timing	None
	Poor Laser Reception	None
	Poor Laser Power	None
	Irregular Laser Shape	None

Operational measures taken to improve relative accuracy:

Low Flight Altitude: Terrain following was employed to maintain a constant above ground level (AGL). Laser horizontal errors are a function of flight altitude above ground (about 1/3000th AGL flight altitude).

Focus Laser Power at narrow beam footprint: A laser return must be received by the system above a power threshold to accurately record a measurement. The strength of the laser return (i.e., intensity) is a function of laser emission power, laser footprint, flight altitude and the reflectivity of the target. While surface reflectivity cannot be controlled, laser power can be increased and low flight altitudes can be maintained.

Reduced Scan Angle: Edge-of-scan data can become inaccurate. The scan angle was reduced to a maximum of ±20° from nadir, creating a narrow swath width and greatly reducing laser shadows from trees and buildings.

Quality GPS: Flights took place during optimal GPS conditions (e.g., 6 or more satellites and PDOP [Position Dilution of Precision] less than 3.0). Before each flight, the PDOP was determined for the survey day. During all flight times, a dual frequency DGPS base station recording at 1 second epochs was utilized and a maximum baseline length between the aircraft and the control points was less than 13 nm at all times.

Ground Survey: Ground survey point accuracy (<1.5 cm RMSE) occurs during optimal PDOP ranges and targets a minimal baseline distance of 4 miles between GPS rover and base. Robust statistics are, in part, a function of sample size (n) and distribution. Ground survey points are distributed to the extent possible throughout multiple flight lines and across the survey area.

50% Side-Lap (100% Overlap): Overlapping areas are optimized for relative accuracy testing. Laser shadowing is minimized to help increase target acquisition from multiple scan angles. Ideally, with a 50% side-lap, the nadir portion of one flight line coincides with the swath edge portion of overlapping flight lines. A minimum of 50% side-lap with terrain-followed acquisition prevents data gaps.

Opposing Flight Lines: All overlapping flight lines have opposing directions. Pitch, roll and heading errors are amplified by a factor of two relative to the adjacent flight line(s), making misalignments easier to detect and resolve.

APPENDIX B – HYDROLOGIC AND HYDRAULIC ANALYSES

Quillayute River Project
Geomorphic Assessment and Action Plan
Hydrologic and Hydraulic Analyses

Appendix B

Submitted to:

Quileute Natural Resources
401 Main Street
La Push, WA 98350

Submitted by:

TETRA TECH

19803 North Creek Parkway
Bothell, WA 98011
Tel 425.482.7600 | Fax 425.482.7652
www.tetratech.com

September 2020

TABLE OF CONTENTS

1 Introduction B-1

2 Hydrologic Analysis B-2

2.1 Quillayute River Drainage B-3

2.2 Climate B-5

2.3 Streamflow B-6

2.3.1 Mean Annual Streamflow B-6

2.3.2 Peak Streamflow B-7

2.3.3 Low-Flow Characteristics B-10

2.4 Water Levels at the River Mouth B-10

2.4.1 Astronomical Tide Levels B-10

2.4.2 Extent of Tidal Influence B-12

2.4.3 Storm Surge B-14

2.4.4 Seasonal Variation in Mean Sea Level B-16

2.4.5 Relative Sea Level Rise B-16

2.4.6 Coastal Flooding B-17

2.4.7 Tsunami Flooding B-19

3 Hydraulic Analysis B-21

3.1 Hydraulic Modeling B-21

3.1.1 Terrain B-21

3.1.2 Calibration B-22

3.1.3 Validation B-26

3.2 Hydraulic Modeling Results B-28

4 References Cited B-30

Attachment 1: River Basin Characteristics

Attachment 2: Hydraulic Modeling Figures

LIST OF TABLES

Table 2-1. River Characteristics B-5
Table 2-2. Mean Annual Streamflow B-7
Table 2-3. USGS StreamStats Peak Streamflow B-8
Table 2-4. USGS (Leonard 1982) Peak Streamflow B-8
Table 2-5. HEC-SSP Bulletin 17C Peak Streamflow B-9
Table 2-6. Peak Streamflow Comparison B-9
Table 2-7. Low-Flow Characteristics B-10
Table 2-8. OCCRI 1D HEC-RAS 100-Year Design Events B-14
Table 2-9. Highest and Lowest Tides, Station 9442396, La Push, Quillayute River, WA B-15
Table 3-1 Manning's Roughness Values by Land Use B-22
Table 3-2. USGS Streamflow Measurements B-24
Table 3-3. HEC-SSP Bulletin 17C Calawah River Peak Streamflow B-27
Table 3-4. Hydraulic Model Design Events B-29

LIST OF FIGURES

Figure 2-1. Quillayute River Drainage HUC-10 Watershed Boundaries B-2
Figure 2-2. Profiles of the Quillayute River and Major Named Tributaries B-4
Figure 2-3. Quillayute River Gage Locations B-7
Figure 2-4. NOS 9442396 Tide Station La Push B-11
Figure 2-5. Tidal and Geodetic Datum Levels at NOS Station La Push B-12
Figure 2-6. Present and Historic Tidal Estuary Extents B-13
Figure 2-7. Water Levels at La Push on February 4, 2006 ..... B-15
Figure 2-8. Relative Sea Level Rise for Project Area under RCP 8.5 ..... B-17
Figure 2-9. FEMA Flood Map for the Lower Quillayute River B-18
Figure 2-10. Tsunami Inundation Limits, Quillayute River Area B-19
Figure 2-11. Tsunami Wave Height History B-20
Figure 3-1. USGS Streamflow Measurement Locations B-23
Figure 3-2. Longitudinal Profile of the Quillayute River – May 4-6, 2010 ..... B-25
Figure 3-3. Hydraulic Model Calibration B-26
Figure 3-4. Hydraulic Model Validation B-28

1 Introduction

The Quileute Natural Resources (QNR) Quillayute River – Assessment, Hydraulic Model, Engineering Design for Thunder Field, and Flood Engineering Project (Project) is designed to address the environmental and economic threats to Thunder Field and adjacent Quileute Tribe reservation lands and the community of La Push, Washington. As a part of the Project, the Quillayute River Geomorphic Assessment (Assessment) is being developed to evaluate existing conditions and impairments in the Quillayute River and provide a Restoration Action Plan (Action Plan). The Assessment is not limited to geomorphology but also documents elements of biology (aquatic and terrestrial species and habitats), hydrology, climate-change, history, land use, and planning.

In support of the Assessment and Action Plan, and as an objective of the Project, the hydrologic and hydraulic analyses presented in this Appendix were completed to identify the 1- and 100-year peak flow events and tidal stages for the Quillayute River. The results from these hydrologic and hydraulic analyses for the Project will be used for engineering design development associated with restoration and enhancement actions and flood engineering focused on protecting La Push from the Quillayute River 100-year recurrence interval. In addition to engineering design development, these analyses will be used as part of the geomorphic and biologic analyses being completed for the Assessment and Action Plan. The geomorphic analyses will integrate and build upon the hydrologic and hydraulic analyses results to identify and evaluate geomorphic change (i.e., historic, current, and future) and prioritize restoration action alternatives. The biologic analyses will integrate the hydraulic modeling output into habitat suitability modeling for various fish species. Combined, the hydrologic and hydraulic analyses provide the foundation for the development of the Assessment and Action Plan, as well as assist in accomplishing the goals and objectives of the Project.

2 Hydrologic Analysis

To determine the 1- and 100-year peak flow recurrence intervals for the Quillayute River, the rainfall-runoff processes (hydrology) for the drainage were analyzed. The Quillayute River drainage is a part of the U.S. Geological Survey's (USGS) Hoh-Quillayute subbasin (8-digit Hydrologic Unit Code [HUC-8] 17100101). The Quillayute River is in the Sol Duc-Quillayute River HUC 10 watershed (10-digit HUC-10 1710010106) and receives major flow contributions from the Dickey River (HUC-10 1710010103), Calawah River (HUC-10 1710010104), and Bogachiel River (HUC-10 1710010105) watersheds (Figure 2-1).

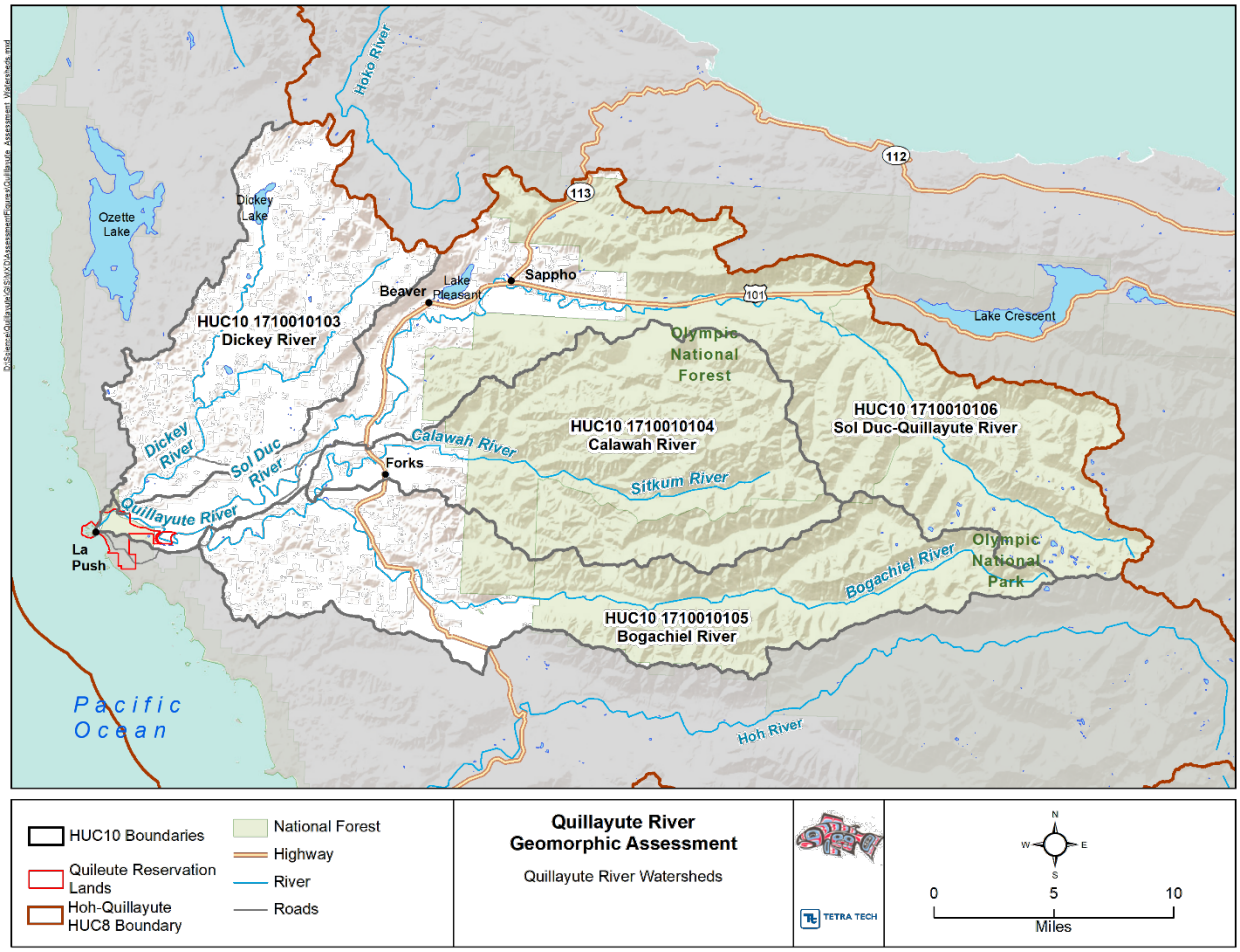

Figure 2-1. Quillayute River Drainage HUC-10 Watershed Boundaries

In order to analyze the hydrology for the Quillayute River and estimate the 1- and 100-year peak flows and tidal stages, the following steps were employed:

1. Compile hydrologic reports describing the Quillayute River drainage.
2. Compile climate information for the Quillayute River drainage.
3. Compile and evaluate data sets to be used in estimating mean annual, peak, and low-flow streamflows for the Quillayute River drainage.
4. Compile and evaluate data sets to be used in estimating water level changes at the mouth of the Quillayute River near La Push, Washington.
5. Utilize the information from the previous steps to calibrate and validate a hydraulic model to perform unsteady flow analyses, evaluate water level changes at the Quillayute River mouth, and generate hydraulic modeling results for the Quillayute River (see Section 3 for hydraulic modeling methods).

Compiled hydrologic reports and data sets to be used in estimating mean annual, peak, and low-flow streamflows for the Quillayute River drainage included (1) a USGS study of Clallam County, including the Quillayute River (Leonard 1982), (2) the USGS StreamStats peak streamflow data (USGS 2019), and (3) a statistical evaluation of peak flow frequency using records from stream gages following Bulletin 17C procedures (England et al. 2019). Climate information for the drainage primarily came from the National Oceanic and Atmospheric Administration (NOAA). Water level data associated with tides for the Quillayute River near its confluence with the Pacific Ocean came from the National Ocean Services (NOS). These reports, information sources, data sets, and other cited publications were each utilized to evaluate and estimate the 1- and 100-year peak flows and tidal stages for the Quillayute River.

2.1 QUILLAYUTE RIVER DRAINAGE

The Quillayute River drains approximately 627 square miles of the northwestern Olympic Peninsula (see Figure 2-1 above). Major named rivers within the Quillayute River drainage from west to east include the Quillayute, Dickey, Sol Duc, and Bogachiel rivers[1]. The elevation of the Quillayute River drainage ranges from over 6,070 feet mean sea level (MSL) near Appleton Pass to 0 feet MSL at the Pacific Ocean. The drainage is within the Cascade Mixed Forest – Coniferous Forest – Alpine Meadow Province as identified by the U.S. Forest Service (USFS; Bailey 2004). The Quillayute River begins at the confluence of the Sol Duc and Bogachiel rivers and flows for approximately 6 miles before entering the Pacific Ocean at La Push, Washington. The Dickey River is the only major named tributary of the mainstem Quillayute River and enters at River Mile (RM) 1.7 referenced from the river mouth at the Pacific Ocean (Czuba et al. 2010).

[1] The Calawah River is a named tributary to the Bogachiel River and is part of the Bogachiel River watershed. Information regarding the Calawah River is presented in Section 3. For the purposes of the Assessment and this Appendix, and unless specified, the Calawah River information is not separated out as major named tributary and is instead combined with the Bogachiel River as part of that watershed.

The major named tributaries of the Quillayute River drainage have headwaters on the western slopes of the Olympic Mountains, about 33 miles east of Forks, Washington. The Sol Duc and Bogachiel rivers flow westward down the steep slopes from the mountains to the coastal terraces. The coastal terraces extend upstream about 30 miles from the mouth of the Quillayute River. The Bogachiel and Sol Duc rivers join approximately 6 miles east of La Push, Washington to form the mainstem of the Quillayute River. All rivers on the coastal terraces have similar low gradients. The Dickey River is a major named tributary that drains the northwest portion of the Quillayute River drainage and has headwaters primarily on the coastal terraces (Leonard 1982). Figure 2-2 shows the gradients of the Quillayute River and named major tributaries. Attachment 1 provides full details of the characteristics of the Quillayute, Dickey, Sol Duc, and Bogachiel rivers.

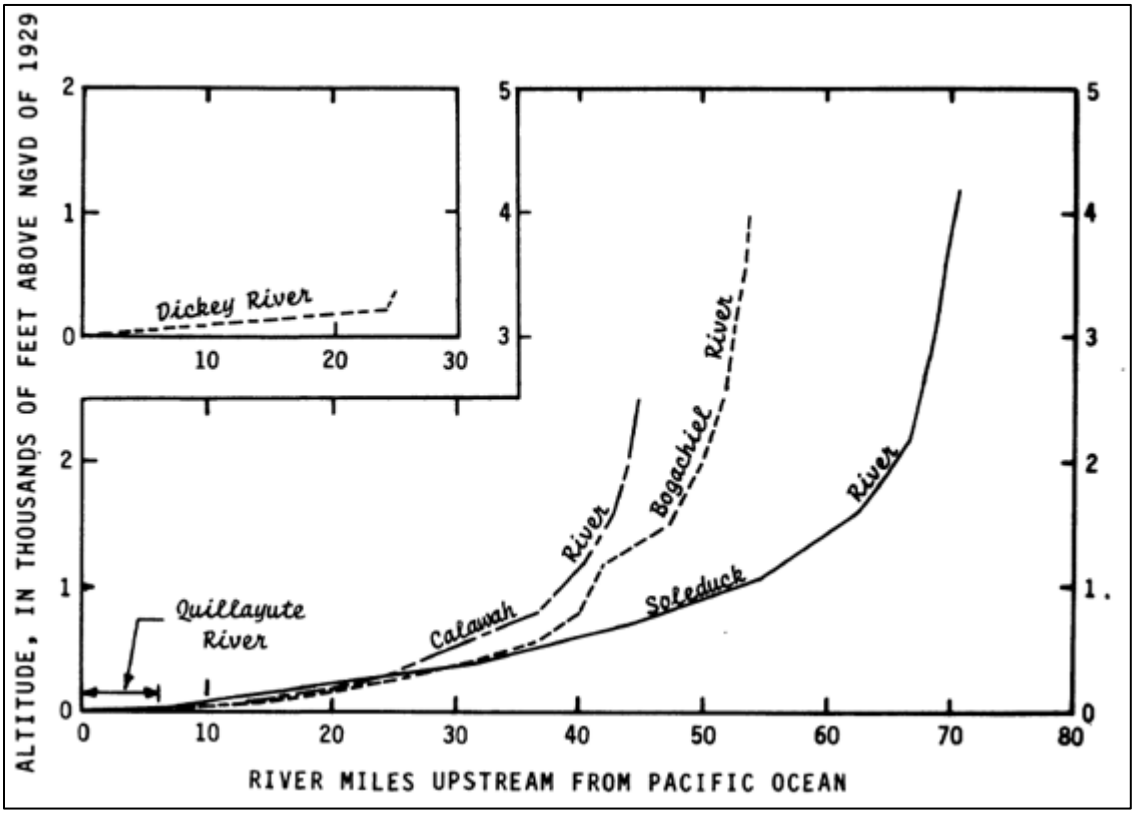

Source: Leonard (1982)

Figure 2-2. Profiles of the Quillayute River and Major Named Tributaries

The USGS developed StreamStats, a Web application that provides access to an assortment of Geographic Information Systems (GIS) analytical tools that are useful for water-resources planning and management, and for engineering and design purposes (USGS 2019). The map-based user interface can be used to delineate drainage areas for user-selected sites on streams, and then get basin characteristics and estimates of flow statistics for the selected sites anywhere this functionality is available. StreamStats users also can select the locations of USGS data-collection stations and get flow statistics and other information for the stations.

Based on StreamStats (USGS 2019), the Quillayute River drainage is approximately 627 square miles. Most of the drainage area lies in the major named tributaries watersheds. Table 2-1 provides the primary characteristics of the drainage.

Table 2-1. River Characteristics

Rivers	Drainage Area (square miles)	Average Slope (Percent)	Average Annual Rainfall (inches)
Dickey River	105	13.9	108
Sol Duc River	225	35.4	115
Bogachiel River	289	38.4	131
Quillayute River	627[1/]	32.8	121

1/ A small portion of the drainage area lies in the contributing area between the confluence of the Sol Duc and Bogachiel rivers and the mouth of the Quillayute River in La Push. This table provides the primary characteristics of the major named rivers.

2.2 CLIMATE

Average annual precipitation varies throughout the Quillayute River drainage as well as with elevation and proximity to the crest of the Olympic Mountains. Annual precipitation in the drainage ranges from 105 inches near the coast to 140 inches in the headwaters (Fretwell 1984) with most of the precipitation occurring in fall and winter. The upper elevations are characterized by heavy precipitation, with snow accumulation in winter months.

NOAA details the climate of the Quillayute River drainage. The area falls within the West Olympic-Coastal climate region for western Washington (NOAA 2019). The region includes the Olympic Mountains, which are part of the Coastal Range extending from the Columbia River to the Strait of Juan de Fuca. This area receives the full force of storms moving inland from the ocean. Therefore, heavy precipitation and gale force winds occur frequently during the winter season.

Seasonal snowfall in the lower elevations ranges from 10 to 30 inches and between 250 and 500 inches in the higher elevations during the winter. In the lower elevations, snow melts rapidly and depths rarely exceed 6 to 15 inches. During the mid-winter months, the snow line in the Olympic Mountains is between 1,500 and 3,000 feet above sea level.

The average maximum temperature in July along the coast is near 70 degrees Fahrenheit (°F) and in the foothills is near 75°F, while minimum temperatures are near 50°F. In winter, the warmer areas are near the coast. The maximum temperatures in January range from 43° to 48°F and the minimum temperatures range from 32° to 38°F.

Unlike many other large rivers of the Olympic Peninsula, the headwaters of the Bogachiel River and other Quillayute River tributaries are not glacier-fed. As a result, they do not experience a spring and summer flood pulse (Wikipedia 2019).

Areas along the southwestern and western slopes of the Olympic Mountains receive the heaviest precipitation in the continental United States. The annual precipitation ranges from 70 to 100 inches over the coastal plains and up to 150 inches on the windward slopes of the mountains. The

Bogachiel Rainforest is one of four rainforest areas in the Olympic National Park. The Bogachiel Rainforest is just south of Forks and gets about 14 feet of rain annually (Outdoor Society 2019).

2.3 STREAMFLOW

Streamflow in the Quillayute River drainage is not artificially stored or diverted and, except for snowmelt in the higher elevations, is primarily influenced by precipitation. Streamflow reflects precipitation levels gradually increasing above base flow with fall and winter rains from September through February, decreasing from February to May, and continuing to decrease to a groundwater discharge regime from June to early September (Leonard 1982).

2.3.1 Mean Annual Streamflow

In general, the highest monthly flows occurring in the winter are about 10 times as great as the lowest monthly flows occurring in the summer. The exception is the Dickey River where the highest monthly flows are about 20 times greater than the lowest monthly flows. Annual mean discharges may vary greatly from year to year, ranging from about 0.5 to 1.5 times the mean annual flow at a gaging station (Leonard 1982). Table 2-2 reports the mean annual flow at gaging stations (Figure 2-3) in the Quillayute River drainage as reported by Leonard (1982).

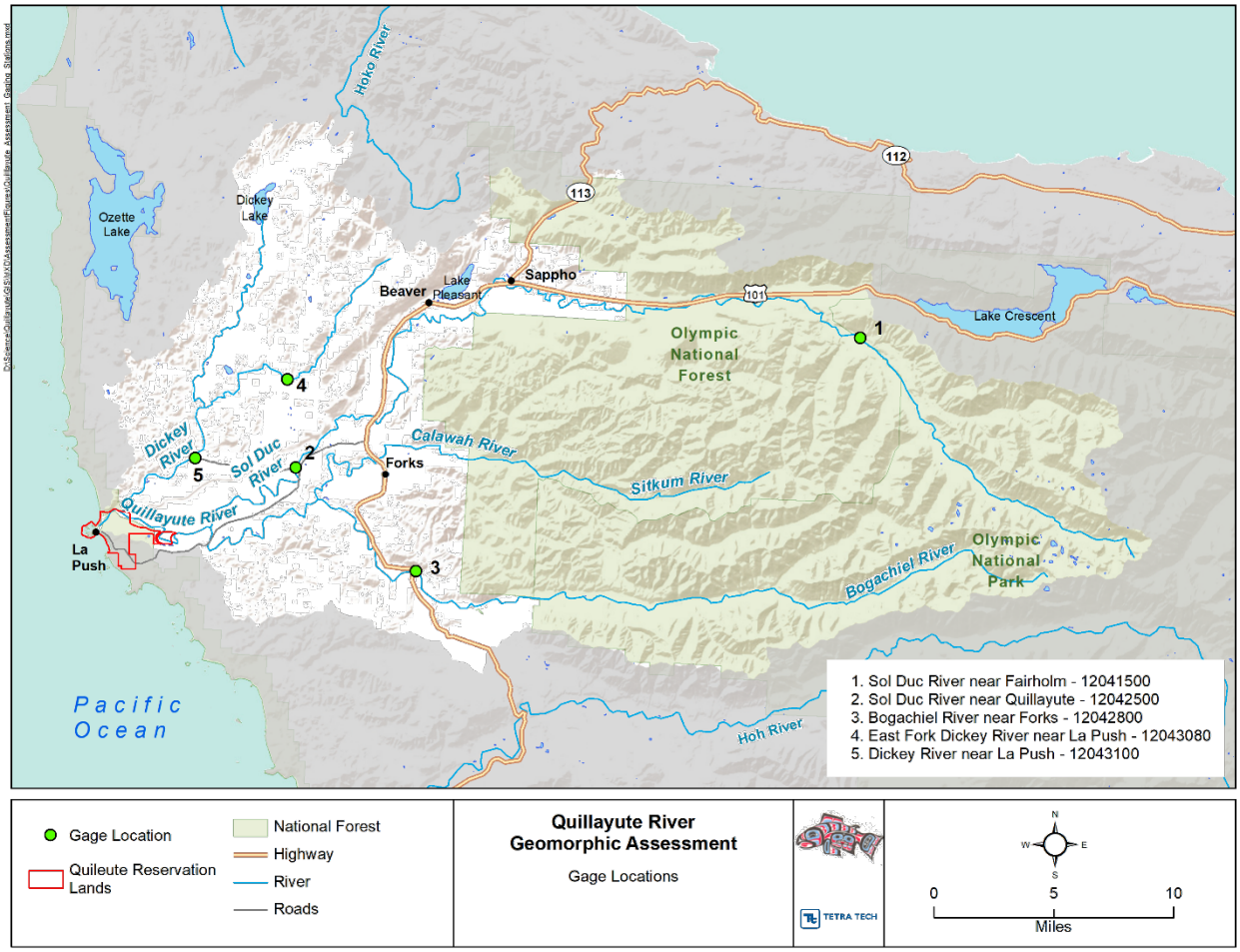

Figure 2-3. Quillayute River Gage Locations

Table 2-2. Mean Annual Streamflow

Gaging Station	Location	Mean Annual Flow (cfs)
12041500	Sol Duc River near Fairholm	621
12042500	Sol Duc River near Quillayute	1,301
12042800	Bogachiel River near Forks	1,061
12043080	East Fork Dickey River near La Push	281
12043100	Dickey River near La Push	528

Source: Leonard 1982
cfs – cubic feet per second

2.3.2 Peak Streamflow

An investigation (Mastin et al. 2016) into the magnitude and frequency of floods in Washington State computed the annual exceedance probability (AEP) statistics for 649 USGS unregulated stream gages in and near the borders of Washington using recorded annual peak flows through the water year 2014. Multivariate regression analysis and the AEP statistics at long-term unregulated and un-urbanized stream gages were used to develop equations to estimate AEP statistics at ungaged

basins. Washington was divided into four regions to improve the accuracy of the regression equations. The Quillayute River drainage falls within Region 4. The pseudo-coefficient of determination (where a value of 100 signifies a perfect regression model) is 95.44 for Region 4. The USGS StreamStats peak streamflow statistics for Washington are based upon this investigation (USGS 2019). Table 2-3 provides the AEP statistics for the Quillayute River and major tributaries.

Table 2-3. USGS StreamStats Peak Streamflow

Recurrence Intervals	Peak Streamflow (cfs)			
	Quillayute River	Dickey River	Sol Duc River	Bogachiel River
2-year	41,500	6,560	14,700	24,200
5-year	56,800	9,300	20,500	32,100
10-year	68,700	11,400	25,000	38,300
25-year	82,400	13,900	30,100	45,100
50-year	93,300	15,900	34,300	50,500
100-year	105,000	18,000	38,700	56,400
200-year	113,000	19,600	41,900	60,300
500-year	131,000	22,800	48,500	69,000

cfs – cubic feet per second

Additional peak streamflow data sets were reviewed for comparison. For example, the USGS developed a streamflow and sediment transport study of the Quillayute River that included a hydrologic analysis to establish peak discharge of selected frequencies (10-, 50-, and 100-year) at gaging stations on streams throughout Clallam County (Leonard 1982). The results of the analysis are tabulated in Table 2-4. The 25-year recurrence interval was calculated based on the 10-, 50-, and 100-year logarithmic trendlines for each river.

Table 2-4. USGS (Leonard 1982) Peak Streamflow

Recurrence Intervals	Peak Streamflow (cfs)			
	Quillayute River	Dickey River	Sol Duc River	Bogachiel River
10-year	78,900	14,300	28,900	42,200
25-year[1/]	94,589	17,613	35,194	50,846
50-year	106,000	20,000	39,700	56,600
100-year	119,000	22,800	45,100	63,600

cfs – cubic feet per second
1/ The 25-year recurrence interval was calculated based on the 10-, 50-, and 100-year logarithmic trendlines for each river.

Utilizing the Hydraulic Engineering Center's (HEC) Statistical Software Package (SSP), a Bulletin 17C Flood Flow Frequency analysis (England et al. 2019) was performed for gaging stations on the Dickey, Sol Duc, and Bogachiel rivers (see Figure 2-3). Results of the Bulletin 17C Flood Flow Frequency analysis are tabulated in Table 2-5.

Table 2-5. HEC-SSP Bulletin 17C Peak Streamflow

Recurrence Intervals	Peak Flood Flows (cfs)		
	Dickey River (USGS 12043100)	Sol Duc River (USGS 12042500)	Bogachiel River (USGS 12042800)
2-year	8,112	19,870	16,004
5-year	11,070	30,024	23,841
10-year	13,258	35,360	29,150
25-year	16,295	40,659	35,924
50-year	18,764	43,740	40,993
100-year	21,416	46,230	46,070
200-year	24,278	48,257	51,183
500-year	28,427	50,381	58,024

cfs – cubic feet per second

In performing the Bulletin 17C Flood Flow Frequency analysis, the number of annual peak streamflow records at each gaging station for each river varied. The Sol Duc River had only 3 years of record, while the Bogachiel River only had 5 years of record. Therefore, it was determined that Bulletin 17C results for the Sol Duc and Bogachiel rivers would not be utilized in the comparison of the peak streamflows due to the lack of annual peak streamflow records at the gaging stations. However, the Dickey River had 18 years of annual peak streamflow records. Comparison results for the selected peak streamflows for the Dickey River are tabulated in Table 2-6.

Table 2-6. Peak Streamflow Comparison

Recurrence Intervals	Dickey River[1/] Peak Streamflow (cfs)		
	USGS StreamStats	Leonard (1982)	Bulletin 17C
10-year	11,400	14,300	13,258
25-year	13,900	17,613[2/]	16,295
50-year	15,900	20,000	18,764
100-year	18,000	22,800	21,416

cfs – cubic feet per second
1/ USGS Gage 12043100
2/ Calculated based on logarithmic trendline of the 10-, 50-, and 100-year peak streamflow values

Results reported in Table 2-6 indicate that USGS StreamStats (USGS 2019) may be under-predicting peak streamflow versus Leonard (1982) and Bulletic 17C peak streamflows. In contrast, peak streamflows reported by Leonard (1982) and the Bulletin 17C streamflow values for the Dickey River match more closely. Based on the peak streamflow comparison (Table 2-6) between the Bulletin 17C analysis and the Leonard (1982) peak streamflow values for the Dickey River, the results favor utilizing the peak streamflow values published by Leonard (1982) because they provide an engineering conservative approach to peak streamflow. Therefore, and to remain consistent, peak streamflows published by Leonard (1982) for the Dickey, Sol Duc, and Bogachiel Rivers were used in the hydraulic model unsteady flow simulations to evaluate peak streamflow for the Quillayute River.

2.3.3 Low-Flow Characteristics

In addition to evaluating mean annual streamflow and peak streamflow, low-flow characteristics were determined to evaluate potential fish passage conditions in the Quillayute River. The high fish passage flow was taken as the mean annual streamflows identified in Table 2-2 for each of the rivers. To calculate the low fish passage flows, low-flow statistics were utilized to determine the 7-day 10-year flow, defined as the lowest average streamflow for a consecutive 7-day period that recurs on average once every 10 years (Curran et al. 2012). The high and low fish passage flows are reported in Table 2-7.

Table 2-7. Low-Flow Characteristics

Characteristics	Streamflow (cfs)			
	Quillayute River	Dickey River	Sol Duc River	Bogachiel River
Mean Annual Streamflow (High Fish Passage Design Flow)	2,890[1/]	528	1,301	1,061
7-Day 10-Year (Low Fish Passage Design Flow)	423[1/]	56	142	225

cfs – cubic feet per second
1/ Summation of the Dickey, Sol Duc, and Bogachiel Rivers.

2.4 WATER LEVELS AT THE RIVER MOUTH

The Quillayute River discharges into the Pacific Ocean near La Push, Washington. Tides have a direct influence on the flows in the river due to the varying backwater effects that the tides exert on the river. The tidal variation at the river mouth consists of predictable astronomical tides and episodic storm effects. Astronomical tides are those that are only influenced by the relative positions of the earth, sun, and moon. Storm effects can include surge and drawdown where winds and atmospheric pressure changes can cause increases or decreases in the water levels as predicted by astronomical tides.

In addition to the short-term water level changes due to tides and storms, there are seasonal and long-term water level changes that need to be considered. There is a seasonal change in mean sea level along the coast that results in a measurable difference in summer and winter mean sea level. There are also the long-term changes related to sea level rise and uplift/subsidence of the earth's crust. These water level changes were evaluated, and recommended values of these changes are provided for use as hydraulic model inputs.

2.4.1 Astronomical Tide Levels

The NOS and NOAA maintain a tide gage station (NOS 9442396) (NOAA 2019) at the La Push marina near the confluence of the Quillayute River with the Pacific Ocean. The station has been in place since 1924; however, detailed water level records are only available for the site from 2002 to the present. Figure 2-4 shows the location of the tide station, and Figure 2-5 shows tidal and geodetic datum levels for this station.

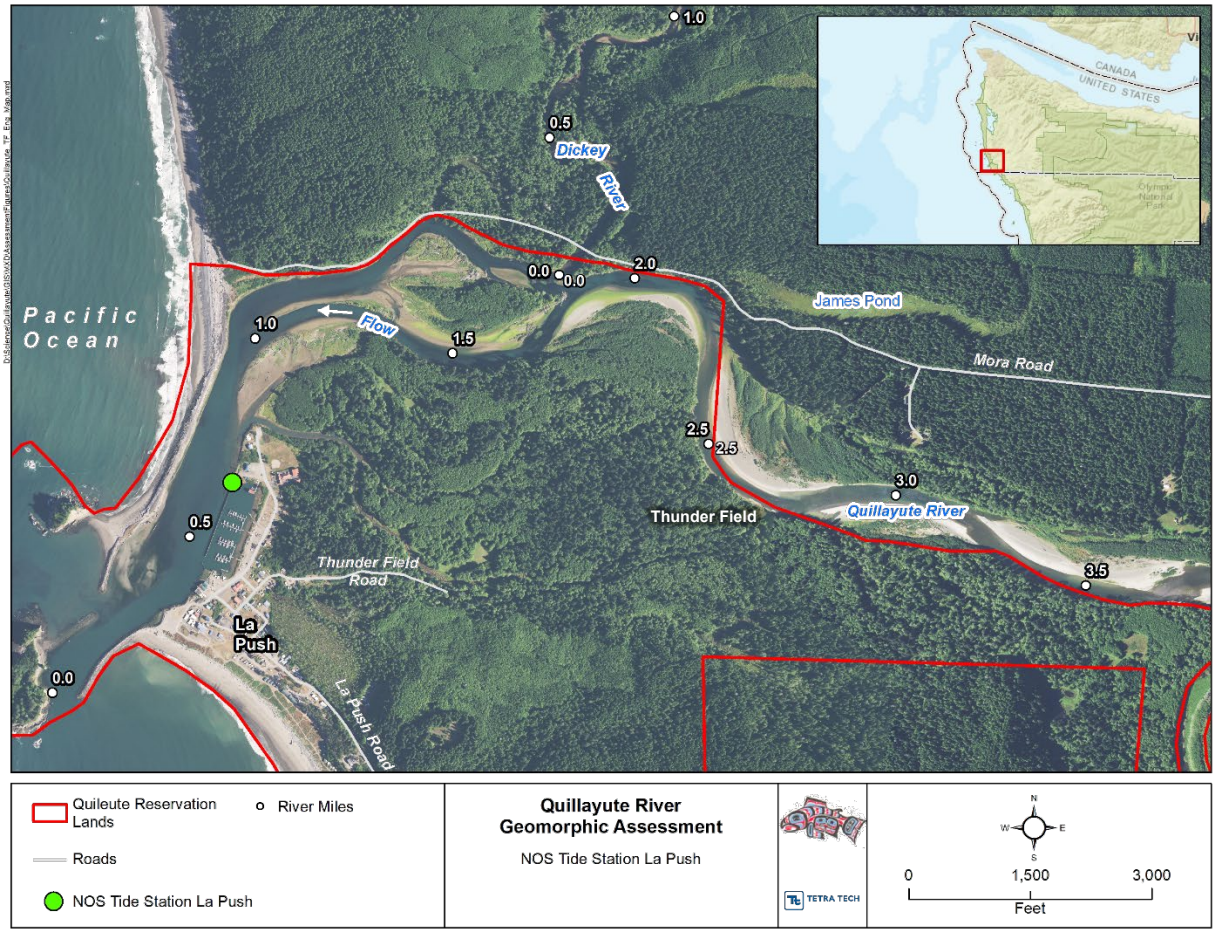

Figure 2-4. NOS 9442396 Tide Station La Push

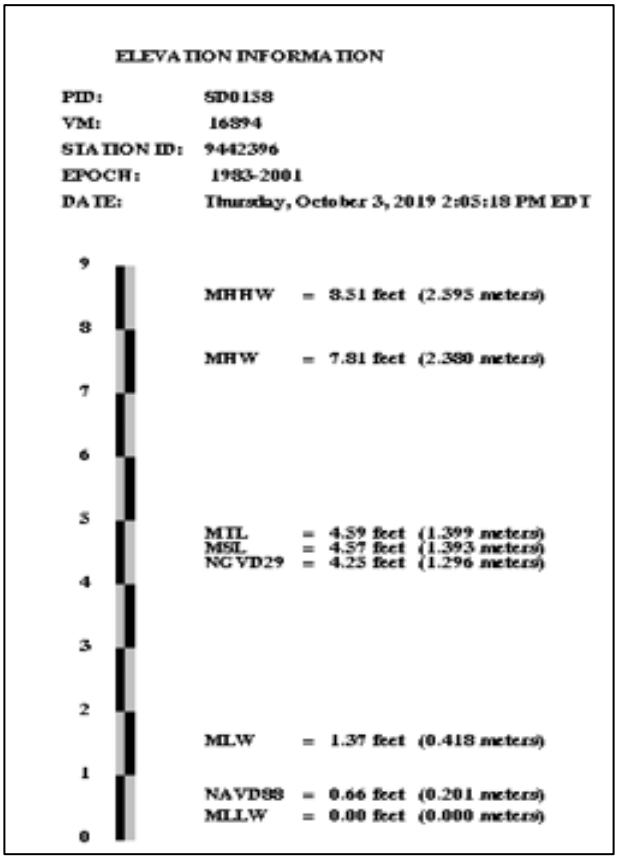

Figure 2-5. Tidal and Geodetic Datum Levels at NOS Station La Push[1/]

1/ The NAVD 88 and the NGVD 29 elevations related to MLLW were computed from Benchmark, 944 2396 TIDAL 7, at the station. Displayed tidal datums are Mean Higher High Water (MHHW), Mean High Water (MHW), Mean Tide Level (MTL), Mean Sea Level (MSL), Mean Low Water (MLW), and Mean Lower Low Water (MLLW) referenced on 1983-2001 Epoch. Elevations of datums referred to Mean Lower Low Water (MLLW).

The tide is semi-diurnal with two high and two low tides per day. The tide range at the site is +8.51 feet. Mean higher high water (MHHW) is at elevation +7.85 feet North American Vertical Datum 1988 (NAVD 88) and mean lower low water (MLLW) is at elevation -0.66 feet NAVD 88.

2.4.2 Extent of Tidal Influence

The tidal level at the Quillayute River mouth varies by 8.51 feet. Therefore, the lower portions of the mainstem Quillayute River experience substantial tidal influence. To determine the extent of tidal influence on the Quillayute River, wetlands associated with the estuary were evaluated and contributions for tidal changes were analyzed.

The Pacific Marine and Estuarine Fish Habitat Partnership (PMEP) has developed GIS mapping of current and historical extents of tidal wetlands the Quillayute River estuary. Figure 2-6 shows the tidal wetland limits. The mapping includes areas currently inundated by the tides ("current tidal wetlands") from the ocean to the head of tide, including the freshwater tidal zone. To assist restoration planning, the mapping also includes areas that were historically inundated by the dikes and tide gates ("historical tidal wetlands"). Although the mapping does not yet distinguish current from historical (disconnected) tidal wetlands, a future mapping phase will provide this information (PMEP 2019).

Figure 2-6. Present and Historic Tidal Estuary Extents

In addition to tidal wetlands, an Oregon Climate Change Research Institute (OCCRI) report from 2019 assessed the relative contributions of the various processes that drive extreme coastal tide water levels, quantified the impact of a range of climate change scenarios on each of the drivers and on the resulting combined tide water levels, and assessed the impact of present-day and forecasted future coastal flooding events on infrastructure in several communities within the Treaty of Olympia area (Serafin et al. 2019). The report included results of a one-dimensional (1D) Hydraulic Engineering Center – River Analysis System (HEC-RAS) hydraulic hybrid model with compound flooding along the Quillayute River. The model was utilized to simulate streamflow with probabilistic simulations of co-occurring streamflow and tidal events. The probabilistic model allows for generation of multiple synthetic water level records to produce numerous estimates of low-probability events not captured in the observational record (Serafin et al. 2019). The model was developed to approximate the response of a HEC-RAS simulation at several transects for the 100-year recurrence interval. Results are presented in Table 2-8 for La Push and Thunder Field.

Table 2-8. OCCRI 1D HEC-RAS 100-Year Design Events

Statistic	Project Locations			
	La Push		Thunder Field[2/]	
	Quillayute Streamflow (cubic feet per second)	North Pacific Ocean Tide El. (feet[1/])	Quillayute Streamflow (cubic feet per second)	North Pacific Ocean Tide El. (feet[1/])
100-year (Avg. Max)	145,522	14.5	136,159	14.5
100-year (Avg. Mean)	108,582	13.4	121,650	11.7
100-year (Avg. Min)	64,026	12.2	111,490	6.6

1/ North American Vertical Datum of 1988
2/ Thunder Field is part of the Project and is a culturally important site along the left bank of the Quillayute River used for Tribal fishing access, ceremonies, and community access via Thunder Road (see Figure 2-3 for Thunder Field area).

The research published from OCCRI (Serafin et al. 2019) determined a statistical technique to estimate and approximate high-water levels at multiple locations along an ungaged river with co-occurring streamflow and tidal events. The OCCRI 100-year average mean Quillayute Streamflow and the North Pacific Ocean Tide Elevation results match up well with the peak streamflow values from the Leonard (1982) report and the high tide elevations listed in Table 2-9. However, the research used a 1D HEC-RAS model with limited geometric controls as a function of hydraulic characteristics between transects and may be considered overpredicting in certain areas. Therefore, the 1D HEC-RAS model used in the OCCRI research was not used for engineering design, and instead a two-dimensional (2D) hydraulic model specific to the Quillayute River was developed using the peak streamflow values from the Leonard (1982) report and tidal elevation values from the NOS 9442396 Tide Station and from the OCCRI (Serafin et al. 2019) research.

2.4.3 Storm Surge

Storm surge is the local change in elevation of the ocean along the shore due to a storm. The storm surge is measured by subtracting the astronomical tidal elevation from the total elevation. Figure 2-7 shows the predicted astronomical tide and the recorded water level for February 4, 2006 (NOAA 2019). The surge increased the predicted tide by about 3.7 feet to yield the highest recorded water level for the La Push station at 13.19 feet (MLLW) or 12.53 feet (NAVD 88).

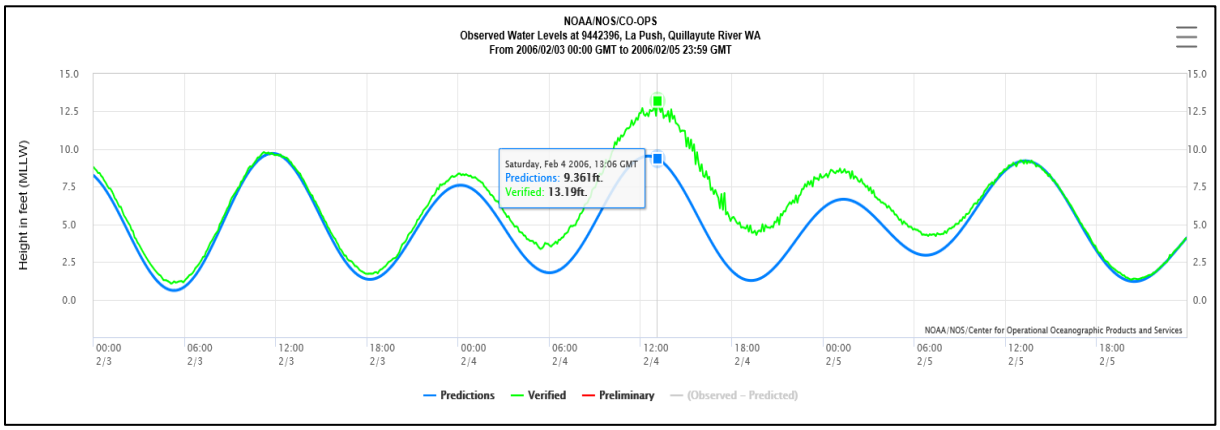

Source: NOAA Tides and Currents website (2019)

Figure 2-7. Water Levels at La Push on February 4, 2006

Table 2-9 lists the 10 highest and lowest water levels recorded at the La Push NOS tide station. Meteorological effects can also result in an actual water level that is less than the predicted astronomical tide. Low-water events in 2007 and 2008 suggest that persistent offshore winds may have contributed to significant dropping of coastal water elevations lasting at least one day. Also of note is a difference between the highest tide value for February 4, 2006, shown in Figure 2-7 versus that shown in Table 2-9. Verified water levels are made at a high frequency and the variations are apparent in the plot as seen in Figure 2-7. However, tide values are recorded with dampeners to minimize high-frequency variations as reflected in Table 2-9.

Table 2-9. Highest and Lowest Tides, Station 9442396, La Push, Quillayute River, WA

Rank	Highest Tide, feet MLLW	Date/Time, GMT	Lowest Tide, feet MLLW	Date/Time GMT
1	12.70	4 Feb 2006/13:00	-3.59	7 May 2008/15:48
2	12.66	6 Nov 2006/20:12	-3.50	6 May 2008/ 14:54
3	12.54	23 Nov 2011/17:54	-3.38	23 Jun 2009/14:42
4	12.47	24 Nov 2011/18:54	-3.37	25 May 2009/14:54
5	12.46	10 Mar 2016/09:18	-3.36	28 Oct 2007/03:12
6	12.33	1 Jan 2006/20:36	-3.35	17 May 2007/14:42
7	12.33	20 Dec 2018/18:24	-3.34	18 May 2007/15:24
8	12.14	10 Dec 2015/19:00	-3.32	13 Jul 2018/14:30
9	12.06	31 Dec 2005/19:36	-3.32	26 Nov 2007/03:06
10	11.85	10 Mar 2016/21:18	-3.30	24 Jun 2017/14:30

Source: NOAA Tides and Currents Website (2019)

Based on the records for the La Push NOS tidal station, it appears the storm surge resulting from onshore wind conditions may contribute to an increase of up to 4.2 feet above MHHW. In contrast, offshore winds may contribute to a decrease of the coastal water levels up to 3.6 feet below MLLW.

As noted in previous sections, storms typically bring strong winds and heavy rainfall to the Assessment Area.[2] Therefore, hydraulic analysis must consider the coincident occurrence of storm surge with high streamflow for the maximum flooding conditions. In addition, high streamflows should be considered together with low tide levels to evaluate high-velocity flow conditions that might contribute to erosion and deposition along the Quillayute River.

2.4.4 Seasonal Variation in Mean Sea Level

Mean wintertime sea levels are 20 inches (1.67 feet) higher than summertime sea levels along Washington State's coasts and estuaries (Mote et al. 2008). This seasonal sea level variation is driven by the strong northward wind along the Washington coast during winter. This variation combines with the effects of the earth's rotation to push ocean water toward shore, thus elevating sea levels. Since the tidal datums presented in Figure 2-5 are based on a 19-year period of water level measurements that include both winter and summer conditions, this analysis approximates a seasonal wintertime sea level increase of half, or 10 inches (0.84 feet), above the NOAA tidal datums for use in hydraulic model inputs. As noted in the previous section, winter season values should apply for hydraulic model inputs because winter storms result in both storm surge and high precipitation conditions.

2.4.5 Relative Sea Level Rise

Relative sea level (RSL) is the net change resulting from vertical land movements and sea level rise. The Washington State Coastal Resiliency Project (Miller et al. 2018) completed RSL evaluations for 171 locations on the coast. The vertical land movement in the Assessment Area is relatively small at +0.2 feet to +/- 0.3 feet per century. The study completed RSL rise projections for two different representative carbon dioxide (CO_2) concentration pathways climate change scenarios. A representative concentration pathway (RCP) is a scenario of long-term global emission of greenhouse gases, short-lived species, and land-use cover that stabilizes radiative forcing at a specified level of watts per square meter. The two RCP scenarios used are RCP 4.5 and RCP 8.5. Figure 2-8 shows the probabilities of exceedance of various levels of sea level rise at time increments from the present to 2150 under RCP 8.5 conditions. The design values recommended for the Assessment Area hydraulic modeling are based upon RCP 8.5 and are as follows:

a) 2050: +0.6 feet (50% probability of exceedance)

b) 2100: +1.9 feet (50% probability of exceedance)

[2] The Assessment Area is the extent to which the geomorphic analyses were performed for the Quillayute River Geomorphic Assessment (Assessment). The Assessment Area includes the entire Quillayute River from the mouth at La Push to the confluence with the Sol Duc and Bogachiel rivers, as well as the Sol Duc River to RM 7.0, the Bogachiel River to RM 6.0, and the Dickey River to RM 1.0.

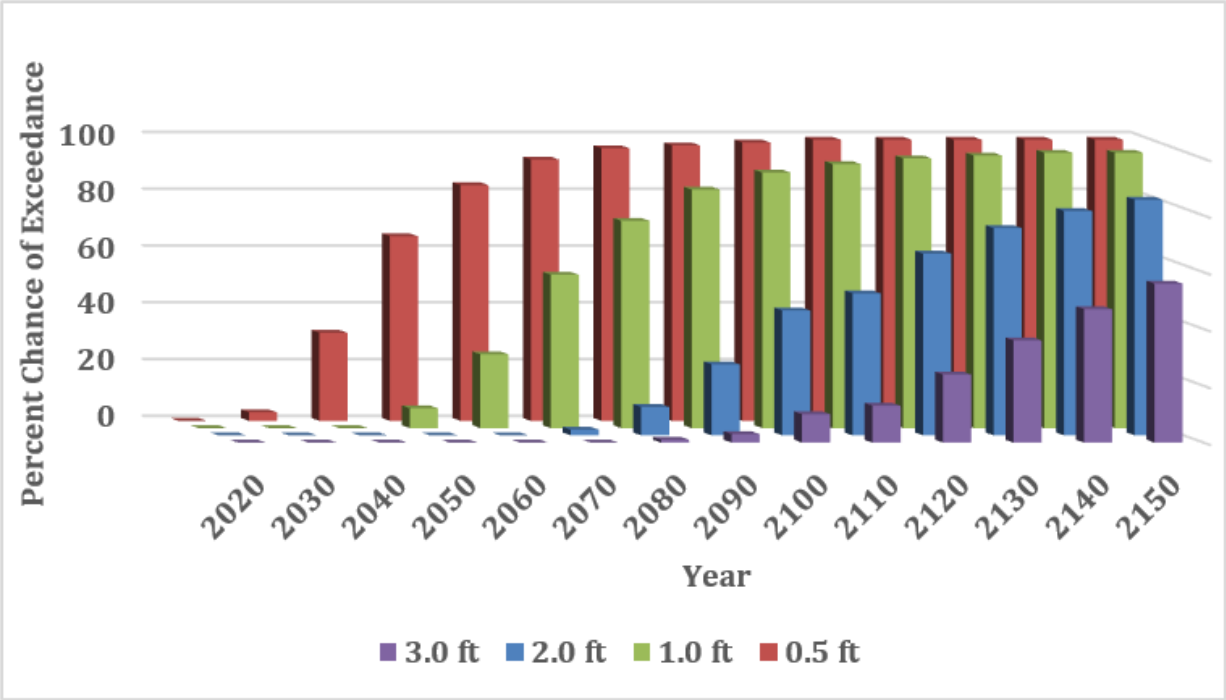

Source: Miller et al. 2018

Figure 2-8. Relative Sea Level Rise for the Assessment Area under RCP 8.5

Parts of the Washington coast may be subject to vertical land level change in the event of a subduction zone earthquake. If a subduction zone earthquake does occur, the Assessment Area may be subject to a significant vertical land level change of -1.3 feet to -5.5 feet based on the predictions of multiple seismic deformation models. Negative values have the effect of raising the local RSL (Miller et al. 2018).

2.4.6 Coastal Flooding

The Federal Emergency Management Agency (FEMA) has developed a Flood Insurance Rate Map (FIRM) for Clallam County (FEMA 1983). The Flood Insurance Study (FEMA 2001) was revised in 2001 (Figure 2-9). The Quileute Indian Reservation is not included in the flood insurance study or FIRM. Methods used to evaluate flood risks in the balance of the general vicinity of the Assessment Area deemed the area to have low development potential or minimal flood risk. As a result, only very limited flood data are available. The flood mapping does not provide elevations for the base flood (100-year mean recurrence interval) and only nominal limits of the areas flooded under base flood conditions are mapped.

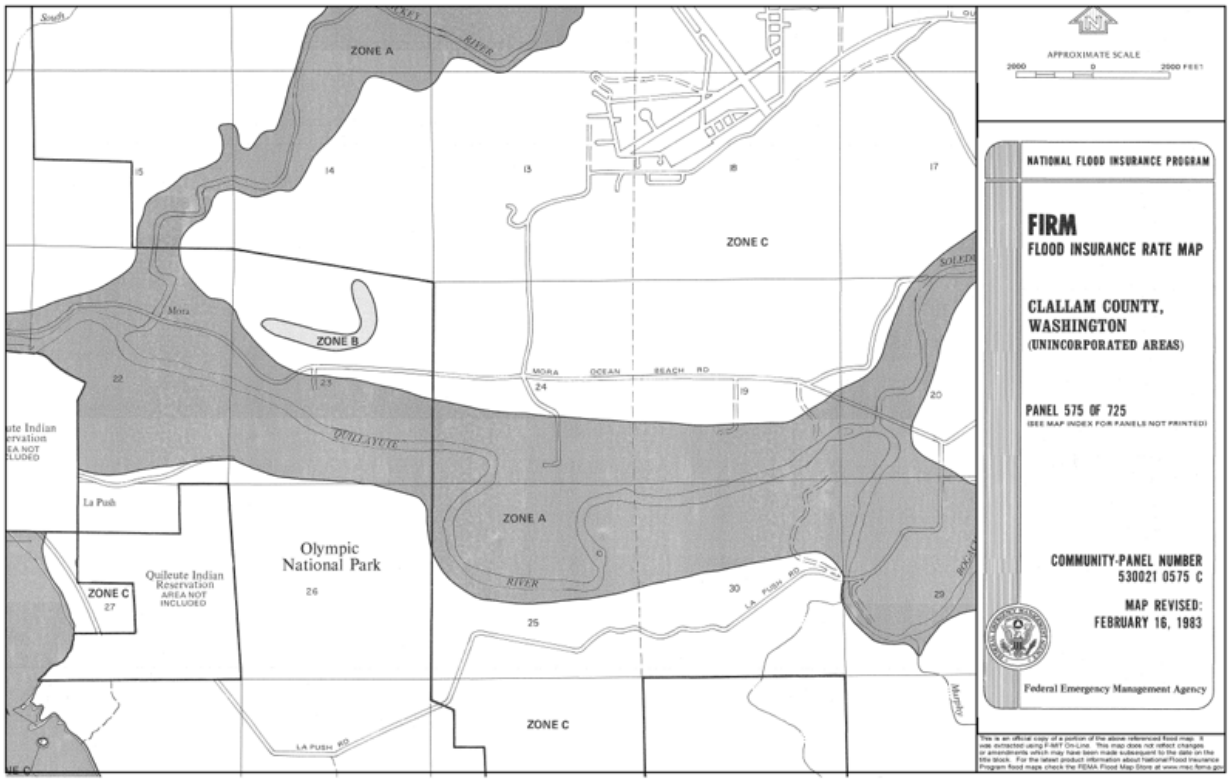

Figure 2-9. FEMA Flood Map for the Lower Quillayute River

2.4.7 Tsunami Flooding

Tsunami inundation mapping is based on multiple simulations of a 9.1 magnitude earthquake on the Cascadia subduction zone. Figure 2-10 shows the tsunami inundation extents in the La Push area. The nominal inundation limits are roughly similar to the base flood limits in the lower Quillayute River as shown on the FEMA FIRM in Figure 2-9.

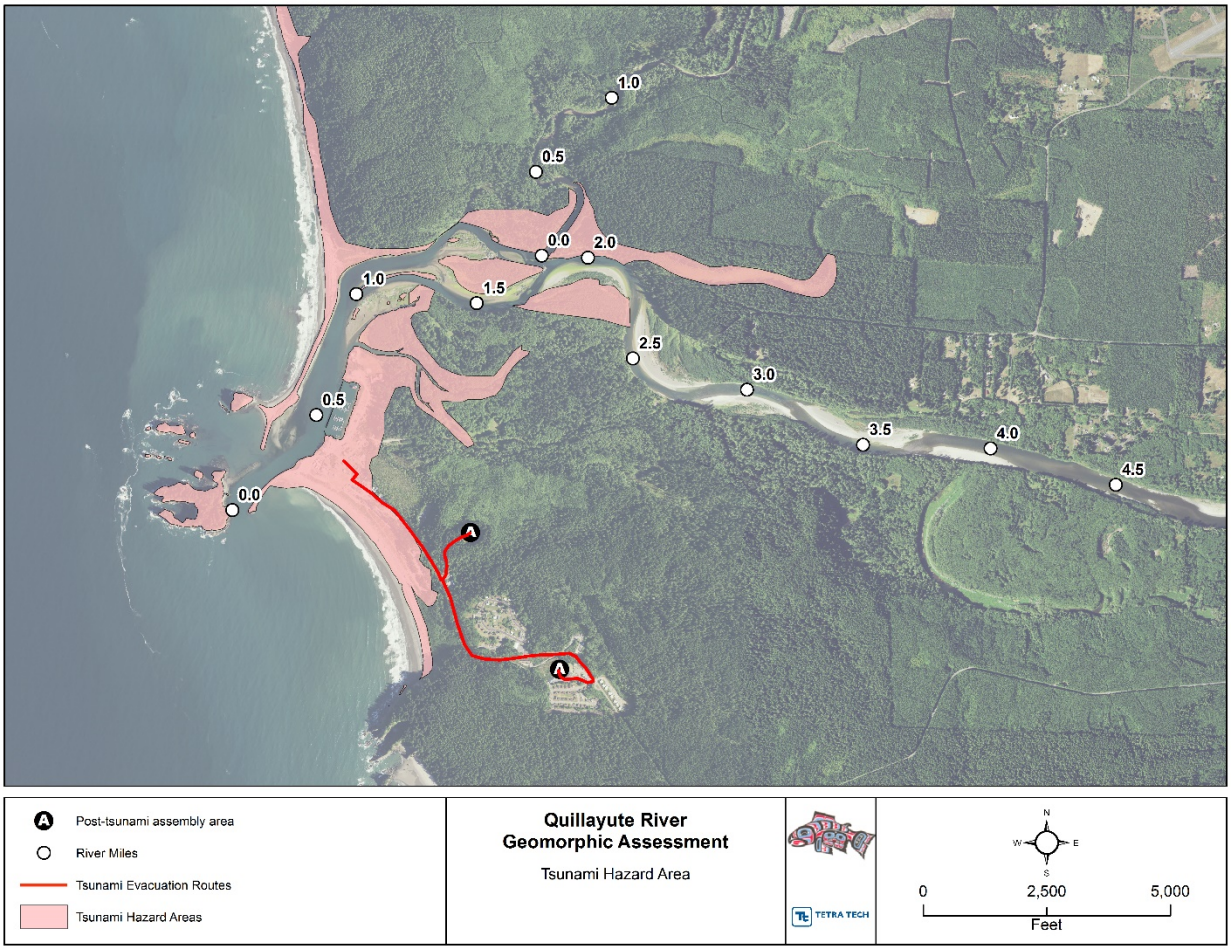

Figure 2-10. Tsunami Inundation Limits, Quillayute River Area

Figure 2-11 shows the simulated time history of the resulting tsunami waves in open water. The simulation was run at a mean tide level of +4 feet. With a peak wave height of +9 feet, the resulting water level is roughly comparable to the highest storm surge level shown in Figure 2-7.

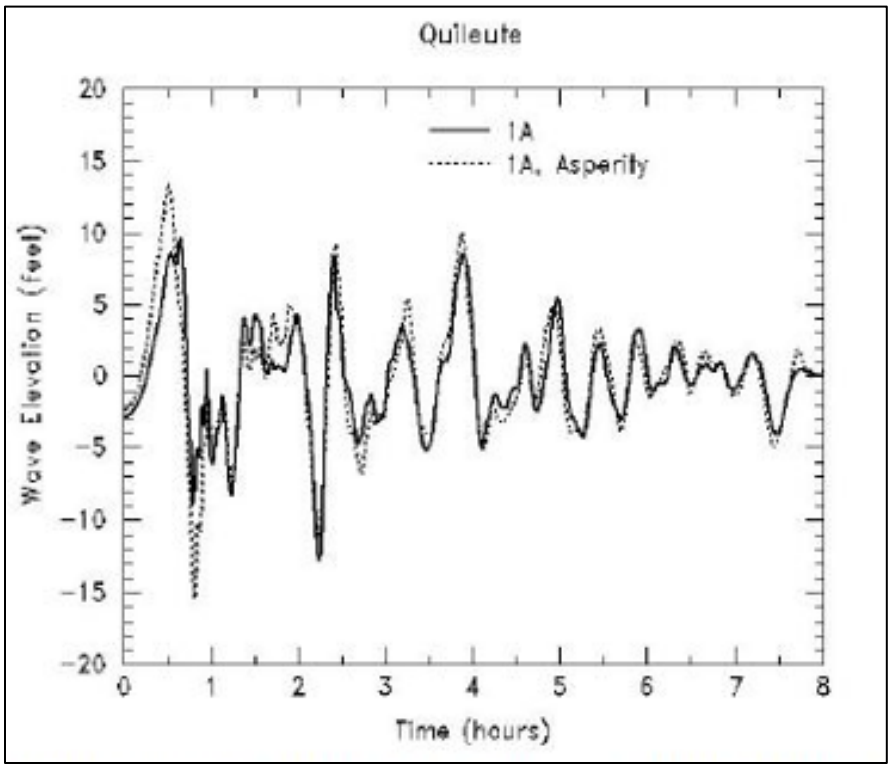

Source: Walsh et al. 2003

Figure 2-11. Tsunami Wave Height History

3 HYDRAULIC ANALYSIS

The streamflow values (see Section 2.3) and tidal stages (see Section 2.4) determined from the hydrologic analysis were used in the hydraulic analyses of flow conditions within the Quillayute River channel and floodplain. Utilizing the results from the hydrologic analysis discussed in Sections 2.3 and 2.4, a 2D hydraulic model was developed for the 1-year and 100-year recurrence intervals and tidal stages. Once the 2D model was developed, the model was calibrated, and the results validated.

3.1 HYDRAULIC MODELING

The 2D hydraulic model entailed utilizing GeoHECRAS version 2.7 coupled with Civil 3D 2018 as the primary software applications. GeoHECRAS combines GIS and HEC-RAS version 5.0.7 software into one user interface, while Civil 3D was used as the main engine behind surface terrain generation. In addition to utilizing the hydrologic analysis results, the existing conditions terrain of the Quillayute River channel and floodplain was integrated into the 2D hydraulic model. Once all data inputs (i.e., hydrologic analysis results, terrain, and land cover) had been compiled, the model was calibrated and validated to different flows and tidal stages across the Assessment Area

3.1.1 Terrain

The existing conditions modeling terrain was generated from the topobathymetric Light Detection and Ranging (LiDAR) survey data (see Appendix A of the Assessment) and combined with the United States Army Corps of Engineers (USACE) navigational channel bathymetric data (USACE 2019). The USACE (2019) data were used to supplement the results of the topobathymetric LiDAR where coverage was interrupted by high turbidity levels of the water in the lower portions of the Quillayute River. The combined data sets were used as the terrain component for the 2D modeling mesh. Breaklines were assigned for channel centerlines, banks, bars, and raised linear features (e.g., roads, terraces, embankments, etc.) to accurately define the mesh geometry. The cell spacing was set at 60 feet for the entire terrain and 30 feet for all breaklines. A total of 207 breaklines and 96,577 cells make up the 2D modeling mesh.

The land use for the model was based on aerial imagery and knowledge gained from field reconnaissance. The land use was delineated and assigned a Manning's n roughness value. Roughness values generally follow recommendations provided by Chow (1959) as well as professional experience and judgement. Based on the aerial map, a land cover file was generated for Manning's roughness values ranging from 0.015 to 0.1, representing forested, agriculture, and residential areas, roads and jetties, and channel, wetland, and brush areas. The roughness values used in the model are presented in Table 3-1.

Table 3-1 Manning's Roughness Values by Land Use

Land Use/Land Cover	Manning's n value
Forested	0.08
Channel	0.04
Wetland	0.04
Brush	0.06
Agriculture	0.045
Residential	0.1
Road	0.015
Jetty	0.055

3.1.2 Calibration

The USGS (Czuba et al. 2010) conducted a bathymetric and streamflow field study in support of a USACE effort to update a 2D hydrodynamic model of the Quillayute River. The 2D hydrodynamic modeling effort was focused on the design of repairs to the jetty that protects about a mile of the right bank of the Quillayute River near the mouth. The Czuba et al. (2010) report provides a longitudinal profile of the riverbed and the water surface elevation (WSE) for the 7-mile studies from the Bogachiel River gaging station to the mouth of the Quillayute River. Measurements of tributary streamflow for periods in April and May 2010 were also recorded. Streamflow in the Quillayute River ranged from 3,630 cfs to 7,800 cfs. The sum of the mean annual streamflow at five gaging stations in the Quillayute River drainage was 3,720 cfs (Czuba et al. 2010) at the time of the survey. Therefore, the 2010 streamflow measurements are roughly equivalent to the mean annual streamflow for the drainage. Based on this, the 2010 data served as a basis to calibrate the 2D hydraulic model developed for the Project for normal flow conditions within the drainage as described in the following sections.

3.1.2.1 Streamflow Measurements

As described above, the USGS collected a series of streamflow measurements on the Quillayute, Dickey, and Bogachiel rivers in April and May 2010 (Czuba et al. 2010). Figure 3-1 shows the location of the streamflow measurements. Table 3-2 provides the details of the streamflow measurements. These streamflow measures served as a basis to calibrate the 2D hydraulic model developed for the Project.

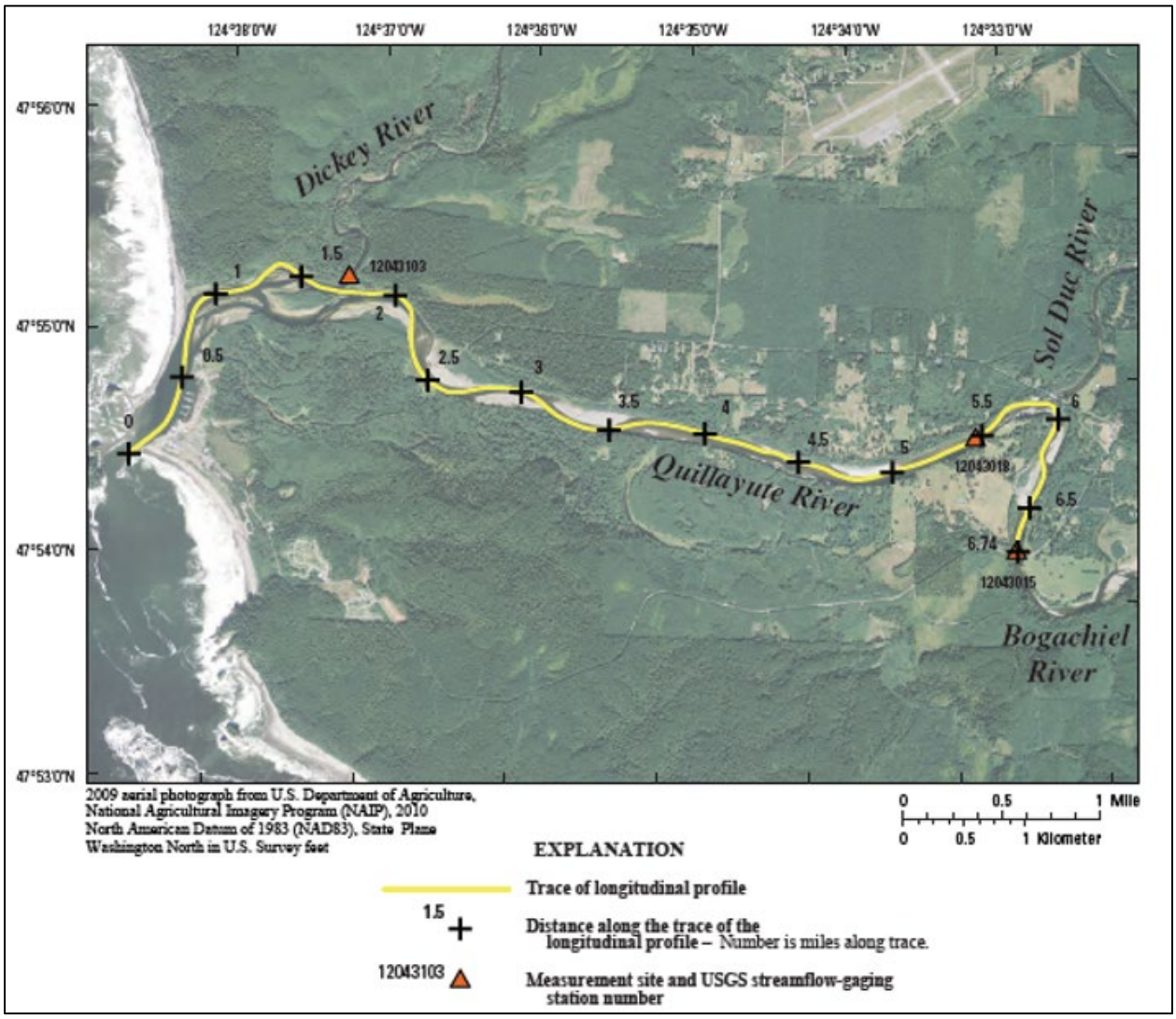

Figure 3-1. USGS Streamflow Measurement Locations

Table 3-2. USGS Streamflow Measurements

Location	Date	Time, PDT, 24:00	Streamflow (cfs)
Quillayute River, USGS gaging station 12043018	April 20, 2010	15:11-15:33	4,110
	April 21, 2010	09:28-09:38	3,830
		10:45-10:56	3,630
		15:02-15:13	3,780
	May 4, 2010	10:44-10:56	7,800
		16:18-16:27	7,310
	May 5, 2010	13:04-13:17	6,000
	May 6, 2010	13:19-13:29	4,830
Dickey River, USGS gaging station No. 12043103	April 20, 2010	08:31-09:31	317[1/]
		16:26-17:10	178[1/]
	April 21, 2010	07:56-08:36	396[1/]
		11:41-12:24	249[1/]
		16:43-17:01	193[1/]
Bogachiel River, USGS gaging station No. 12043015	May 6, 2010	13:58-14:13	3,250

cfs – cubic feet per second
1/ Streamflow was tidally influenced.

3.1.2.2 Bathymetric and Water Surface Elevation Profile

Figure 3-1 shows the RM distances measured from the mouth of the Quillayute River. Figure 3-2 is a longitudinal profile of the river reach and shows the WSE and river channel bottom as surveyed by the USGS on May 4-6, 2010 (Czuba et al. 2010).

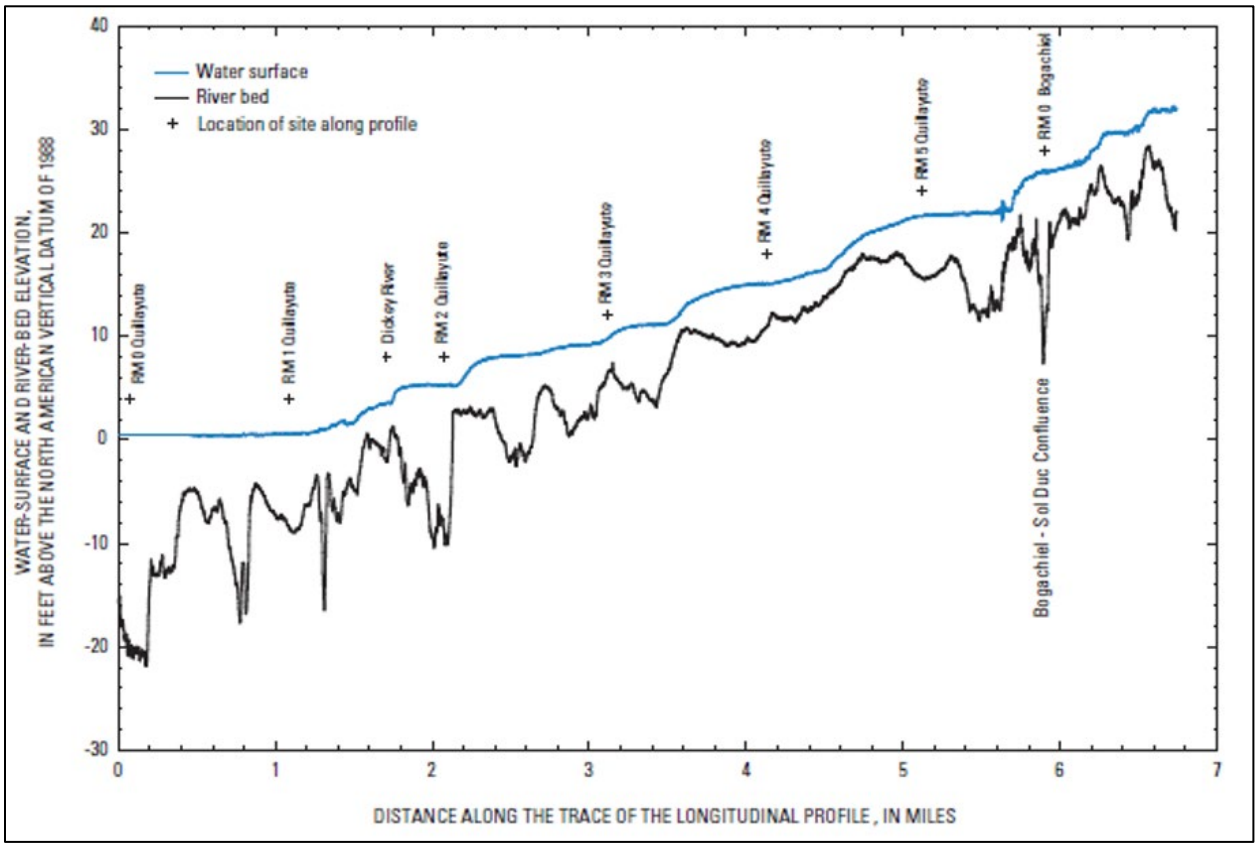

Figure 3-2. Longitudinal Profile of the Quillayute River – May 4-6, 2010

3.1.2.3 Evaluation

Figure 3-2 illustrates a WSE of approximately 22 feet at RM 5.5 (USGS gaging station 12043018) on the Quillayute River during the May 4-6, 2010, flow measurement activities performed by USGS (Czuba et al. 2010). Calibration of the 2D hydraulic model completed for the Assessment Area consisted of utilizing the streamflow measurements on the Quillayute and Bogachiel rivers on May 6, 2010. The difference between the two flows was applied to the Sol Duc River so that the combined streamflows for the Bogachiel and Sol Duc rivers equaled 4,830 cfs, the measured streamflow on May 6, 2010 for the Quillayute River.

The May 6, 2010 measured streamflows were inserted into the model as the upstream boundary condition. The downstream boundary conditions were set to tide elevations of -0.66 feet NAVD 88 and 7.85 feet NAVD 88, MLLW and MHHW, respectively. The model calibration is primarily focused on the observed WSE at RM 5.5 (Quillayute River observation gage) approximately 2 miles upstream of tidal influence. Results of the model calibration are provided as Figure 3-3. Results of the model calibration simulation indicate a WSE of approximately 22 feet, equivalent to the streamflow measurement data collected by the USGS in 2010 (Czuba et al. 2010) as indicated by the arrow.

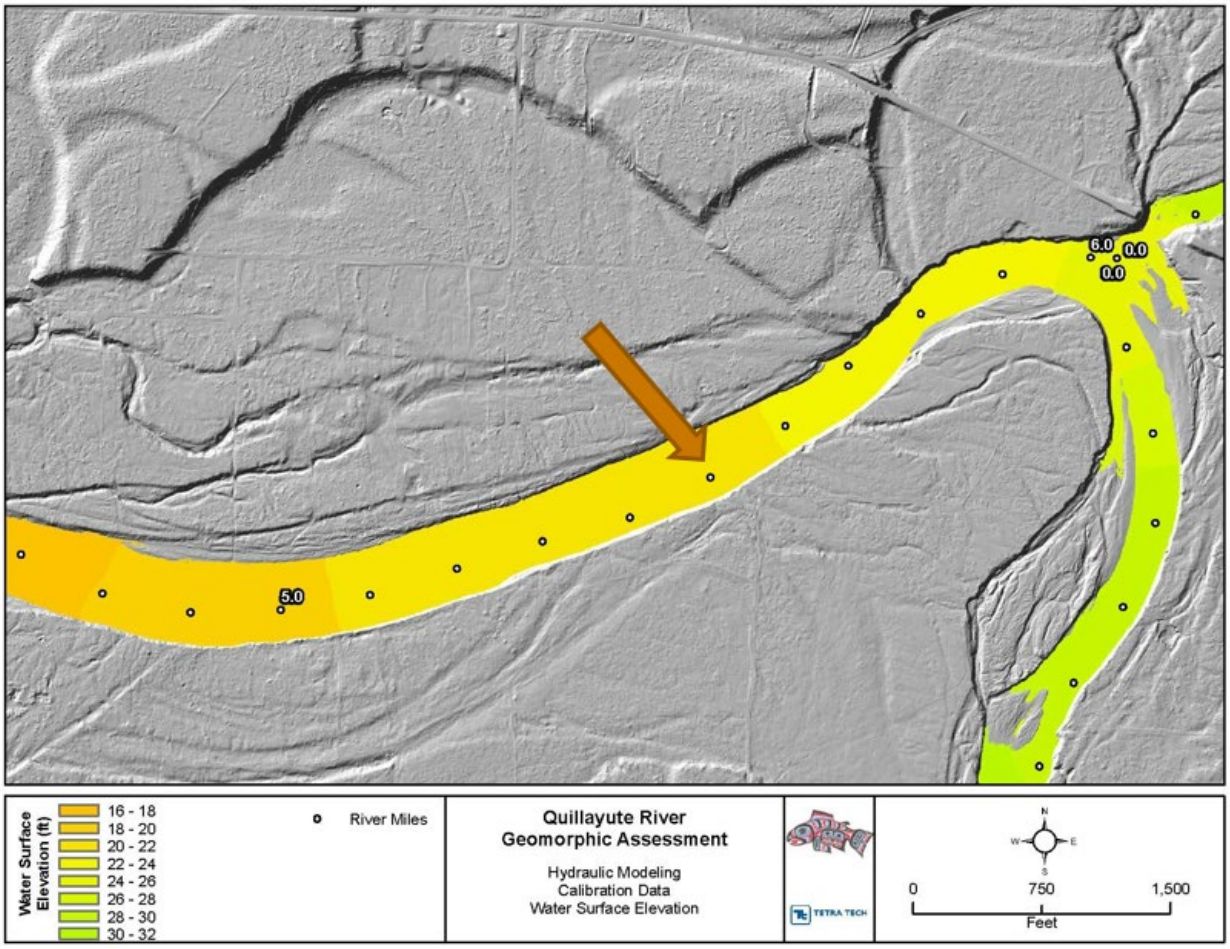

Figure 3-3. Hydraulic Model Calibration

3.1.3 Validation

Once the hydraulic model was calibrated, several unsteady flow analyses were performed utilizing the peak streamflow values from Leonard (1982), described in Section 2.3.2. To validate these peak streamflow values, historic events were investigated on the Bogachiel River, because the Bogachiel River watershed contains both a flow gage and a stage gage that could be used to match a flow event with an elevation. The validation process included the USGS 12043000 flow gage on the Calawah River and Station 12043015, the stage gage on the Bogachiel River.

The USGS gage 12043000 located on the Calawah River, a major tributary to the Bogachiel River, was identified to support model validation. This gage has recorded 42 years and counting of peak streamflow data, making it the prime contender for a Bulletin 17C Flood Flow Frequency analysis to determine peak streamflow on the Calawah River and identify a historic peak streamflow event that took place on the Calawah River that would influence the flows on the Bogachiel River. Results of the Bulletin 17C Flood Flow Frequency analysis are tabulated in Table 3-3.

Table 3-3. HEC-SSP Bulletin 17C Calawah River Peak Streamflow

Recurrence Intervals	Calawah River Peak Streamflow (cfs) USGS 12043000
2-year	21,204
5-year	28,301
10-year	32,657
25-year	37,825
50-year	41,462
100-year	44,939
200-year	48,294
500-year	52,585

cfs – cubic feet per second

On November 6, 2006, the Calawah River flow gage recorded a value of 38,100 cfs. Results of the Bulletin 17C Flood Flow Frequency analysis calculated a value of 37,825 cfs for the 25-year recurrence interval for the Calawah River (Table 3-3). Therefore, November 6, 2006, was identified as a historic 25-year peak streamflow event that could be used for model validation on the Bogachiel River. On the same day, USGS 12043015, the Bogachiel River stage gage just upstream from the Highway 110 bridge, recorded a stage WSE value of approximately 43 feet.

Utilizing the Leonard (1982) peak streamflow values (Section 2.3.2), a 25-year recurrence interval for the Bogachiel River was calculated as 50,846 cfs (see Table 2-4). Similarly, the 25-year recurrence intervals were calculated for the Sol Duc (35,194 cfs) and Dickey (17,613 cfs) rivers (Table 2-4). These 25-year peak streamflow values were routed through the 2D hydraulic model to compare the WSE results at the Bogachiel River gage location. Model results at the Bogachiel River gage location for the 25-year recurrence interval yielded a WSE of 45 feet, shown in Figure 3-4.

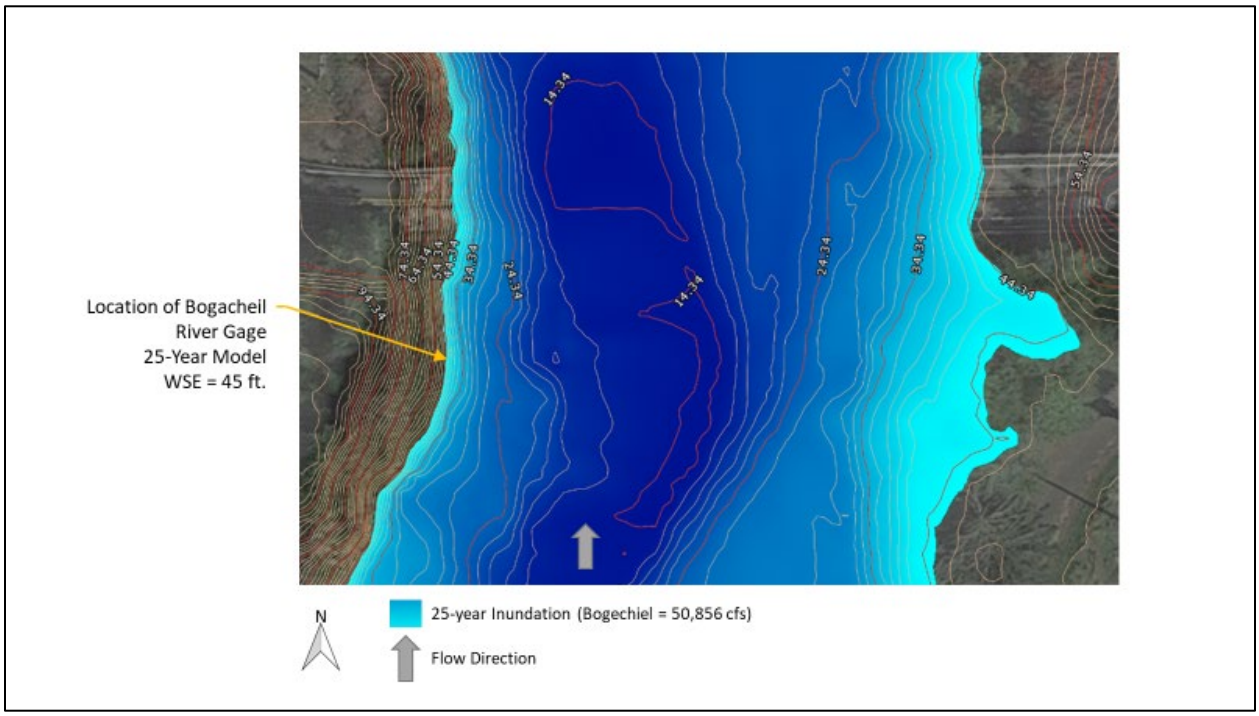

Figure 3-4. Hydraulic Model Validation

3.2 HYDRAULIC MODELING RESULTS

As described in Section 3.1.2, bathymetric and streamflow data collected by the USGS for the Quillayute, Dickey, and Bogachiel rivers (Czuba et al. 2010) were used in combination with field data collected as part of the Project. Regional curves and regression equations, and gaging station data from USGS 12043018 Quillayute River near La Push WA, 12043015 Bogachiel River near La Push, WA, 12042800 Bogachiel River near Forks, WA, and 12043000 Calawah River near Forks, WA to calibrate and validate the hydrologic and hydraulic analysis for this Project. These data sources were used to evaluate the 1-year and 100-year recurrence intervals for the Quillayute River.

Upon completion of model calibration and validation, it was determined the peak streamflow analysis performed for Leonard (1982) was adequate for the Quillayute River drainage. Furthermore, the findings of the OCCRI research (Serafin et al. 2019) on tidal influence and the recorded high and low tide values (see Figure 2-4) were appropriate for evaluating water levels at the mouth of the Quillayute River. Based on these data sets, design scenarios for the 1- and 100-year recurrence intervals were determined (Table 3-4). Each design event was modeled with a high tide WSE of 13.5 feet and a low tide WSE of -4.25 feet NAVD 88. The 1-year recurrence interval was calculated based on the 10-, 50-, and 100-year logarithmic trendlines for each river.

Table 3-4. Hydraulic Model Design Events

Statistic	Peak Streamflows (cfs)			
	Quillayute River	Dickey River	Sol Duc River	Bogachiel River
1-year	39,381	5,815	12,732	20,834
100-year	131,500[1/]	22,800	45,100	63,600

cfs – cubic feet per second
1/ Summation of all flows from Leonard (1982)

Utilizing the values reported in Table 3-4, inundation depths, velocities, and shear stresses were determined. The 2D hydraulic model has the capability to export the grid cell–based inundation depths, velocities, and shear stresses. Results of the hydraulic model are provided in Attachment 2, with figures representing inundation depths, velocities, and shear stresses for the 1- and 100-year design events. These figures are necessary for engineering design development, as well as the geomorphic and biological analyses being completed for the Assessment and Action Plan.

4 REFERENCES CITED

Curran, C.A., K. Eng, and C.P. Konrad. 2012. Analysis of low flows and selected methods for estimating low-flow characteristics at partial-record and ungaged stream sites in western Washington. U.S. Geological Survey Scientific Investigations Report 2012-5078. 46 p.

Czuba, J.A., C. R. Barnas, T. E. McKenna, G. B. Justin, and K.L. Payne. 2010. Bathymetric and Streamflow Data for the Quillayute, Dickey and Bogachiel Rivers, Clallam County, Washington, April – May 2010. U. S. Geological Survey Data Series 537, 12 p. Available online at: https://pubs.usgs.gov/ds/537/ (Accessed September 27, 2019).

England, J.F., Jr., T.A. Cohn, B.A. Faber, J.R. Stedinger, W.O. Thomas, Jr., A.G. Veilleux, J.E. Kinag, and R.R. Mason, Jr. 2019. Guidelines for determining flood flow frequency-Bulletin 17C (ver. 1.1, May 2019). U.S. Geological Survey Techniques and Methods. Book 4, chap. B5, 148p. Available online at: https://doi.org.10.3133/tm4B5

FEMA (Federal Emergency Management Agency). 1983. Flood Insurance Rate Map, Clallam County, Washington (Unincorporated Areas). Panel 575 of 725. Community-Panel Number 530021 0575 C. February 16, 1983.

FEMA. 2001. Flood Insurance Study, Clallam County, Washington (Unincorporated Areas), Community Number 530021. Revised February 23, 2001.

Fretwell, M.O. 1984. Quality of Water, Quillayute River Basin, Washington. U.S. Geological Survey. Water Resources Investigations. Report 83-4162.

Leonard, N.M. 1982. Streamflow and Sediment Transport in the Quillayute River Basin, Washington. USGS Open File Report 82-627. Tacoma, WA. Available online at: https://pubs.er.usgs.gov/publication/ofr82627 (Accessed October 16, 2019).

Mastin, M.C., C.P. Konrad, A.G. Veilleux, and A.E. Tecca. 2016. Magnitude, Frequency and Trends of Floods at Gaged and Ungaged Site in Washington, based on Data Through Water Year 2014 (version 1.2, November 2017). U. S. Geological Survey Scientific Investigations Report 2016-5118. 70 p. Available online at: https://dx.doi.org/10.3133/sir20165118

Miller, I.L., H. Morgan, G. Mauger,T. Newton, R. Weldon, D. Schmidt, M. Welsh, and E. Grossman. 2018. Projected Sea Level Rise for Washington State – A 2018 Assessment. A collaboration of Washington Sea Grant, University of Washington Climate Impacts Group, University of Oregon, University of Washington, and US Geological Survey. Prepared for the Washington Coastal Resiliency Project. Updated July 2019. Available online at: http://www.wacoastalnetwork.com/wcrp-documents.html (Accessed October 3, 2019).

Mote, P., A. Petersen, S. Reeder, H. Shipman, and L. Whitely Binder. 2008. Sea level Rise in the Coastal Waters of Washington State. University of Washington: http://cses.washington.edu/db/pdf/moteetalslr579.pdf

NOAA (National Oceanic and Atmospheric Administration. 2000. Tide and Current Glossary. Silver Spring MD. January, 2000. Available online at: https://tidesandcurrents.noaa.gov/publications/glossary2.pdf

NOAA. 2019. Climate of Washington: Western Regional Climate Center. Available online at: https://wrcc.dri.edu/narratives/WASHINGTON.htm (Accessed September 27, 2019).

NOAA Tides and Currents. 2019. Tide Station 9442396, La Push, WA. Available online at: https://tidesandcurrents.noaa.gov/map/index.html?id=9442396 (Accessed October 3, 2019).

PMEP (Pacific Marine and Estuarine Fish Habitat Partnership). 2019. Current and Historic Estuary Extents. Available online at: http://www.pacificfishhabitat.org/data/estuary-extents/ (Accessed October 16, 2019).

Outdoor Society. 2019. Rediscover the Olympic's Bogachiel Rainforest. Available online at: http://outdoor-society.com/rediscover-the-olympics-bogachiel-rainforest/ (Accessed September 27, 2019).

Serafin, K. A., P. Ruggiero, K. Parker, and D.F. Hill. 2019. What's streamflow got to do with it? A probabilistic simulation of the competing oceanographic and fluvial processes driving extreme along-river water levels. Natural Hazards and Earth Systems Sciences 19: 1415–1431. https://doi.org/10.5194/nhess-19-1415-2019

USACE (United States Army Corps of Engineers). 2019. U.S. Army Corps of Engineers Hydro Hydrographic Survey of the Quillayute River and La Push Marina. Collected July 2019.

USGS (United States Geological Survey). 2019. StreamStats. Available online at: https://www.usgs.gov/mission-areas/water-resources/science/streamstats-streamflow-statistics-and-spatial-analysis-tools?qt-science_center_objects=0#qt-science_center_objects

Wikipedia. 2019. Bogachiel River. Available online at: https://en.wikipedia.org/wiki/Bogachiel_River (Accessed September 27, 2019).

Walsh, T. J., E.P. Meyers III, and A.M. Baptista. 2003. Tsunami Inundation Map of the Quileute Washington Area. Washington Division of Geology and Earth Resources, Open File Report: 2003-1. Available online at: http://www.dnr.wa.gov/Publications/ger_ofr2003-1_tsunami_hazard_quileute.pdf

ATTACHMENT 1 – RIVER BASIN CHARACTERISTICS

- Quillayute River
- Dickey River
- Sol Duc River
- Bogachiel River

Quillayute River Basin Characteristics

Region ID: WA
Workspace ID: WA20200218201551931000
Clicked Point (Latitude, Longitude): 47.90886, -124.64127
Time: 2020-02-18 12:16:08 -0800

Basin Characteristics

Parameter Code	Parameter Description	Value	Unit
BSLDEM30M	Mean basin slope computed from 30 m DEM	32.8	percent
CANOPY_PCT	Percentage of drainage area covered by canopy as described in OK SIR 2009_5267	81.7	percent
DRNAREA	Area that drains to a point on a stream	627.46	square miles
ELEV	Mean Basin Elevation	1350	feet
ELEVMAX	Maximum basin elevation	6070	feet
MINBELEV	Minimum basin elevation	0	feet

Parameter Code	Parameter Description	Value	Unit
NFSL30	North-Facing Slopes Greater Than 30 Percent	14.1	percent
PRECPRIS10	Basin average mean annual precipitation for 1981 to 2010 from PRISM	121	inches
RELIEF	Maximum - minimum elevation	6070	feet
SLOP30_30M	Percent area with slopes greater than 30 percent from 30-meter DEM.	50.8	percent

USGS Data Disclaimer: Unless otherwise stated, all data, metadata and related materials are considered to satisfy the quality standards relative to the purpose for which the data were collected. Although these data and associated metadata have been reviewed for accuracy and completeness and approved for release by the U.S. Geological Survey (USGS), no warranty expressed or implied is made regarding the display or utility of the data for other purposes, nor on all computer systems, nor shall the act of distribution constitute any such warranty.

USGS Software Disclaimer: This software has been approved for release by the U.S. Geological Survey (USGS). Although the software has been subjected to rigorous review, the USGS reserves the right to update the software as needed pursuant to further analysis and review. No warranty, expressed or implied, is made by the USGS or the U.S. Government as to the functionality of the software and related material nor shall the fact of release constitute any such warranty. Furthermore, the software is released on condition that neither the USGS nor the U.S. Government shall be held liable for any damages resulting from its authorized or unauthorized use.

USGS Product Names Disclaimer: Any use of trade, firm, or product names is for descriptive purposes only and does not imply endorsement by the U.S. Government.

Application Version: 4.3.11

Dickey River Basin Characteristics

Region ID: WA
Workspace ID: WA20200218202508370000
Clicked Point (Latitude, Longitude): 47.92063, -124.62343
Time: 2020-02-18 12:25:24 -0800

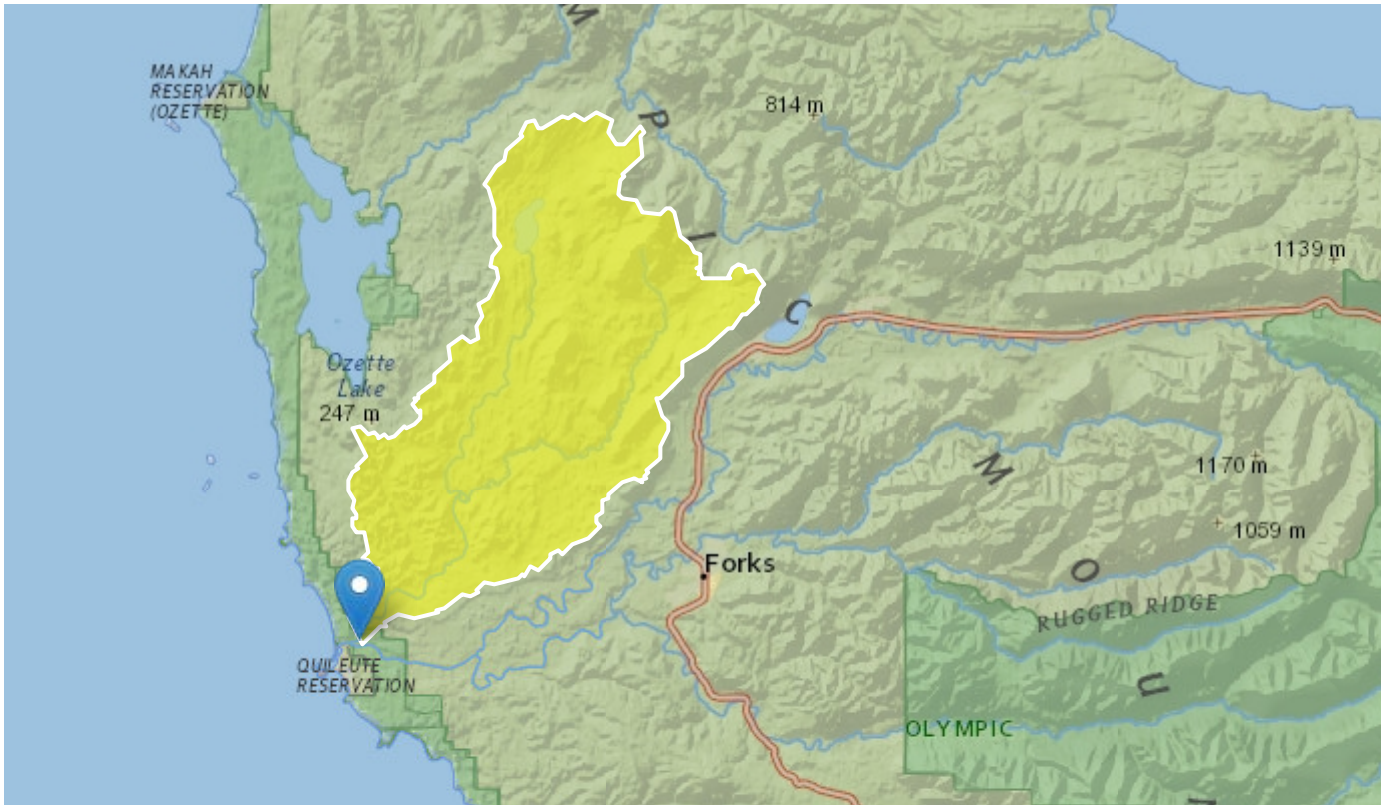

Basin Characteristics

Parameter Code	Parameter Description	Value	Unit
BSLDEM30M	Mean basin slope computed from 30 m DEM	13.9	percent
CANOPY_PCT	Percentage of drainage area covered by canopy as described in OK SIR 2009_5267	80.2	percent
DRNAREA	Area that drains to a point on a stream	105.35	square miles
ELEV	Mean Basin Elevation	401	feet
ELEVMAX	Maximum basin elevation	1940	feet
MINBELEV	Minimum basin elevation	11.3	feet

Parameter Code	Parameter Description	Value	Unit
NFSL30	North-Facing Slopes Greater Than 30 Percent	1.49	percent
PRECIP	Mean Annual Precipitation	98.3	inches
PRECPRIS10	Basin average mean annual precipitation for 1981 to 2010 from PRISM	108	inches
RELIEF	Maximum - minimum elevation	1930	feet
SLOP30_30M	Percent area with slopes greater than 30 percent from 30-meter DEM.	6.61	percent

USGS Data Disclaimer: Unless otherwise stated, all data, metadata and related materials are considered to satisfy the quality standards relative to the purpose for which the data were collected. Although these data and associated metadata have been reviewed for accuracy and completeness and approved for release by the U.S. Geological Survey (USGS), no warranty expressed or implied is made regarding the display or utility of the data for other purposes, nor on all computer systems, nor shall the act of distribution constitute any such warranty.

USGS Software Disclaimer: This software has been approved for release by the U.S. Geological Survey (USGS). Although the software has been subjected to rigorous review, the USGS reserves the right to update the software as needed pursuant to further analysis and review. No warranty, expressed or implied, is made by the USGS or the U.S. Government as to the functionality of the software and related material nor shall the fact of release constitute any such warranty. Furthermore, the software is released on condition that neither the USGS nor the U.S. Government shall be held liable for any damages resulting from its authorized or unauthorized use.

USGS Product Names Disclaimer: Any use of trade, firm, or product names is for descriptive purposes only and does not imply endorsement by the U.S. Government.

Application Version: 4.3.11

Sol Duc River Basin Characteristics

Region ID: WA
Workspace ID: WA20200218202817313000
Clicked Point (Latitude, Longitude): 47.91429, -124.54245
Time: 2020-02-18 12:28:34 -0800

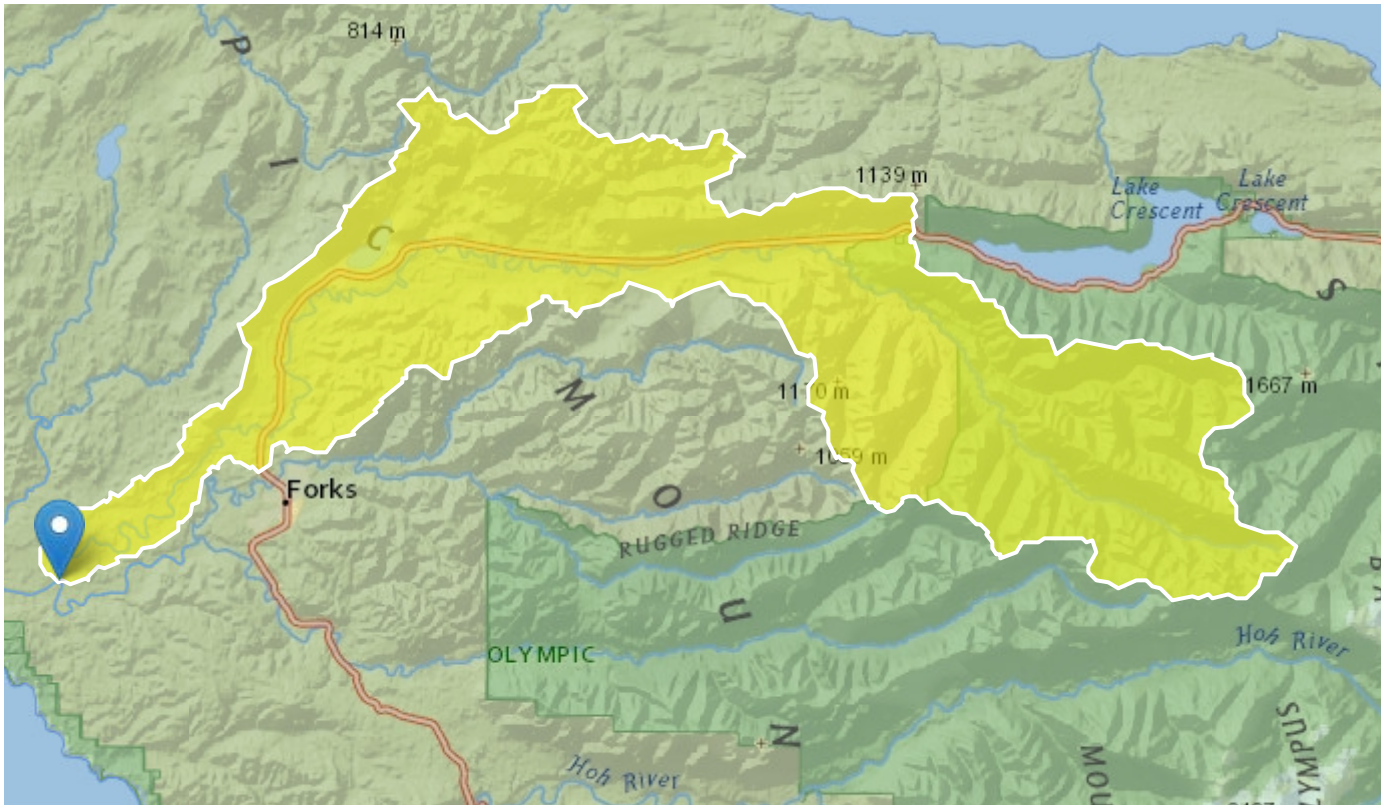

Basin Characteristics

Parameter Code	Parameter Description	Value	Unit
BSLDEM30M	Mean basin slope computed from 30 m DEM	35.4	percent
CANOPY_PCT	Percentage of drainage area covered by canopy as described in OK SIR 2009_5267	78.6	percent
DRNAREA	Area that drains to a point on a stream	225.2	square miles
ELEV	Mean Basin Elevation	1810	feet
ELEVMAX	Maximum basin elevation	6070	feet
MINBELEV	Minimum basin elevation	30.1	feet

Parameter Code	Parameter Description	Value	Unit
NFSL30	North-Facing Slopes Greater Than 30 Percent	16	percent
PRECIP	Mean Annual Precipitation	102	inches
PRECPRIS10	Basin average mean annual precipitation for 1981 to 2010 from PRISM	115	inches
RELIEF	Maximum - minimum elevation	6040	feet
SLOP30_30M	Percent area with slopes greater than 30 percent from 30-meter DEM.	58.3	percent

USGS Data Disclaimer: Unless otherwise stated, all data, metadata and related materials are considered to satisfy the quality standards relative to the purpose for which the data were collected. Although these data and associated metadata have been reviewed for accuracy and completeness and approved for release by the U.S. Geological Survey (USGS), no warranty expressed or implied is made regarding the display or utility of the data for other purposes, nor on all computer systems, nor shall the act of distribution constitute any such warranty.

USGS Software Disclaimer: This software has been approved for release by the U.S. Geological Survey (USGS). Although the software has been subjected to rigorous review, the USGS reserves the right to update the software as needed pursuant to further analysis and review. No warranty, expressed or implied, is made by the USGS or the U.S. Government as to the functionality of the software and related material nor shall the fact of release constitute any such warranty. Furthermore, the software is released on condition that neither the USGS nor the U.S. Government shall be held liable for any damages resulting from its authorized or unauthorized use.

USGS Product Names Disclaimer: Any use of trade, firm, or product names is for descriptive purposes only and does not imply endorsement by the U.S. Government.

Application Version: 4.3.11

Bogachiel River Basin Characteristics

Region ID: WA
Workspace ID: WA20200218203346719000
Clicked Point (Latitude, Longitude): 47.91367, -124.54222
Time: 2020-02-18 12:34:03 -0800

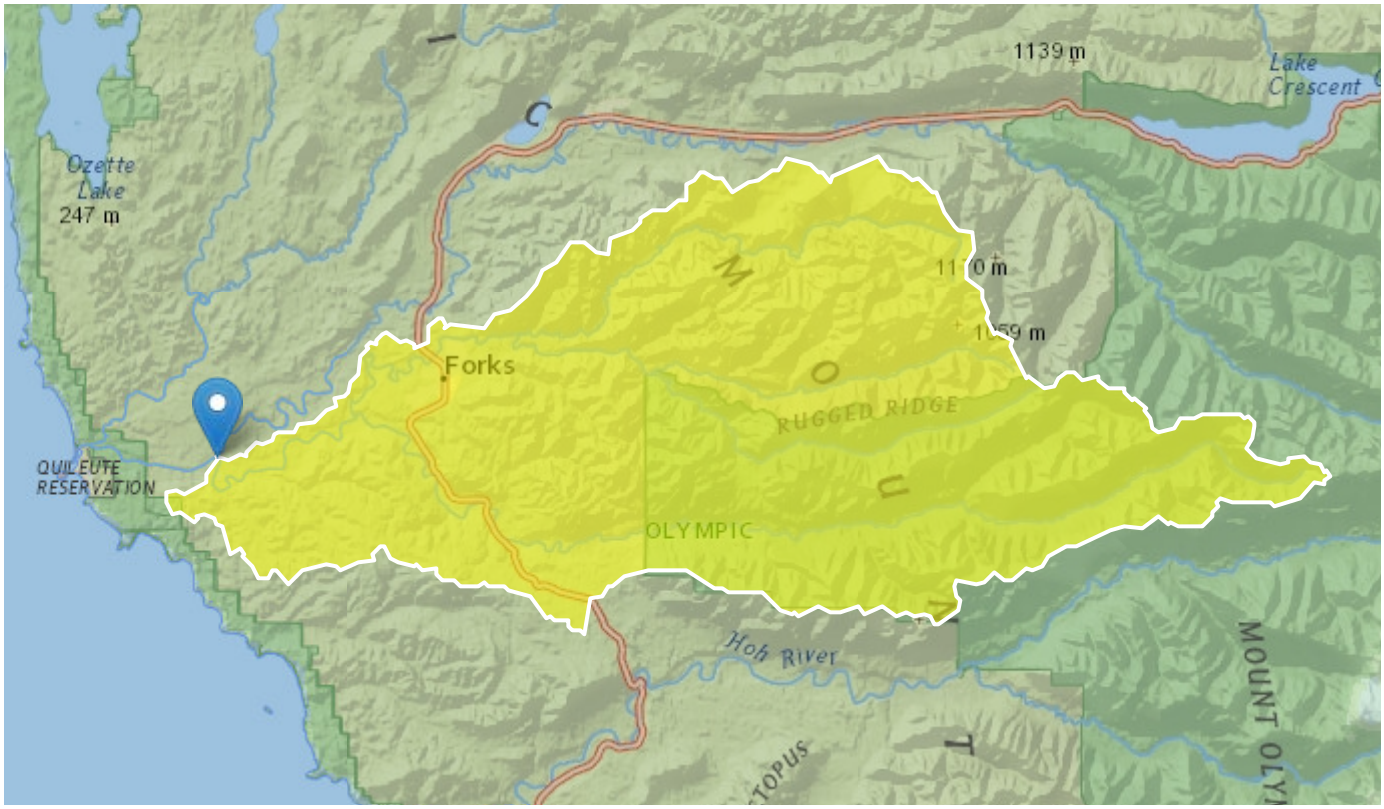

Basin Characteristics

Parameter Code	Parameter Description	Value	Unit
BSLDEM30M	Mean basin slope computed from 30 m DEM	38.4	percent
CANOPY_PCT	Percentage of drainage area covered by canopy as described in OK SIR 2009_5267	85.1	percent
DRNAREA	Area that drains to a point on a stream	289.01	square miles
ELEV	Mean Basin Elevation	1380	feet
ELEVMAX	Maximum basin elevation	5420	feet
MINBELEV	Minimum basin elevation	28.6	feet

Parameter Code	Parameter Description	Value	Unit
NFSL30	North-Facing Slopes Greater Than 30 Percent	17.5	percent
PRECIP	Mean Annual Precipitation	117	inches
PRECPRIS10	Basin average mean annual precipitation for 1981 to 2010 from PRISM	131	inches
RELIEF	Maximum - minimum elevation	5400	feet
SLOP30_30M	Percent area with slopes greater than 30 percent from 30-meter DEM.	62.4	percent

USGS Data Disclaimer: Unless otherwise stated, all data, metadata and related materials are considered to satisfy the quality standards relative to the purpose for which the data were collected. Although these data and associated metadata have been reviewed for accuracy and completeness and approved for release by the U.S. Geological Survey (USGS), no warranty expressed or implied is made regarding the display or utility of the data for other purposes, nor on all computer systems, nor shall the act of distribution constitute any such warranty.

USGS Software Disclaimer: This software has been approved for release by the U.S. Geological Survey (USGS). Although the software has been subjected to rigorous review, the USGS reserves the right to update the software as needed pursuant to further analysis and review. No warranty, expressed or implied, is made by the USGS or the U.S. Government as to the functionality of the software and related material nor shall the fact of release constitute any such warranty. Furthermore, the software is released on condition that neither the USGS nor the U.S. Government shall be held liable for any damages resulting from its authorized or unauthorized use.

USGS Product Names Disclaimer: Any use of trade, firm, or product names is for descriptive purposes only and does not imply endorsement by the U.S. Government.

Application Version: 4.3.11

ATTACHMENT 2 – HYDRAULIC MODELING FIGURES

- Figure B-1: Record High Tide 1 Year Flow Inundation Depth
- Figure B-2: Record High Tide 1 Year Flow Velocity
- Figure B-3: Record High Tide 1 Year Flow Shear Stress
- Figure B-4: Record Low Tide 1 Year Flow Inundation Depth
- Figure B-5: Record Low Tide 1 Year Flow Velocity
- Figure B-6: Record Low Tide 1 Year Flow Shear Stress
- Figure B-7: Record High Tide 100 Year Flow Inundation Depth
- Figure B-8: Record High Tide 100 Year Flow Velocity
- Figure B-9: Record High Tide 100 Year Flow Shear Stress
- Figure B-10: Record Low Tide 100 Year Flow Inundation Depth
- Figure B-11: Record Low Tide 100 Year Flow Velocity
- Figure B-12: Record Low Tide 100 Year Flow Shear Stress

G:\Science\Cameron\Quillayute\GIS\MXD\HydraulicModeling\1yr_RecHighTide_Depth.mxd

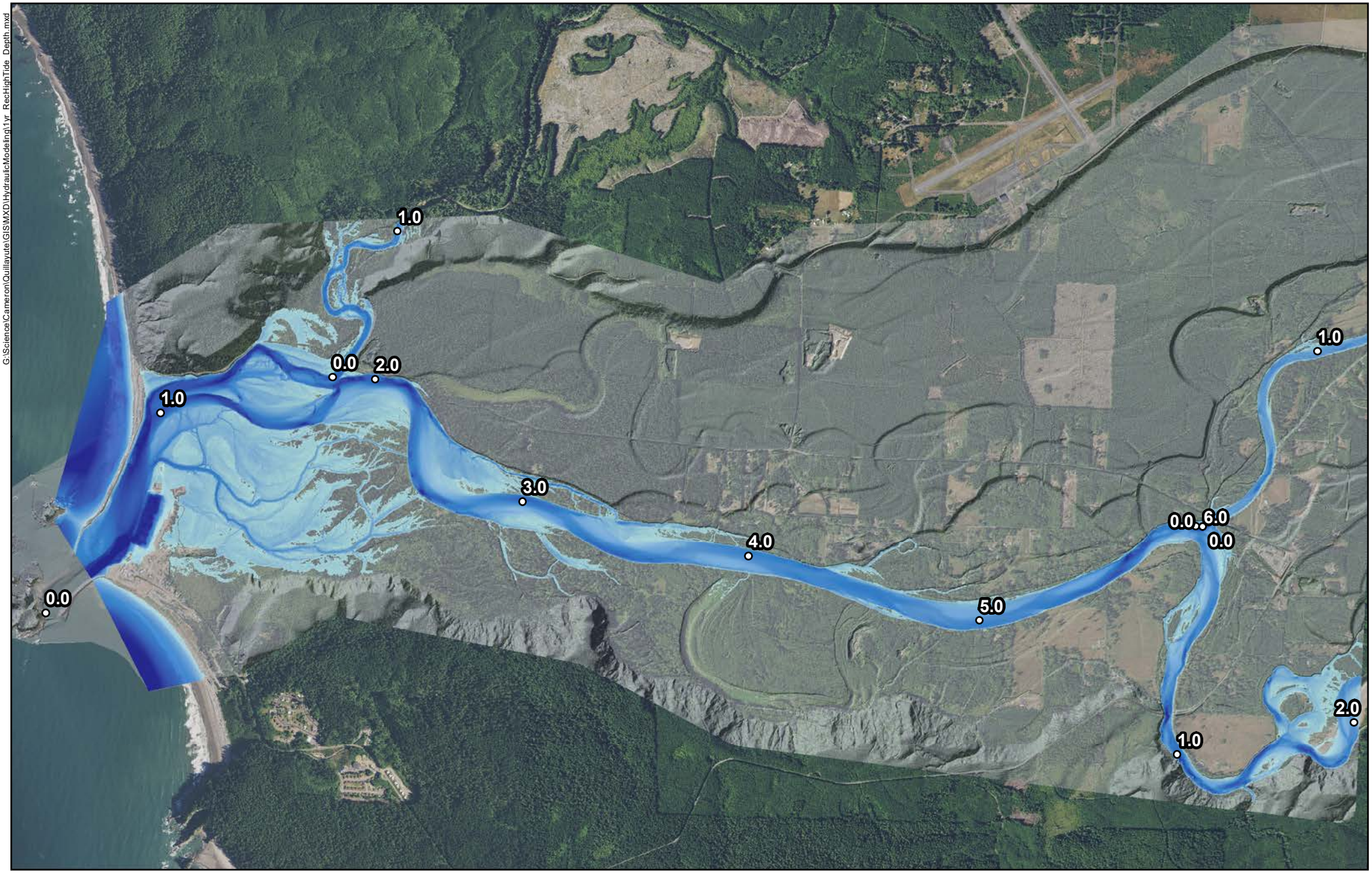

Inundation Depth (ft)

High : 39

Low : 0

River Miles

Quillayute River Flow: 31, 381 cfs

Low Tide: -4.25 ft. (NAVD88) High Tide: 13.5 ft. (NAVD88)

Quillayute River
Geomorphic Assessment

Hydraulic Modeling
1 Year Flow
Record High Tide
Figure B-1

TETRA TECH

N
W E
S

0 3,500 7,000

Feet

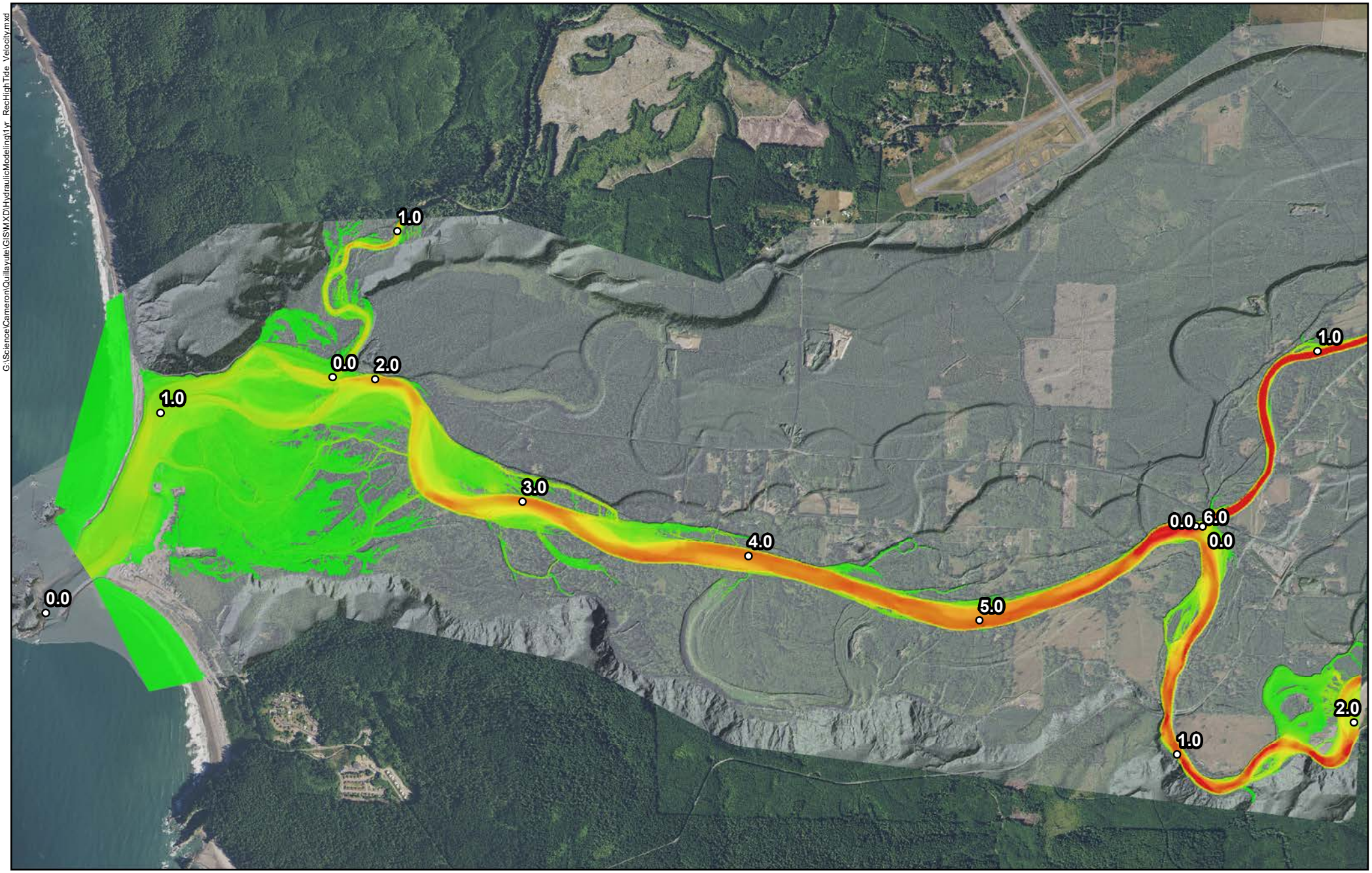

Velocity (ft/second)

High : 11

Low : 0

River Miles

Quillayute River Flow: 31, 381 cfs

Low Tide: -4.25 ft. (NAVD88) High Tide: 13.5 ft. (NAVD88)

Quillayute River Geomorphic Assessment

Hydraulic Modeling
1 Year Flow
Record High Tide
Figure B-2

TETRA TECH

N
W E
S

0 3,500 7,000

Feet

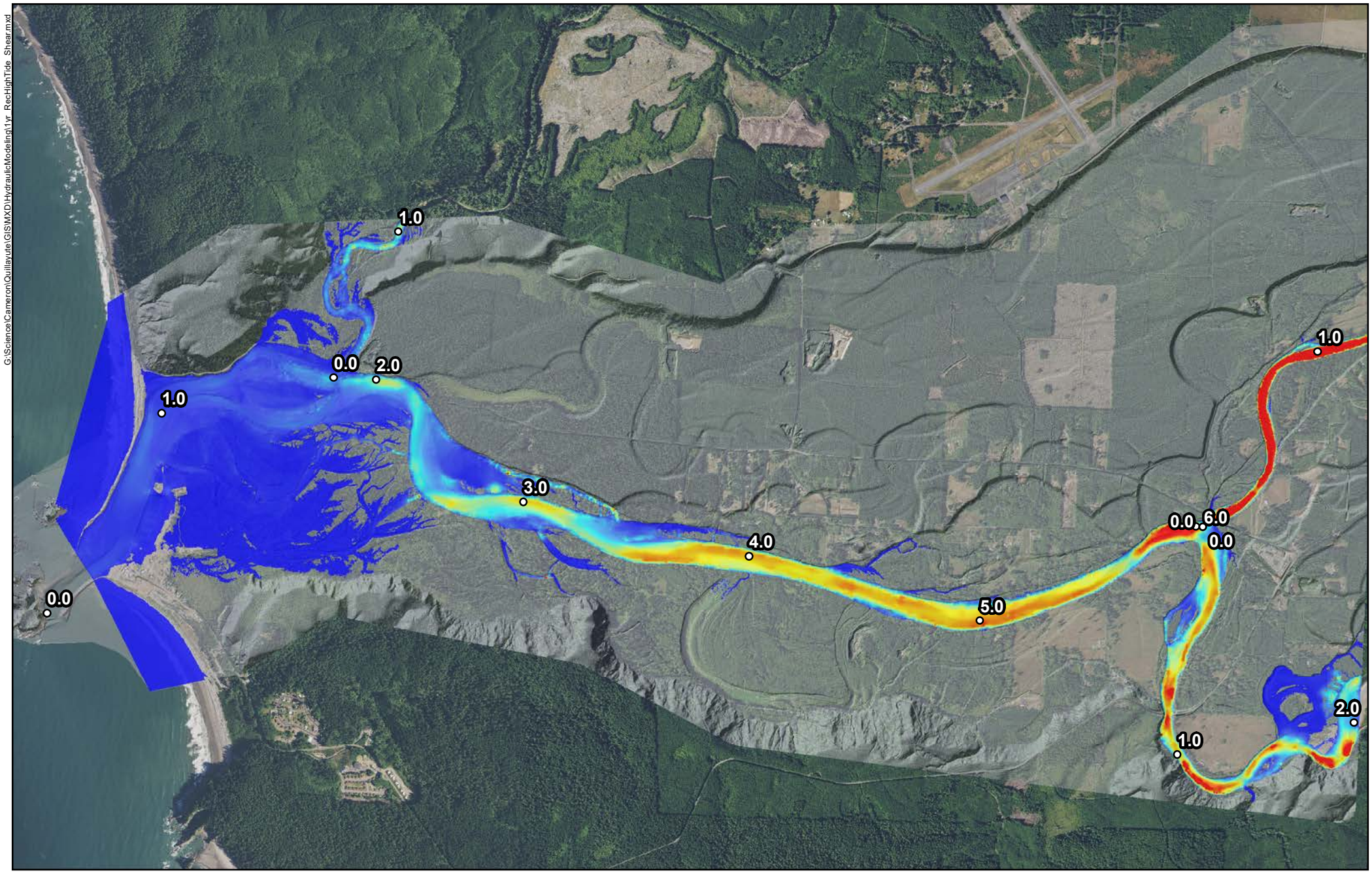

Shear Stress (lb/sq. ft.)

High : 10

Low : 0

River Miles

Quillayute River Flow: 31, 381 cfs

Low Tide: -4.25 ft. (NAVD88) High Tide: 13.5 ft. (NAVD88)

Quillayute River
Geomorphic Assessment

Hydraulic Modeling
1 Year Flow
Record High Tide
Figure B-3

TETRA TECH

N
W E
S

0 3,500 7,000

Feet

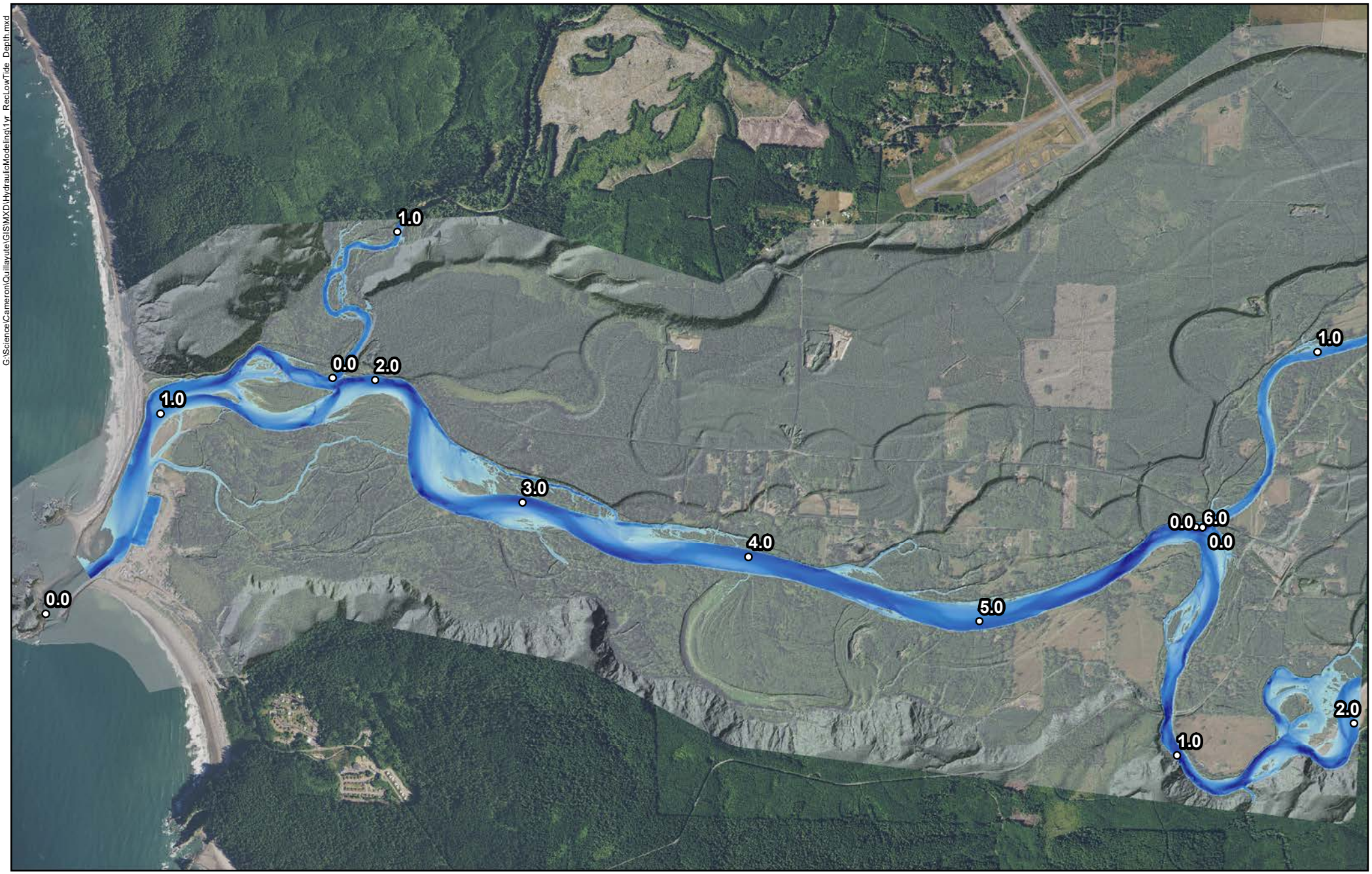

G:\Science\Cameron\Quillayute\GIS\MXD\HydraulicModeling\1yr_RecLowTide_Depth.mxd

Inundation Depth (ft)

High : 25

Low : 0

River Miles

Quillayute River Flow: 31, 381 cfs

Low Tide: -4.25 ft. (NAVD88) High Tide: 13.5 ft. (NAVD88)

Quillayute River
Geomorphic Assessment

Hydraulic Modeling
1 Year Flow
Record Low Tide
Figure B-4

TETRA TECH

N
W E
S

0 3,500 7,000

Feet

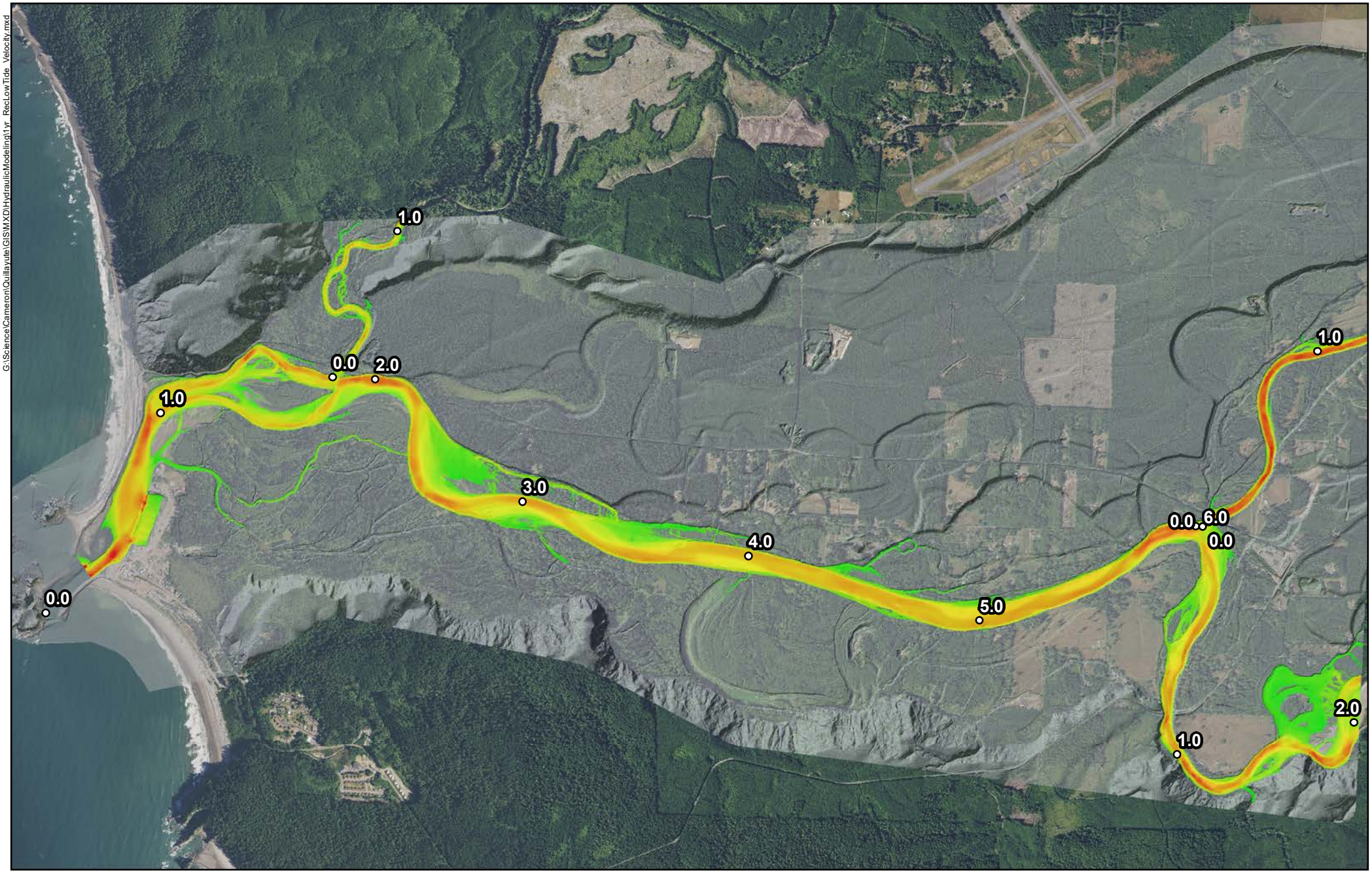

Velocity (ft/s)

High : 15

Low : 0

River Miles

Quillayute River Flow: 31, 381 cfs

Low Tide: -4.25 ft. (NAVD88) High Tide: 13.5 ft. (NAVD88)

Quillayute River Geomorphic Assessment

Hydraulic Modeling
1 Year Flow
Record Low Tide
Figure B-5

TETRA TECH

N
W E
S

0 3,500 7,000

Feet

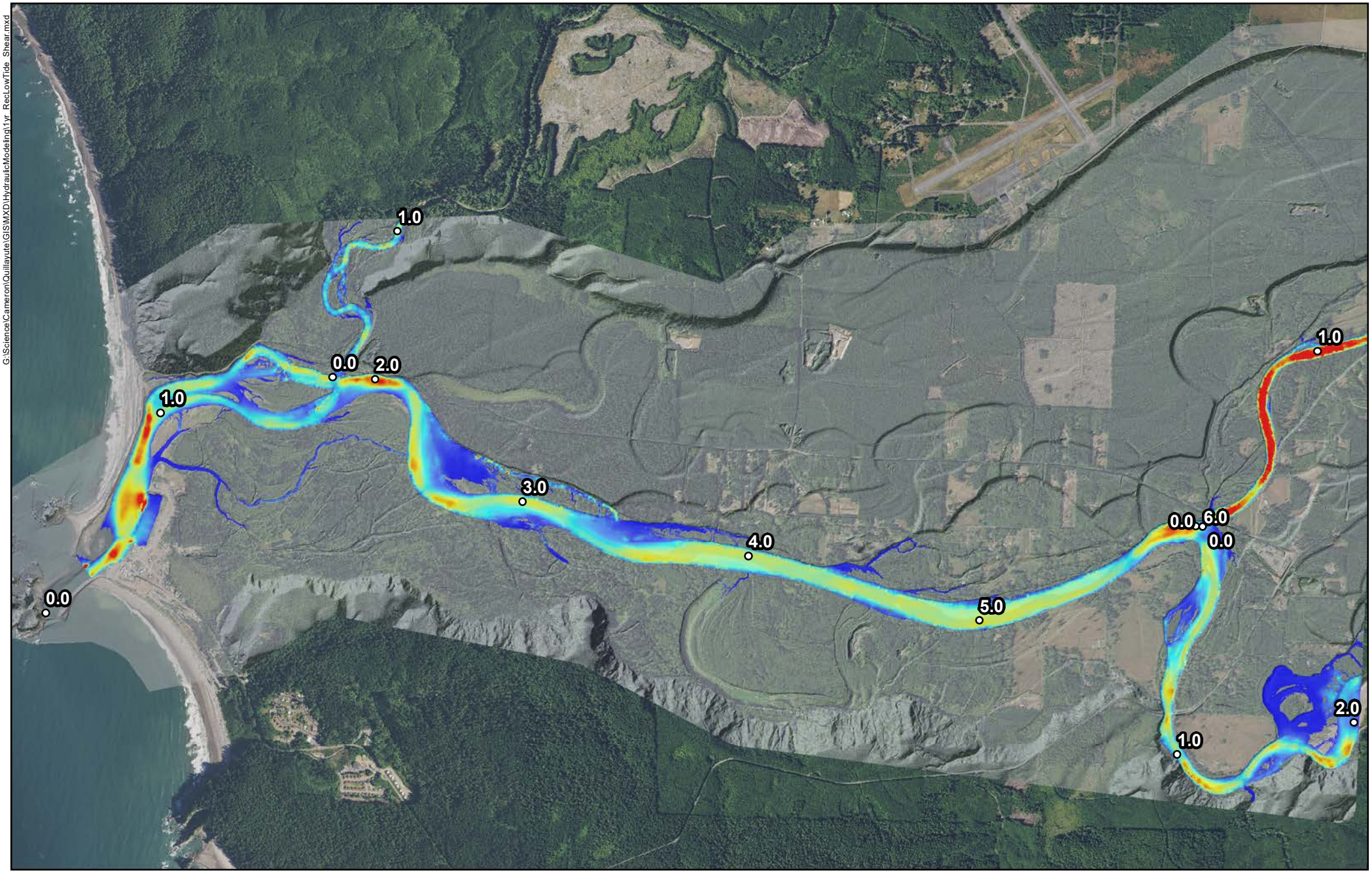

Shear Stress (lb/sq. ft.)

High : 3.8

Low : 0

River Miles

Quillayute River Flow: 31, 381 cfs

Low Tide: -4.25 ft. (NAVD88) High Tide: 13.5 ft. (NAVD88)

Quillayute River
Geomorphic Assessment

Hydraulic Modeling
1 Year Flow
Record Low Tide
Figure B-6

TETRA TECH

N
W E
S

0 3,500 7,000

Feet

G:\Science\Cameron\Quillayute\GIS\MXD\HydraulicModeling\100yr_RecHighTide_Depth.mxd

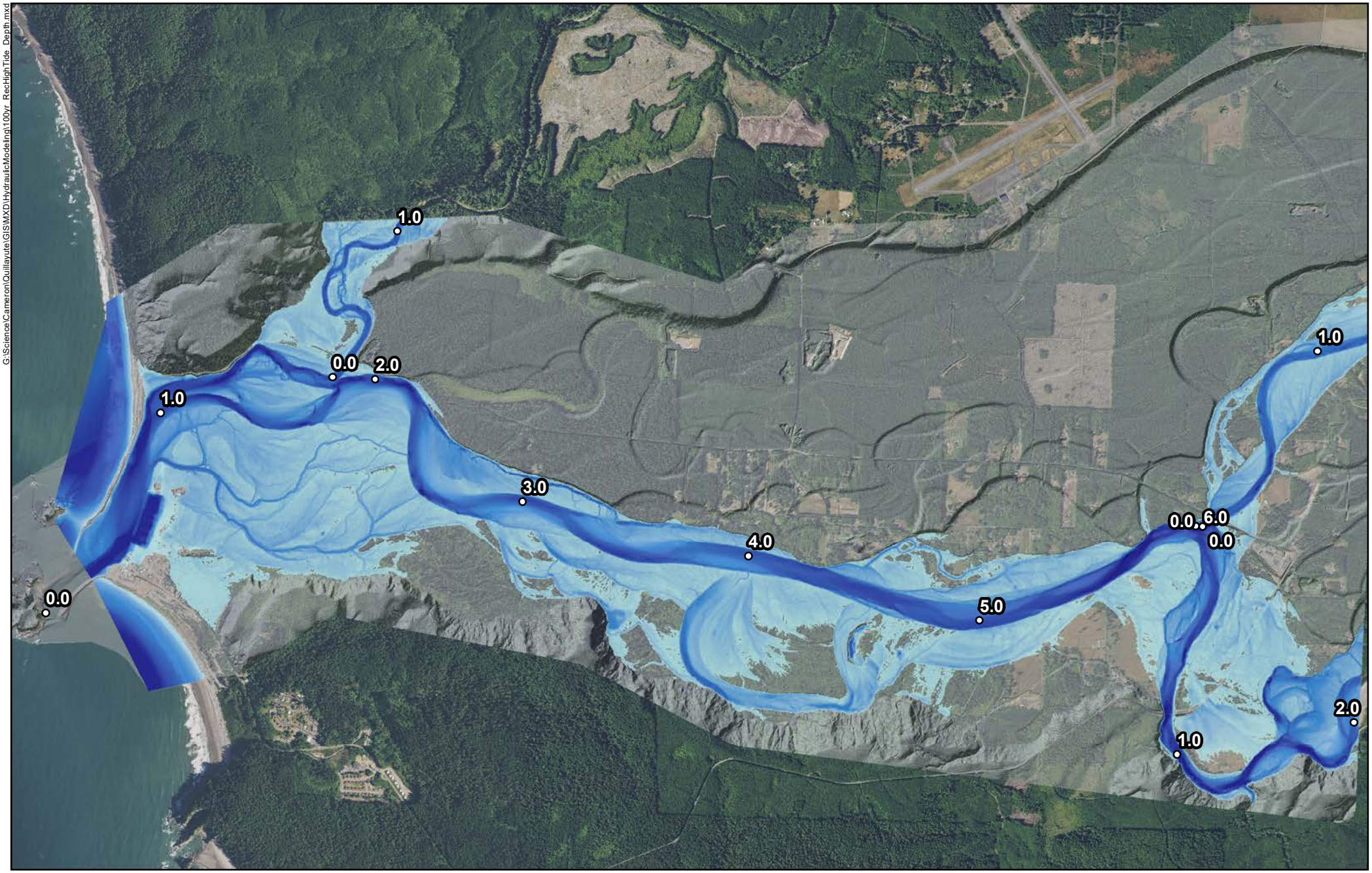

Inundation Depth (ft)

High : 39

Low : 0

River Miles

Quillayute River Flow: 131, 500 cfs

Low Tide: -4.25 ft. (NAVD88) High Tide: 13.5 ft. (NAVD88)

Quillayute River Geomorphic Assessment

Hydraulic Modeling
100 Year Flow
Record High Tide
Figure B-7

TETRA TECH

N
W E
S

0 3,500 7,000

Feet

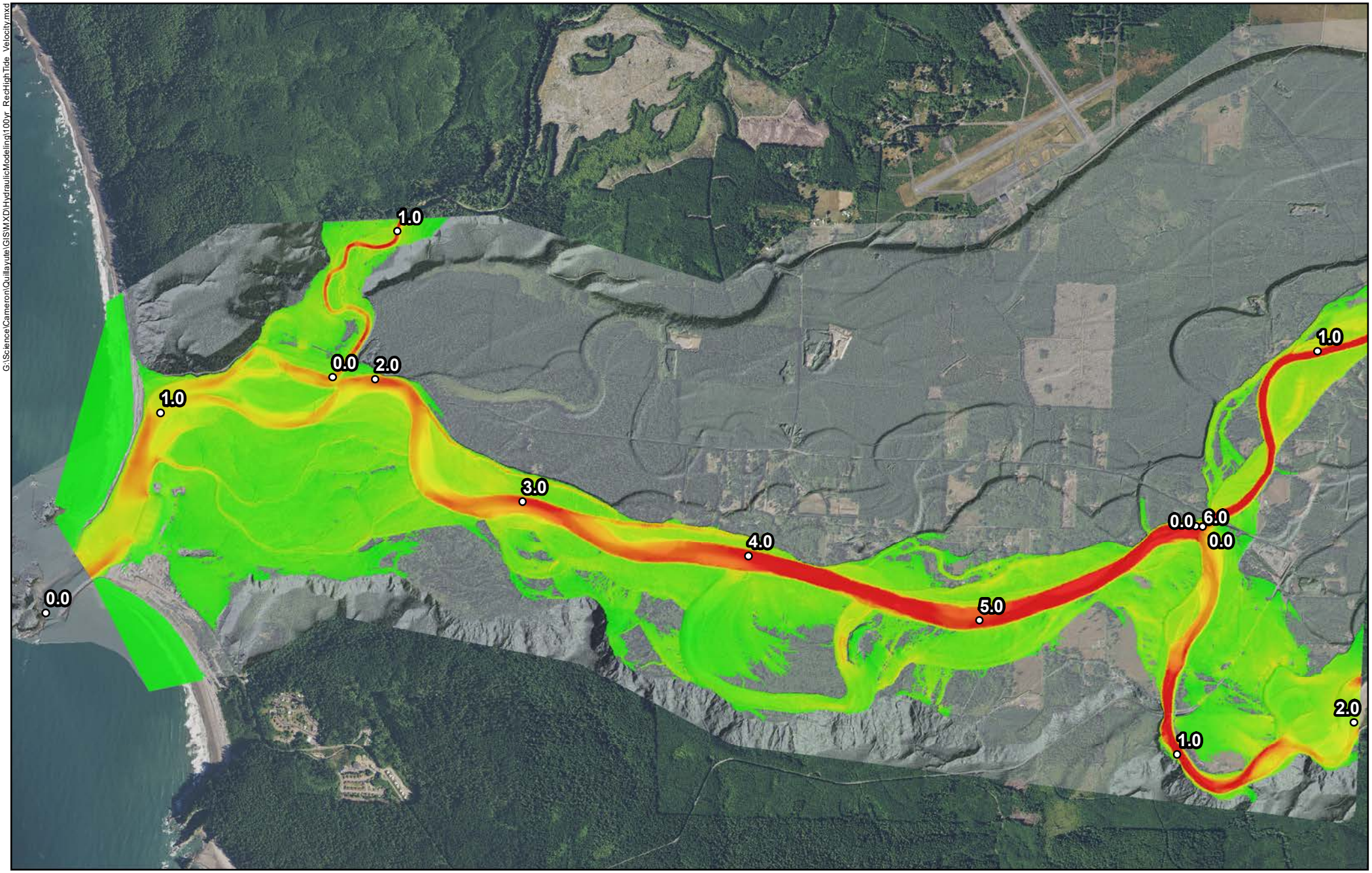

Velocity (ft/second)

High : 17

Low : 0

River Miles

Quillayute River Flow: 131, 500 cfs

Low Tide: -4.25 ft. (NAVD88) High Tide: 13.5 ft. (NAVD88)

Quillayute River
Geomorphic Assessment

Hydraulic Modeling
100 Year Flow
Record High Tide
Figure B-8

TETRA TECH

N
W E
S

0 3,500 7,000

Feet

G:\Science\Cameron\Quillayute\GIS\MXD\HydraulicModeling\100yr_RecHighTide_Shear.mxd

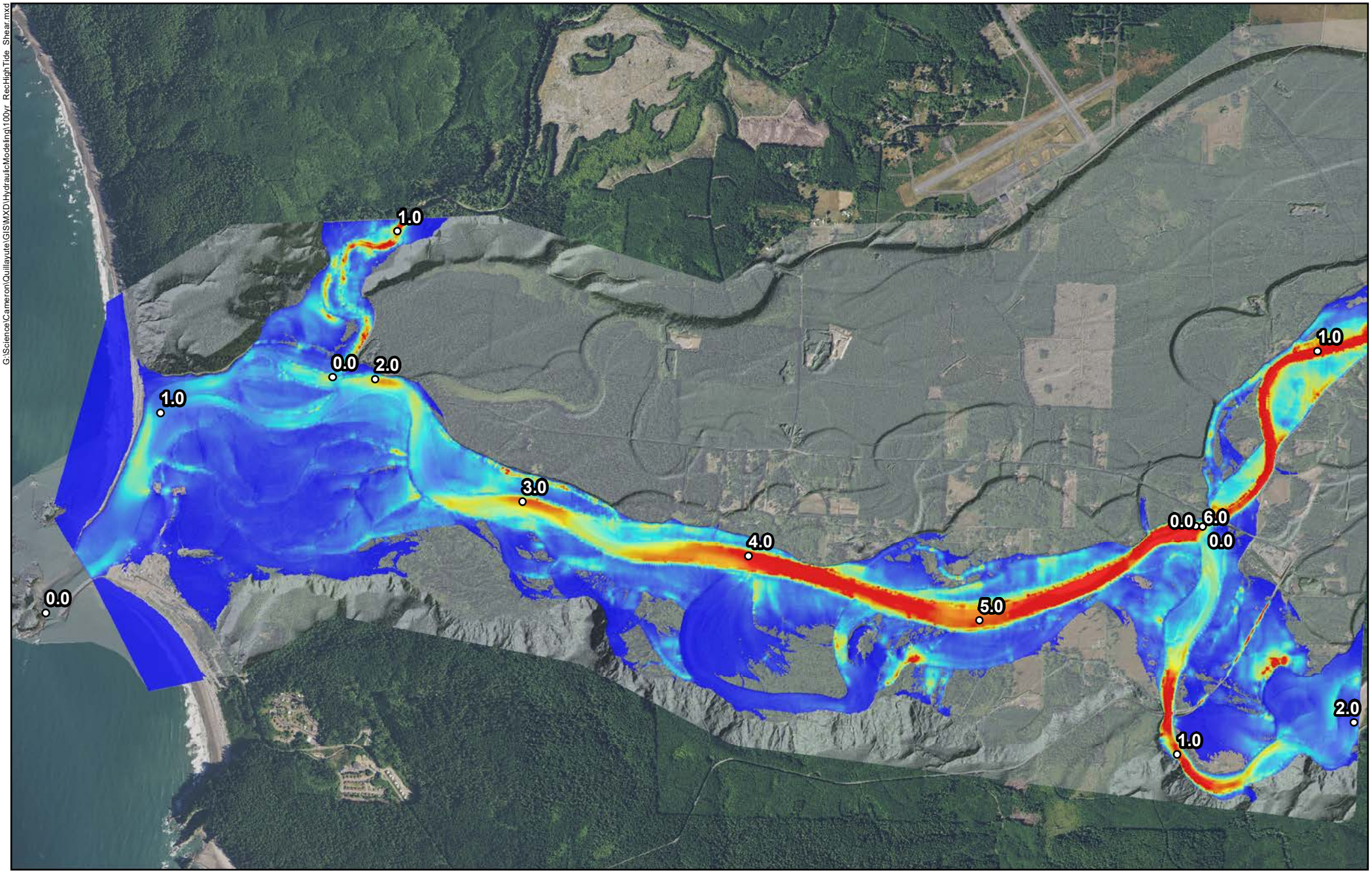

Shear Stress (lb/sq. ft.)

High : 8.0

Low : 0

River Miles

Quillayute River Flow: 131, 500 cfs

Low Tide: -4.25 ft. (NAVD88) High Tide: 13.5 ft. (NAVD88)

Quillayute River
Geomorphic Assessment

Hydraulic Modeling
100 Year Flow
Record High Tide
Figure B-9

TETRA TECH

N
W E
S

0 3,500 7,000
Feet

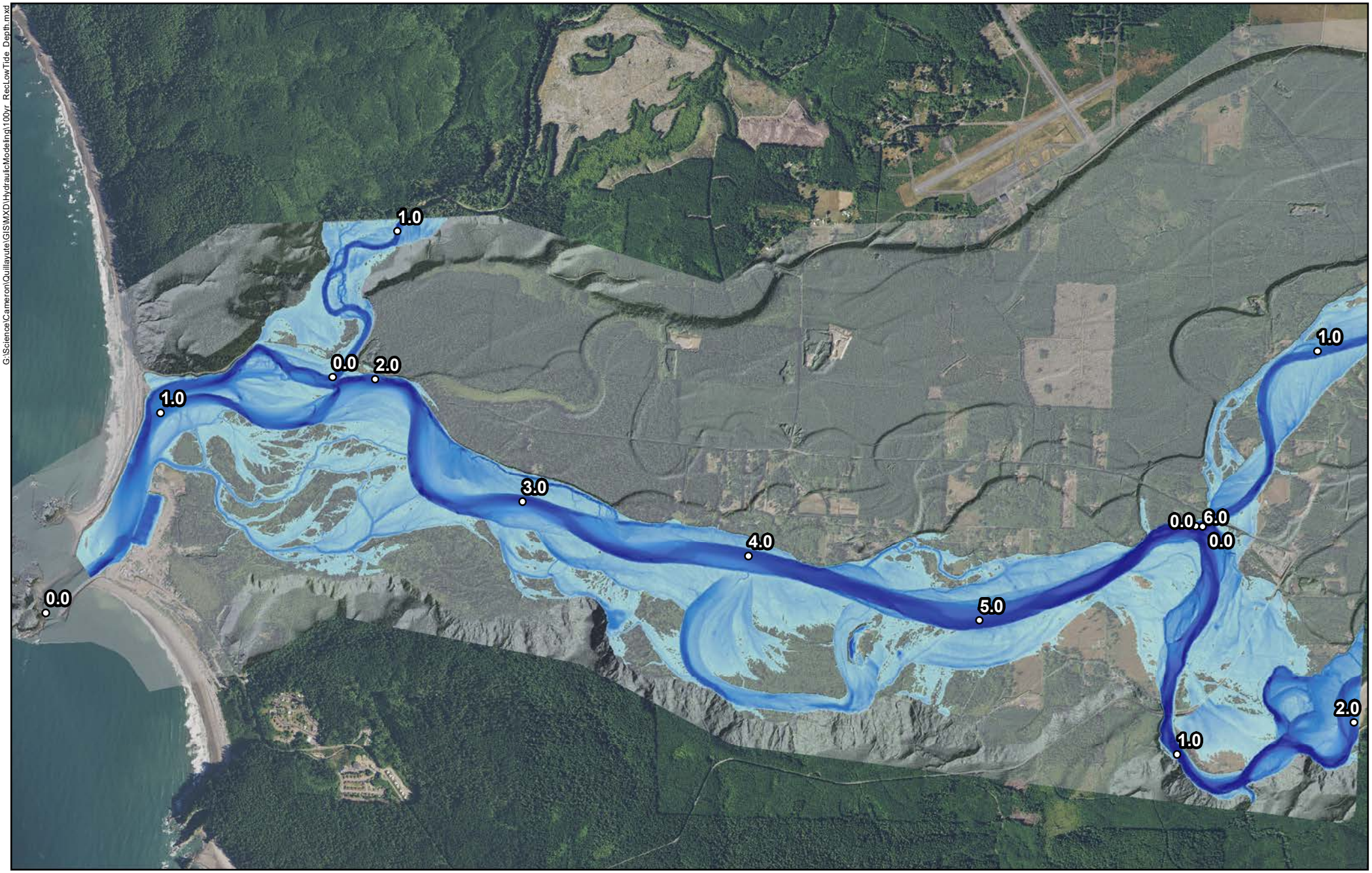

G:\Science\Cameron\Quillayute\GIS\MXD\HydraulicModeling\100yr_RecLowTide_Depth.mxd

Inundation Depth (ft)

High : 34

Low : 0

River Miles

Quillayute River Flow: 131, 500 cfs

Low Tide: -4.25 ft. (NAVD88) High Tide: 13.5 ft. (NAVD88)

Quillayute River
Geomorphic Assessment

Hydraulic Modeling
100 Year Flow
Record Low Tide
Figure B-10

TETRA TECH

N
W E
S

0 3,500 7,000

Feet

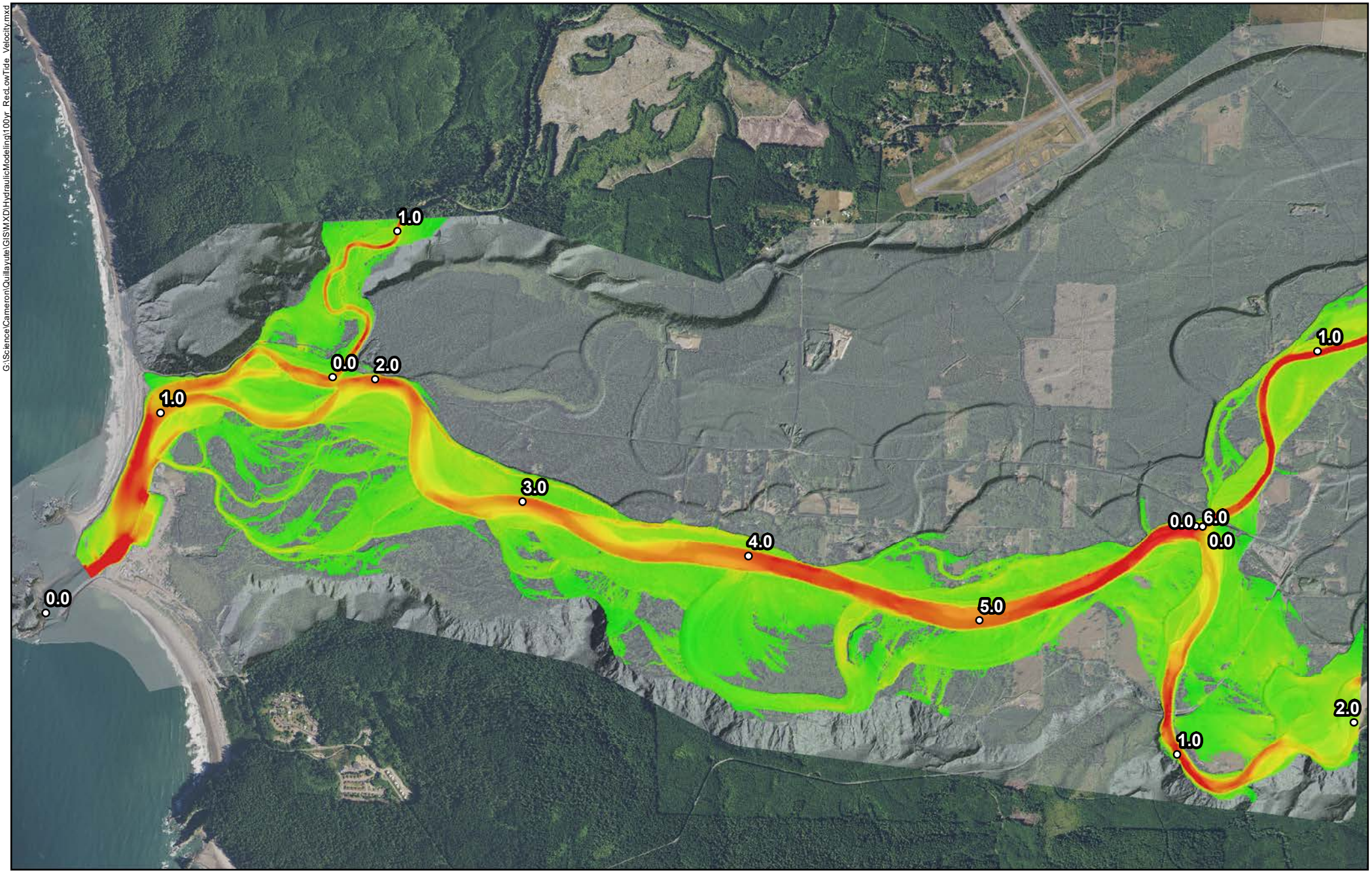

Velocity (ft/s)

High : 30

Low : 0

River Miles

Quillayute River Flow: 131, 500 cfs

Low Tide: -4.25 ft. (NAVD88) High Tide: 13.5 ft. (NAVD88)

Quillayute River
Geomorphic Assessment

Hydraulic Modeling
100 Year Flow
Record Low Tide
Figure B-11

TETRA TECH

N
W E
S

0 3,500 7,000

Feet

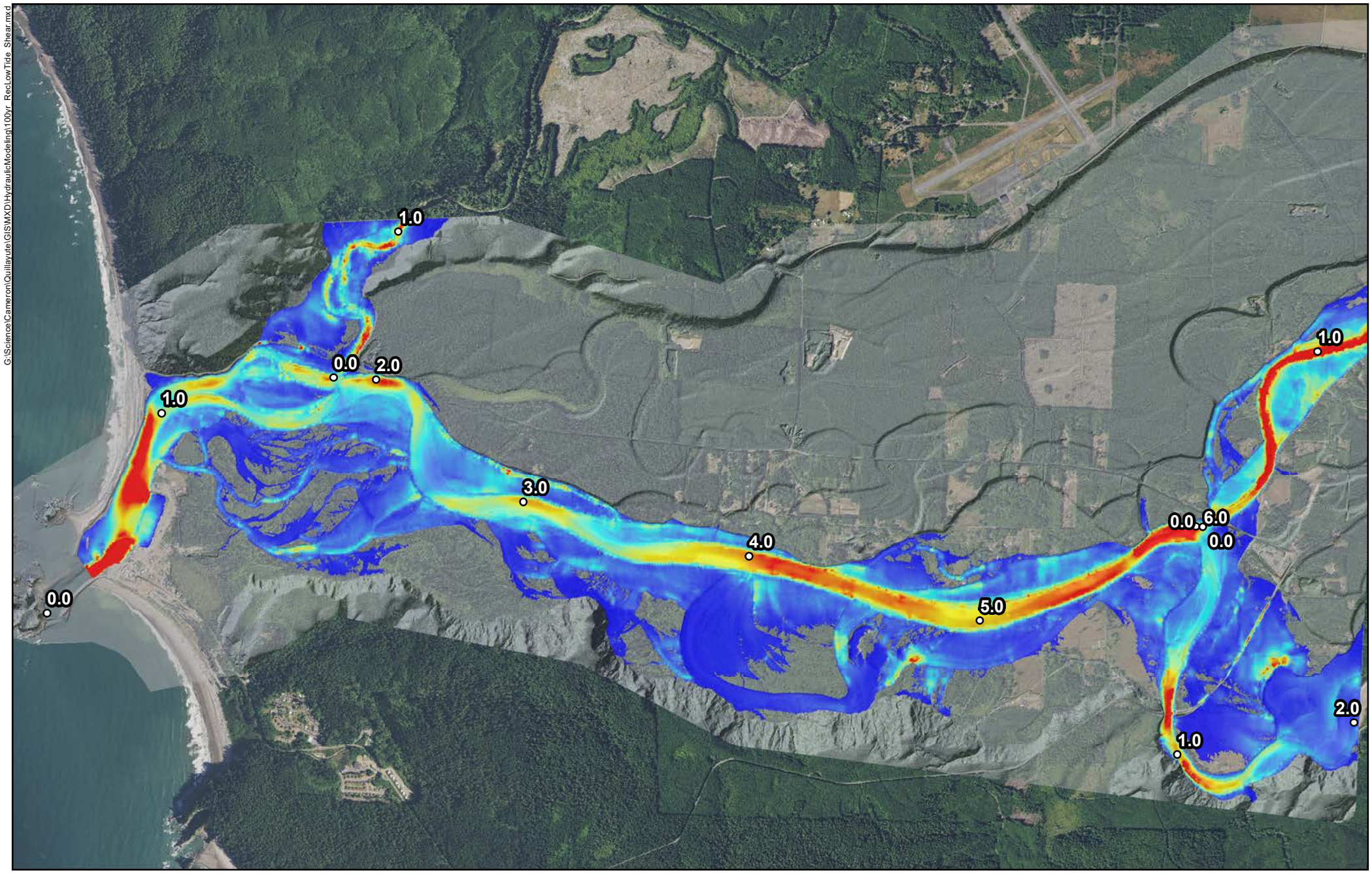

G:\Science\Cameron\Quillayute\GIS\MXD\HydraulicModeling\100yr_RecLowTide_Shear.mxd

Shear Stress (lb/sq. ft.)

High : 9.6

Low : 0

River Miles

Quillayute River Flow: 131, 500 cfs

Low Tide: -4.25 ft. (NAVD88) High Tide: 13.5 ft. (NAVD88)

Quillayute River
Geomorphic Assessment

Hydraulic Modeling
100 Year Flow
Record Low Tide
Figure B-12

TETRA TECH

N
W E
S

0 3,500 7,000
Feet

APPENDIX C – AVULSION RISK RATING ANALYSIS

Quillayute River Project
Geomorphic Assessment and Action Plan
Avulsion Risk Rating Analysis

Appendix C

Submitted to:

Quileute Natural Resources
401 Main Street
La Push, WA 98350

Submitted by:

19803 North Creek Parkway
Bothell, WA 98011
Tel 425.482.7600 | Fax 425.482.7652
www.tetratech.com

September 2020

1. INTRODUCTION

Below is an explanation of each of the factors that went into the avulsion risk analysis. Following the description of each of the factors, the equation for calculating the risk is explained in further detail.

2. Factors

The following section describes the different factors that were used to determine the avulsion risk equation for the identified avulsion pathways.

P_Slope

The slope of the identified avulsion pathways was calculated based on the 2019 topobathymetric LiDAR data collected. This was used in a comparison of the existing channel slope (*E_Slope*).

E_Slope

Existing slope was calculated for the current mainstem of the river starting at the inlet for the identified avulsion pathway and ending at the outlet for the pathway. Each slope was ranked from 1 to 15 with the highest slope being 15 and lowest slope being 1. Existing slope compared to the avulsion pathway slope (*P_Slope*) was also compared.

Slope_Dif

The slope difference was calculated by dividing the avulsion pathway slope by the existing channel slope. Slingerland and Smith (1998) identified avulsion risk as "high" when the avulsion pathway slope is more than 4 times that of the existing channel slope and "moderate" when greater than 2. Any differences greater than 4 were given a rating of 3, between 2 and 4 a rating of 2, and less than 2 a rating of 1.

P_In_Out_Dif

The difference between the avulsion path inlet and outlet was calculated based on the 2019 topobathymetric LiDAR. This measurement was used to further identify the avulsion paths with the greatest change in hydraulic gradient presenting the greater likelihood of avulsion via hydraulic "benefit".

AHA_Veg_Avg_Height

The average canopy height was calculated for each of the Avulsion Hazard Areas. The average canopy height was used as a determining factor in the roughness in the floodplain associated with the avulsion pathways. Higher roughness decreases the likelihood of avulsion. Average canopy height greater than 60 ft. was given a weight factor of 0.5. Canopy height between 30 and 60 feet was given a weight factor of 0.75. Canopy height of less than 30 feet was given a weight factor of 1.

AHA_Mannings

The hydraulic model used for the Assessment has an associated Land Use.shp file that contains the mapped land use and associated Manning's roughness value used in the model. The Manning's roughness factor for each AHA was determined by multiplying the percent of the AHA occupied by the land use type with associated roughness value and adding that to the product of the percent of the AHA occupied by other land use types and their associated roughness values. For example, if 80% of the AHA was labeled as "Forest" and 20% was labeled as "Ag", then the Manning's roughness value used in the calculation would be (0.08*0.80) + (0.045*0.20). Roughness values greater than 0.07 were given a weight factor of 0.5. Values between 0.06 and 0.07 were given a weight factor of 0.75. Values less than 0.60 were given a weight factor of 1.

P_Relative_Elev_19

The average relative elevation (2019) of each avulsion pathway was measured. Pathways with low relative elevations were ranked higher in risk of avulsion due to the fact that lower relative elevation means more frequent inundation.

2018_WSE_to_In

The 2018 water surface elevation compared to the elevation of the inlet of the avulsion pathways was measured for each pathway. Pathways with a lower difference in elevation between the water surface and the inlet were ranked more likely to factor into an avulsion.

100Yr_Avg_Depth

The average depth of the 100 Year Modeled flow was measured along the avulsion pathways. The 100-year modeled flow depth was extracted as the maximum depth from both the 100-year flow with low tide and from the 100-year flow with high tide. This is a more conservative approach to the 100-year modeled flow depth. Average modeled flow depths were ranked from highest average depth (highest risk) to lowest average depth (lowest risk).

100Yr_WSE_Slope

The water surface elevation slope was calculated for each of the avulsion pathways based on the 100-year modeled flow events. Again, the water surface elevation was extracted as the maximum water surface elevation from both the 100-year flow with low tide and from the 100-year flow with high tide.

100Yr_In_Out_Dif

The difference between the inlet and outlet of the 100-year flow water surface elevation was calculated for each avulsion pathway. Those pathways with a higher difference between the inlet and the outlet were ranked as more likely for avulsion than those with lower difference values.

100Yr_Max_V

The maximum velocity from the 100-year modeled flow was measured along the avulsion pathways. Increased water velocities increase the likelihood of erosion and therefore of avulsion in the pathways. The 100-year modeled flow velocity was based on the highest flow velocity values from the 100-year flow at high tide and the 100-year flow at low tide.

100Yr_Avg_V

The average velocity from the 100-year modeled flow was measured along the avulsion pathways. Increased water velocities increase the likelihood of erosion and therefore of avulsion in the pathways. The 100-year modeled flow velocity was based on the highest flow velocity values from the 100-year flow at high tide and the 100-year flow at low tide.

100Yr_Max_SS

The maximum shear stress from the 100-year modeled flow was measured along the avulsion pathways. Increased shear stress increases the likelihood of erosion and therefore of avulsion in the pathways. The 100-year modeled flow shear stress was based on the highest flow shear stress values from the 100-year flow at high tide and the 100-year flow at low tide.

100Yr_Avg_SS

The average shear stress from the 100-year modeled flow was measured along the avulsion pathways. Increased shear stress increases the likelihood of erosion and therefore of avulsion in the pathways. The 100-year modeled flow shear stress was based on the highest flow shear stress values from the 100-year flow at high tide and the 100-year flow at low tide.

Risk_Rating

In order to identify the avulsion pathways at highest risk of increased inundation, the ranking of each of the above factors was taken into consideration. The rating is based on the average ranking of P_In_Out_Dif, 100Yr_Avg_Depth, 100Yr_WSE_Slope, 100Yr_Avg_V, and 100Yr_Avg_SS plus the average of P_Relative_Elev_19 and 2018_WSE_to_In, and multiplied by the weight factors of Slope_Dif, AHA_Veg_Avg_Height, and AHA_Mannings.

3. Risk Rating Equation

The following section describes how the factors described above were used in the calculation of the avulsion risk rating.

$$\text{Risk\_Rating} =$$

1.

$$[average(P\_In\_Out\_Dif, 100Yr\_Avg\_Depth, 100Yr\_WSE\_Slope,$$

$$100Yr\_In\_Out\_Dif, 100Yr\_Avg\_V, 100Yr\_Avg\_SS) +$$

2.

$$average(P\_Relative\_Elev\_19, 2018\_WSE\_to\_In)] \times$$

3.

$$(Slope\_Dif \times AHA\_Veg\_Avg\_Height \times AHA\_Mannings)$$

Where:

1. Compiles the average ranking of the avulsion pathway based on the difference between the pathway inlet and outlet, average 100-year flow depth, WSE slope, WSE slope inlet and outlet difference, average velocity, and average shear stress. This part of the equation gives a rating of the difference between the inlet and outlet (i.e. gradient) of the avulsion pathway and the predicted gradient of the 100-year flow WSE alongside the average depth, velocity, and shear stress at the 100-year flow. Increased avulsion pathway gradient and increased differences between the inlet and outlet of the pathways along with higher flow values lead to an increased likelihood of avulsion in the pathway. This is then added to:

2. The average ranking of the avulsion pathway based on average relative elevation of the pathway and the average ranking of the difference in height between the 2018 water surface and the avulsion pathway inlet. This part of the equation gives a rating of the elevation of the pathway above the active channel. Lower relative elevations and lower inlet elevations compared to the active channel increase the likelihood of avulsion. This number is then multiplied by:

3. The weighted factors of the difference in slope between the avulsion pathway and the existing channel, the average height of vegetation in the avulsion hazard area (AHA), and the Manning's roughness of the AHA. Differences in slope between the avulsion pathway and the existing channel were found to need to be at least a factor of 4 to incite avulsion in crevasse splays on the bank (Slingerland and Smith 1998). Increasing roughness in the channel and in the floodplain decreases the likelihood of a full avulsion as the velocity and shear stress exerted on the pathway is decreased.

Based on quantile sorting of the risk rating data, values less than 8.6 are rated as low risk of increased inundation, values between 8.6 and 11.5 are rated as moderate, and values greater than 11.5 are rated as high.

4. Reoccupation Risk Rating Equation

To calculate the probability and risk of an avulsion pathway being reoccupied by the mainstem channel, a Reoccupation Risk Rating equation was developed. Based on channel migration analysis mapping, pathways with historic channels never mapped or mapped in 1883 by the General Land Office (GLO) surveys were given a risk factor of 0.5. Pathways with historic channels mapped between 1955 and 1990 were given a risk factor of 0.75. Pathways with historic channels mapped between 2002 and 2017 were given a risk factor or 1 (Table 1). These risk factors were then multiplied by the **Risk_Rating** values previously calculated to characterize the reoccupation risk rating for each avulsion pathway.

Table 1. Reoccupation Risk Factors Based on Historic Channel Mapping Dates

Historic Channel Date	Risk Factor
N/A (Not mapped), 1883	0.5
1955 – 1990	0.75
2002 – 2017	1

Path ID	Avulsion Pathway Slope	Existing Channel Slope	Slope Difference	Avulsion Path Inlet/Outlet Difference (ft)	AHA Vegetation Avg. Height (ft)	AHA Mannings Roughness
PID	P_Slope	E_Slope	Slope_Dif	P_In_Out_Dif	AHA_Veg_Avg_Height	AHA_Mannings
Q1	-7.11E-05	2	1	1	0.50	0.50
Q2	6.01E-04	5	1	8	0.50	0.50
Q3	7.48E-04	5	1	12	0.50	0.50
Q4	7.47E-04	8	1	14	0.50	0.50
Q5	4.19E-04	4	1	6	0.50	0.50
Q6	2.72E-03	22	1	27	0.75	0.75
Q7	1.59E-03	19	1	16	0.75	0.75
Q8	6.79E-04	9	1	11	0.75	0.50
Q9	2.08E-04	3	1	4	0.75	0.50
Q10	8.08E-04	10	1	25	0.50	0.75
Q11	8.23E-04	10	1	25	0.50	0.75
Q12	3.48E-04	16	1	9	0.50	0.75
Q13	6.73E-08	1	1	2	0.50	0.75
Q14	6.84E-04	12	1	19	0.50	0.75
Q15	7.01E-04	12	1	19	0.50	0.75
Q16	1.24E-03	12	1	21	0.50	0.50
Q17	1.32E-03	12	1	22	0.50	0.50
B1	5.38E-01	29	1	18	1.00	1.00
B2	6.58E-03	28	1	24	1.00	0.50
B3	1.16E-03	17	1	7	1.00	0.75
B4	2.81E-03	20	1	17	0.75	1.00
B5	4.76E-03	21	2	23	0.75	0.50
B6	3.96E-03	26	1	13	1.00	1.00
B7	4.25E-03	23	1	15	1.00	1.00
B8	1.25E-03	18	1	10	1.00	1.00
SD1	3.60E-03	24	1	28	0.75	0.50
SD2	3.21E-03	24	1	28	0.75	0.50
D1	2.00E-04	7	1	3	0.75	0.50
D2	4.55E-03	27	1	5	1.00	0.50

Avulsion Path Average Relative Elevation (2019) (ft)	2018 WSE to Inlet Elevation (ft)	100 Year Flow Average Inundation Depth (ft)	100 Year Flow WSE Pathway Slope	100 Year Flow WSE Inlet/Outlet Difference (ft)
P_Relative_Elev_19	2018_WSE_to_In	100Yr_Avg_Depth	100Yr_WSE_Slope	100Yr_In_Out_Dif
6	22	11	16	8
13	22	16	8	11
16	22	19	7	10
17	18	18	5	13
19	19	20	6	14
27	28	26	15	16
21	7	15	21	19
10	2	12	22	24
9	2	14	23	21
6	5	6	17	28
8	9	7	18	28
11	9	8	14	27
22	9	13	4	12
14	9	9	12	25
15	9	10	13	25
18	8	17	9	17
20	16	21	24	15
29	25	29	2	1
2	6	5	25	9
25	26	27	10	7
2	1	3	28	18
1	4	1	29	20
12	20	23	11	5
23	17	24	3	2
24	21	28	1	4
5	14	4	27	22
4	14	2	26	22
26	29	22	20	6
28	27	25	19	3

100 Year Flow Average Velocity (ft/s)	100 Year Flow Average Shear Stress (lbs/sq. ft.)	Increased Inundation Risk Rating	Increased Inundation Risk (High, Moderate, Low)	Reoccupation Risk Rating	Reoccupy_Risk (High, Moderate, Low)
100Yr_Avg_V	100Yr_Avg_SS	Risk_Rating	Riv_Risk	Reoccupy_Rating	Reoccupy_Risk
12	13	6.0	Low	3.0	Low
16	17	7.5	Low	3.8	Low
20	18	8.3	Low	4.2	Low
18	19	8.0	Low	4.0	Low
24	26	8.8	Moderate	4.4	Low
29	27	28.6	High	21.4	High
28	23	19.3	High	14.5	High
11	14	8.1	Low	4.1	Low
15	20	8.1	Low	4.1	Low
3	5	7.3	Low	5.5	Moderate
6	10	9.1	Moderate	6.8	Moderate
7	8	8.3	Low	6.2	Moderate
10	6	8.8	Moderate	6.6	Moderate
2	2	8.6	Moderate	6.5	Moderate
9	9	9.8	Moderate	7.4	Moderate
21	24	7.8	Low	3.9	Low
25	25	10.0	Moderate	5.0	Low
19	12	40.5	High	30.4	High
17	15	9.9	Moderate	5.0	Low
22	16	30.3	High	30.3	High
4	4	10.4	Moderate	5.2	Moderate
1	3	11.5	Moderate	5.8	Moderate
27	21	32.7	High	32.7	High
14	7	30.8	High	30.8	High
8	1	31.2	High	31.2	High
13	22	10.8	Moderate	5.4	Moderate
5	11	9.3	Moderate	4.6	Low
26	29	16.9	High	12.7	High
23	28	22.3	High	16.8	High

APPENDIX D – RELATIVE ELEVATION MODEL (REM) MAPPING

Quillayute River Project
Geomorphic Assessment and Action Plan
Relative Elevation Model (REM) Mapping

Appendix D

Submitted to:

Quileute Natural Resources
401 Main Street
La Push, WA 98350

Submitted by:

TETRA TECH

19803 North Creek Parkway
Bothell, WA 98011
Tel 425.482.7600 | Fax 425.482.7652
www.tetratech.com

September 2020

LIST OF FIGURES

Figure D-1. ..... Relative Elevation Model Overview 2019
Figure D-2. ..... Reach 1 Relative Elevation Model 2019
Figure D-3. ..... Reach 2 Relative Elevation Model 2019
Figure D-4. ..... Reach 3 Relative Elevation Model 2019
Figure D-5. ..... Reach 4 Relative Elevation Model 2019
Figure D-6. ..... Reach 5 Relative Elevation Model 2019
Figure D-7. ..... Reach 6 Relative Elevation Model 2019
Figure D-8. ..... Lower Bogachiel Relative Elevation Model 2019
Figure D-9. ..... Lower Sol Duc Relative Elevation Model 2019
Figure D-10. ..... Lower Dickey Relative Elevation Model 2019

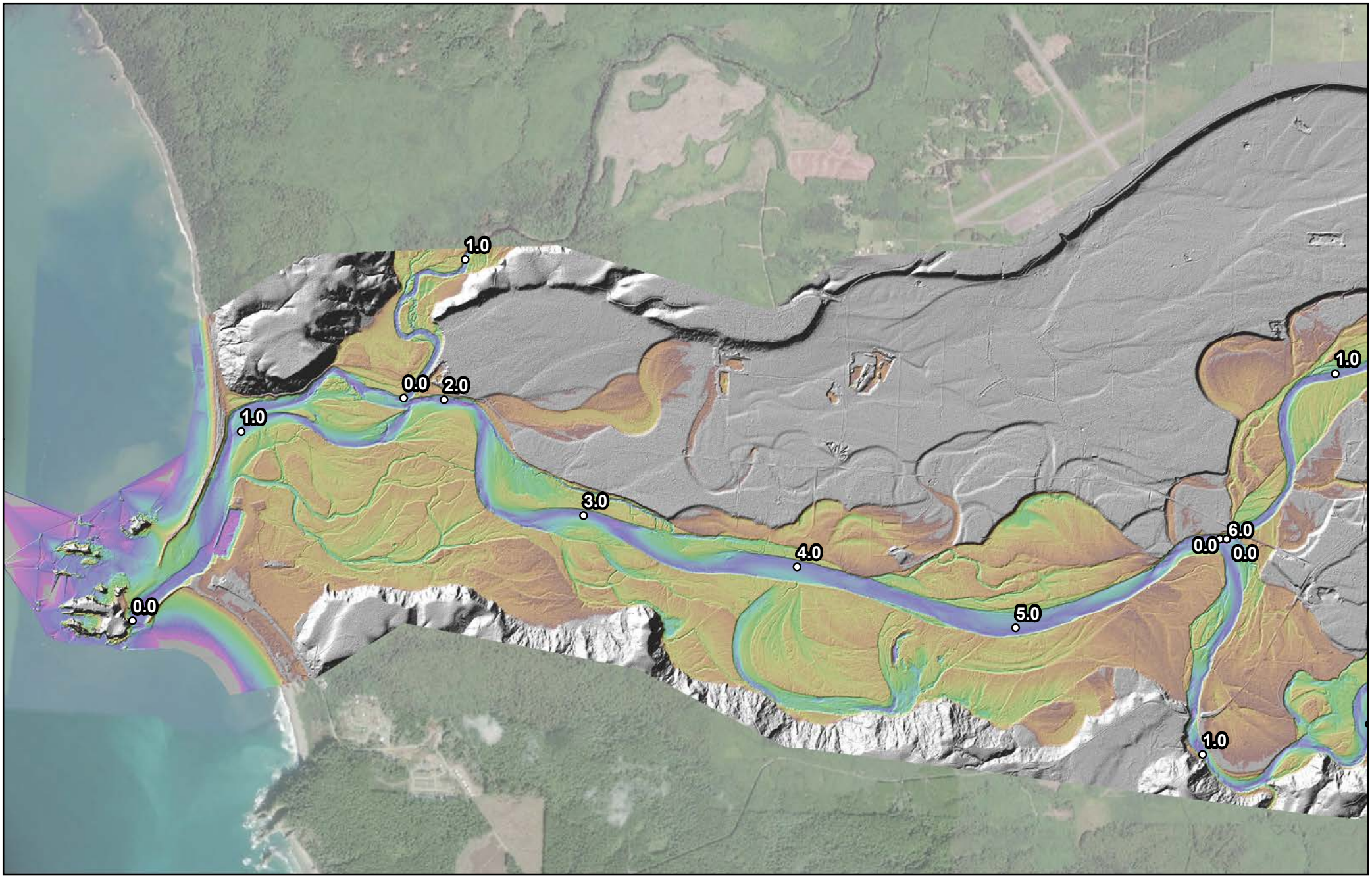

River Miles

Relative Elevation Model

Height Above Channel Bottom (ft)

High : 25

Low : -5

Quillayute River Geomorphic Assessment

Relative Elevation Model
2019 Topobathymetric LiDAR

Figure D-1

TETRA TECH

N
W E
S

0 3,000 6,000

Feet

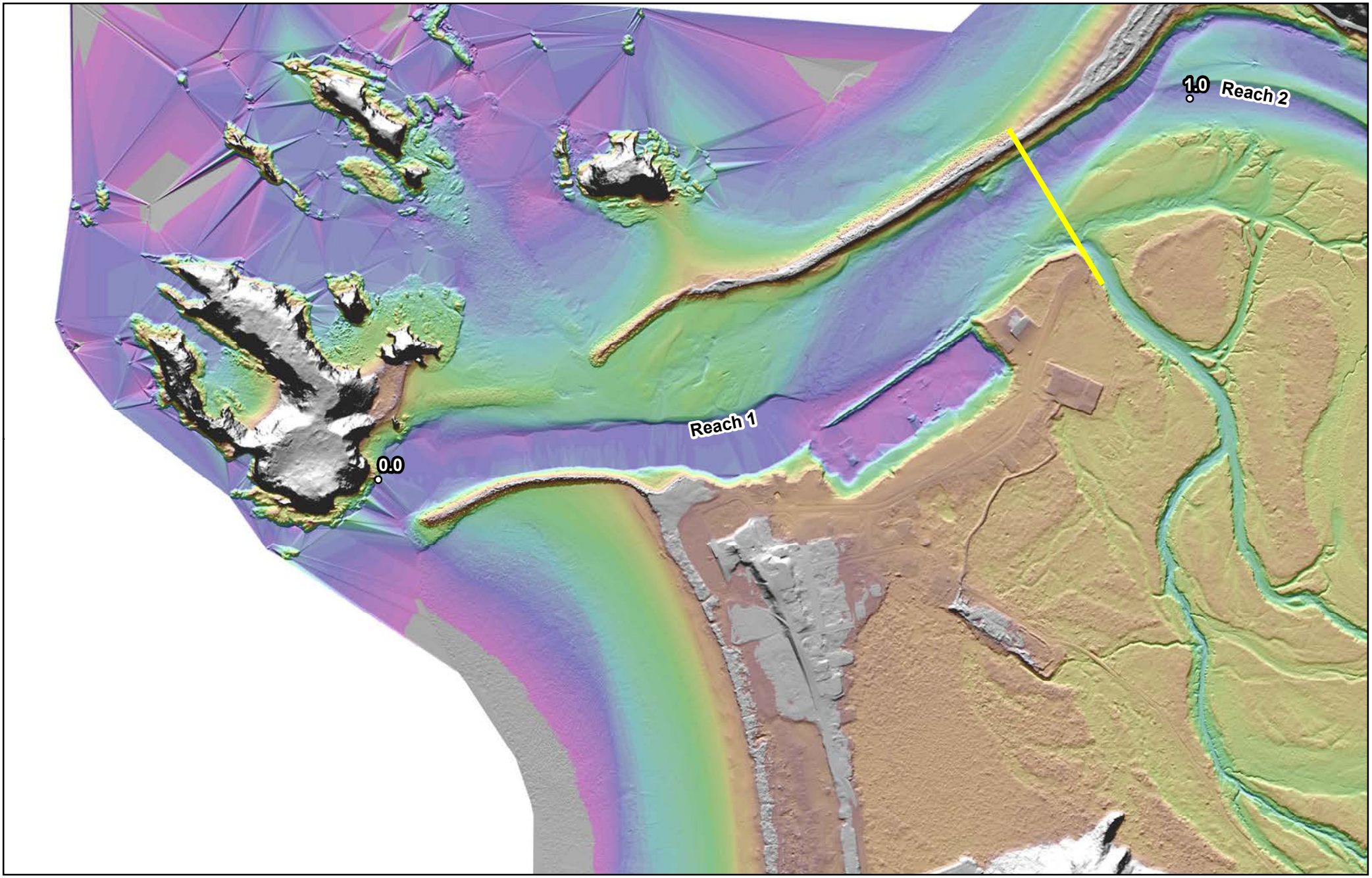

Relative Elevation Model

Height Above Channel Bottom (ft)

High : 25

Low : -5

River Miles

Geomorphic Reaches

Quillayute River Geomorphic Assessment

Relative Elevation Model
2019 Topobathymetric LiDAR
Reach 1

Figure D-2

TETRA TECH

N
W
E
S

0 750 1,500

Feet

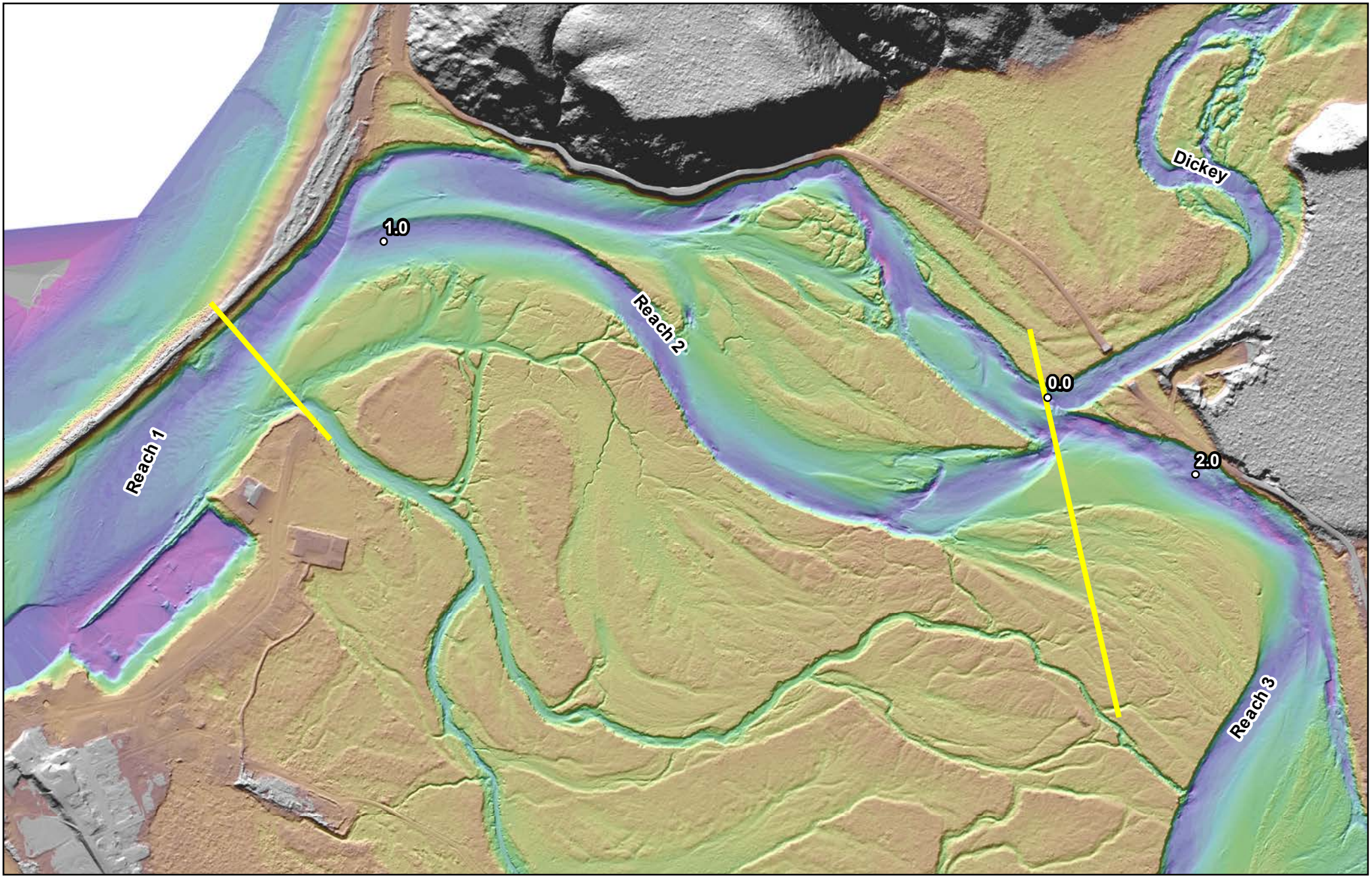

Relative Elevation Model

Height Above Channel Bottom (ft)

High : 25

Low : -5

River Miles

Geomorphic Reaches

Quillayute River Geomorphic Assessment

Relative Elevation Model
2019 Topobathymetric LiDAR
Reach 2
Figure D-3

TETRA TECH

N
W
E
S

0 750 1,500

Feet

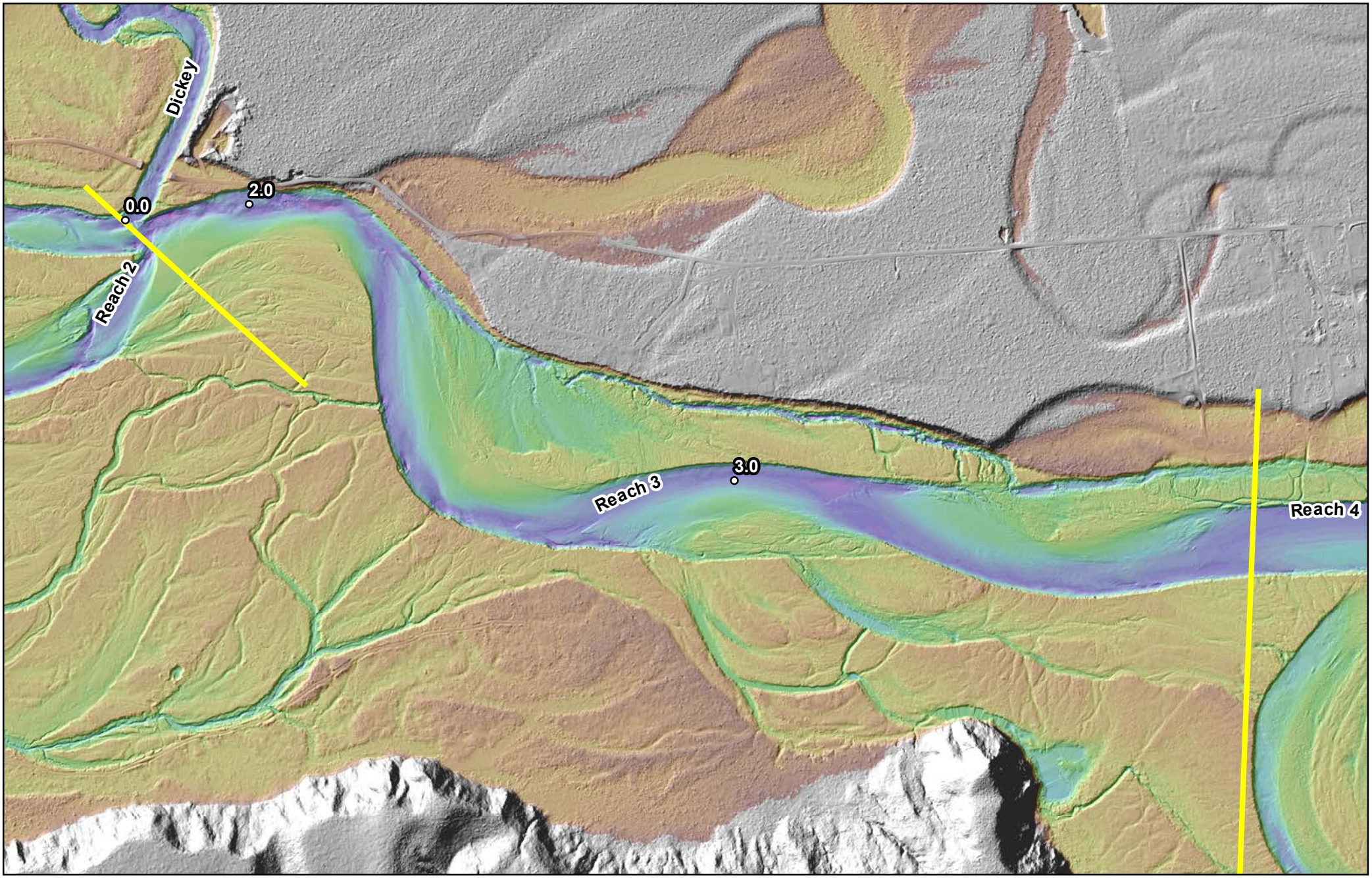

Relative Elevation Model

Height Above Channel Bottom (ft)

High : 25

Low : -5

River Miles

Geomorphic Reaches

Quillayute River Geomorphic Assessment

Relative Elevation Model
2019 Topobathymetric LiDAR
Reach 3
Figure D-4

TETRA TECH

N
W
E
S

0 1,000 2,000

Feet

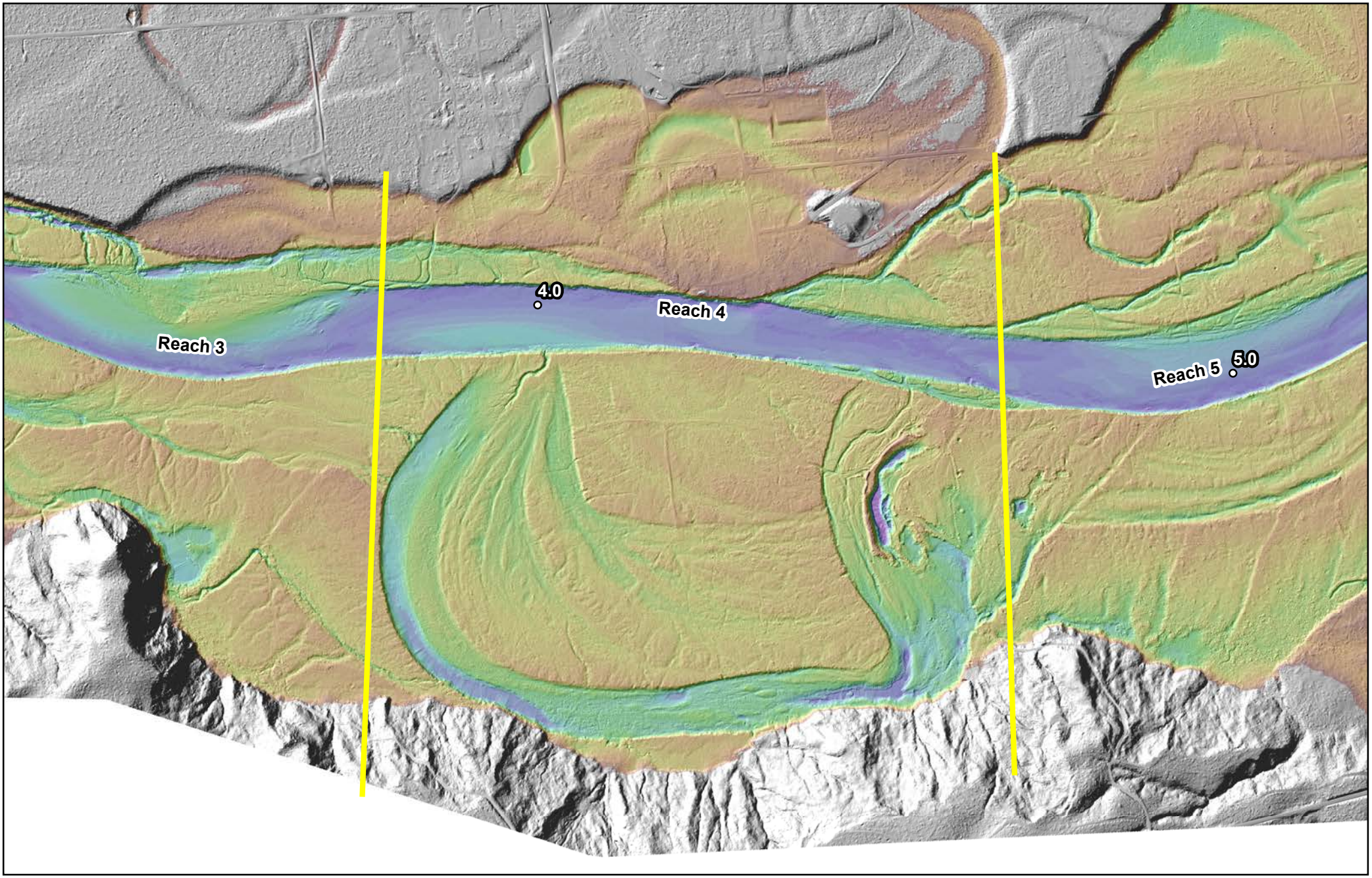

Relative Elevation Model

Height Above Channel Bottom (ft)

High : 25

Low : -5

River Miles

Geomorphic Reaches

Quillayute River Geomorphic Assessment

Relative Elevation Model
2019 Topobathymetric LiDAR
Reach 4
Figure D-5

TETRA TECH

N
W
E
S

0 1,000 2,000

Feet

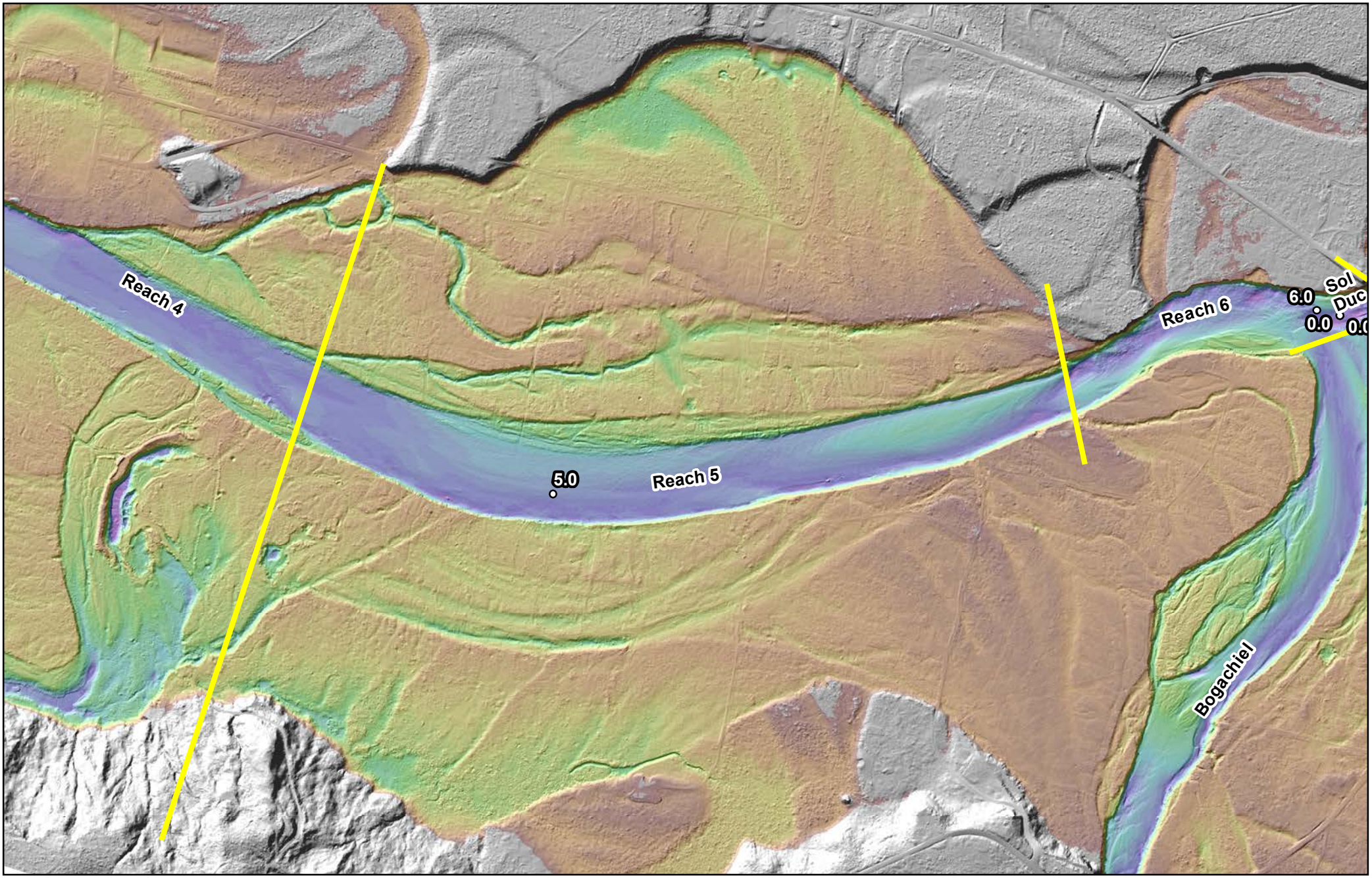

Relative Elevation Model

Height Above Channel Bottom (ft)

High : 25

Low : -5

River Miles

Geomorphic Reaches

Quillayute River Geomorphic Assessment

Relative Elevation Model
2019 Topobathymetric LiDAR
Reach 5
Figure D-6

TETRA TECH

N
W
E
S

0 875 1,750

Feet

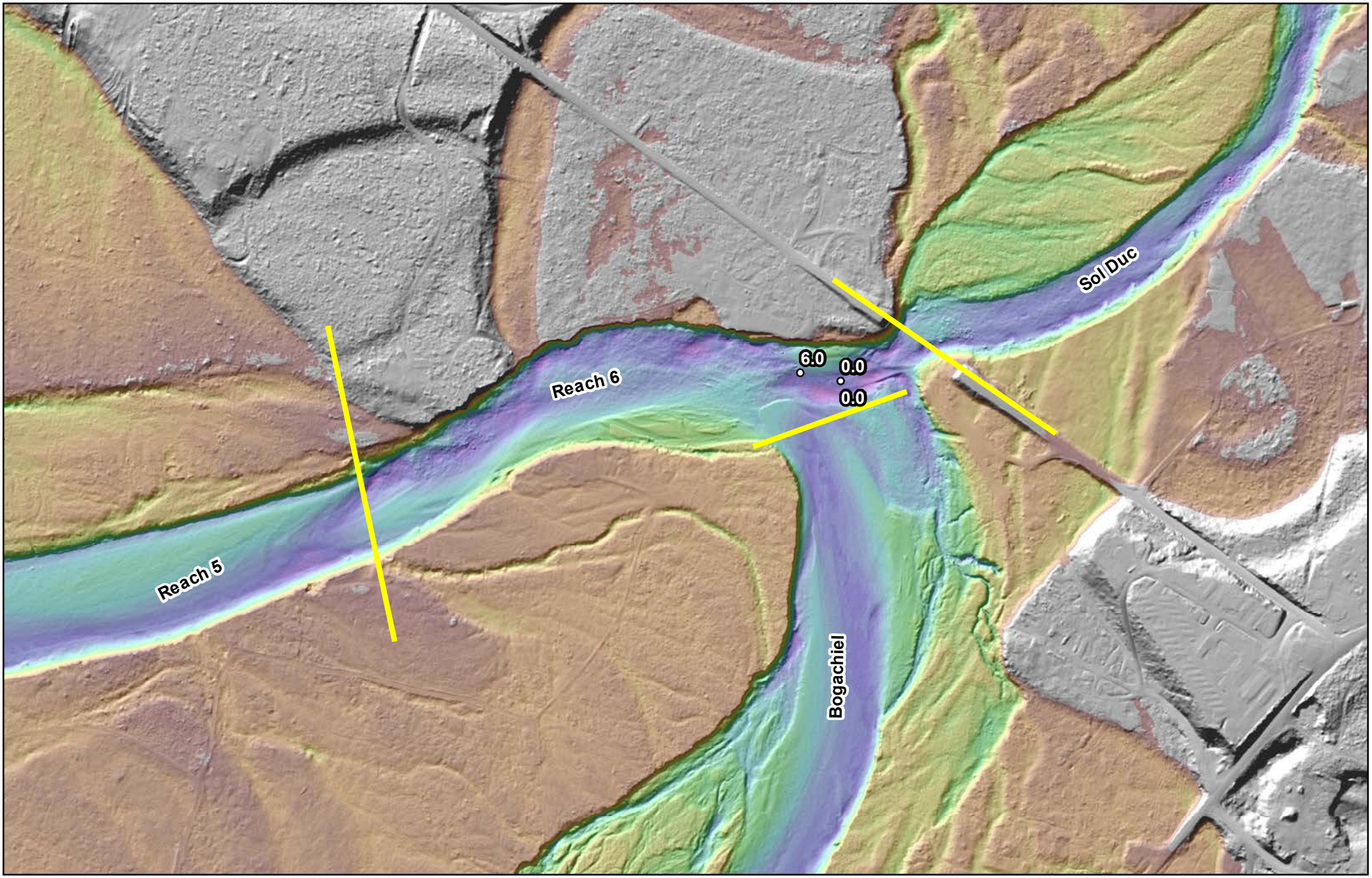

Relative Elevation Model

Height Above Channel Bottom (ft)

High : 25

Low : -5

River Miles

Geomorphic Reaches

Quillayute River Geomorphic Assessment

Relative Elevation Model
2019 Topobathymetric LiDAR
Reach 6

Figure D-7

TETRA TECH

N
W
E
S

0 500 1,000

Feet

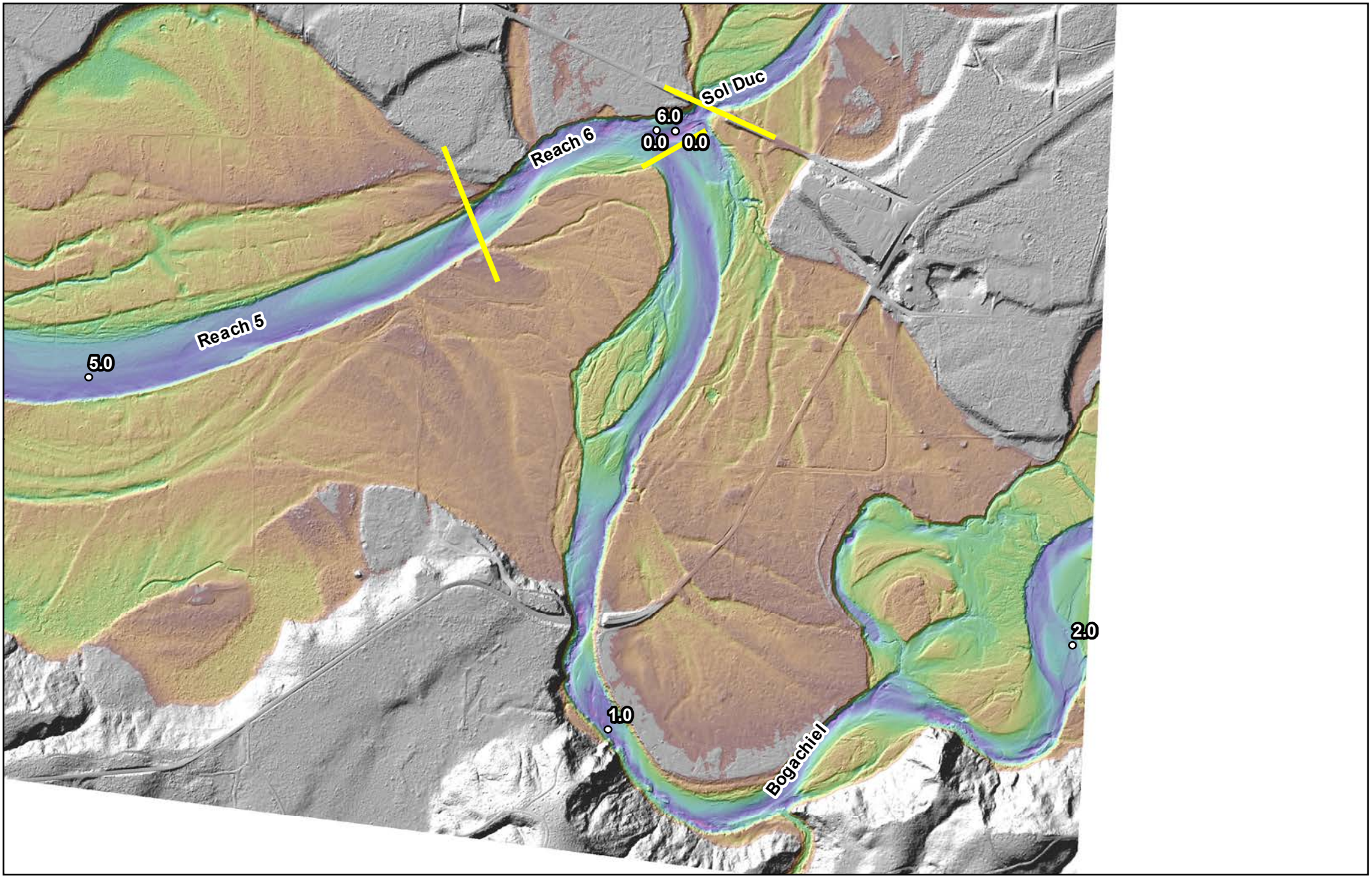

Relative Elevation Model

Height Above Channel Bottom (ft)

High : 25

Low : -5

River Miles

Geomorphic Reaches

Quillayute River Geomorphic Assessment

Relative Elevation Model
2019 Topobathymetric LiDAR
Lower Bogachiel River
Figure D-8

TETRA TECH

N
W E
S

0 1,000 2,000

Feet

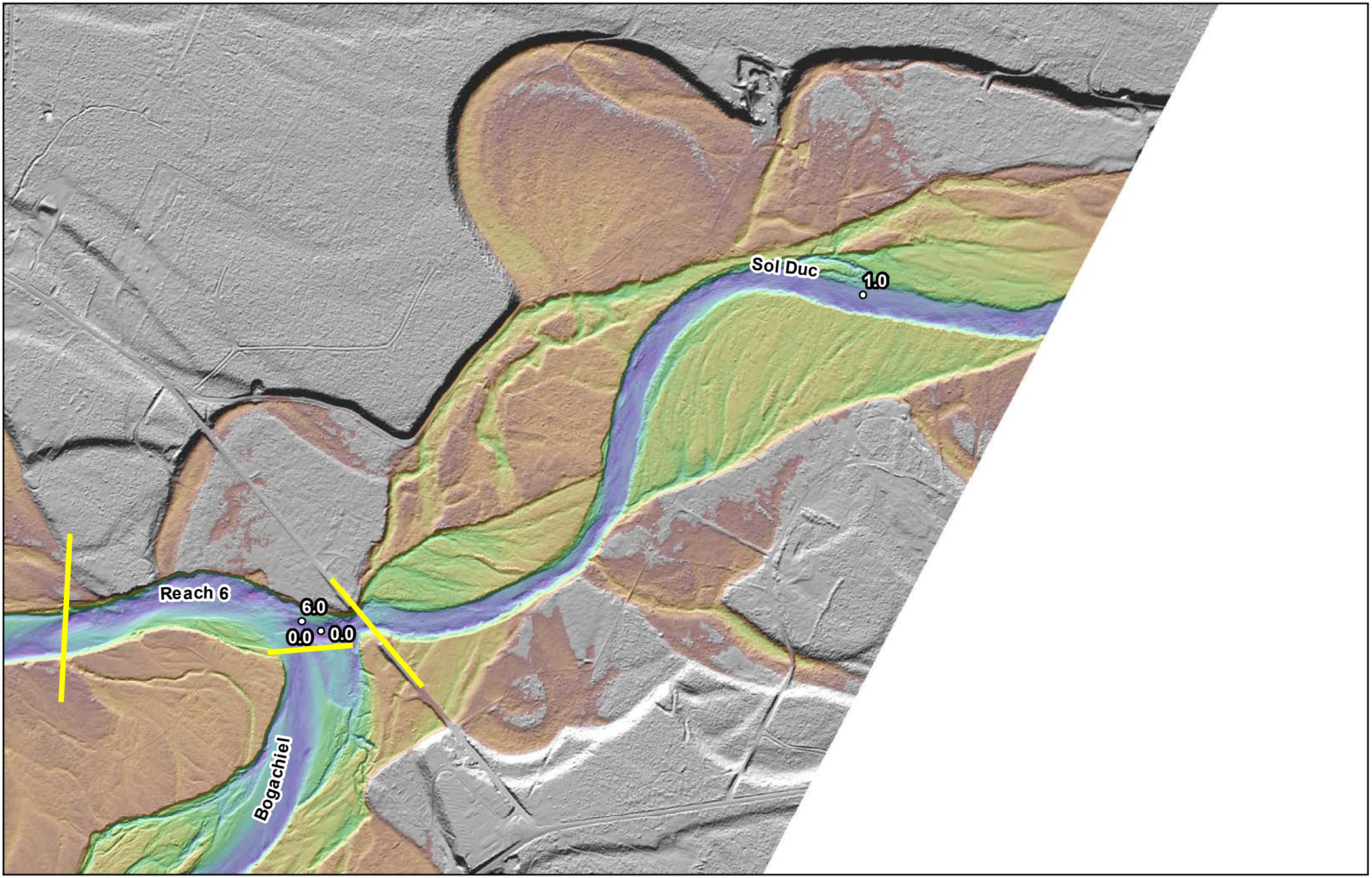

Relative Elevation Model

Height Above Channel Bottom (ft)

High : 25

Low : -5

River Miles

Geomorphic Reaches

Quillayute River Geomorphic Assessment

Relative Elevation Model
2019 Topobathymetric LiDAR
Lower Sol Duc River

Figure D-9

TETRA TECH

N
W
E
S

0 1,000 2,000

Feet

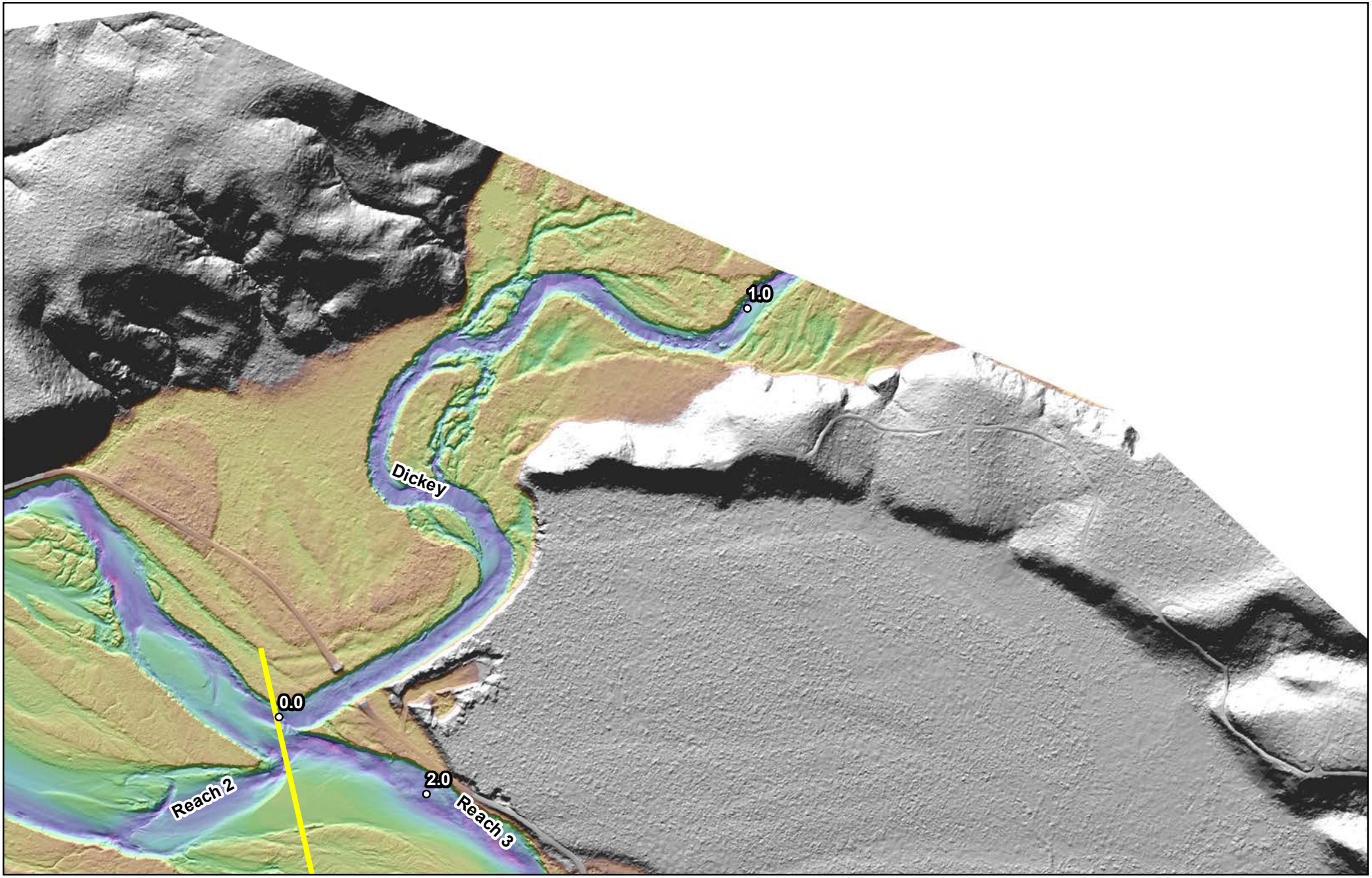

Relative Elevation Model

Height Above Channel Bottom (ft)

High : 25

Low : -5

River Miles

Geomorphic Reaches

Quillayute River Geomorphic Assessment

Relative Elevation Model
2019 Topobathymetric LiDAR
Lower Dickey River

Figure D-10

TETRA TECH

N
W
E
S

0 750 1,500

Feet

APPENDIX E – CANOPY COVERAGE MAPPING

Quillayute River Project
Geomorphic Assessment and Action Plan
Canopy Coverage Mapping

Appendix E

Submitted to:

Quileute Natural Resources
401 Main Street
La Push, WA 98350

Submitted by:

TETRA TECH

19803 North Creek Parkway
Bothell, WA 98011
Tel 425.482.7600 | Fax 425.482.7652
www.tetratech.com

September 2020

LIST OF FIGURES

Figure E-1. Canopy Cover Height Assessment Overview
Figure E-2. Canopy Cover Height Reach 1
Figure E-3. Canopy Cover Height Reach 2
Figure E-4. Canopy Cover Height Reach 3
Figure E-5. Canopy Cover Height Reach 4
Figure E-6. Canopy Cover Height Reach 5
Figure E-7. Canopy Cover Height Reach 6
Figure E-8. Canopy Cover Height Lower Bogachiel River
Figure E-9. Canopy Cover Height Lower Sol Duc River
Figure E-10. Canopy Cover Height Lower Dickey River

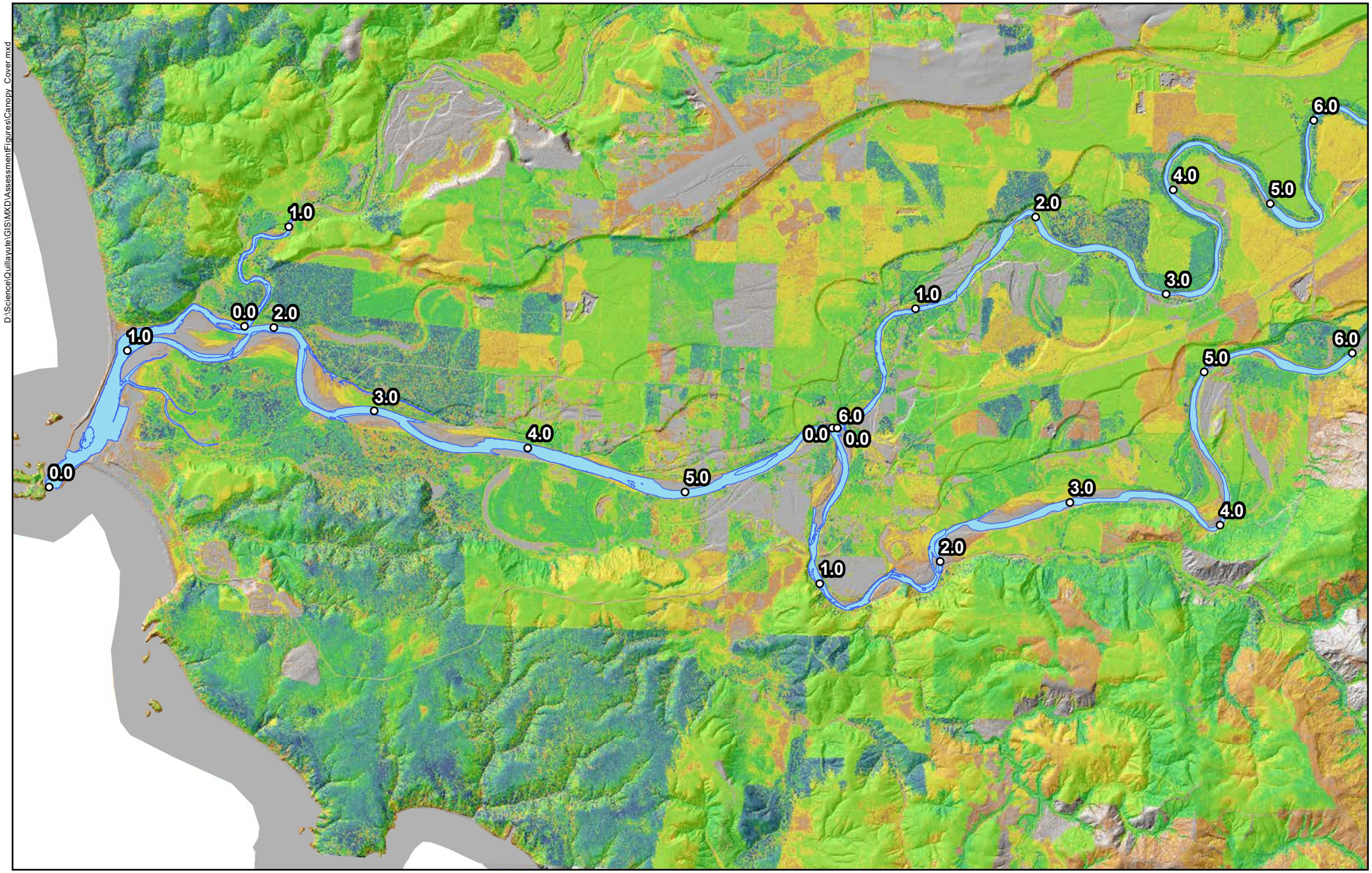
D:\Science\Quillayute\GIS\MXD\AssessmentFigures\Canopy_Cover.mxd
0.0
1.0
2.0
3.0
4.0
5.0
6.0
Canopy Cover Height (feet)
0 - 3
3 - 15
15 - 25
25 - 50
50 - 80
80 - 100
100 - 120
120 - 140
140 +
River Miles
Quillayute River
Geomorphic Assessment
Canopy Cover Height
2018 LiDAR
Figure E-1
TETRA TECH
N
W
E
S
0
5,000
10,000
Feet

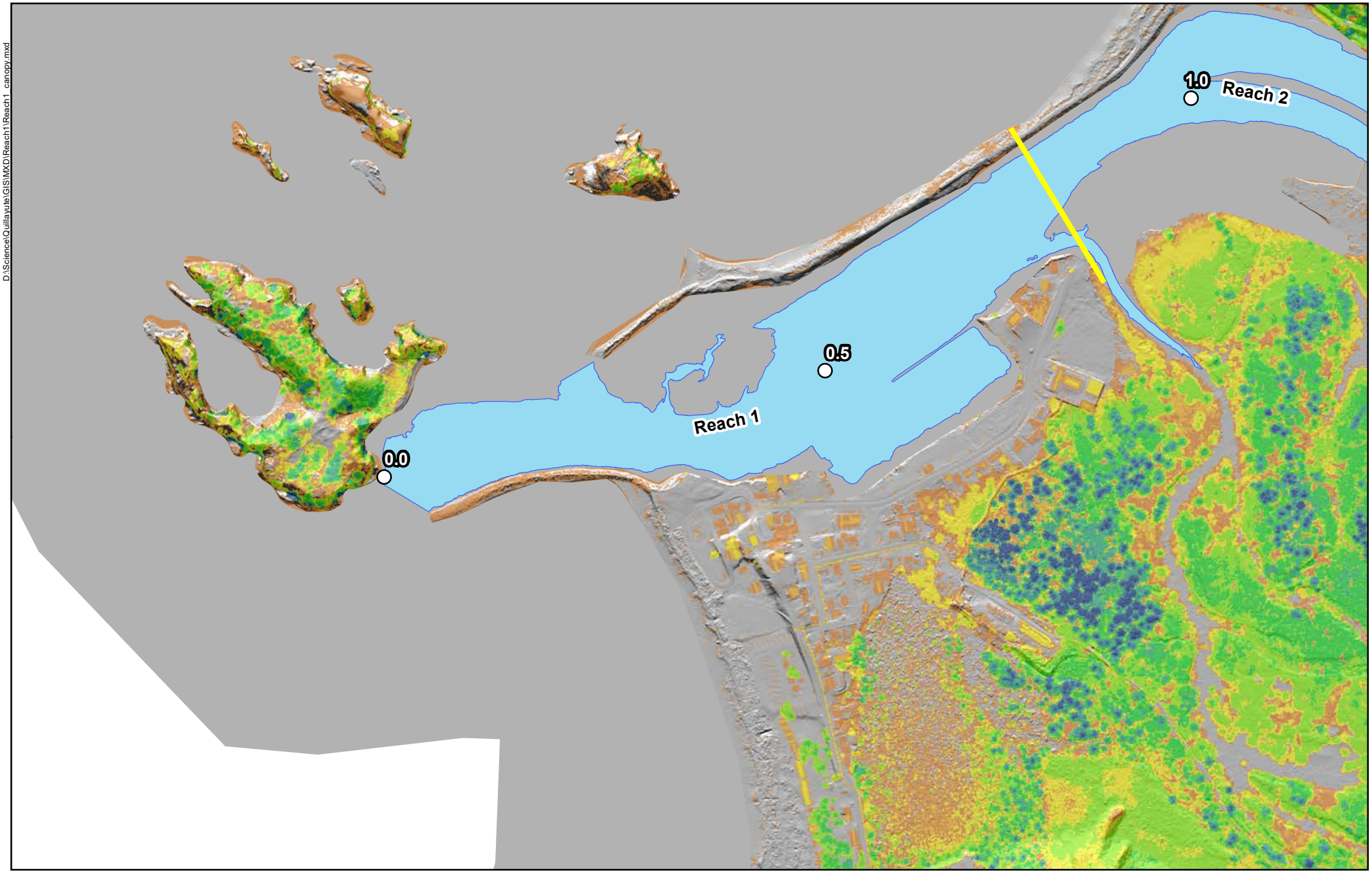

Canopy Cover Height (feet)

- 0 - 3
- 3 - 15
- 15 - 25
- 25 - 50
- 50 - 80
- 80 - 100
- 100 - 120
- 120 - 140
- 140 +
- River Miles

Quillayute River Geomorphic Assessment

Canopy Cover
2018 LiDAR
Reach 1
Figure E-2

TETRA TECH

N W E S

0 750 1,500
Feet

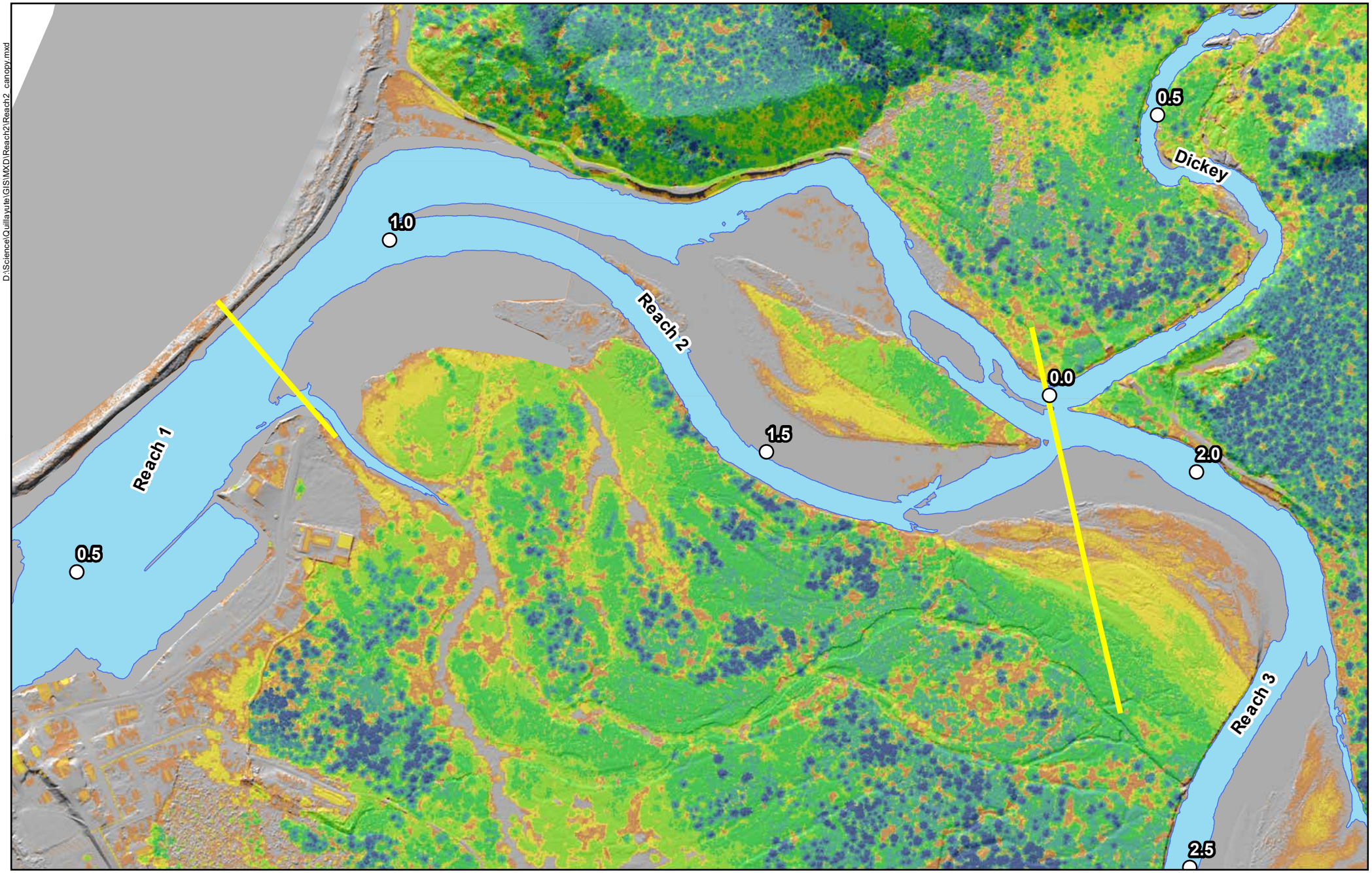

Canopy Cover Height (feet)

- 0 - 3
- 3 - 15
- 15 - 25
- 25 - 50
- 50 - 80
- 80 - 100
- 100 - 120
- 120 - 140
- 140 +
- River Miles

Quillayute River Geomorphic Assessment

Canopy Cover
2018 LiDAR
Reach 2
Figure E-3

TETRA TECH

N
W
E
S

0 750 1,500
Feet

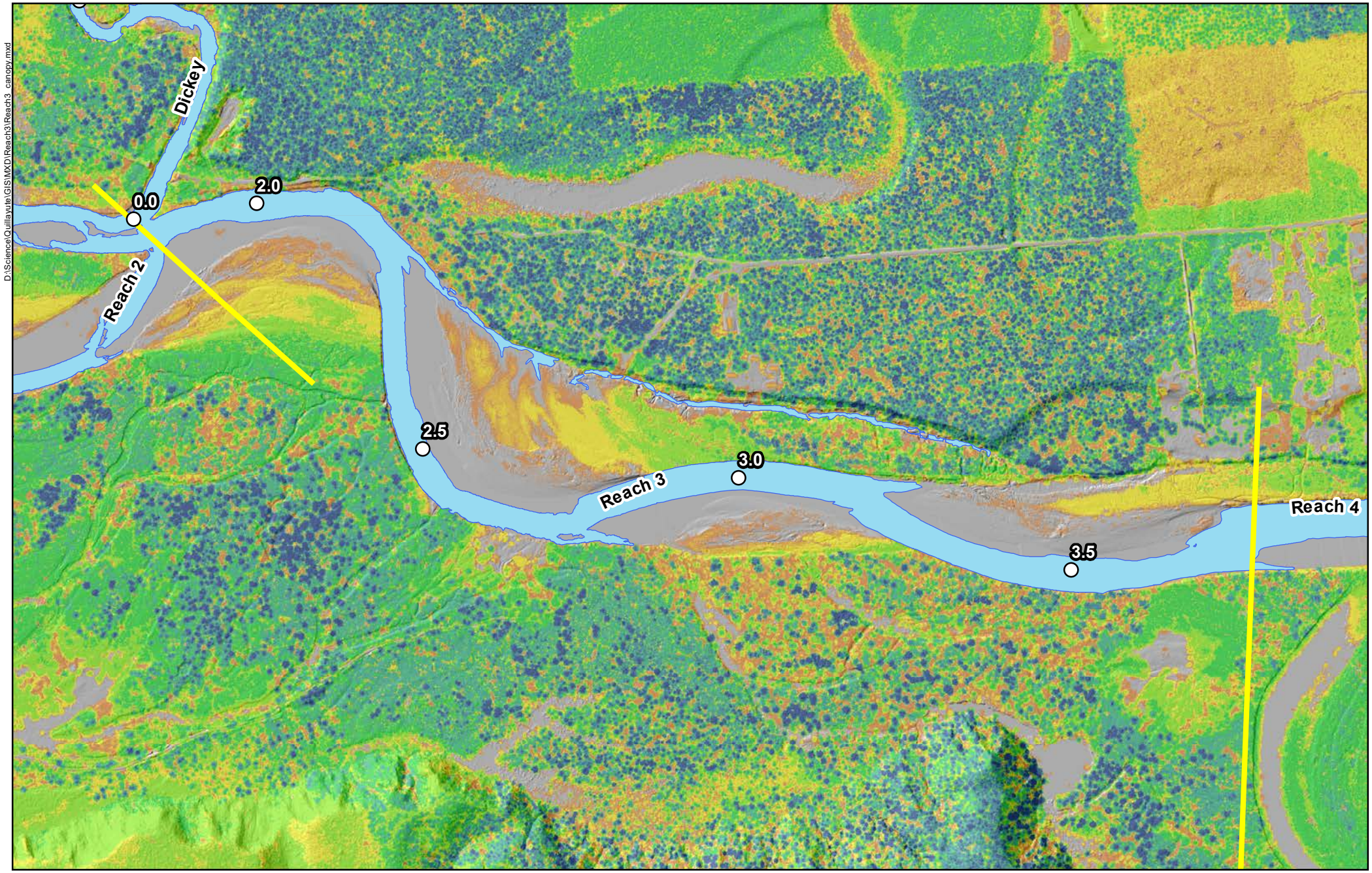

Canopy Cover Height (feet)

- 0 - 3
- 3 - 15
- 15 - 25
- 25 - 50
- 50 - 80
- 80 - 100
- 100 - 120
- 120 - 140
- 140 +
- River Miles

Quillayute River Geomorphic Assessment

Canopy Cover
2018 LiDAR
Reach 3
Figure E-4

TETRA TECH

N
W
E
S

0 1,000 2,000
Feet

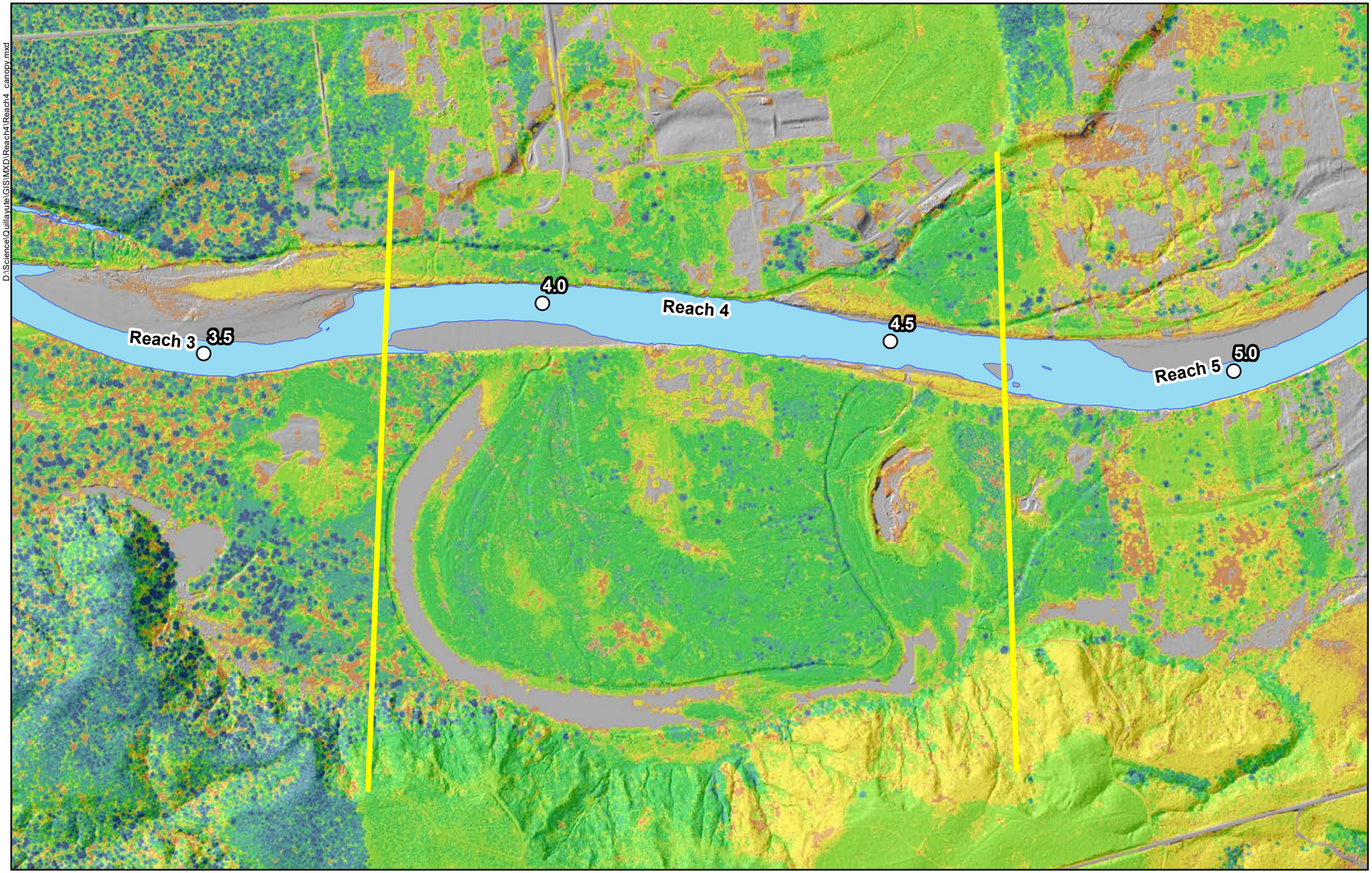

Canopy Cover Height (feet)

- 0 - 3
- 3 - 15
- 15 - 25
- 25 - 50
- 50 - 80
- 80 - 100
- 100 - 120
- 120 - 140
- 140 +
- River Miles

Quillayute River Geomorphic Assessment

Canopy Cover
2018 LiDAR
Reach 4
Figure E-5

TETRA TECH

N
W
E
S

0 1,000 2,000
Feet

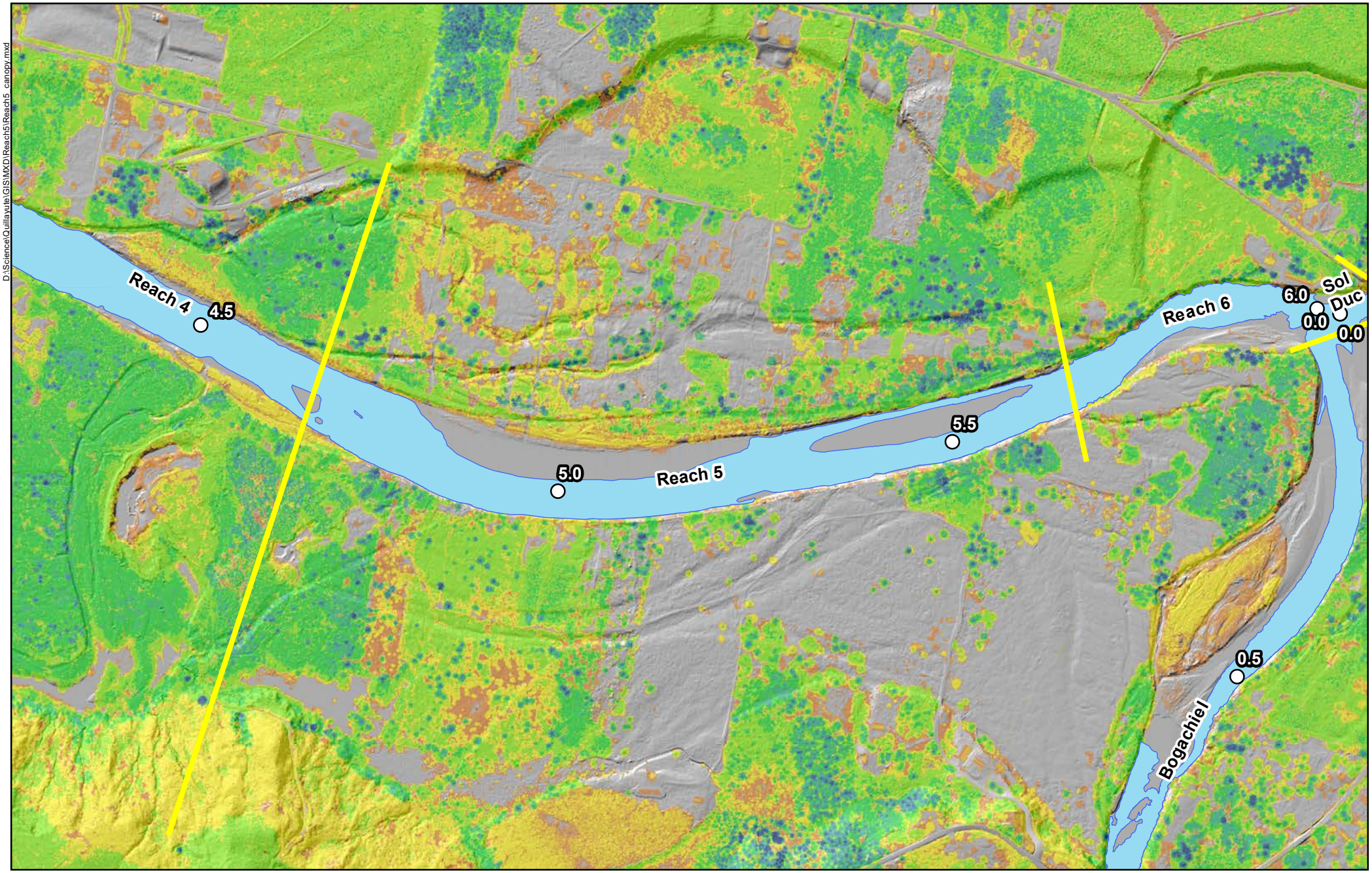

Canopy Cover Height (feet)

- 0 - 3
- 3 - 15
- 15 - 25
- 25 - 50
- 50 - 80
- 80 - 100
- 100 - 120
- 120 - 140
- 140 +
- River Miles

Quillayute River Geomorphic Assessment

Canopy Cover
2018 LiDAR
Reach 5
Figure E-6

TETRA TECH

N
W
E
S

0 875 1,750
Feet

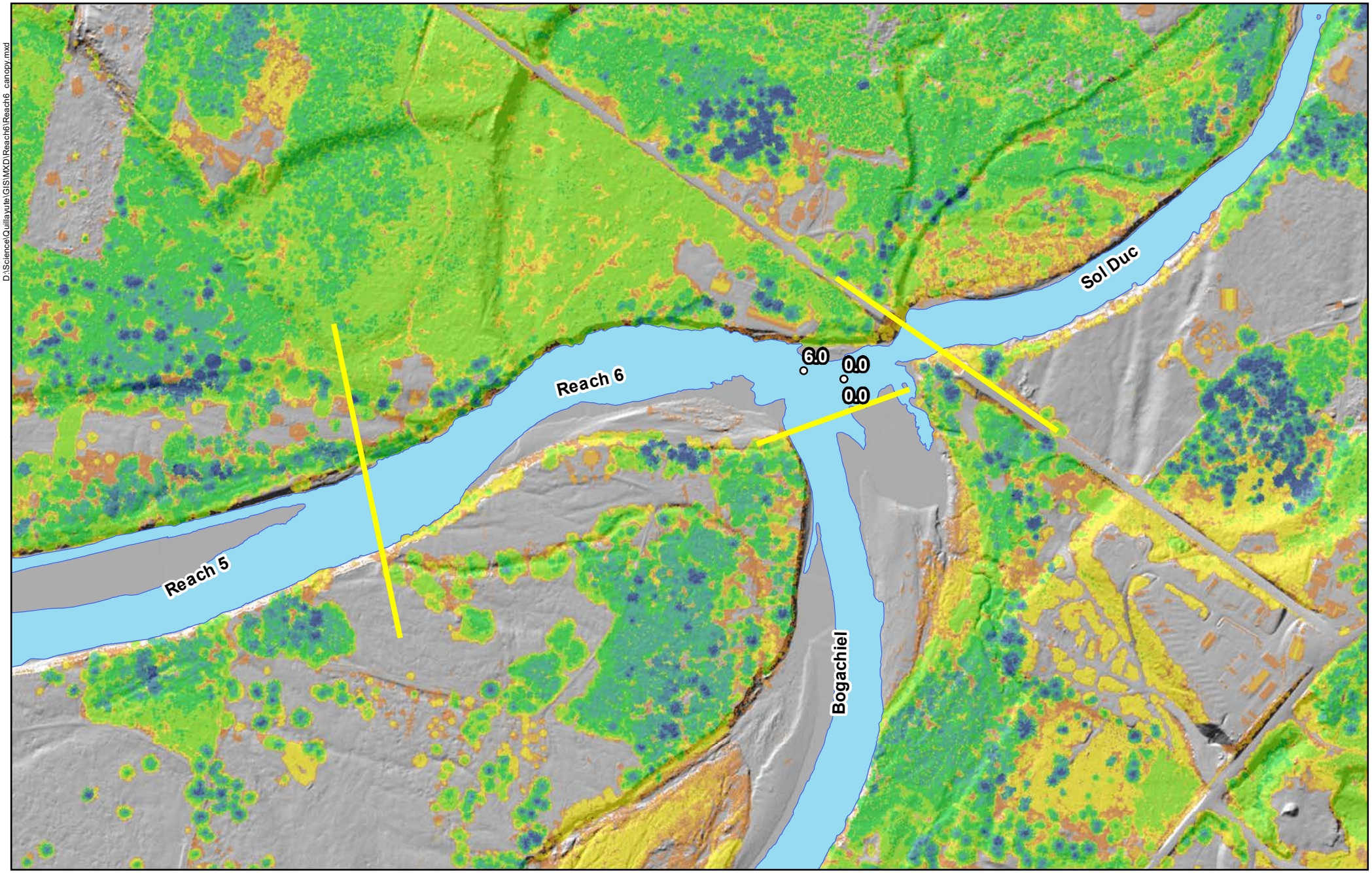

Canopy Cover Height (feet)

- 0 - 3
- 3 - 15
- 15 - 25
- 25 - 50
- 50 - 80
- 80 - 100
- 100 - 120
- 120 - 140
- 140 +
- River Miles

Quillayute River Geomorphic Assessment

Canopy Cover
2018 LiDAR
Reach 6
Figure E-7

TETRA TECH

N
W
E
S

0 500 1,000
Feet

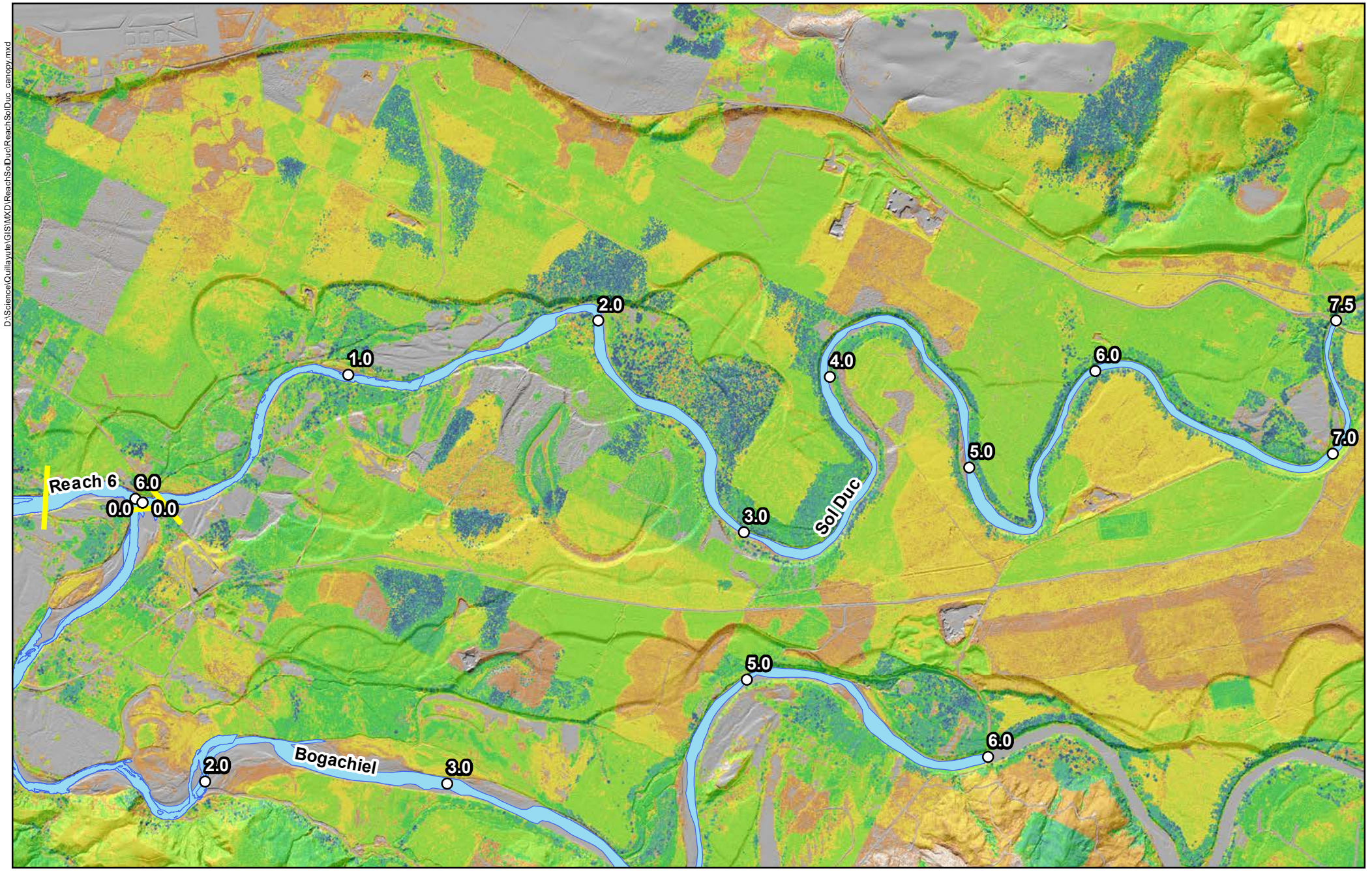

Canopy Cover Height (feet)

- 0 - 3
- 3 - 15
- 15 - 25
- 25 - 50
- 50 - 80
- 80 - 100
- 100 - 120
- 120 - 140
- 140 +
- River Miles

Quillayute River Geomorphic Assessment

Canopy Cover
2018 LiDAR
Lower Sol Duc River
Figure E-8

TETRA TECH

N
W
E
S

0 2,500 5,000
Feet

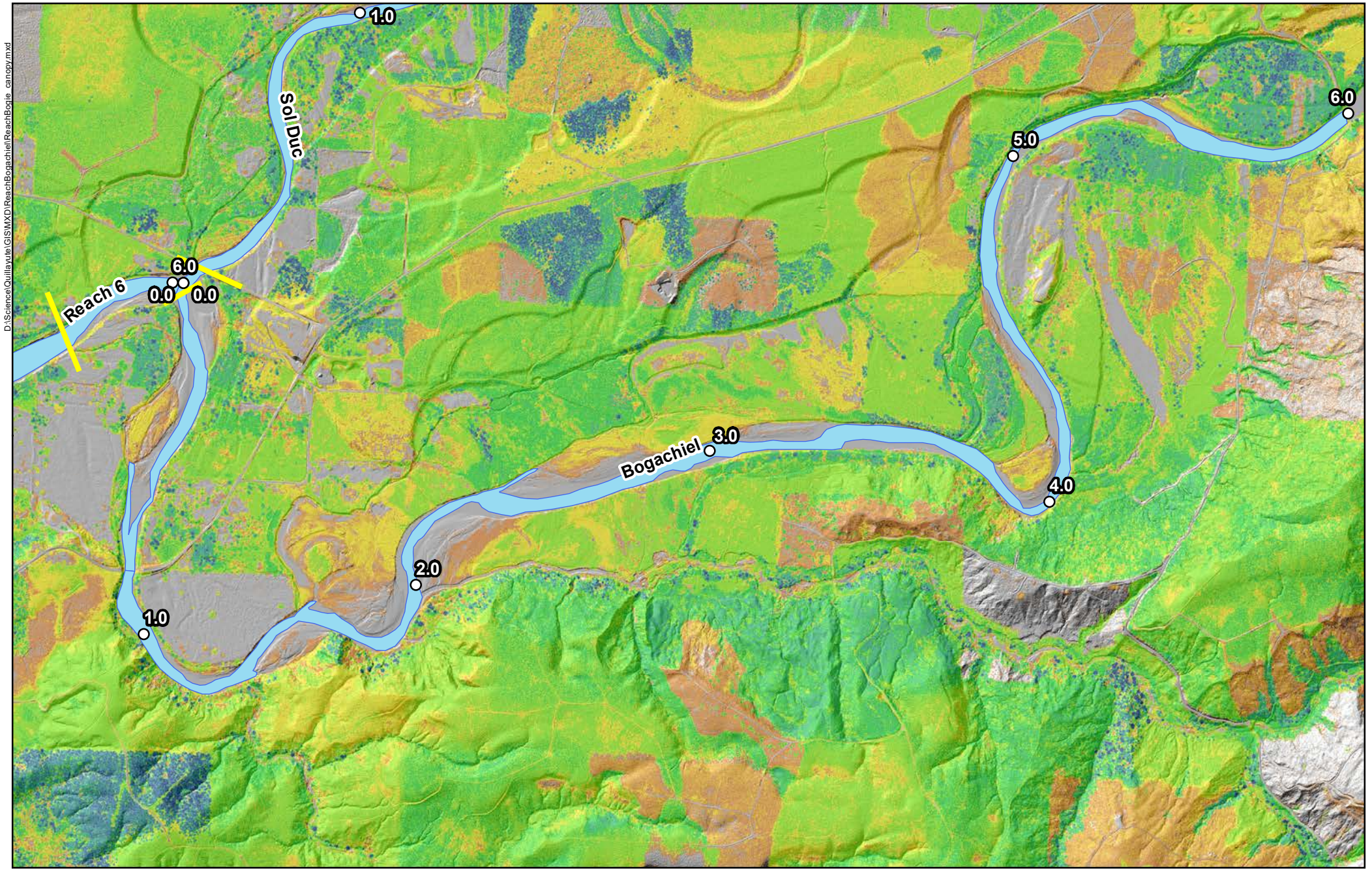

Canopy Cover Height (feet)

- 0 - 3
- 3 - 15
- 15 - 25
- 25 - 50
- 50 - 80
- 80 - 100
- 100 - 120
- 120 - 140
- 140 +
- River Miles

Quillayute River Geomorphic Assessment

Canopy Cover
2018 LiDAR
Lower Bogachiel River
Figure E-9

TETRA TECH

N
W E
S

0 2,000 4,000
Feet

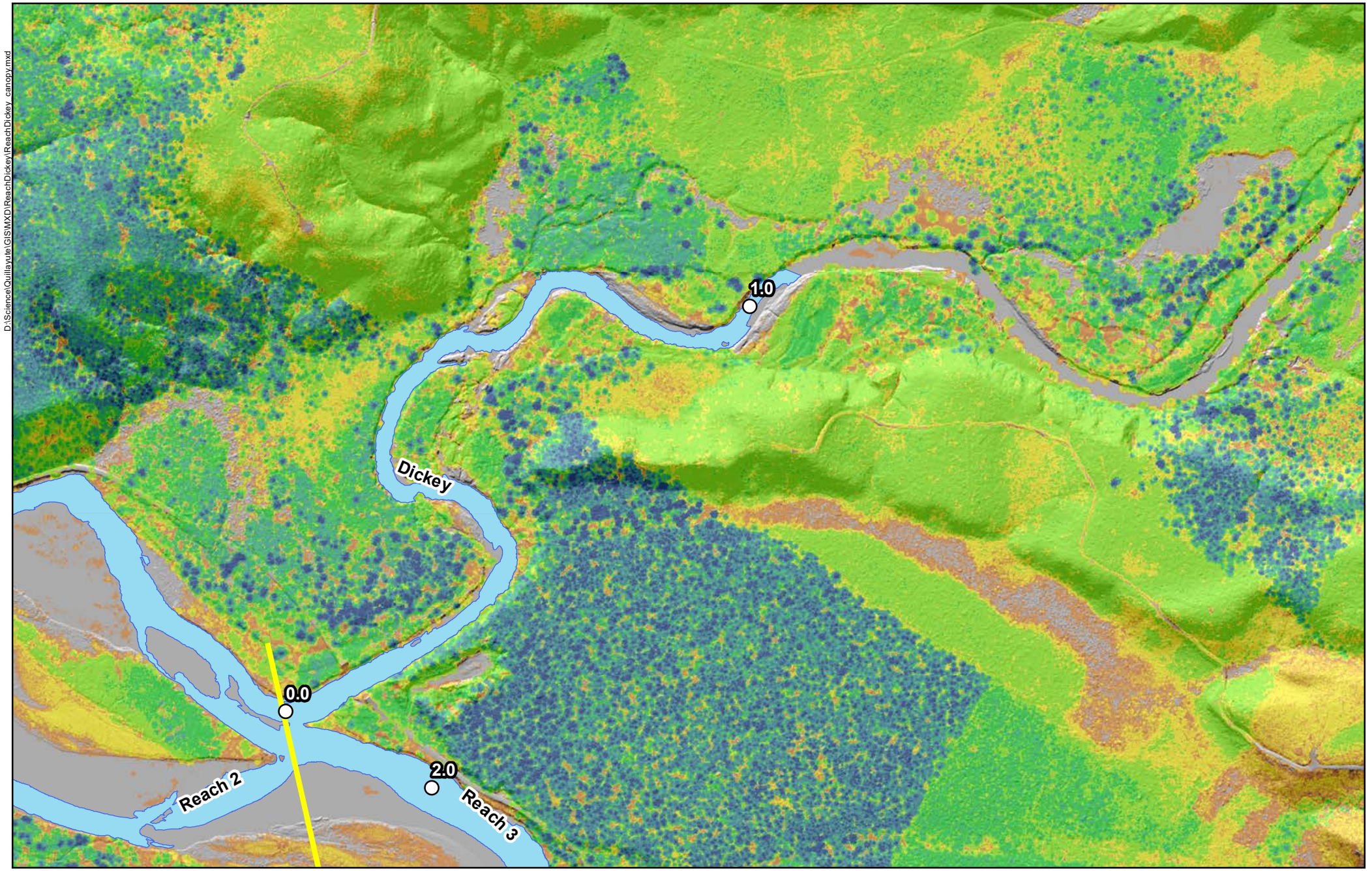

Canopy Cover Height (feet)

- 0 - 3
- 3 - 15
- 15 - 25
- 25 - 50
- 50 - 80
- 80 - 100
- 100 - 120
- 120 - 140
- 140 +
- River Miles

Quillayute River Geomorphic Assessment

Canopy Cover
2018 LiDAR
Lower Dickey River
Figure E-10

TETRA TECH

N
W
E
S

0 750 1,500
Feet

APPENDIX F – DIFFRENCE OF DEM (DOD) MAPING

Quillayute River Project
Geomorphic Assessment and Action Plan
Difference of DEM (DoD) Mapping

Appendix F

Submitted to:

Quileute Natural Resources
401 Main Street
La Push, WA 98350

Submitted by:

19803 North Creek Parkway
Bothell, WA 98011
Tel 425.482.7600 | Fax 425.482.7652
www.tetratech.com

September 2020

LIST OF FIGURES

Figure F-1. ..... Erosion/Deposition Overview 2002 - 2018
Figure F-2. ..... Reach 1 Erosion/Deposition 2002 - 2018
Figure F-3. ..... Reach 2 Erosion/Deposition 2002 - 2018
Figure F-4. ..... Reach 3 Erosion/Deposition 2002 - 2018
Figure F-5. ..... Reach 4 Erosion/Deposition 2002 - 2018
Figure F-6. ..... Reach 5 Erosion/Deposition 2002 - 2018
Figure F-7. ..... Reach 6 Erosion/Deposition 2002 - 2018
Figure F-8. ..... Lower Bogachiel Erosion/Deposition 2002 - 2018
Figure F-9. ..... Lower Sol Duc Erosion/Deposition 2002 - 2018
Figure F-10. ..... Lower Dickey Erosion/Deposition 2002 -2018

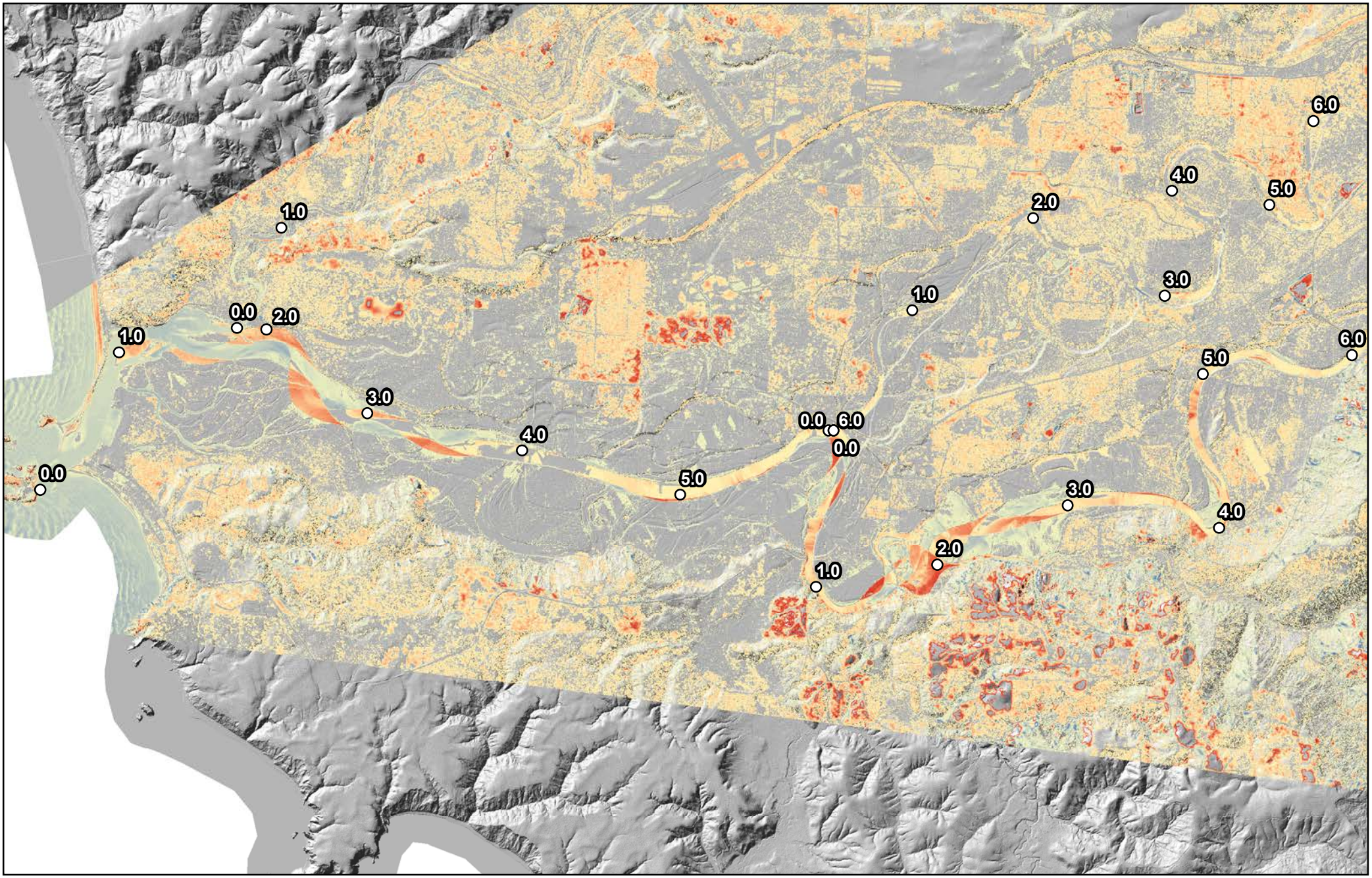

Erosion/Deposition

Between 2002 and 2018

-20 ft.

+20 ft.

River Miles

Quillayute River Geomorphic Assessment

Erosion/Deposition
2002 - 2018

Figure F-1

TETRA TECH

N
W E
S

0 5,000 10,000

Feet

Erosion/Deposition

Between 2002 and 2018

-20 ft.

+20 ft.

River Miles

Quillayute River
Geomorphic Assessment

Erosion/Deposition
2002 - 2018
Reach 1
Figure F-2

TETRA TECH

N
W
E
S

0 900 1,800
Feet

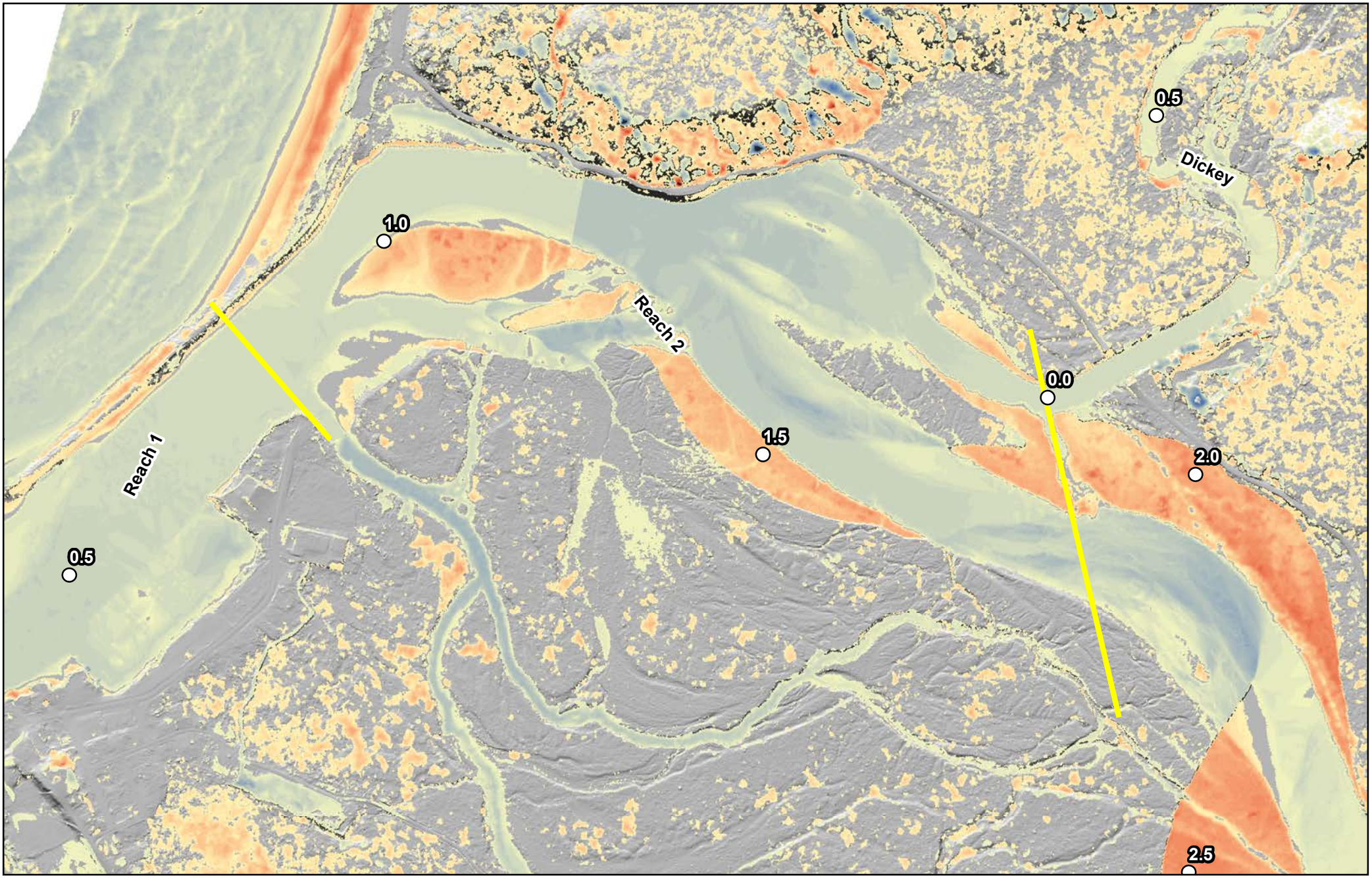

Erosion/Deposition

Between 2002 and 2018

-20 ft.

+20 ft.

River Miles

Quillayute River
Geomorphic Assessment

Erosion/Deposition
2002 - 2018
Reach 2
Figure F-3

TETRA TECH

N
W
E
S

0 900 1,800
Feet

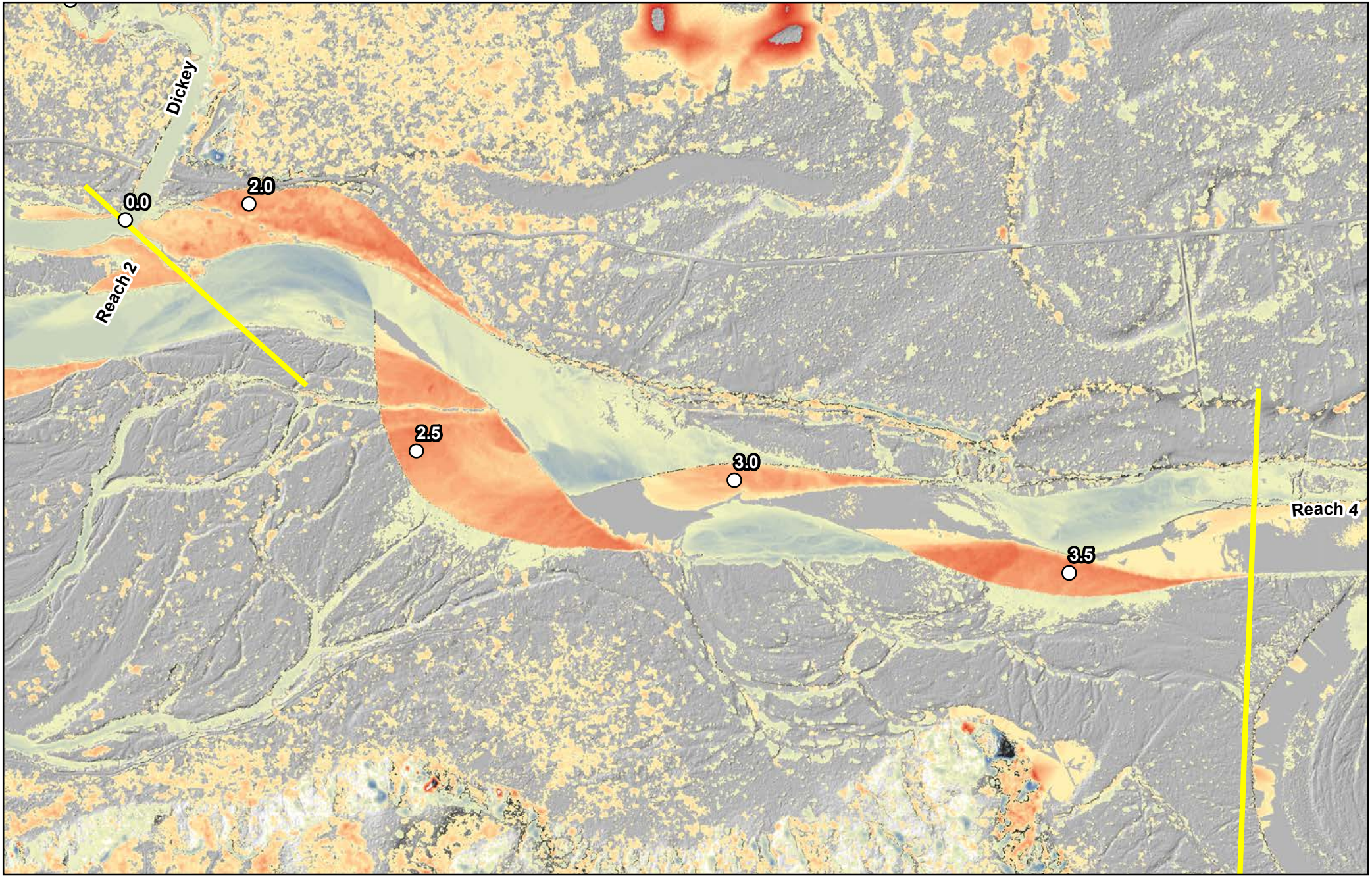

Erosion/Deposition

Between 2002 and 2018

-20 ft.

+20 ft.

River Miles

Quillayute River
Geomorphic Assessment

Erosion/Deposition
2002 - 2018
Reach 3
Figure F-4

TETRA TECH

N
W
E
S

0 1,200 2,400
Feet

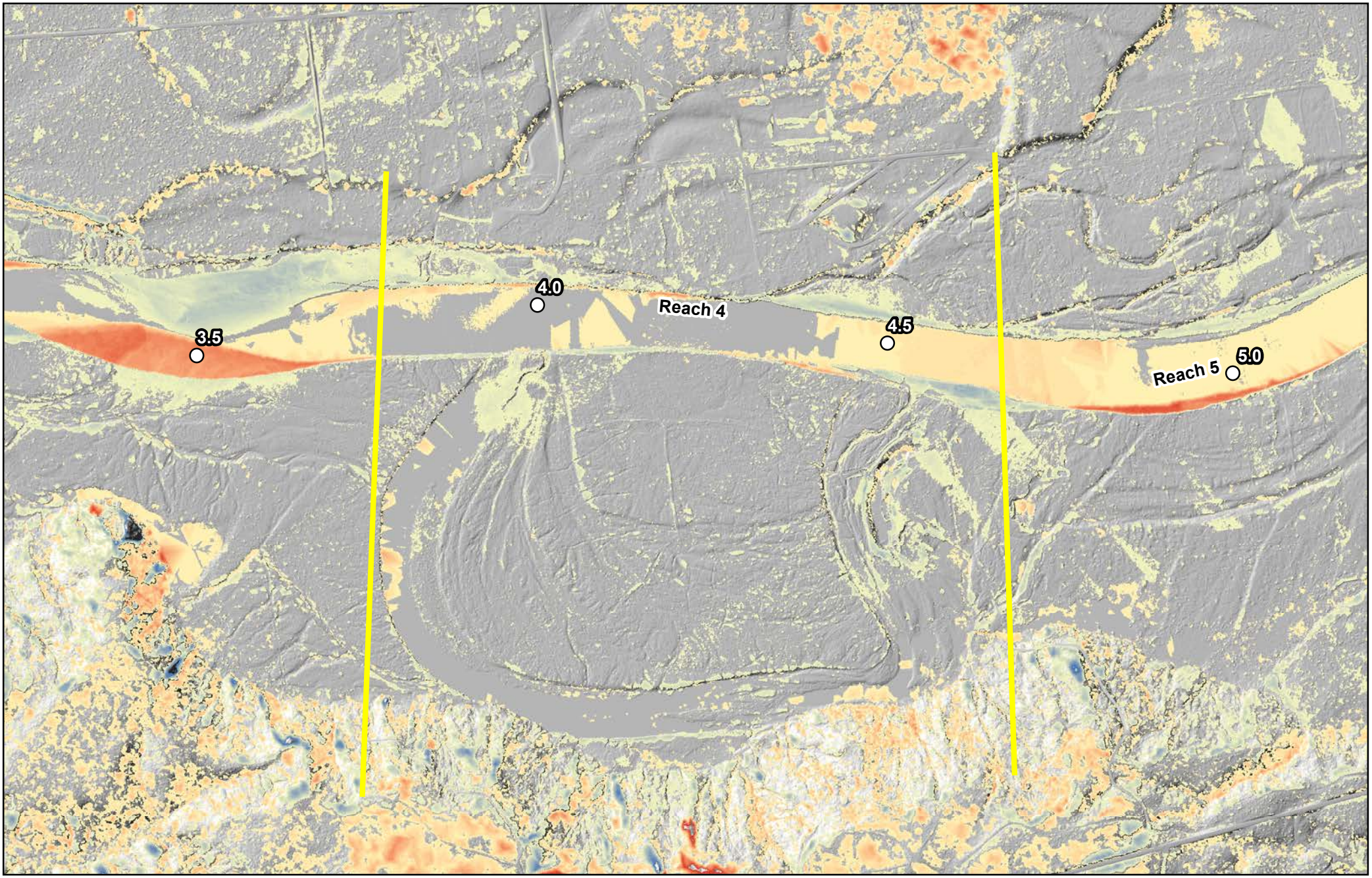

Erosion/Deposition

Between 2002 and 2018

-20 ft.

+20 ft.

River Miles

Quillayute River
Geomorphic Assessment

Erosion/Deposition
2002 - 2018
Reach 4
Figure F-5

TETRA TECH

N
W
E
S

0 1,200 2,400
Feet

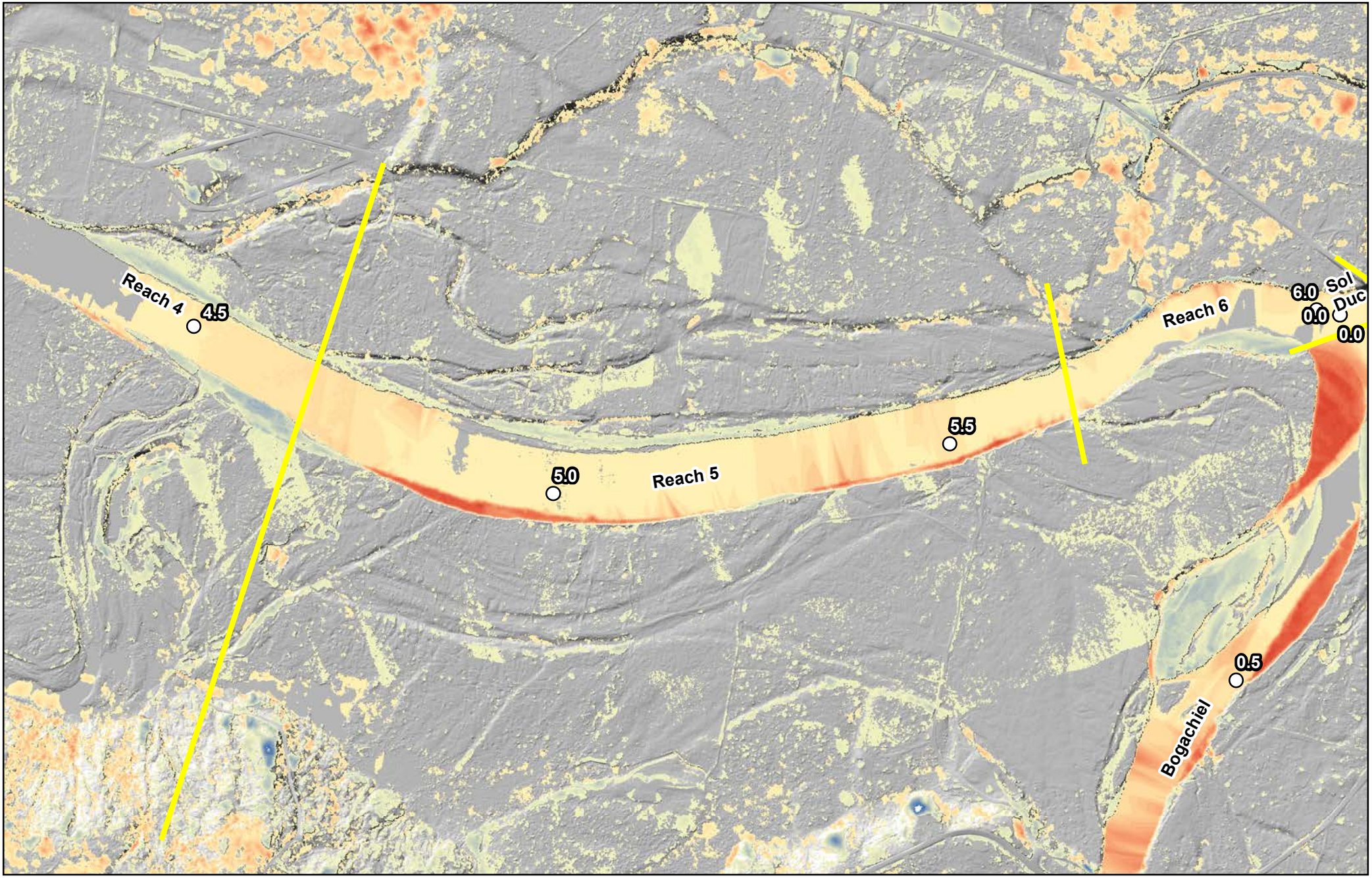

Erosion/Deposition

Between 2002 and 2018

-20 ft.

+20 ft.

River Miles

Quillayute River
Geomorphic Assessment

Erosion/Deposition
2002 - 2018
Reach 5
Figure F-6

TETRA TECH

N
W
E
S

0 1,050 2,100
Feet

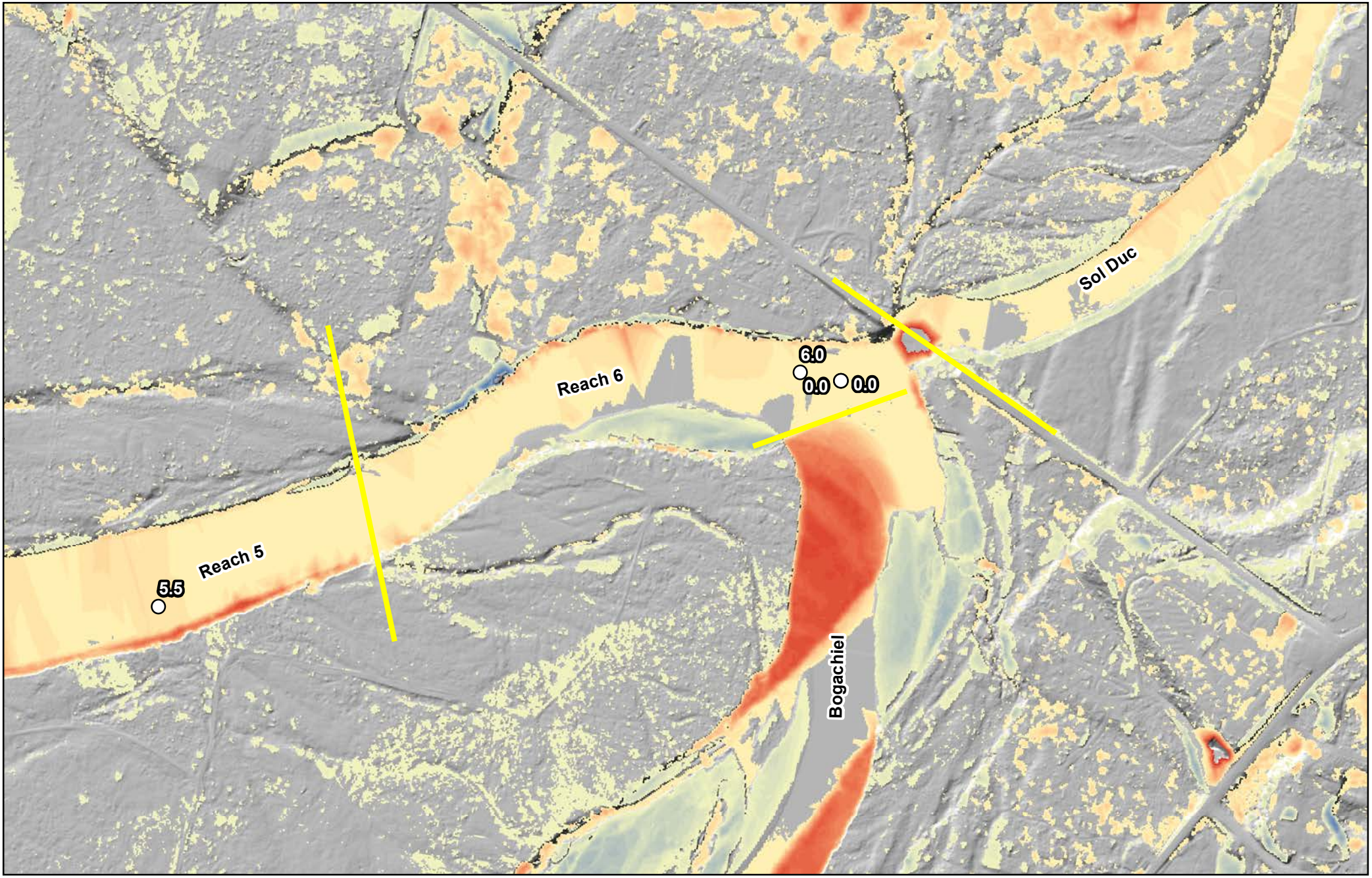

Erosion/Deposition

Between 2002 and 2018

-20 ft.

+20 ft.

River Miles

Quillayute River
Geomorphic Assessment

Erosion/Deposition
2002 - 2018
Reach 6
Figure F-7

TETRA TECH

N
W
E
S

0 600 1,200
Feet

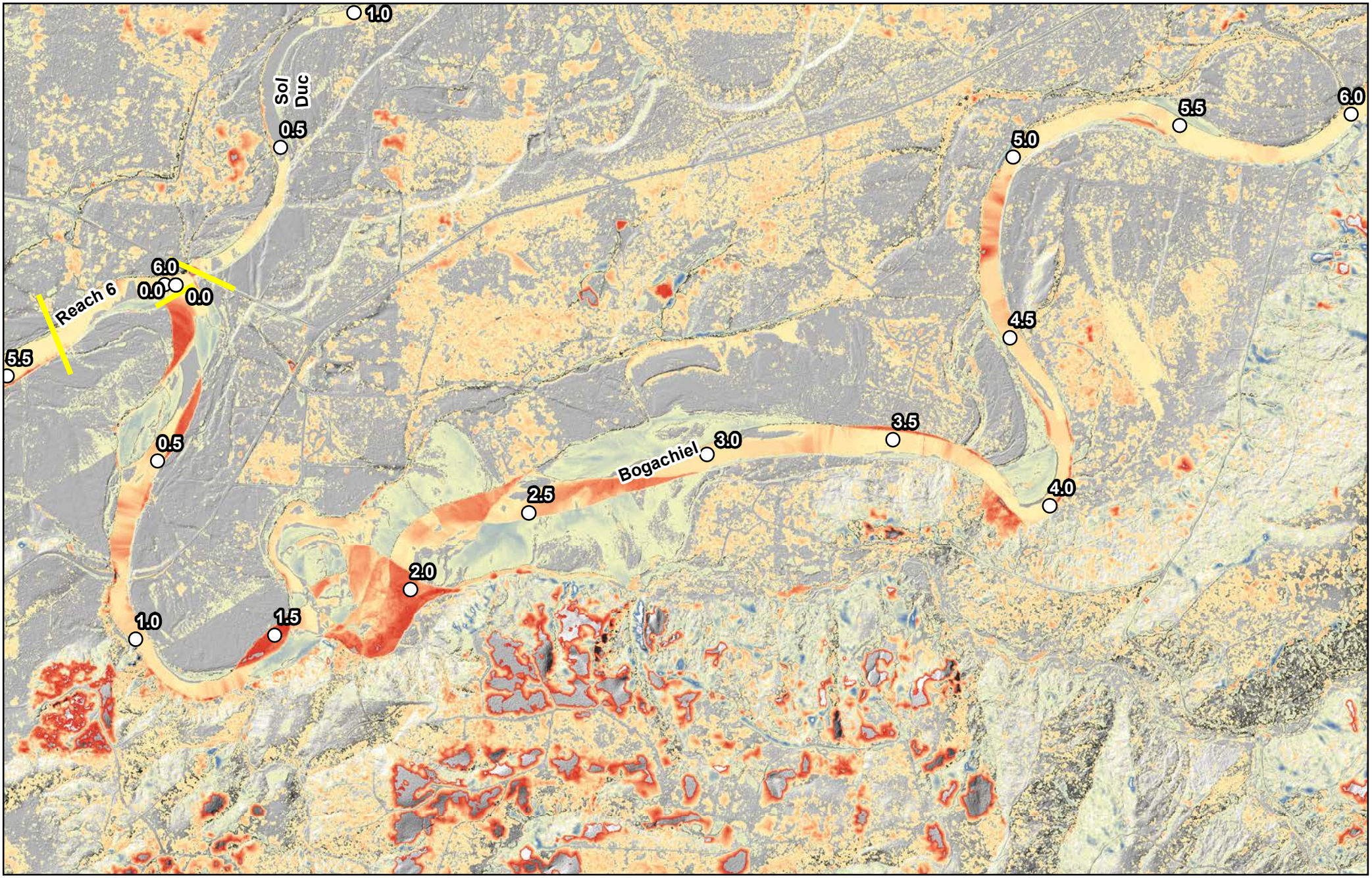

Erosion/Deposition

Between 2002 and 2018

-20 ft.

+20 ft.

River Miles

Quillayute River
Geomorphic Assessment

Erosion/Deposition
2002 - 2018
Lower Bogachiel River
Figure F-8

TETRA TECH

N
W E
S

0 2,300 4,600
Feet

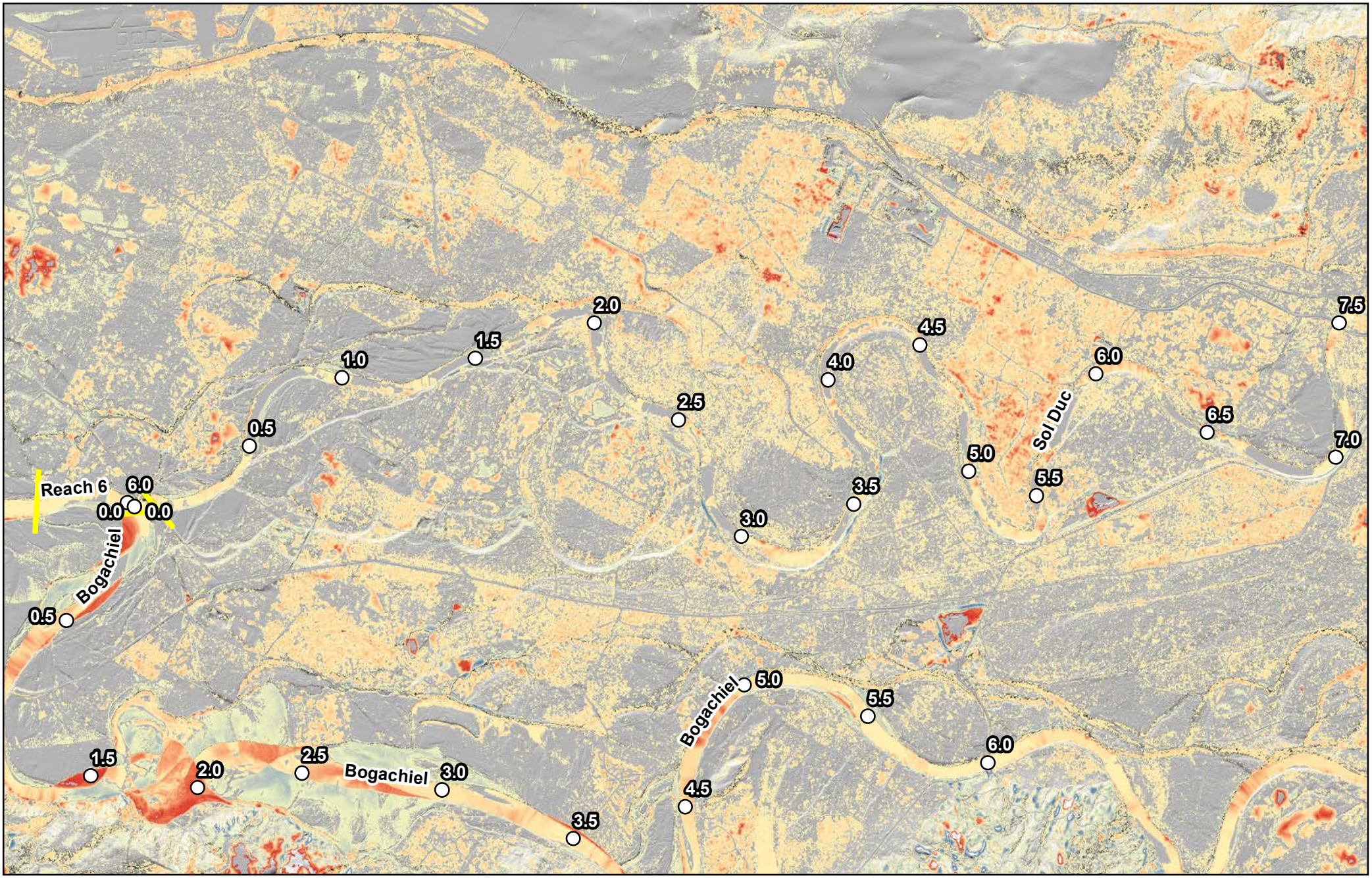

Erosion/Deposition

Between 2002 and 2018

-20 ft.

+20 ft.

River Miles

Quillayute River Geomorphic Assessment

Erosion/Deposition
2002 - 2018
Lower Sol Duc River
Figure F-9

TETRA TECH

N
W
E
S

0 3,100 6,200

Feet

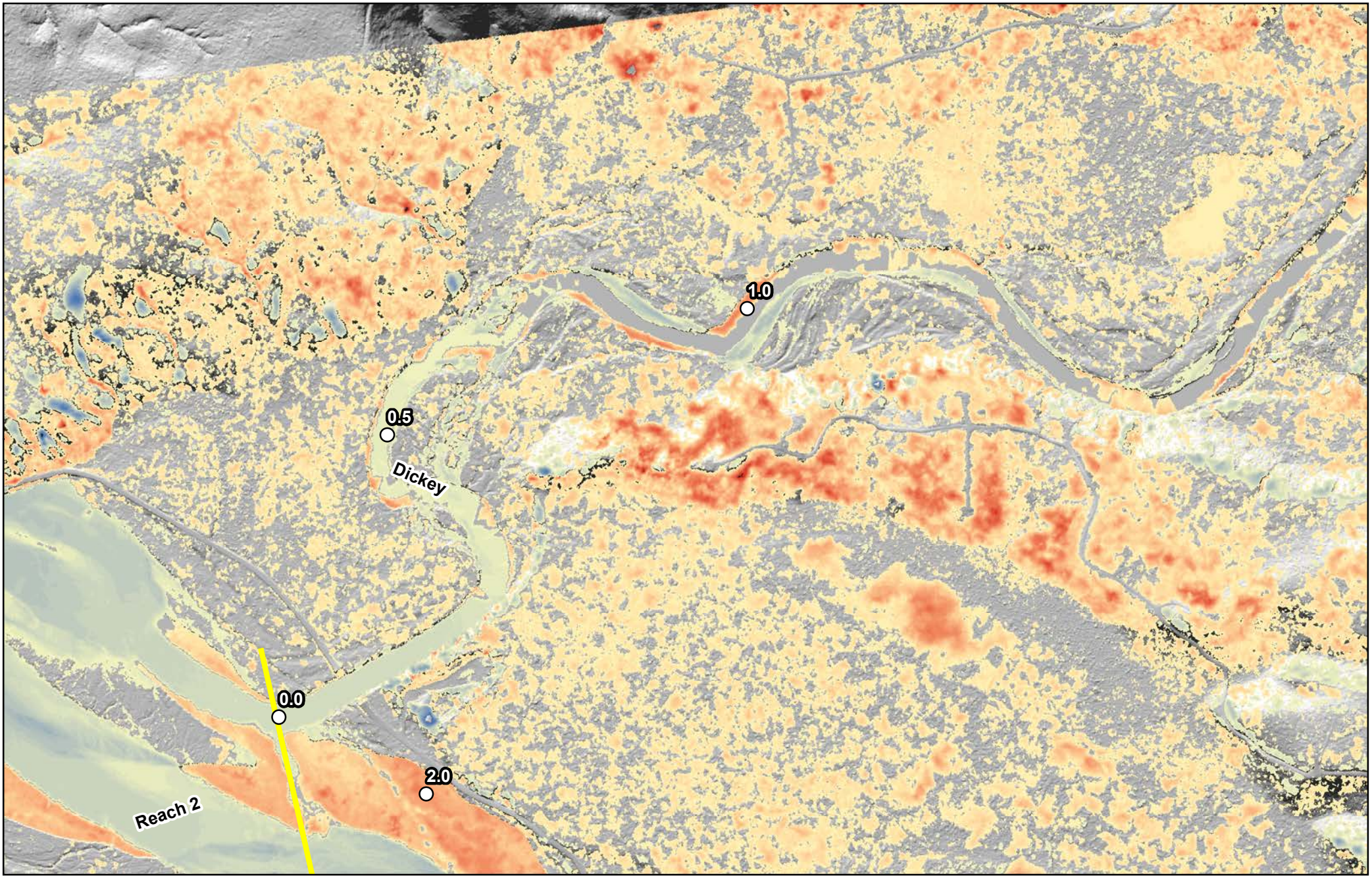

Erosion/Deposition

Between 2002 and 2018

-20 ft.

+20 ft.

River Miles

Quillayute River
Geomorphic Assessment

Erosion/Deposition
2002 - 2018
Lower Dickey River
Figure F-10

TETRA TECH

N
W
E
S

0 900 1,800
Feet

APPENDIX G – CHANNEL MIGRATION ANALYSIS MAPPING

Quillayute River Project
Geomorphic Assessment and Action Plan
Channel Migration Analysis Mapping

Appendix G

Submitted to:

Quileute Natural Resources
401 Main Street
La Push, WA 98350

Submitted by:

19803 North Creek Parkway
Bothell, WA 98011
Tel 425.482.7600 | Fax 425.482.7652
www.tetratech.com

September 2020

LIST OF FIGURES

Figure G-1. ..... Channel Migration Overview 1883 - 2019
Figure G-2. ..... Channel Migration Overview 1883 - 1990
Figure G-3. ..... Channel Migration Overview 2002 - 2011
Figure G-4. ..... Channel Migration Overview 2013 - 2019
Figure G-5. ..... Reach 1 Channel Migration 1883 - 2019
Figure G-6. ..... Reach 1 Channel Migration 1883 - 1990
Figure G-7. ..... Reach 1 Channel Migration 2002 - 2011
Figure G-8. ..... Reach 1 Channel Migration 2013 - 2019
Figure G-9. ..... Reach 2 Channel Migration 1883 - 2019
Figure G-10. ..... Reach 2 Channel Migration 1883 - 1990
Figure G-11. ..... Reach 2 Channel Migration 2002 - 2011
Figure G-12. ..... Reach 2 Channel Migration 2013 - 2019
Figure G-13. ..... Reach 3 Channel Migration 1883 - 2019
Figure G-14. ..... Reach 3 Channel Migration 1883 - 1990
Figure G-15. ..... Reach 3 Channel Migration 2002 - 2011
Figure G-16. ..... Reach 3 Channel Migration 2013 - 2019
Figure G-17. ..... Reach 4 Channel Migration 1883 - 2019
Figure G-18. ..... Reach 4 Channel Migration 1883 - 1990
Figure G-19. ..... Reach 4 Channel Migration 2002 - 2011
Figure G-20. ..... Reach 4 Channel Migration 2013 - 2019
Figure G-21. ..... Reach 5 Channel Migration 1883 - 2019
Figure G-22. ..... Reach 5 Channel Migration 1883 - 1990
Figure G-23. ..... Reach 5 Channel Migration 2002 - 2011
Figure G-24. ..... Reach 5 Channel Migration 2013 - 2019
Figure G-25. ..... Reach 6 Channel Migration 1883 - 2019
Figure G-26. ..... Reach 6 Channel Migration 1883 - 1990
Figure G-27. ..... Reach 6 Channel Migration 2002 - 2011
Figure G-28. ..... Reach 6 Channel Migration 2013 - 2019
Figure G-29. ..... Lower Sol Duc Channel Migration 1883 - 2019
Figure G-30. ..... Lower Sol Duc Channel Migration 1883 - 1990
Figure G-31. ..... Lower Sol Duc Channel Migration 2002 - 2011
Figure G-32. ..... Lower Sol Duc Channel Migration 2013 - 2019
Figure G-33. ..... Lower Bogachiel Channel Migration 1883 - 2019
Figure G-34. ..... Lower Bogachiel Channel Migration 1883 - 1990
Figure G-35. ..... Lower Bogachiel Channel Migration 2002 - 2011
Figure G-36. ..... Lower Bogachiel Channel Migration 2013 - 2019
Figure G-37. ..... Lower Dickey Channel Migration 1883 - 2019
Figure G-38. ..... Lower Dickey Channel Migration 1883 - 1990
Figure G-39. ..... Lower Dickey Channel Migration 2002 - 2011
Figure G-40. ..... Lower Dickey Channel Migration 2013 - 2019

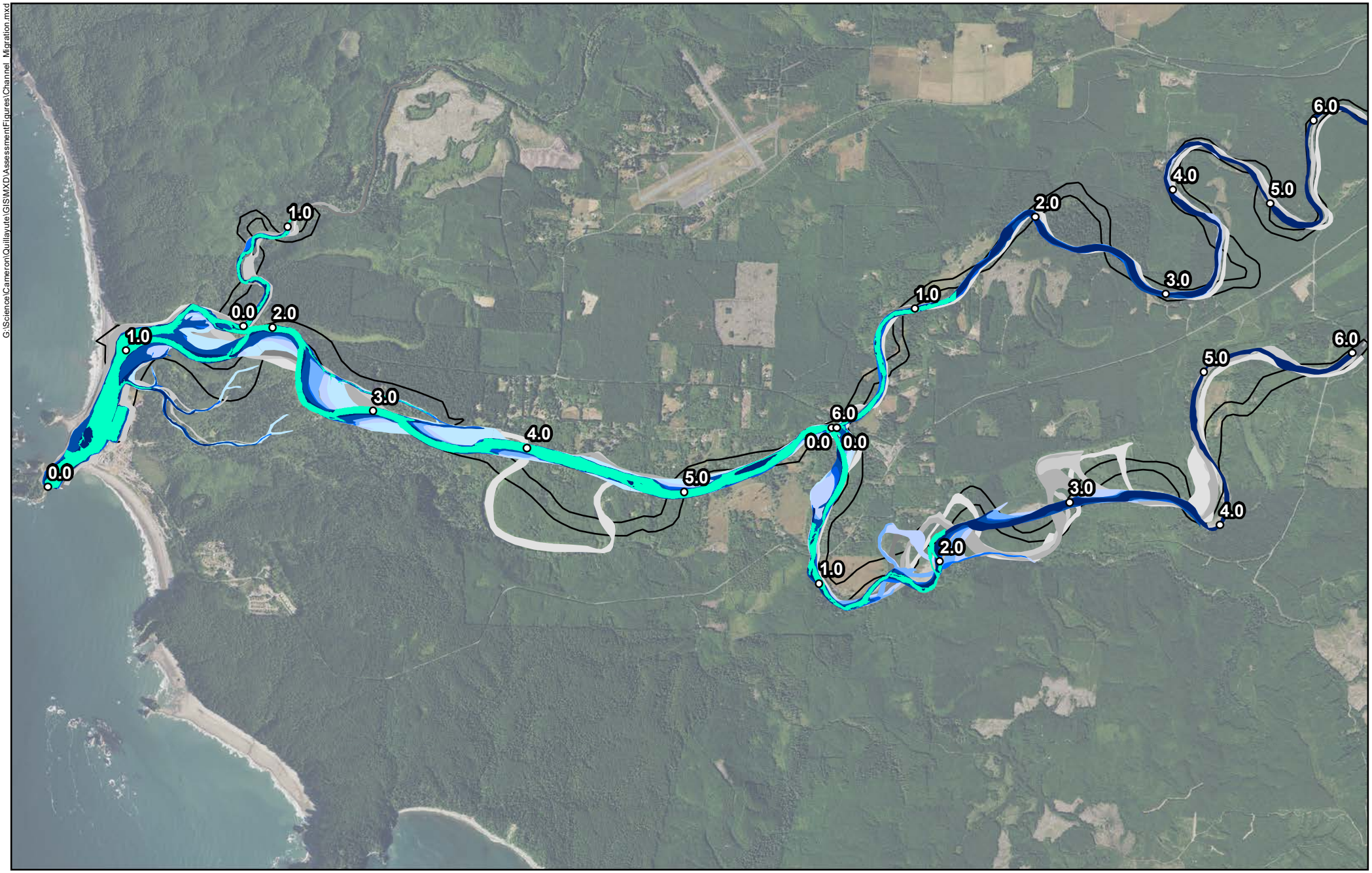

Channel

2019	2011	1990	1883*	
2017	2009	1980	River Miles	
2015	2006	1977		
2013	2002	1955	*GLO Survey	

Quillayute River Geomorphic Assessment

Channel Migration Analysis
1883 - 2019

Figure G-1

TETRA TECH

N
W E
S

0 5,000 10,000
Feet

G:\Science\Cameron\Quillayute\GIS\MXD\AssessmentFigures\Channel_Migration.mxd
0.0
1.0
2.0
3.0
4.0
5.0
6.0
Channel
1990
1980
1977
1955
1883*
River Miles
*GLO Survey
Quillayute River
Geomorphic Assessment
Channel Migration Analysis
1883 - 1990
Figure G-2
TETRA TECH
N
W
E
S
0
5,000
10,000
Feet

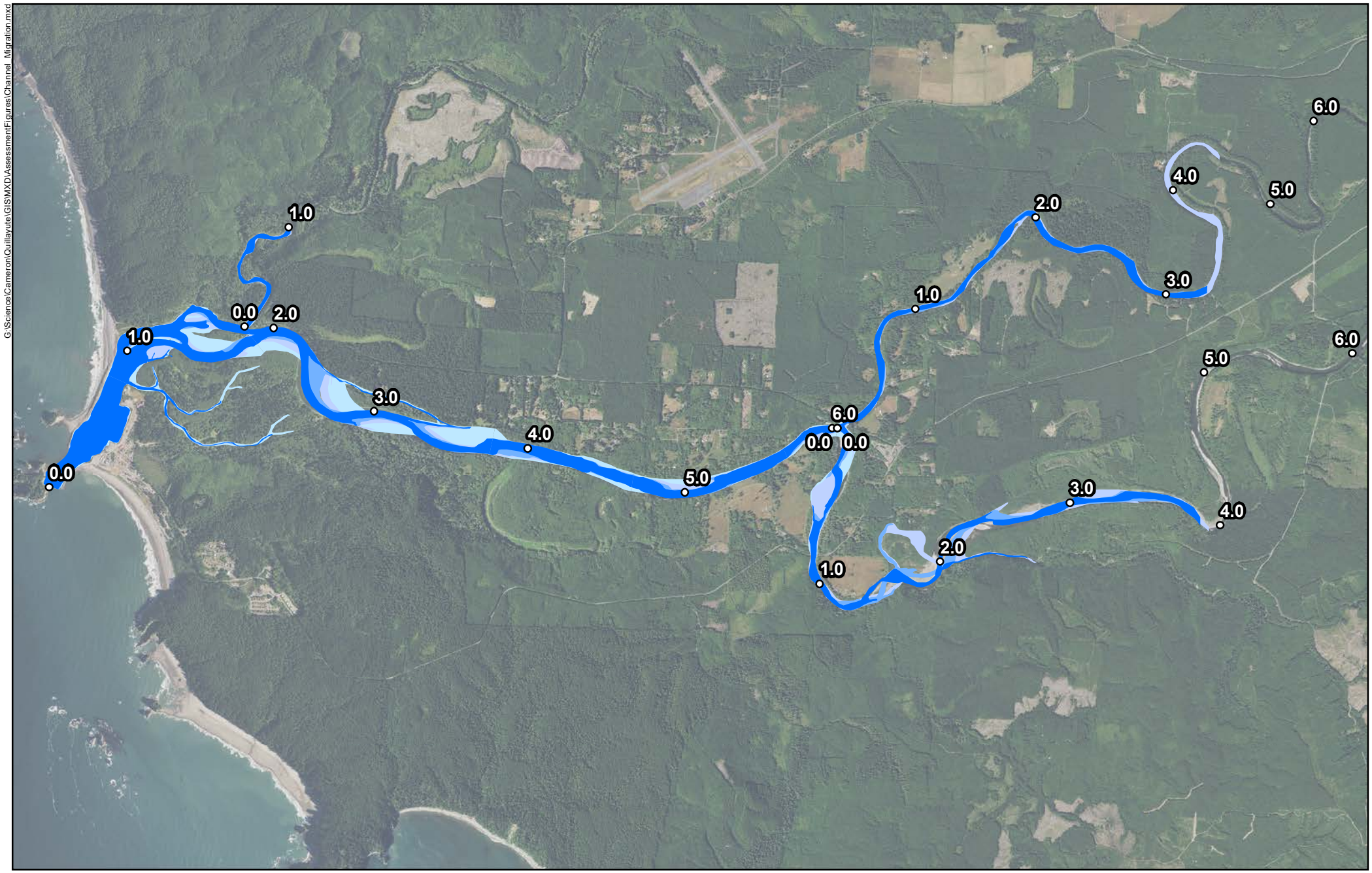

Channel

2011 | 2006

2009 | 2002

River Miles

Quillayute River Geomorphic Assessment

Channel Migration Analysis
2002 - 2011

Figure G-3

TETRA TECH

N
W E
S

0 5,000 10,000
Feet

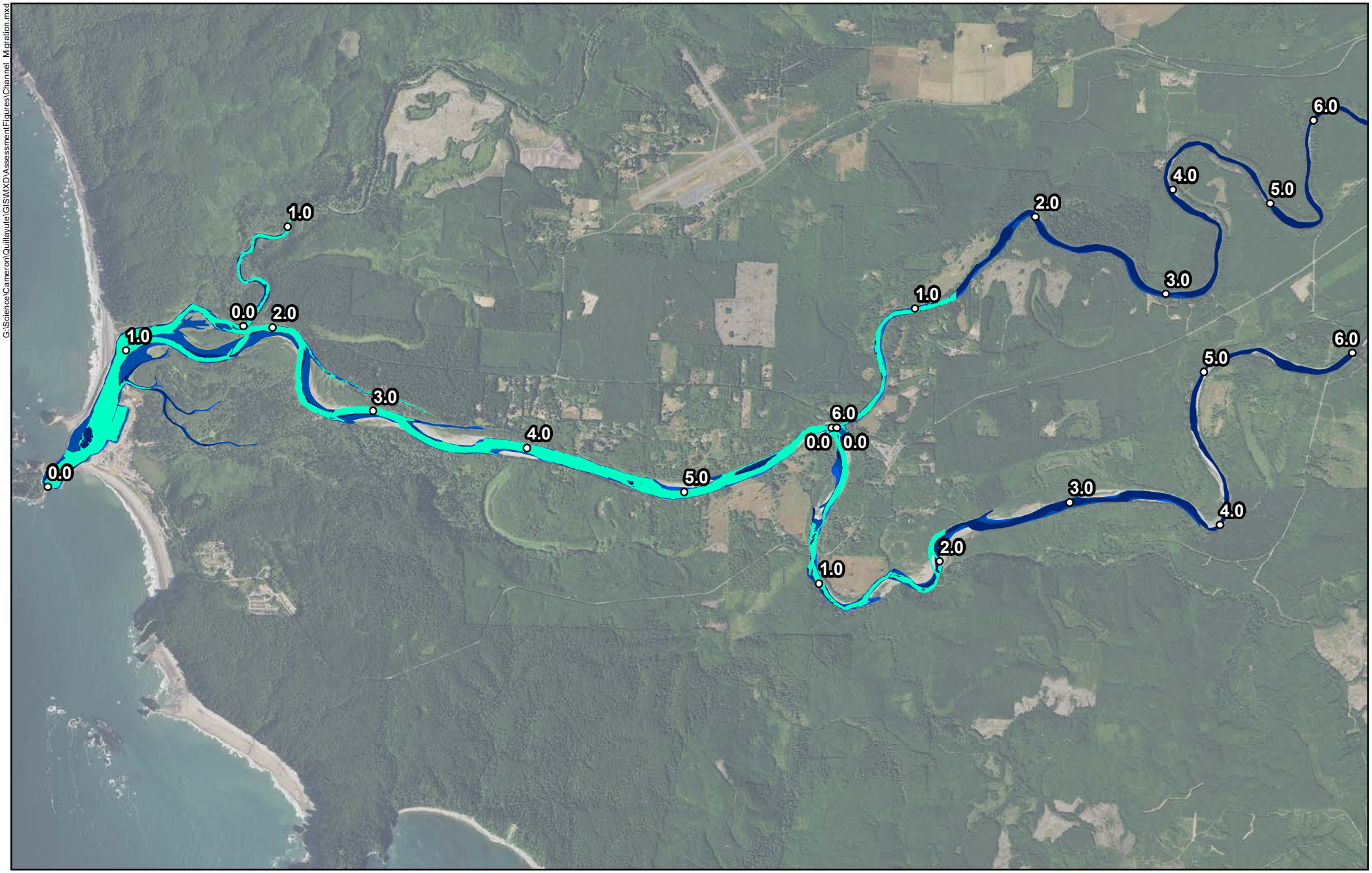
G:\Science\Cameron\Quillayute\GIS\MXD\AssesssmentFigures\Channel_Migration.mxd
1.0
0.0
2.0
1.0
3.0
4.0
5.0
0.0
6.0
0.0
0.0
1.0
2.0
3.0
4.0
5.0
6.0
1.0
2.0
3.0
4.0
5.0
6.0
Channel
2019
2015
2017
2013
River Miles
Quillayute River
Geomorphic Assessment
Channel Migration Analysis
2013 - 2019
Figure G-4
TETRA TECH
N
W
E
S
0
5,000
10,000
Feet

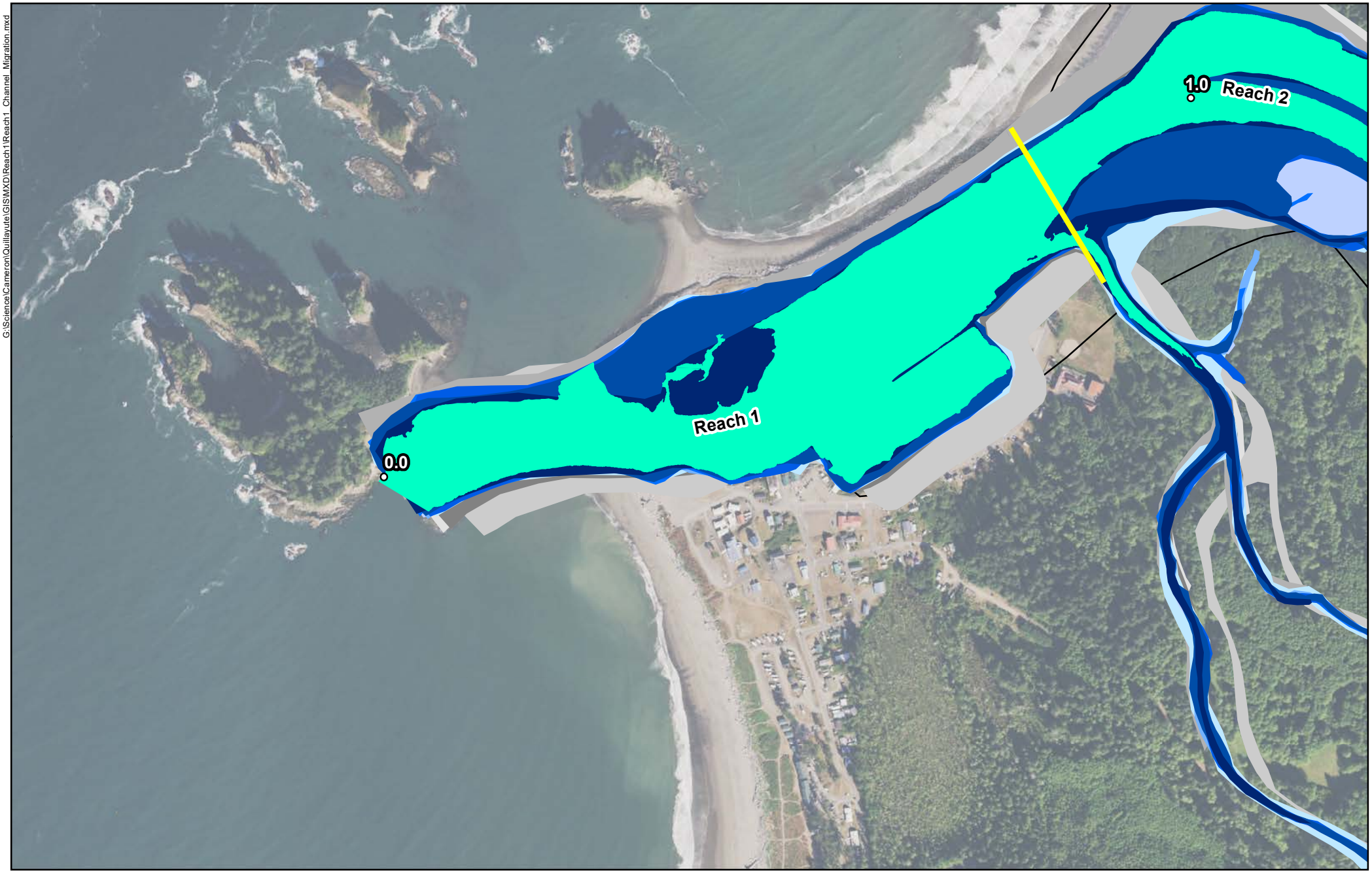
G:\Science\Cameron\Quillayute\GIS\MXD\Reach1\Reach1_Channel_Migration.mxd
1.0
Reach 2
Reach 1
0.0
Channel
2019
2017
2015
2013
2011
2009
2006
2002
1990
1980
1977
1955
1883*
Geomorphic Reaches
River Miles
Quillayute River
Geomorphic Assessment
Reach 1
Channel Migration Analysis
1883 - 2019
Figure G-5
*GLO Survey
TETRA TECH
N
W
E
S
0
750
1,500
Feet

Channel

1990
1980
1977
1955
1883*

*GLO Survey

Geomorphic Reaches

River Miles

Quillayute River
Geomorphic Assessment

Reach 1
Channel Migration Analysis
1883 - 1990
Figure G-6

TETRA TECH

N
W
E
S

0 750 1,500
Feet

Channel

2011 2006

2009 2002

Geomorphic Reaches

River Miles

Quillayute River Geomorphic Assessment

Reach 1
Channel Migration Analysis
2002 - 2011
Figure G-7

TETRA TECH

N E S W

0 750 1,500

Feet

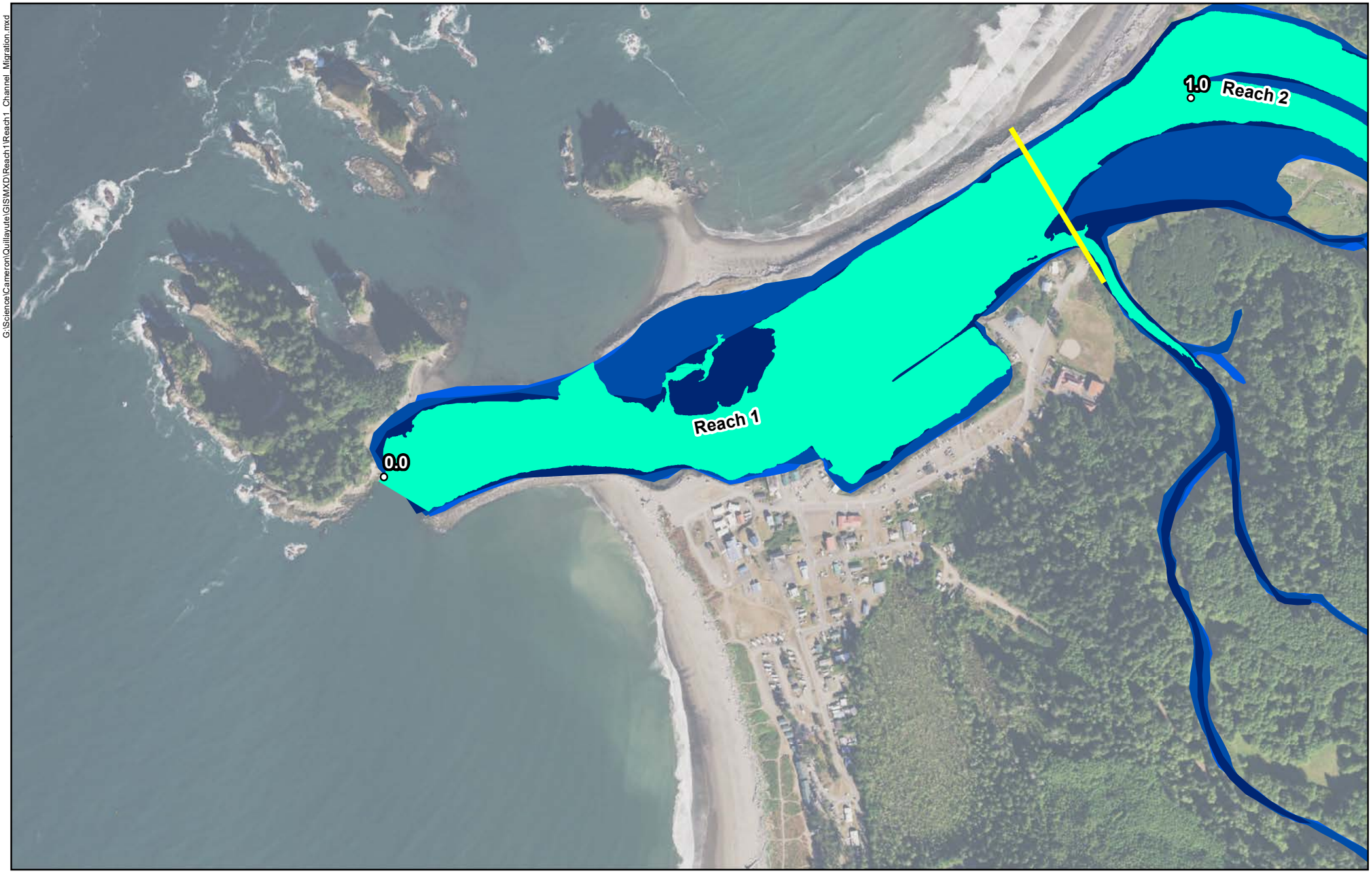

Channel

2019 2015

2017 2013

Geomorphic Reaches

River Miles

Quillayute River Geomorphic Assessment

Reach 1
Channel Migration Analysis
2013 - 2019
Figure G-8

TETRA TECH

0 750 1,500

Feet

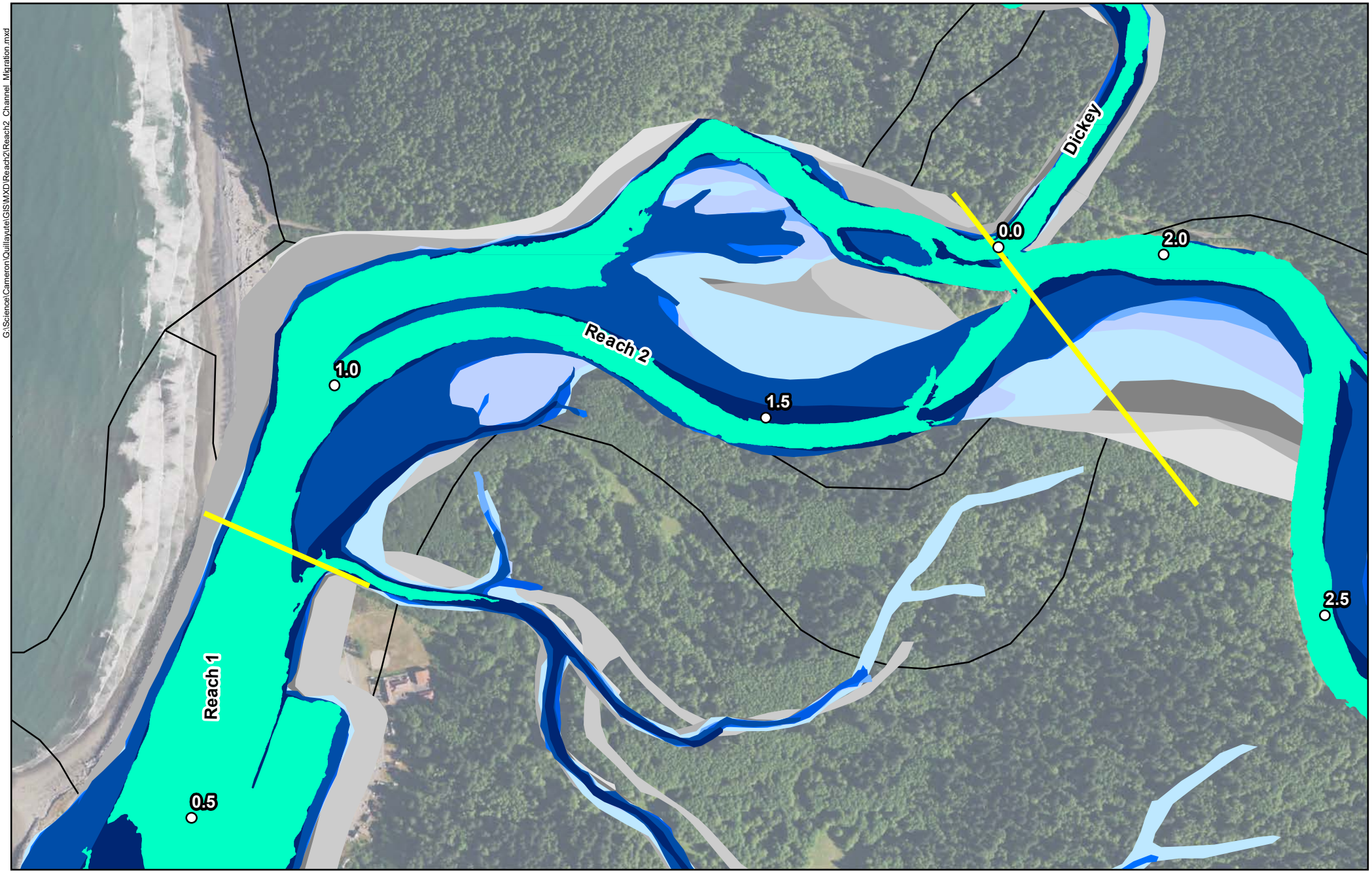

Channel

2019	2011	1990	1883*
2017	2009	1980	Geomorphic Reaches
2015	2006	1977	River Miles
2013	2002	1955	

Quillayute River Geomorphic Assessment

Channel Migration Analysis
1883 - 2019
Reach 2
Figure G-9

*GLO Survey

TETRA TECH

N
W E
S

0 750 1,500
Feet

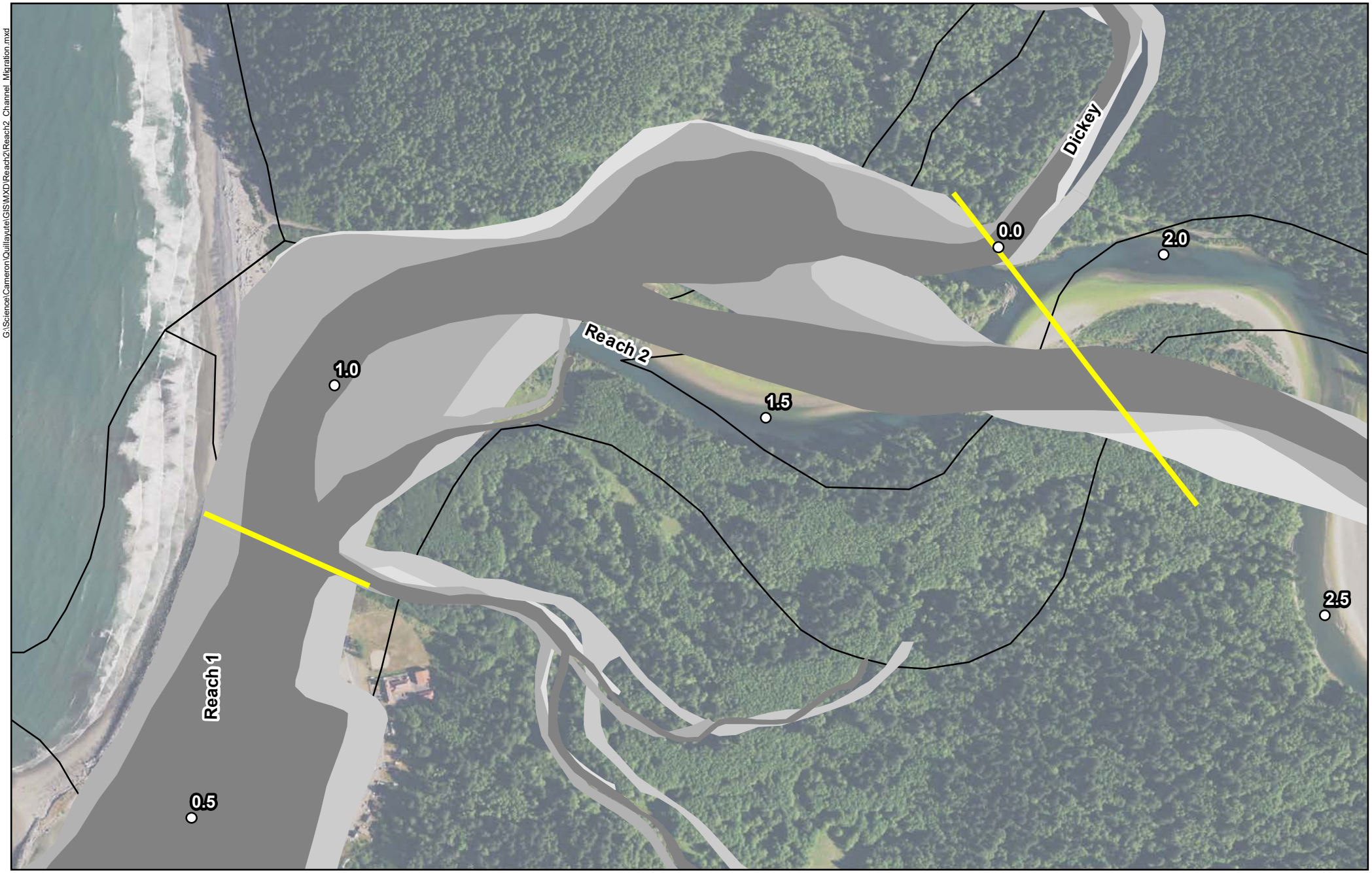

Channel

- 1990
- 1980
- 1977
- 1955
- 1883*

*GLO Survey

Geomorphic Reaches

River Miles

Quillayute River
Geomorphic Assessment

Channel Migration Analysis
1883 - 1990
Reach 2
Figure G-10

TETRA TECH

N
W E
S

0 750 1,500
Feet

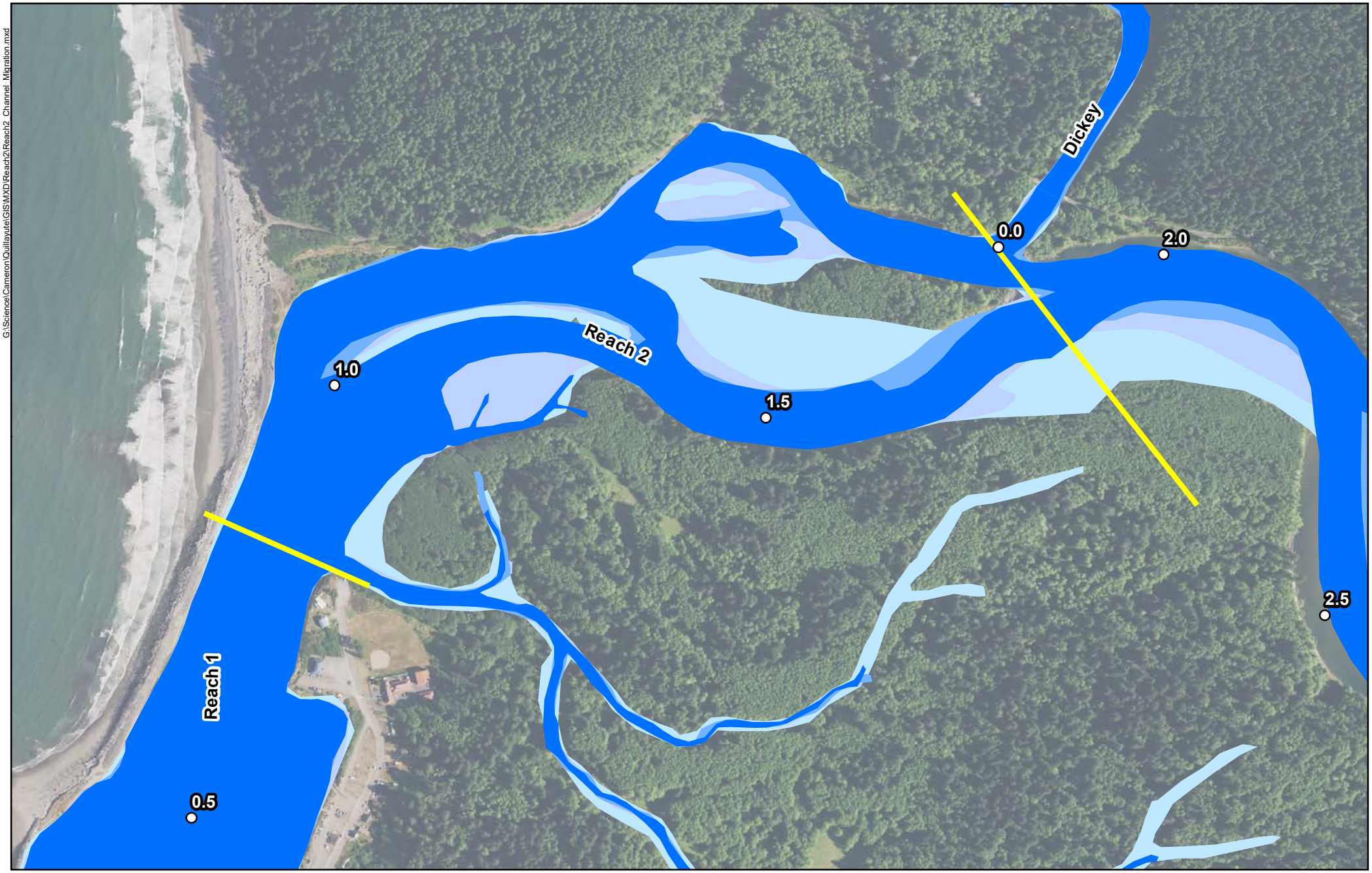

Channel

2011 | 2006

2009 | 2002

Geomorphic Reaches

River Miles

Quillayute River
Geomorphic Assessment

Channel Migration Analysis
2002 - 2011
Reach 2
Figure G-11

TETRA TECH

N
W E
S

0 750 1,500
Feet

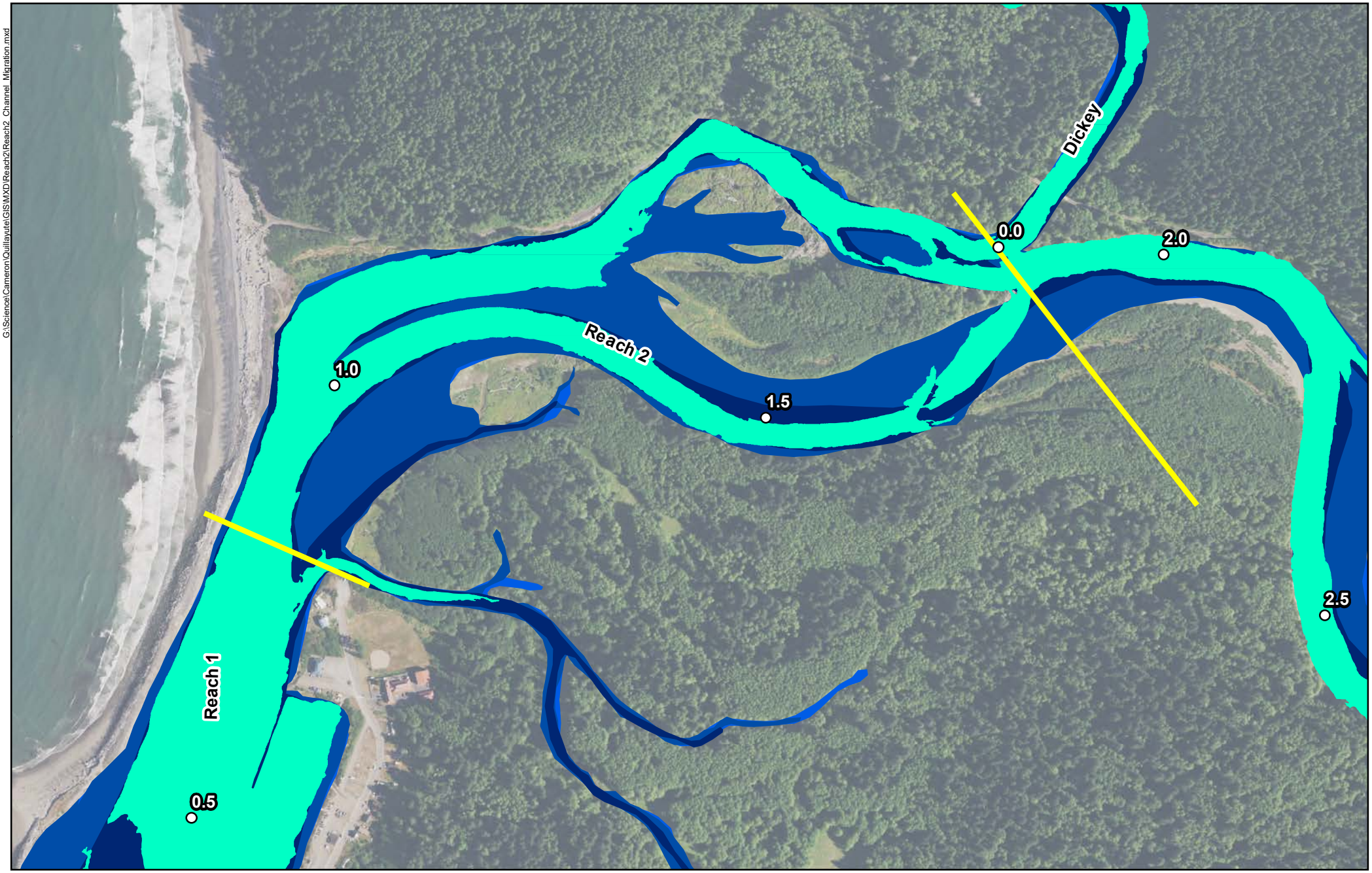

Channel

2019 2015

2017 2013

Geomorphic Reaches

River Miles

Quillayute River
Geomorphic Assessment

Channel Migration Analysis
2013 - 2019
Reach 2
Figure G-12

TETRA TECH

N
W E
S

0 750 1,500
Feet

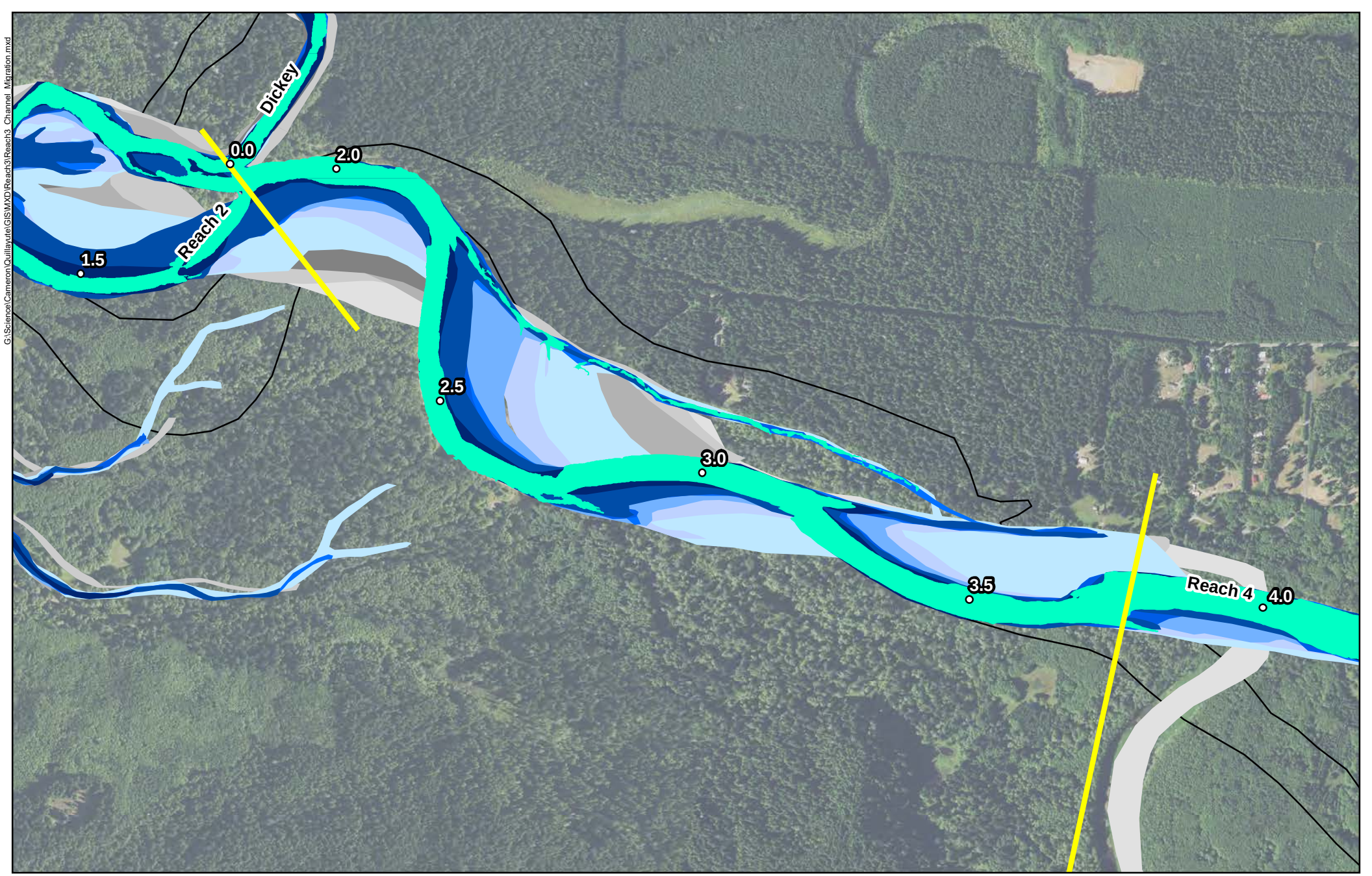

Channel

2019	2011	1990	1883*
2017	2009	1980	Geomorphic Reaches
2015	2006	1977	River Miles
2013	2002	1955	

*GLO Survey

Quillayute River Geomorphic Assessment

Channel Migration Analysis
1883 - 2019
Reach 3
Figure G-13

TETRA TECH

N
W E
S

0 1,250 2,500
Feet

Channel

1990	1955
1980	1883*
1977	

*GLO Survey

Geomorphic Reaches

River Miles

Quillayute River
Geomorphic Assessment

Channel Migration Analysis
1883 - 1990
Reach 3
Figure G-14

TETRA TECH

N
W E
S

0 1,250 2,500
Feet

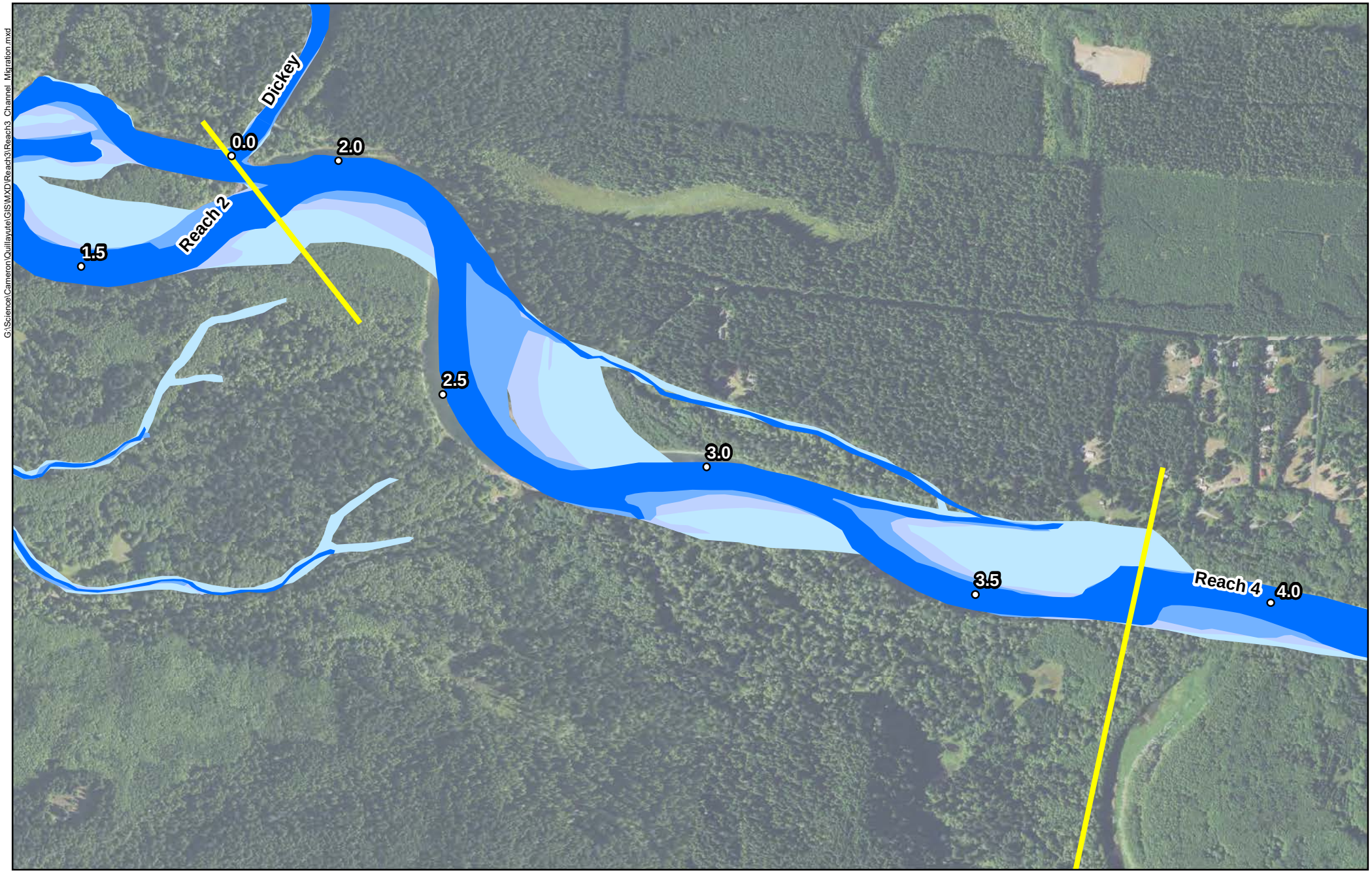

Channel

2011 | 2006

2009 | 2002

Geomorphic Reaches

River Miles

Quillayute River Geomorphic Assessment

Channel Migration Analysis
2002 - 2011
Reach 3
Figure G-15

TETRA TECH

N
W E
S

0 1,250 2,500
Feet

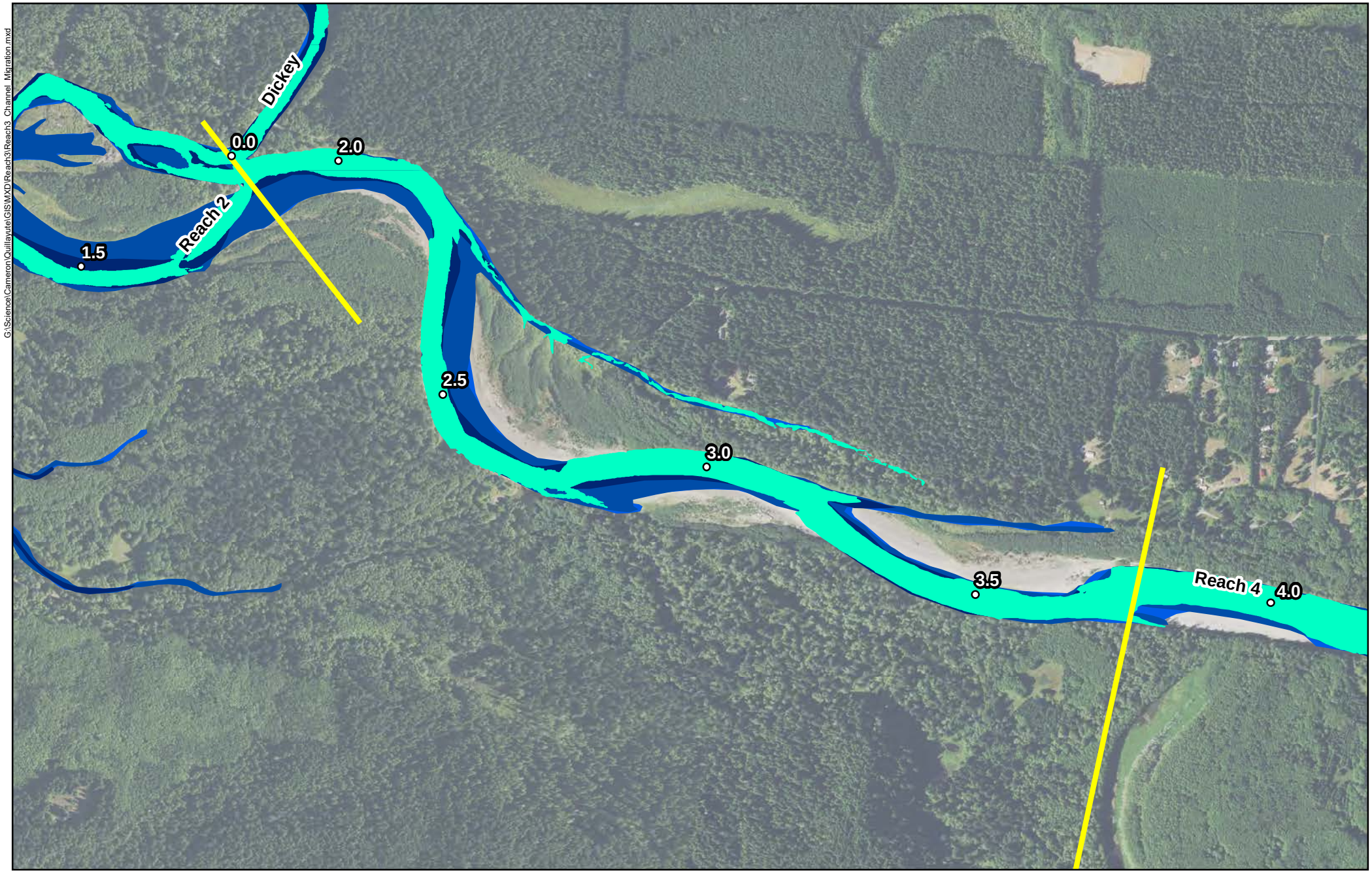

Channel

2019 2015

2017 2013

Geomorphic Reaches

River Miles

Quillayute River Geomorphic Assessment

Channel Migration Analysis
2013 - 2019
Reach 3
Figure G-16

TETRA TECH

N
W E
S

0 1,250 2,500
Feet

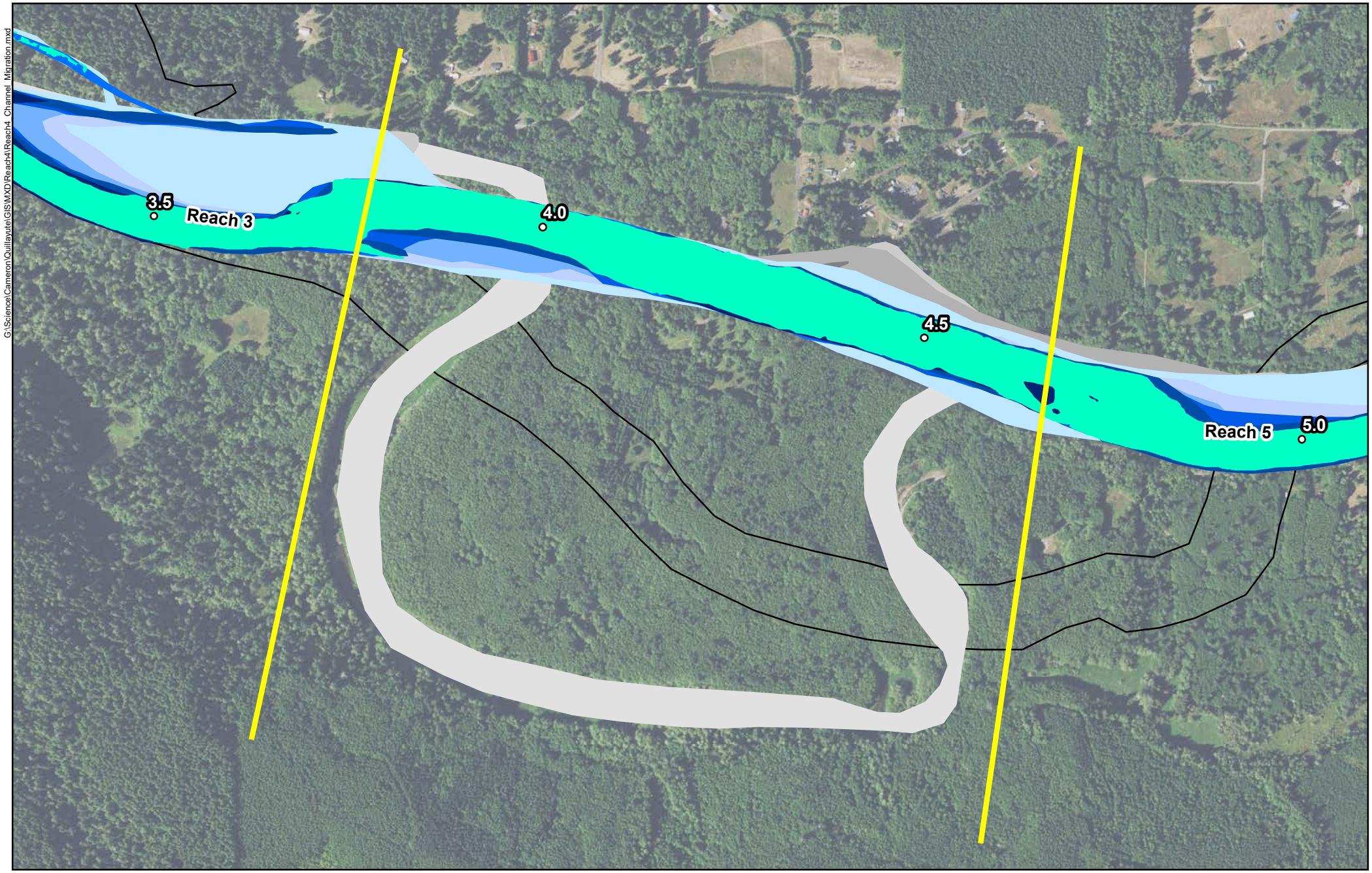

Channel

2019	2011	1990	1883*
2017	2009	1980	Geomorphic Reaches
2015	2006	1977	River Miles
2013	2002	1955	

*GLO Survey

Quillayute River Geomorphic Assessment

Channel Migration Analysis
1883 - 2019
Reach 4
Figure G-17

TETRA TECH

N
W E
S

0 1,000 2,000
Feet

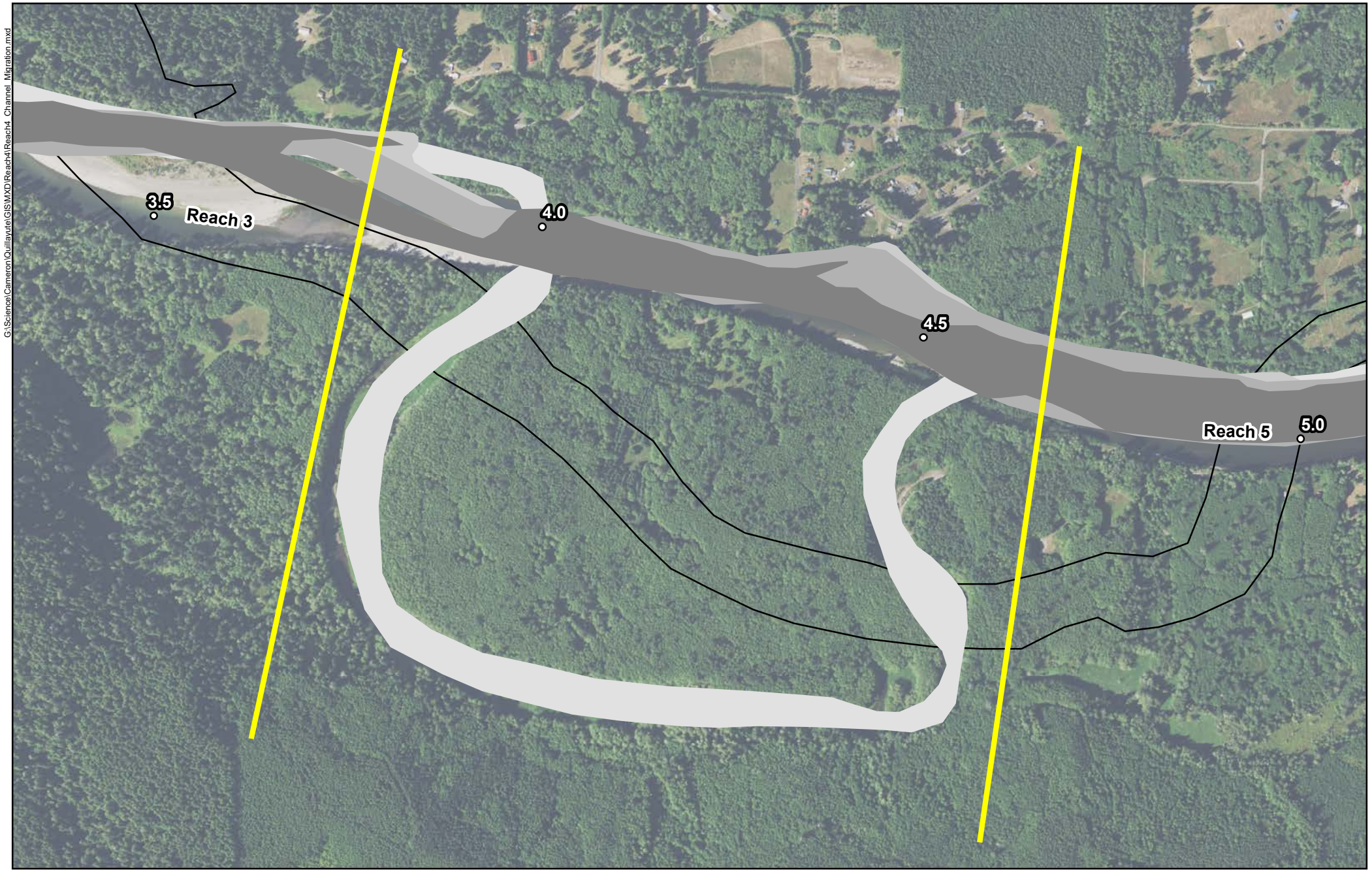

Channel

1990
1980
1977
1955
1883*

*GLO Survey

Geomorphic Reaches

River Miles

Quillayute River
Geomorphic Assessment

Channel Migration Analysis
1883 - 1990
Reach 4
Figure G-18

TETRA TECH

N
W E
S

0 1,000 2,000
Feet

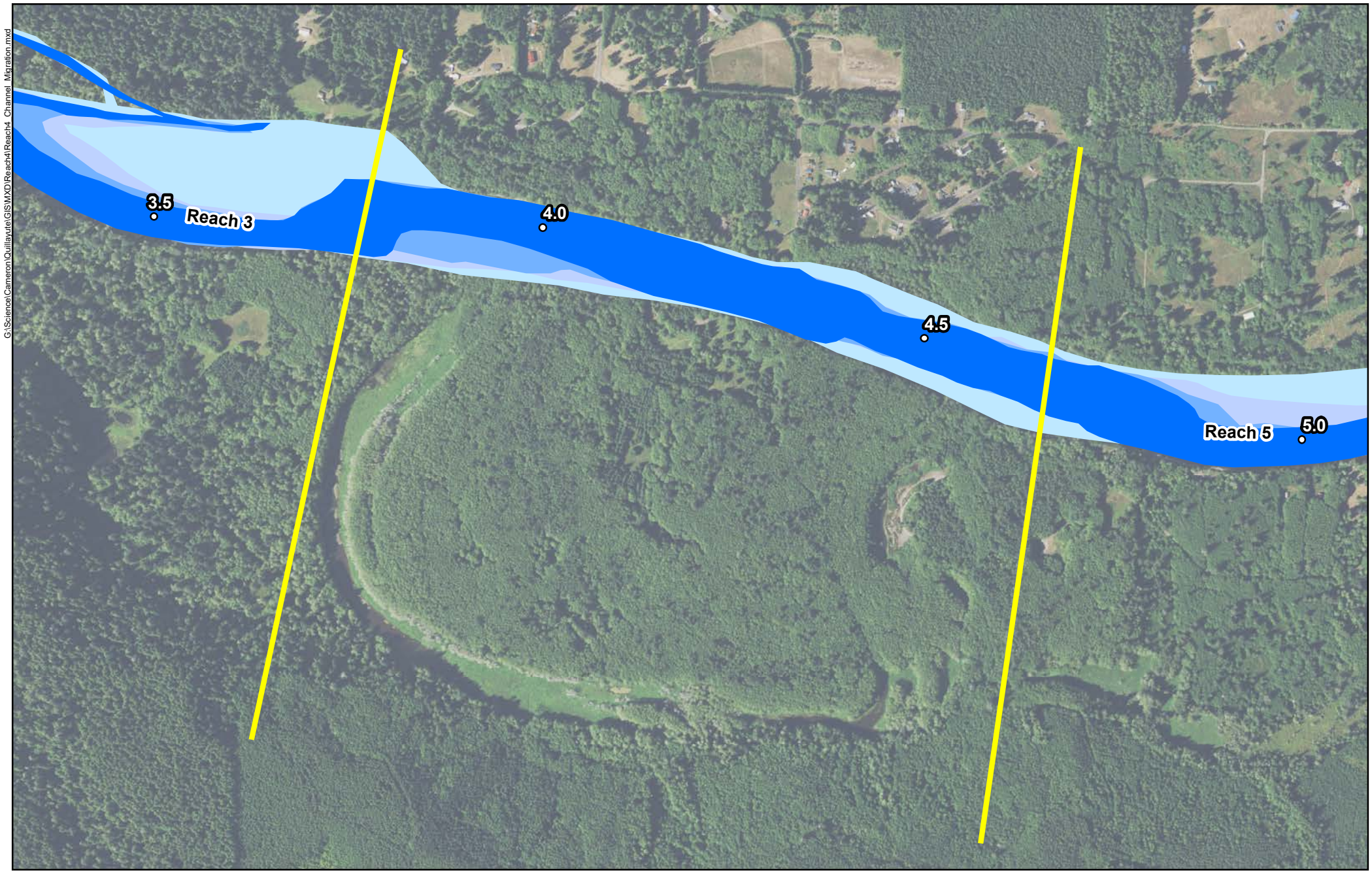

Channel

2011 | 2006

2009 | 2002

Geomorphic Reaches

River Miles

Quillayute River
Geomorphic Assessment

Channel Migration Analysis
2002 - 2011
Reach 4
Figure G-19

TETRA TECH

N
W E
S

0 1,000 2,000
Feet

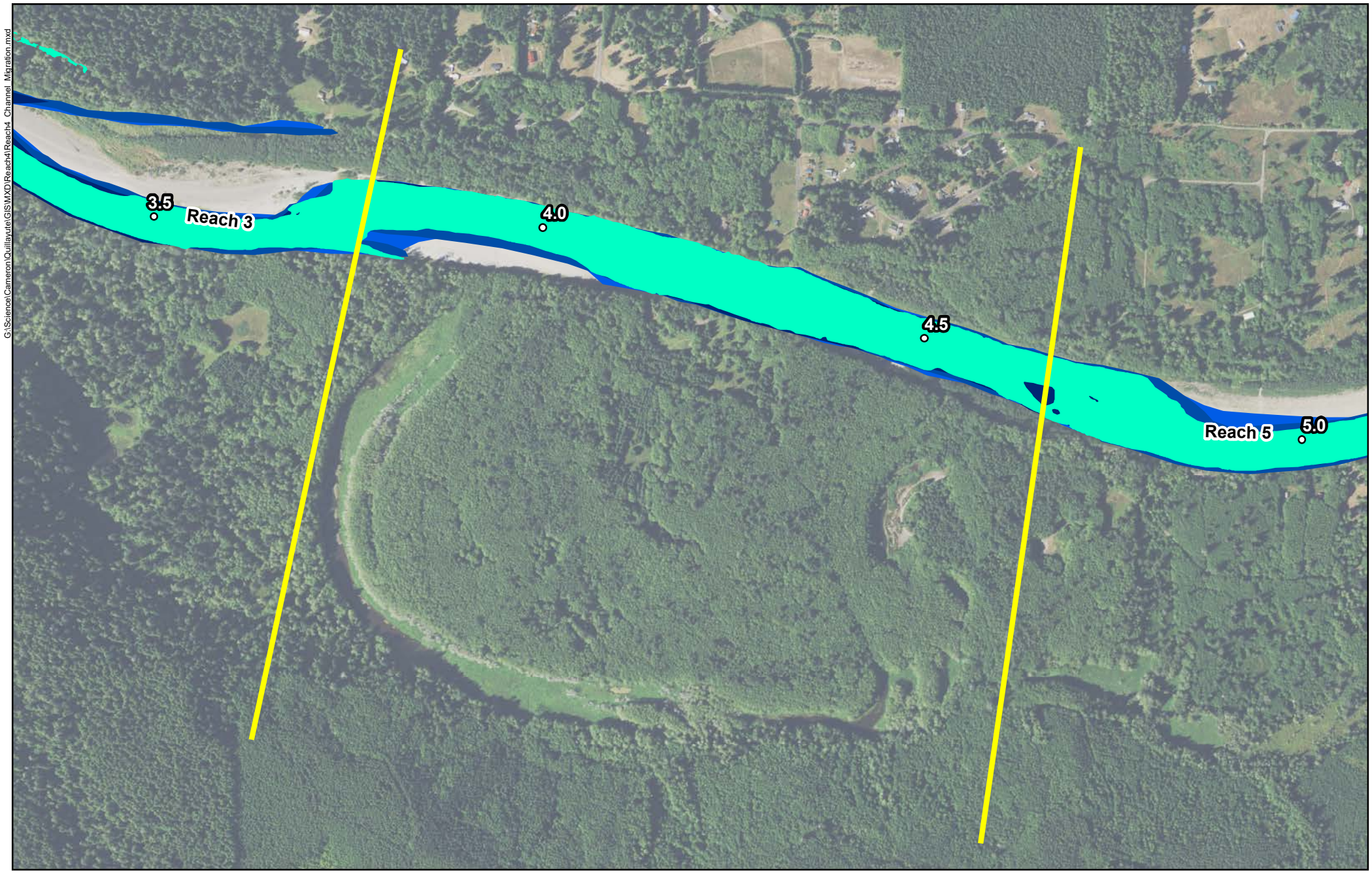

Channel

2019 2015

2017 2013

Geomorphic Reaches

River Miles

Quillayute River
Geomorphic Assessment

Channel Migration Analysis
2013 - 2019
Reach 4
Figure G-20

TETRA TECH

N
W E
S

0 1,000 2,000
Feet

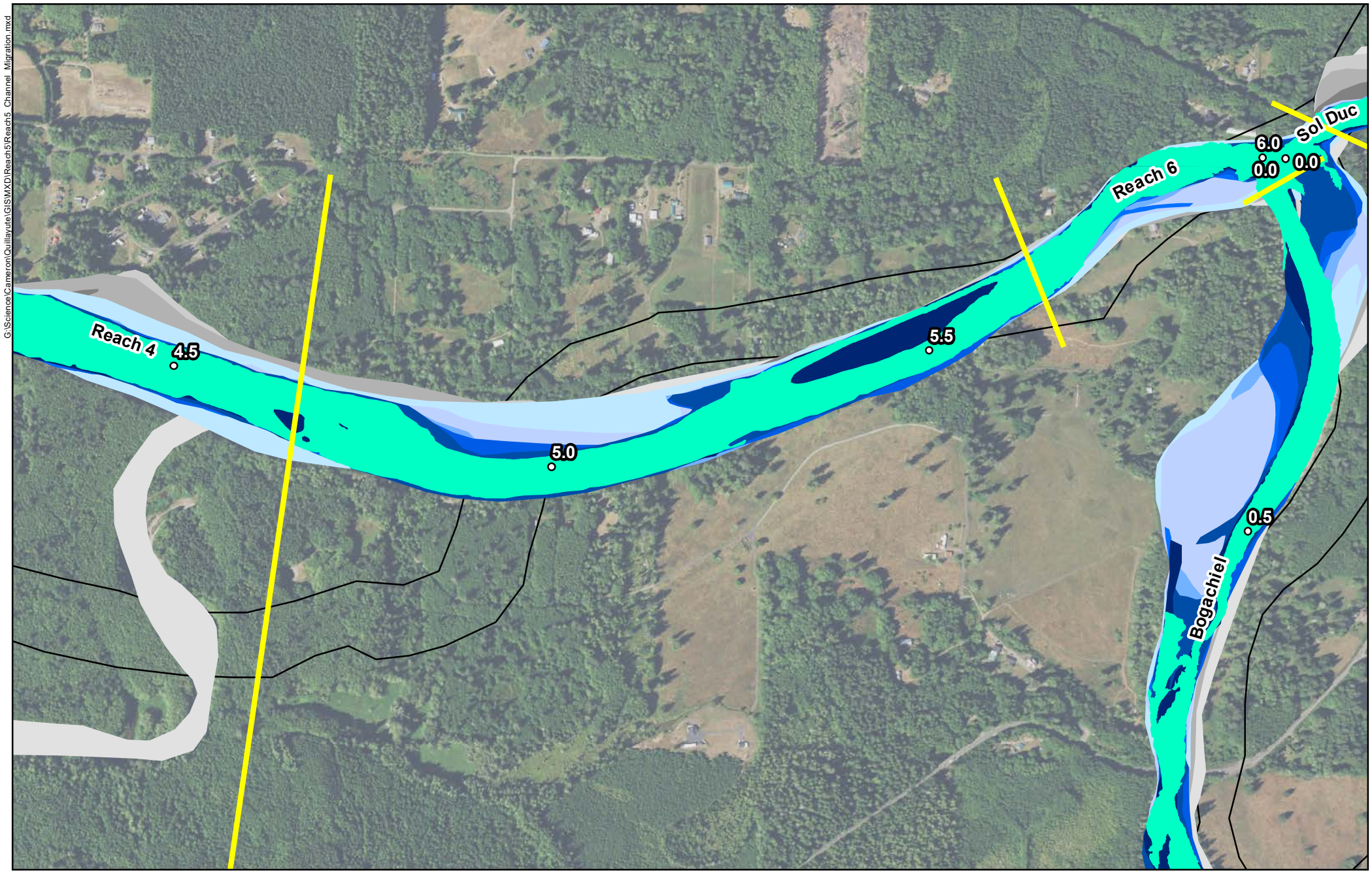

Channel

2019	2011	1990	1883*
2017	2009	1980	Geomorphic Reaches
2015	2006	1977	River Miles
2013	2002	1955	

Quillayute River Geomorphic Assessment

Channel Migration Analysis
1883 - 2019
Reach 5
Figure G-21

*GLO Survey

TETRA TECH

N
W E
S

0 1,000 2,000
Feet

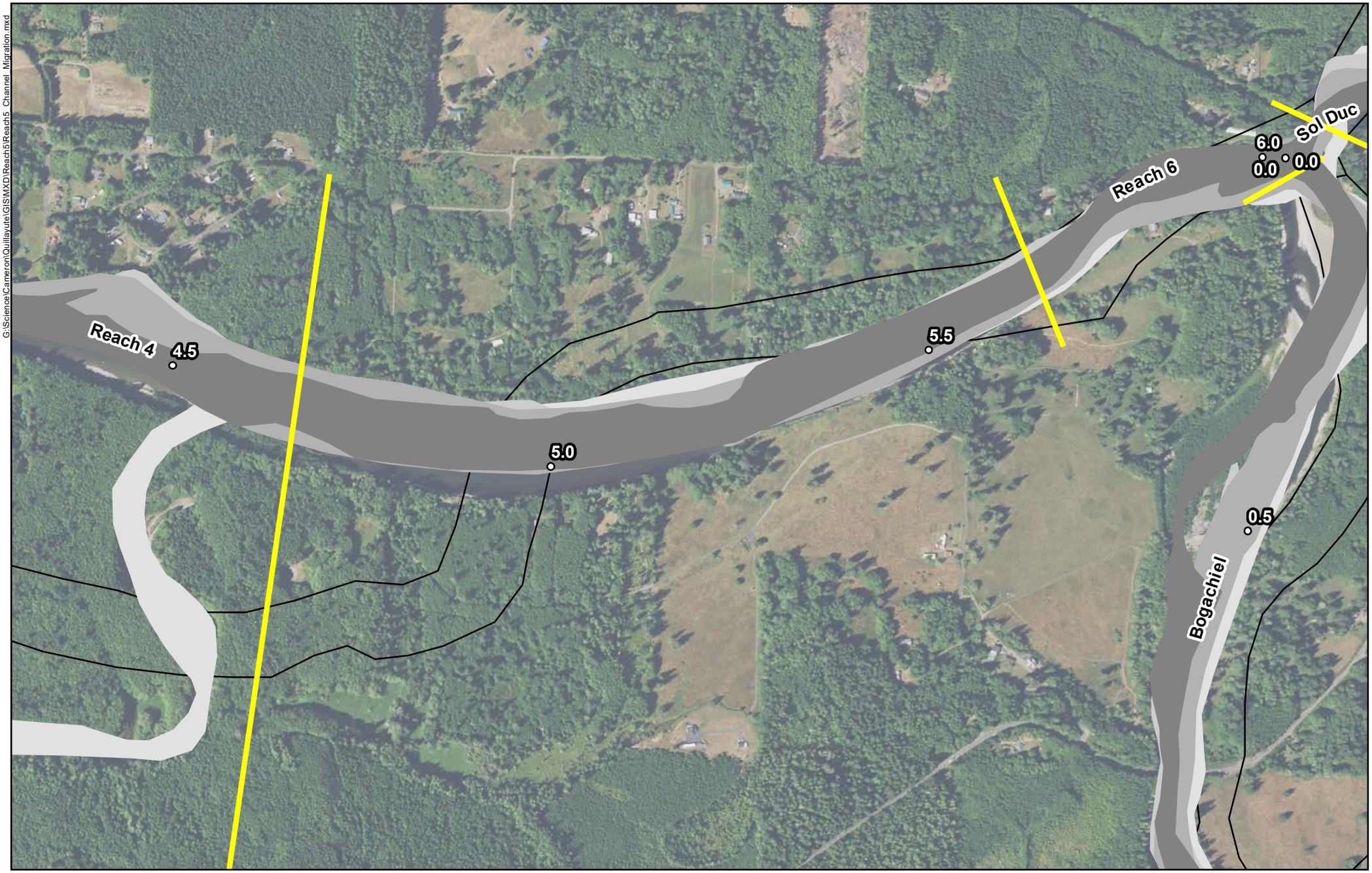

Channel

1990	1955
1980	1883*
1977	

*GLO Survey

Geomorphic Reaches

River Miles

Quillayute River
Geomorphic Assessment

Channel Migration Analysis
1883 - 1990
Reach 5
Figure G-22

TETRA TECH

N
W E
S

0 1,000 2,000
Feet

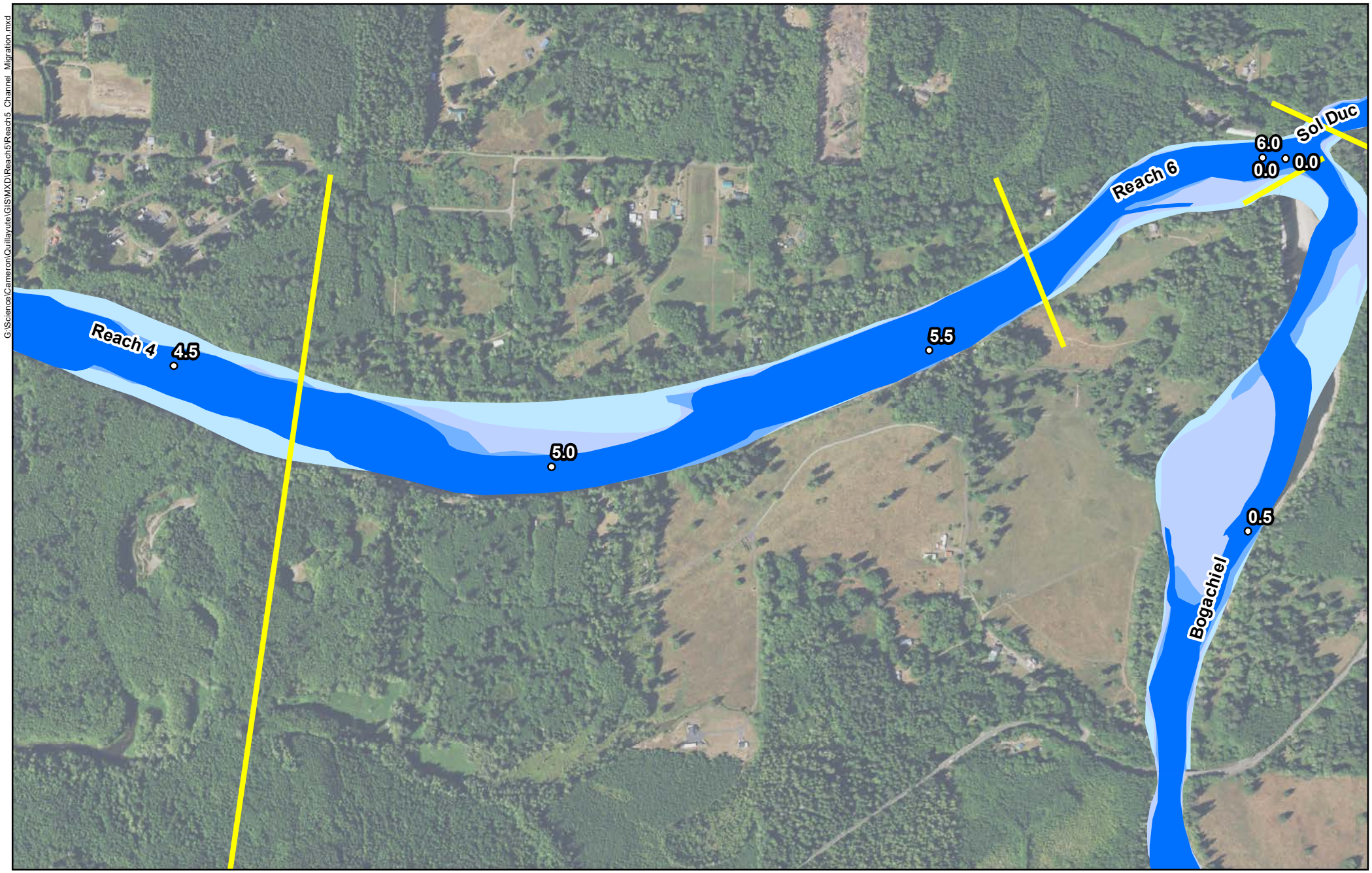

Channel

2011 | 2006

2009 | 2002

Geomorphic Reaches

River Miles

Quillayute River
Geomorphic Assessment

Channel Migration Analysis
2002 - 2011
Reach 5
Figure G-23

TETRA TECH

N
W E
S

0 1,000 2,000
Feet

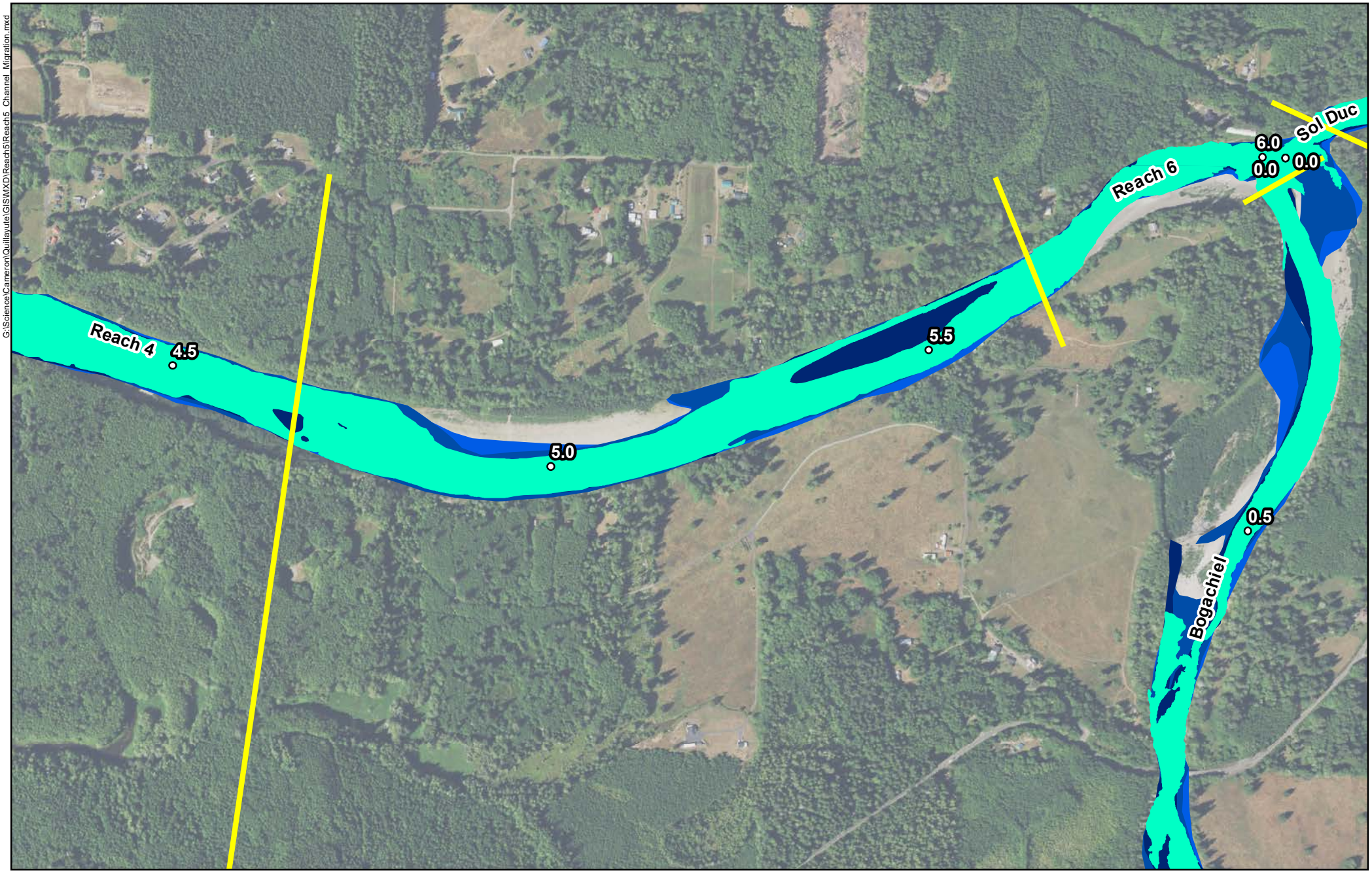

Channel

2019 2015

2017 2013

Geomorphic Reaches

River Miles

Quillayute River Geomorphic Assessment

Channel Migration Analysis
2013 - 2019
Reach 5
Figure G-24

TETRA TECH

N W E S

0 1,000 2,000

Feet

G:\Science\Cameron\Quillayute\GIS\MXD\Reach6\Reach6_Channel_Migration.mxd

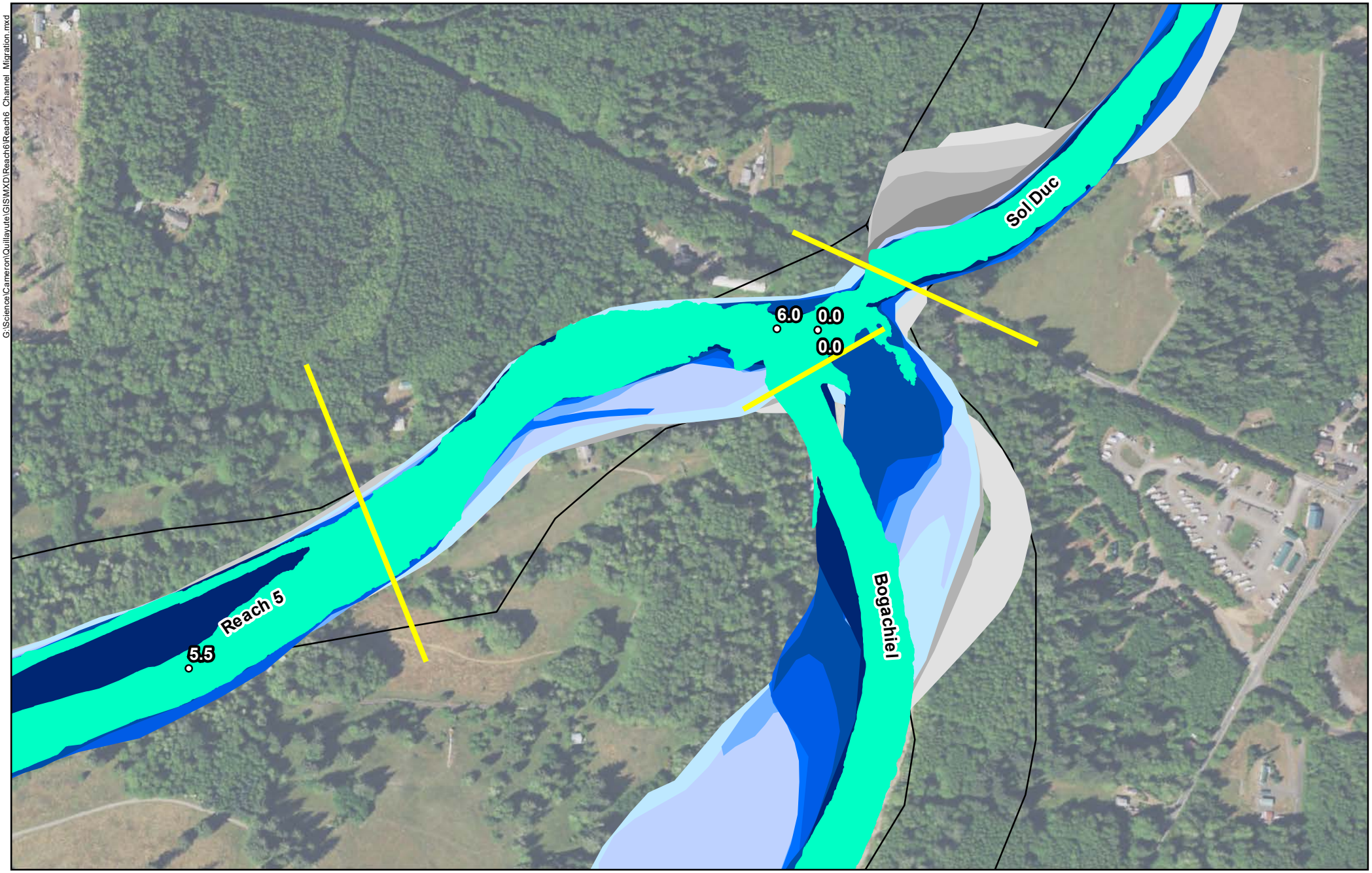

Channel

2019	2011	1990	1883*	Geomorphic Reaches
2017	2009	1980		
2015	2006	1977		River Miles
2013	2002	1955		

Quillayute River Geomorphic Assessment

Channel Migration Analysis
1883 - 2019
Reach 6
Figure G-25

*GLO Survey

TETRA TECH

N
W E
S

0 500 1,000
Feet

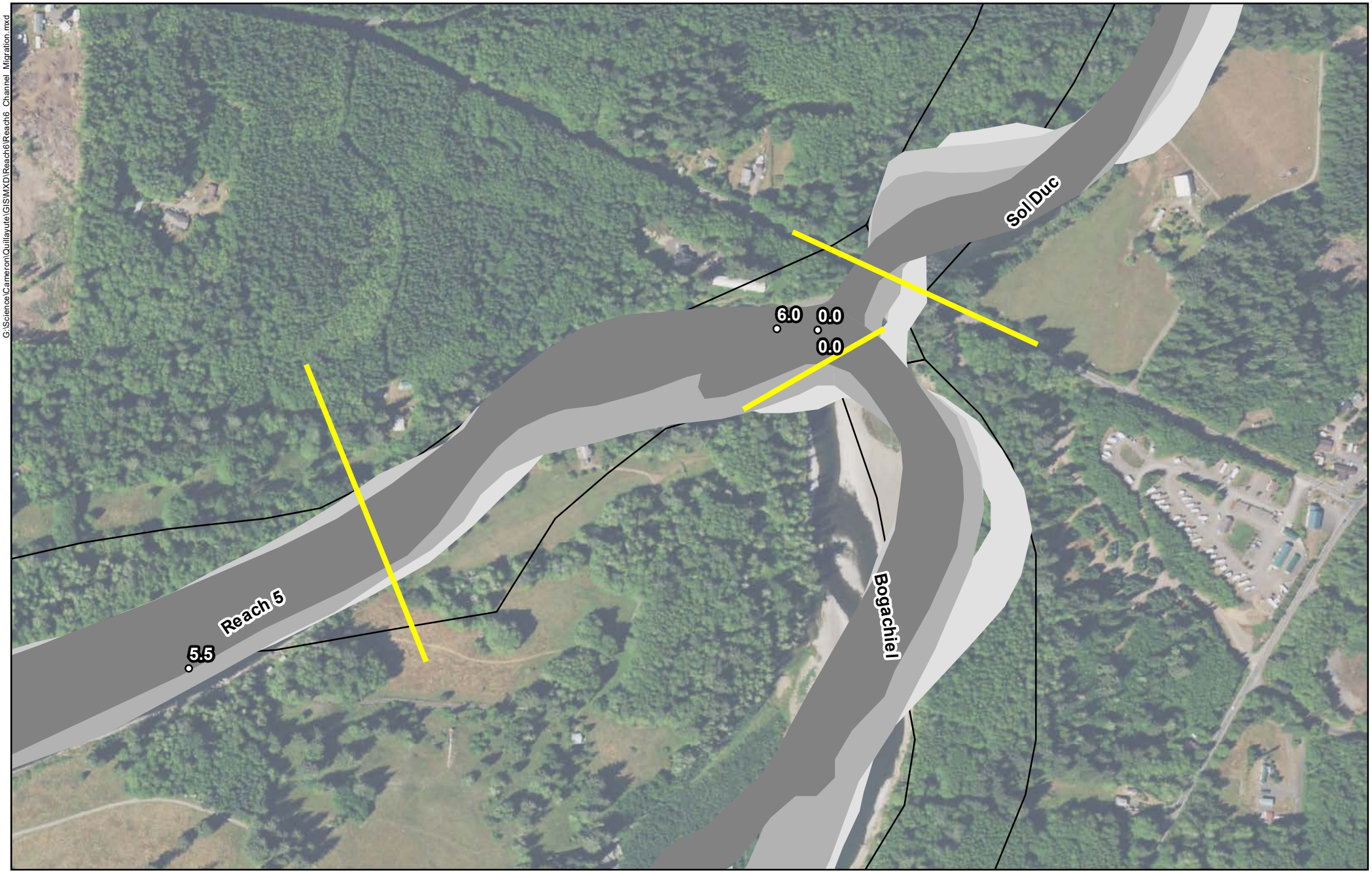

Channel

1990	1955
1980	1883*
1977	

*GLO Survey

Geomorphic Reaches

River Miles

Quillayute River
Geomorphic Assessment

Channel Migration Analysis
1883 - 1990
Reach 6
Figure G-26

TETRA TECH

N
W E
S

0 500 1,000
Feet

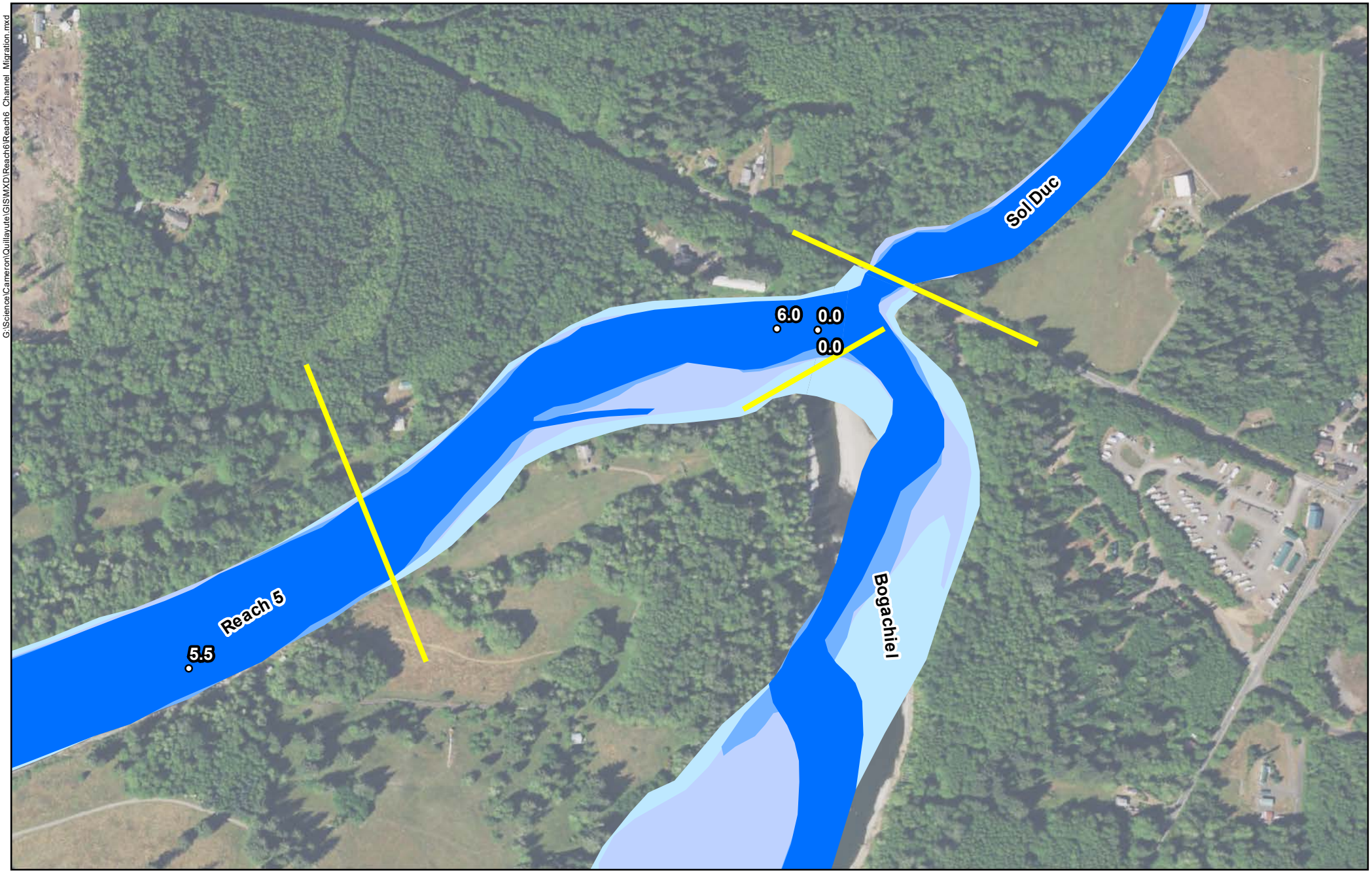

Channel

2011 | 2006

2009 | 2002

Geomorphic Reaches

River Miles

Quillayute River
Geomorphic Assessment

Channel Migration Analysis
2002 - 2011
Reach 6
Figure G-27

TETRA TECH

N
W E
S

0 500 1,000
Feet

G:\Science\Cameron\Quillayute\GIS\MXD\Reach6\Reach6_Channel_Migration.mxd

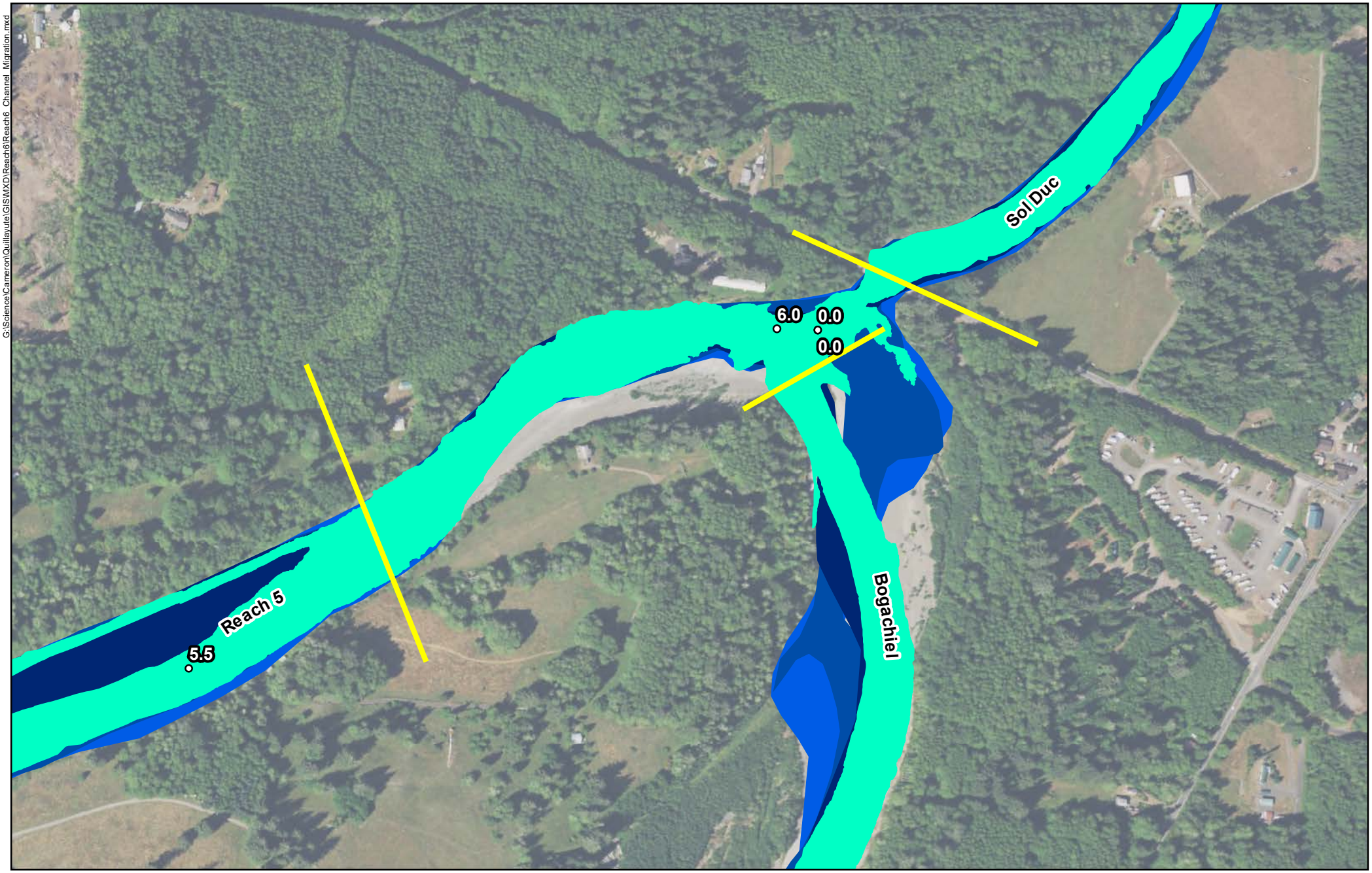

Channel

2019 2015

2017 2013

Geomorphic Reaches

River Miles

Quillayute River Geomorphic Assessment

Channel Migration Analysis
2013 - 2019
Reach 6
Figure G-28

TETRA TECH

N
W E
S

0 500 1,000
Feet

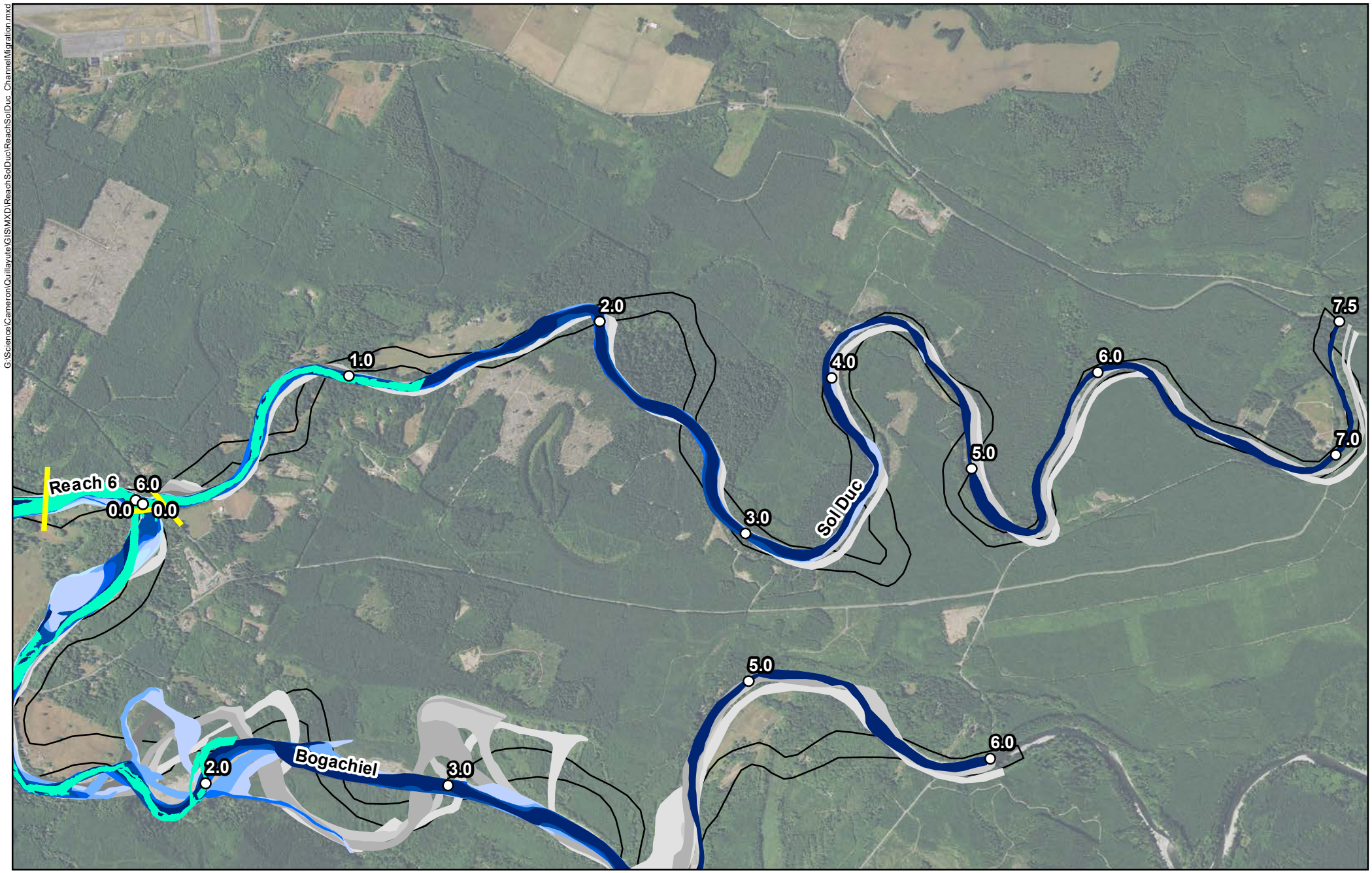
G:\Science\Cameron\Quillayute\GIS\MXD\ReachSolDuc\ReachSolDuc_ChannelMigration.mxd
Reach 6
6.0
0.0
0.0
1.0
2.0
3.0
4.0
5.0
6.0
7.0
7.5
Sol Duc
Bogachiel
2.0
3.0
5.0
6.0
Channel
2019
2017
2015
2013
2011
2009
2006
2002
1990
1980
1977
1955
1883*
Geomorphic Reaches
River Miles
Quillayute River
Geomorphic Assessment
Channel Migration Analysis
1883 - 2019
Lower Sol Duc River
Figure G-29
*GLO Survey
TETRA TECH
N
W
E
S
0
2,500
5,000
Feet

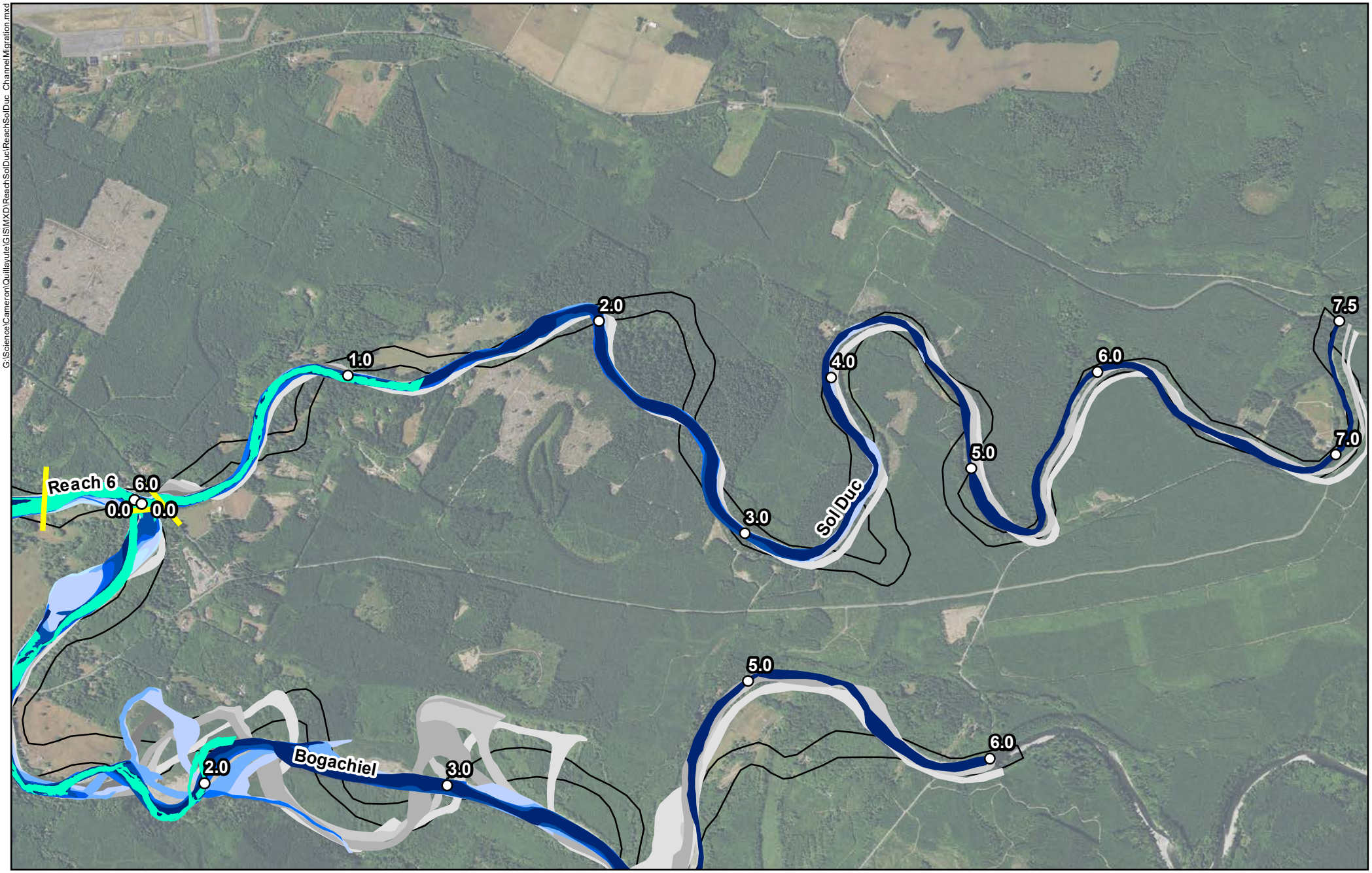

Channel

1990 | 1955

1980 | 1883*

1977

*GLO Survey

Geomorphic Reaches

River Miles

Quillayute River
Geomorphic Assessment

Channel Migration Analysis
1883 - 1990
Lower Sol Duc River
Figure G-30

TETRA TECH

N
W
E
S

0 2,500 5,000
Feet

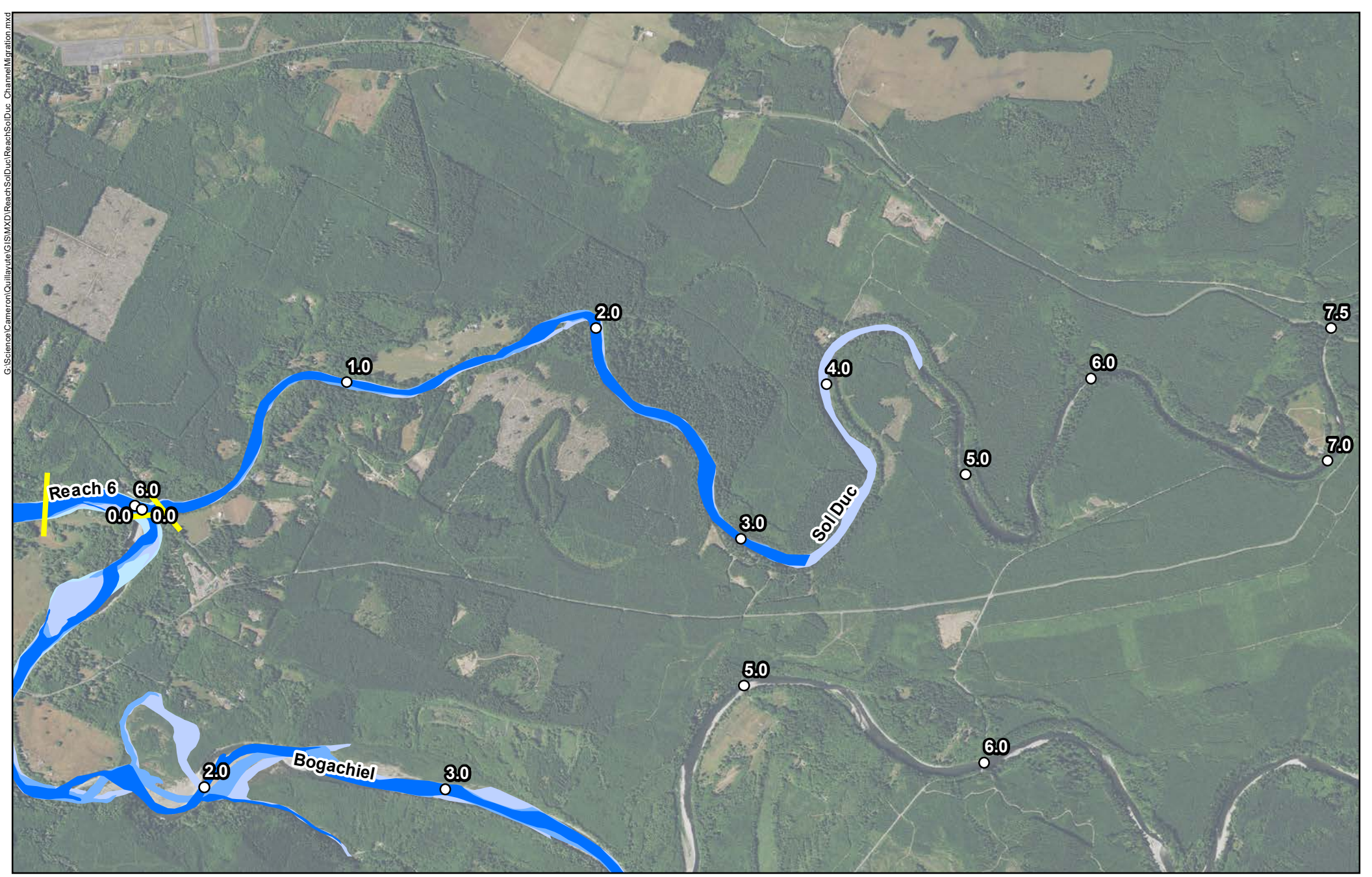

Channel

2011 | 2006

2009 | 2002

Geomorphic Reaches

River Miles

Quillayute River Geomorphic Assessment

Channel Migration Analysis
2002 - 2011
Lower Sol Duc River
Figure G-31

TETRA TECH

N
W
E
S

0 2,500 5,000
Feet

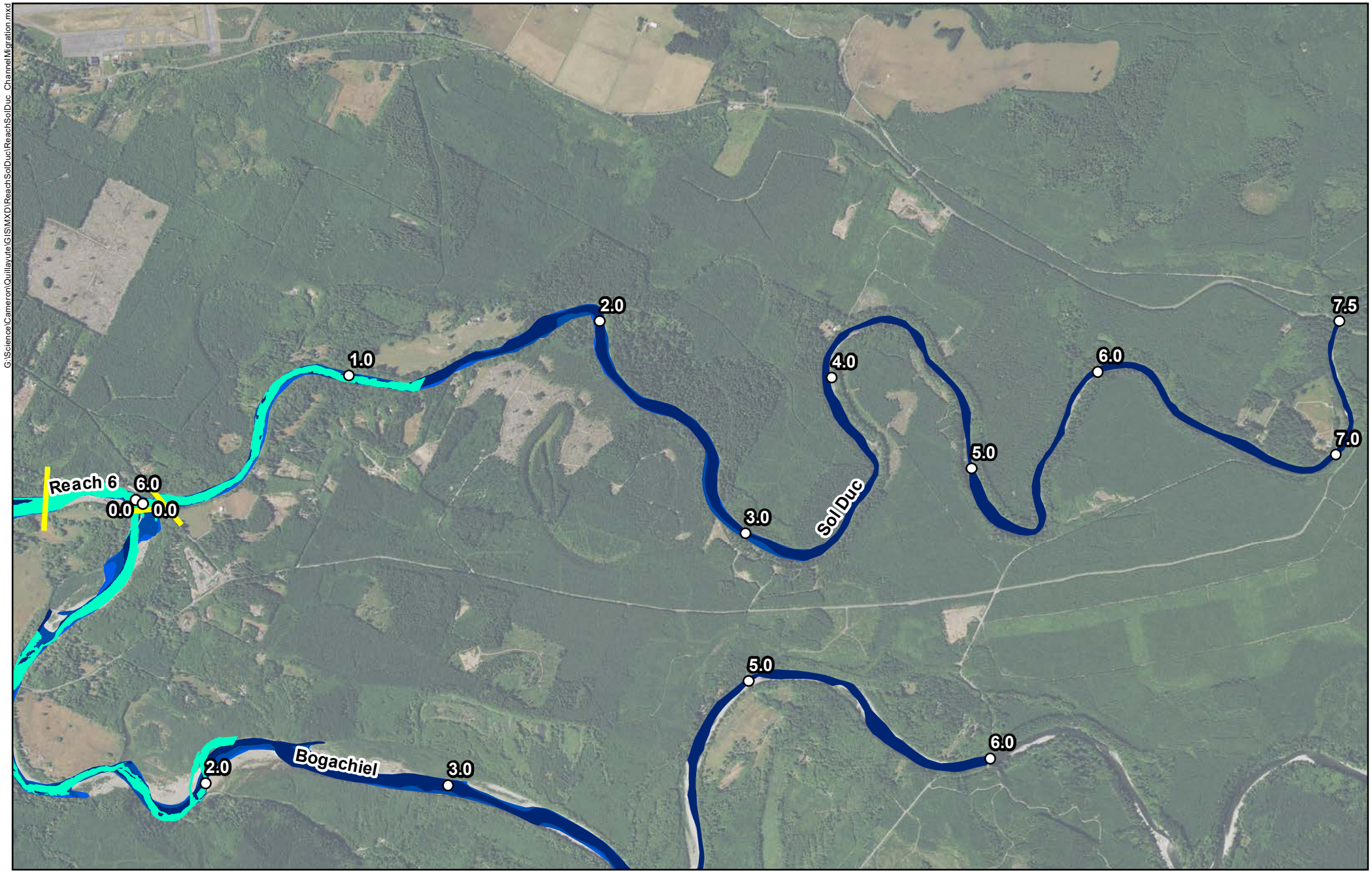

Channel

2019 2015

2017 2013

Geomorphic Reaches

River Miles

0

Quillayute River Geomorphic Assessment

Channel Migration Analysis
2013 - 2019
Lower Sol Duc River
Figure G-32

TETRA TECH

N W E S

0 2,500 5,000

Feet

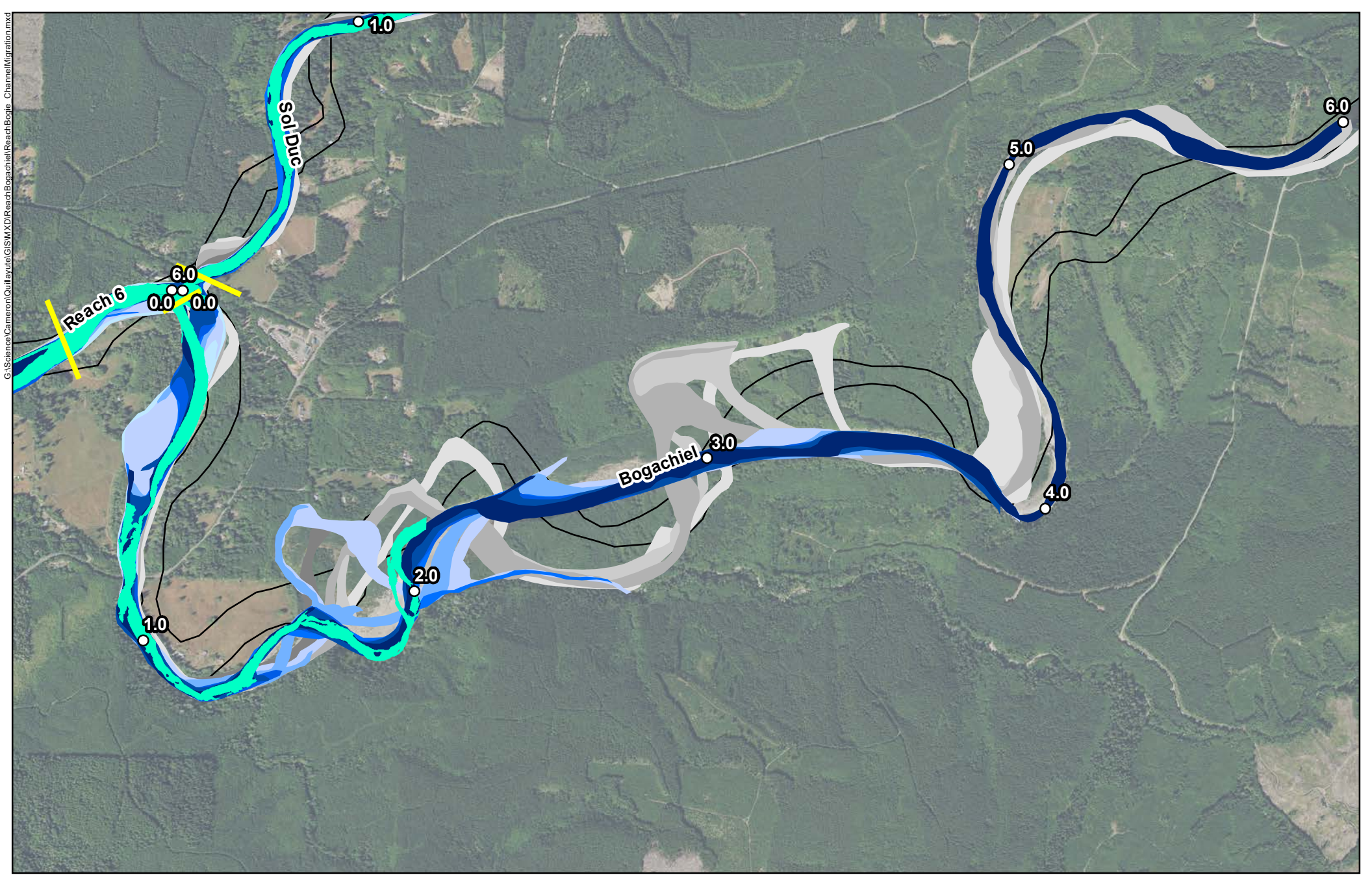

Channel

2019	2011	1990	1883*
2017	2009	1980	Geomorphic Reaches
2015	2006	1977	River Miles
2013	2002	1955	

Quillayute River Geomorphic Assessment

Channel Migration Analysis
1883 - 2019
Lower Bogachiel River
Figure G-33

*GLO Survey

TETRA TECH

N
W E
S

0 2,000 4,000
Feet

Channel

1990
1980
1977
1955
1883*

*GLO Survey

Geomorphic Reaches

River Miles

Quillayute River
Geomorphic Assessment

Channel Migration Analysis
1883 - 1990
Lower Bogachiel River
Figure G-34

TETRA TECH

N
W
E
S

0 2,000 4,000
Feet

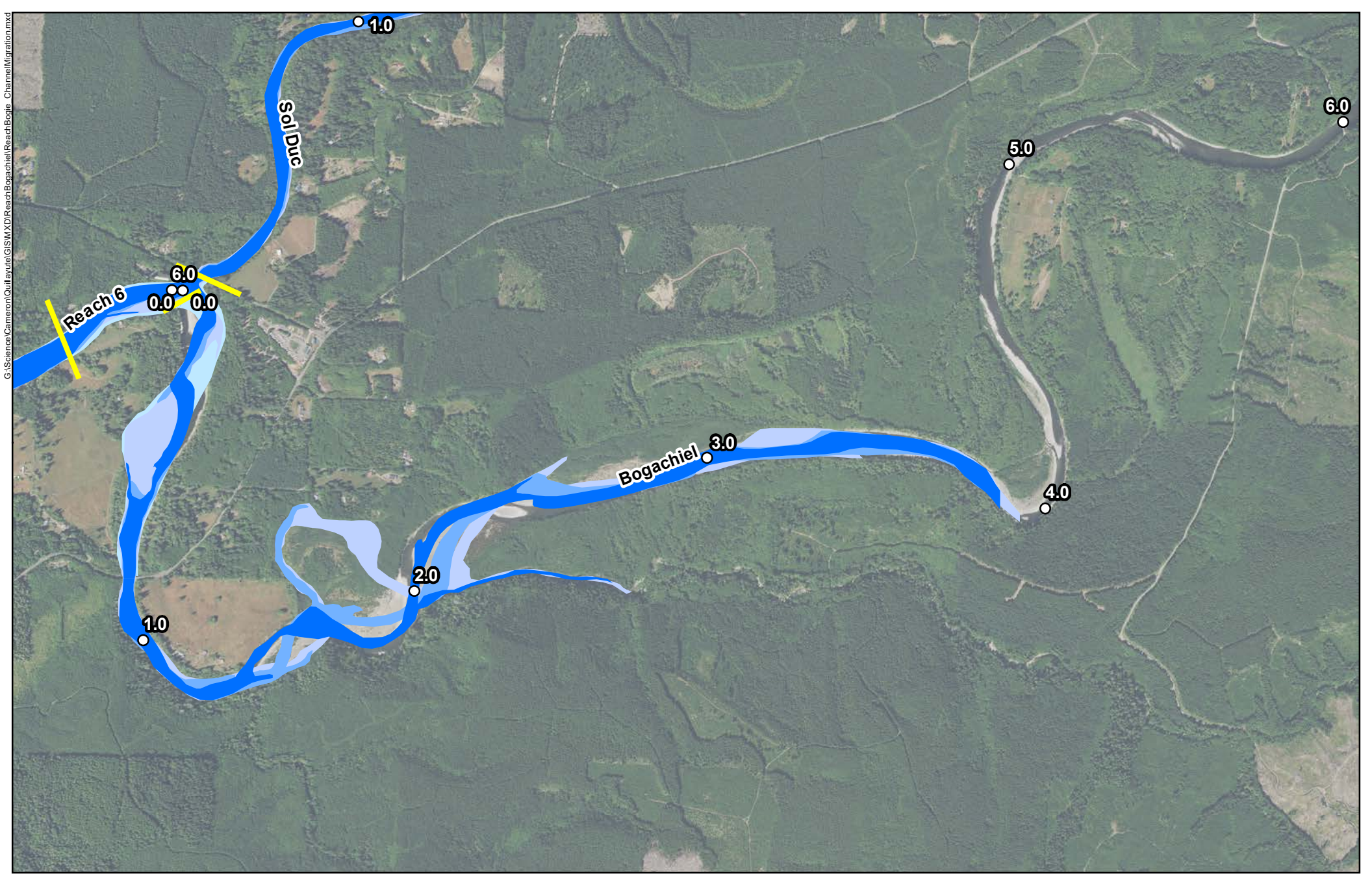

Channel

2011 | 2006

2009 | 2002

Geomorphic Reaches

River Miles

Quillayute River Geomorphic Assessment

Channel Migration Analysis
2002 - 2011
Lower Bogachiel River
Figure G-35

TETRA TECH

N
W E
S

0 2,000 4,000
Feet

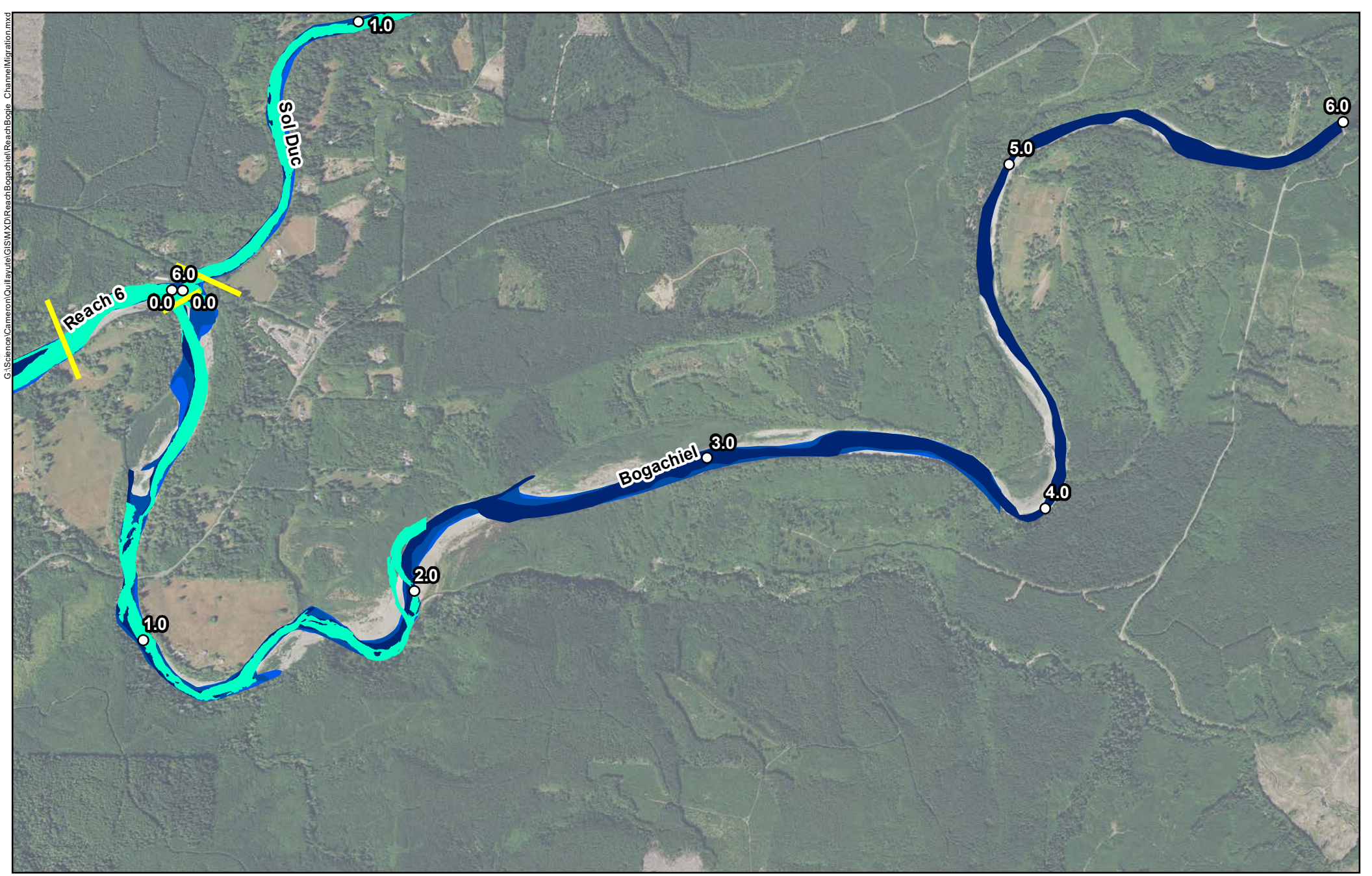

Channel

2019 2015

2017 2013

Geomorphic Reaches

River Miles

Quillayute River Geomorphic Assessment

Channel Migration Analysis
2013 - 2019
Lower Bogachiel River
Figure G-36

TETRA TECH

N
W E
S

0 2,000 4,000
Feet

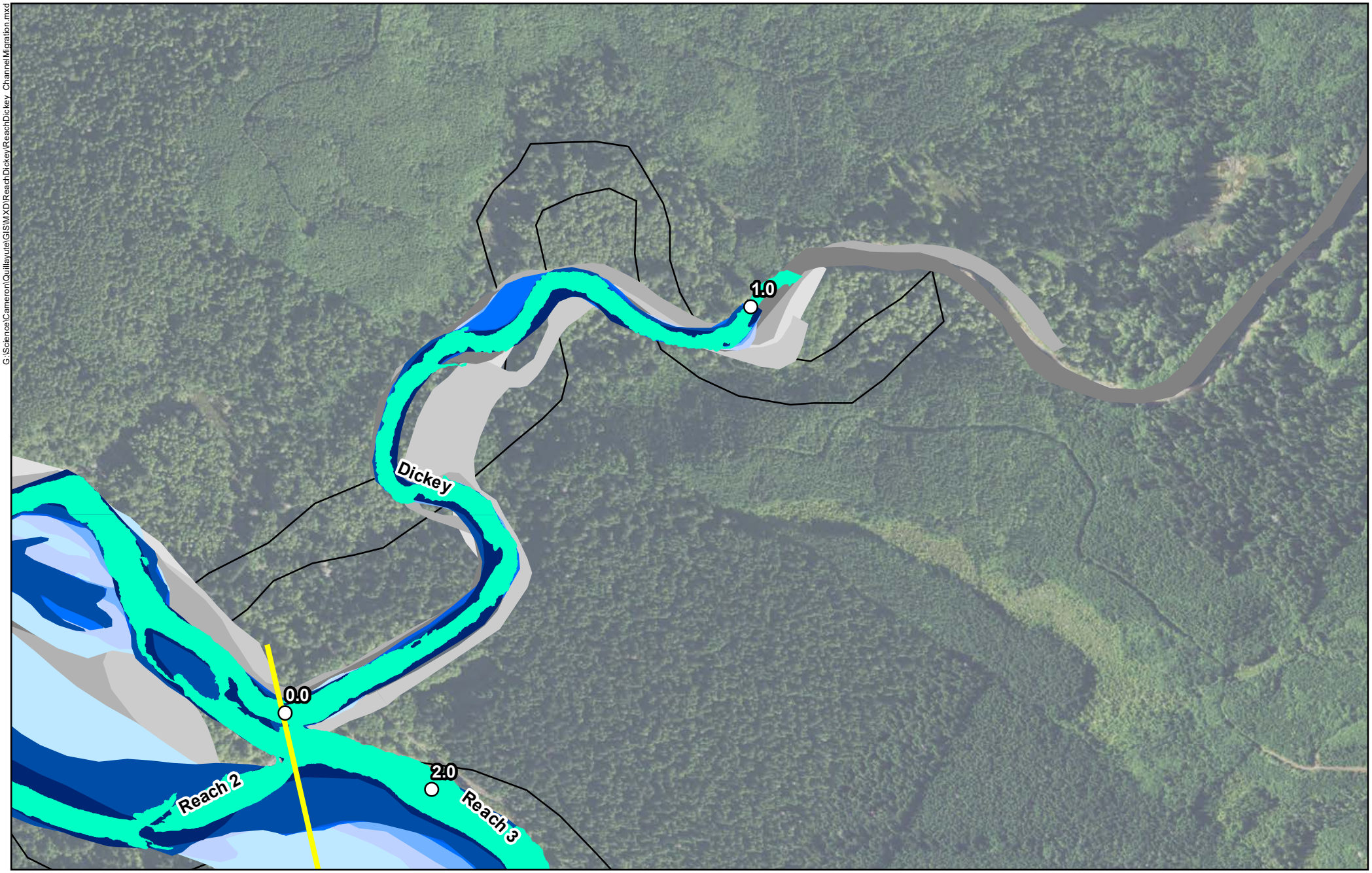

Channel

2019	2011	1990	1883*
2017	2009	1980	Geomorphic Reaches
2015	2006	1977	River Miles
2013	2002	1955	

*GLO Survey

Quillayute River Geomorphic Assessment

Channel Migration Analysis
1883 - 2019
Lower Dickey River
Figure G-37

TETRA TECH

N
W
E
S

0 750 1,500
Feet

Channel

1990
1980
1977
1955
1883*

*GLO Survey

Geomorphic Reaches

River Miles

Quillayute River
Geomorphic Assessment

Channel Migration Analysis
1883 - 1990
Lower Dickey River
Figure G-38

TETRA TECH

N
W
E
S

0 750 1,500
Feet

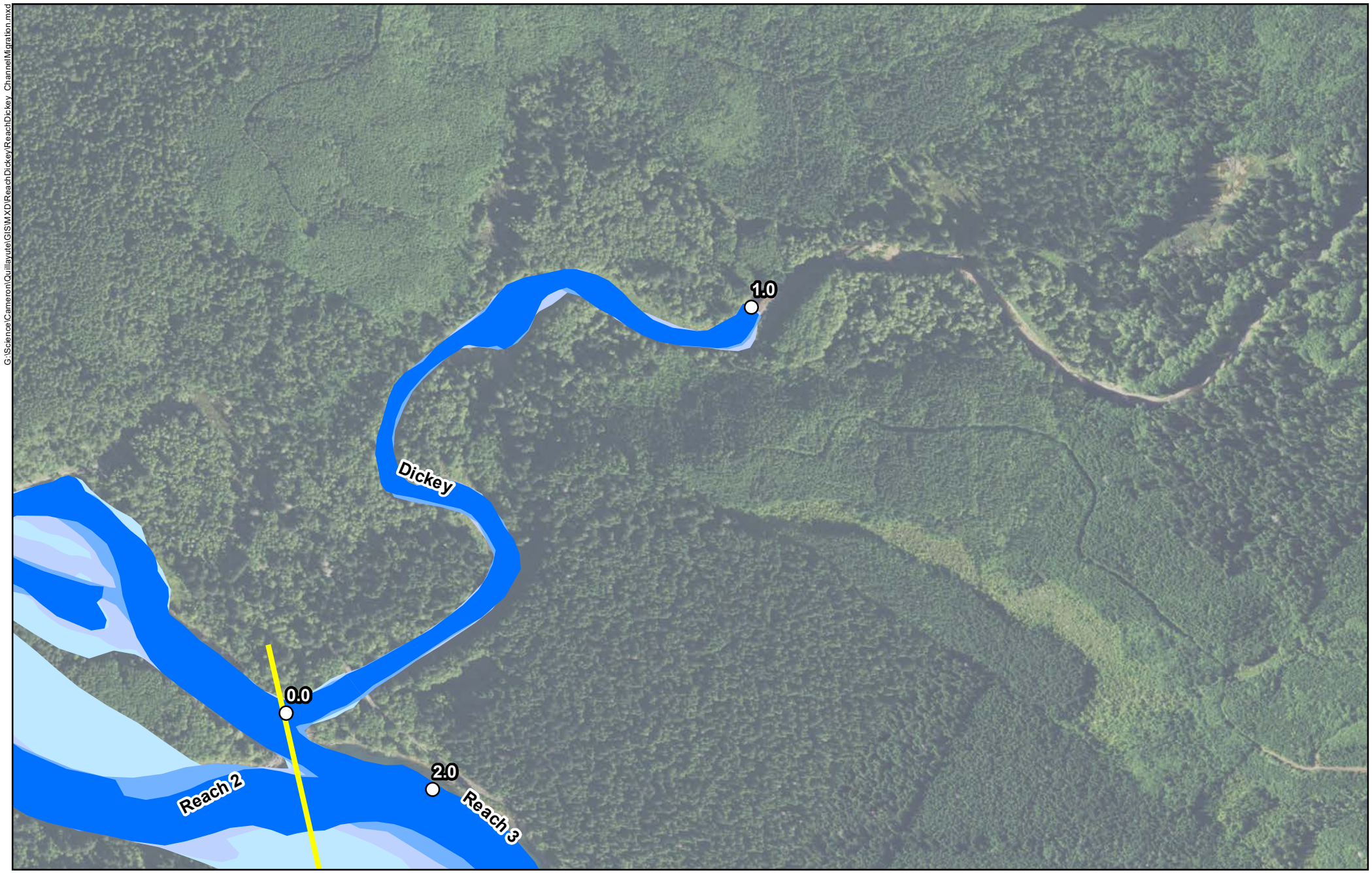

Channel

2011 | 2006

2009 | 2002

Geomorphic Reaches

River Miles

Quillayute River Geomorphic Assessment

Channel Migration Analysis
2002 - 2011
Lower Dickey River
Figure G-39

TETRA TECH

N
W
E
S

0 750 1,500
Feet

G:\Science\Cameron\Quillayute\GIS\MXD\ReachDickey\ReachDickey_ChannelMigration.mxd

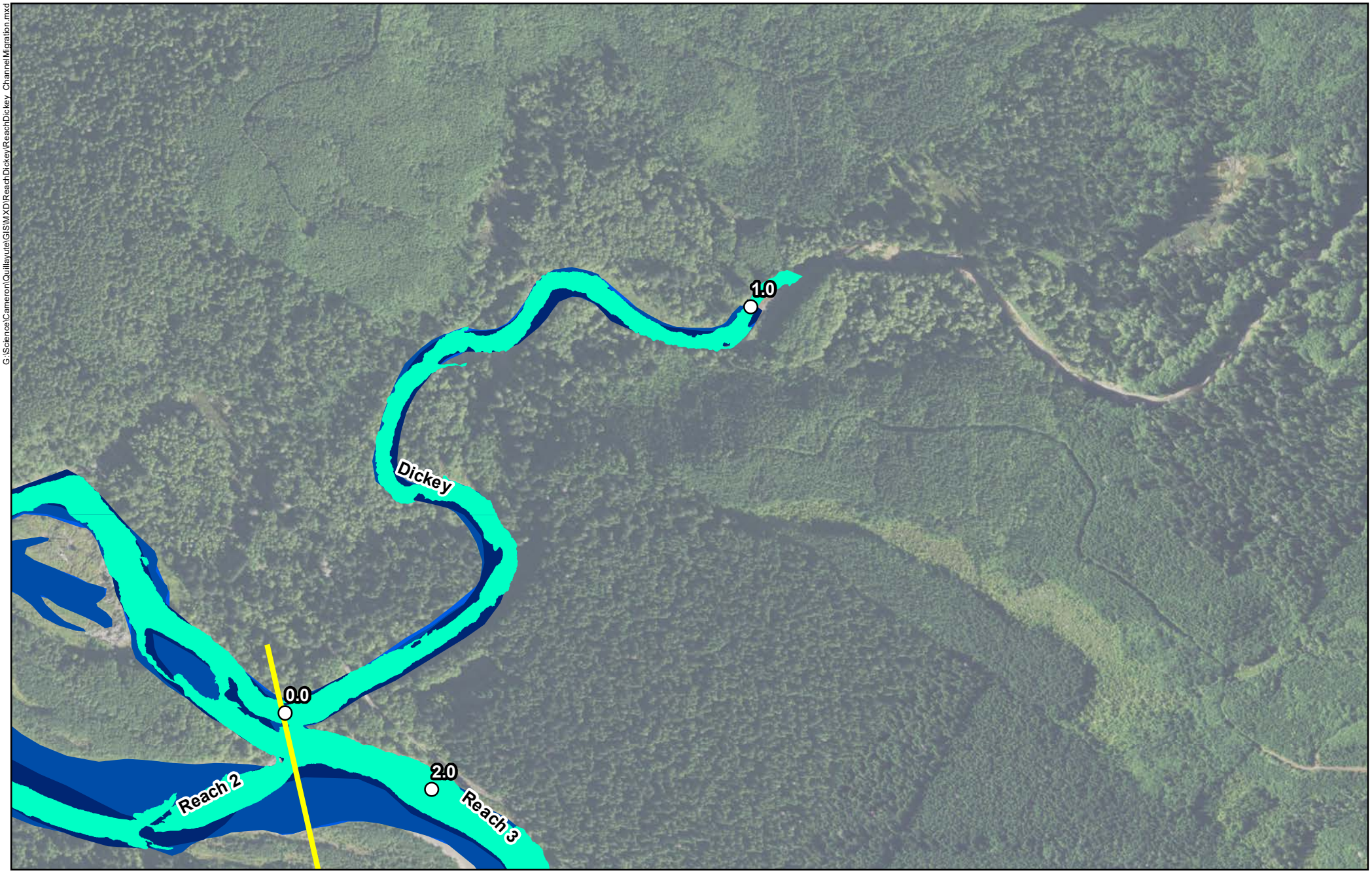

Channel

2019 | 2015

2017 | 2013

Geomorphic Reaches

River Miles

Quillayute River
Geomorphic Assessment

Channel Migration Analysis
2013 - 2019
Lower Dickey River
Figure G-40

TETRA TECH

N
W
E
S

0 750 1,500
Feet

APPENDIX H – CHANNEL MIGRATION ZONE (CMZ) MAPPING

Quillayute River Project
Geomorphic Assessment and Action Plan
Channel Migration Zone (CMZ) Mapping

Appendix H

Submitted to:

Quileute Natural Resources
401 Main Street
La Push, WA 98350

Submitted by:

19803 North Creek Parkway
Bothell, WA 98011
Tel 425.482.7600 | Fax 425.482.7652
www.tetratech.com

September 2020

LIST OF FIGURES

Figure H-1. ..... Channel Migration Zone Analysis Overview
Figure H-2. ..... Reach 1 Channel Migration Zone Analysis
Figure H-3. ..... Reach 2 Channel Migration Zone Analysis
Figure H-4. ..... Reach 3 Channel Migration Zone Analysis
Figure H-5. ..... Reach 4 Channel Migration Zone Analysis
Figure H-6. ..... Reach 5 Channel Migration Zone Analysis
Figure H-7. ..... Reach 6 Channel Migration Zone Analysis
Figure H-8. ..... Lower Bogachiel Channel Migration Zone Analysis
Figure H-9. ..... Lower Sol Duc Channel Migration Zone Analysis
Figure H-10. ..... Lower Dickey Channel Migration Zone Analysis

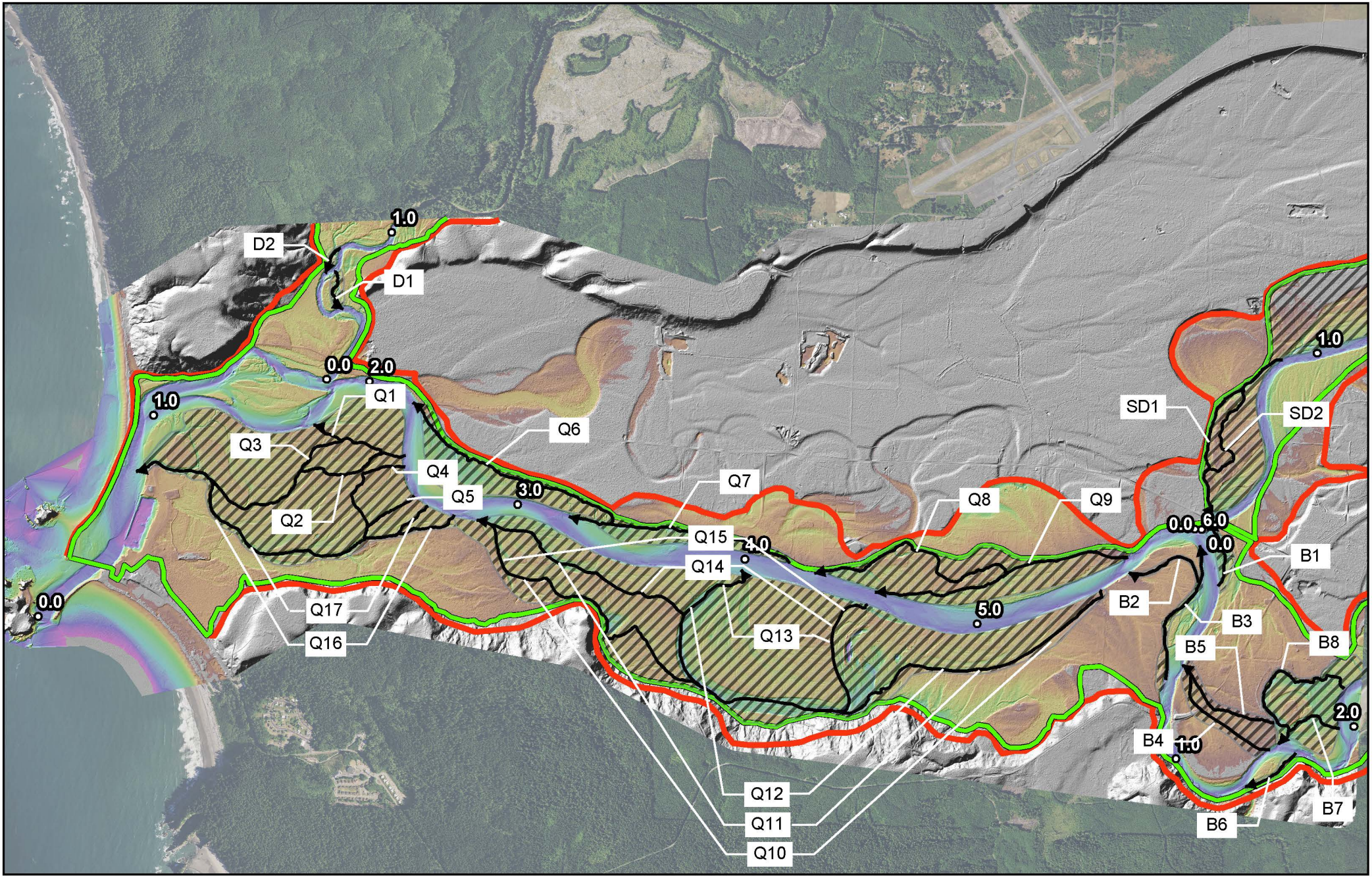

Avulsion Pathways

AHA

MVB

CMZ

Relative Elevation Model

Height Above Channel Bottom (ft)

High : 25

Low : -5

River Miles

Quillayute River Geomorphic Assessment

Channel Migration Zone (CMZ) Analysis
Quillayute and Bogachiel Rivers

Figure H-1

TETRA TECH

N
W E
S

0 3,500 7,000

Feet

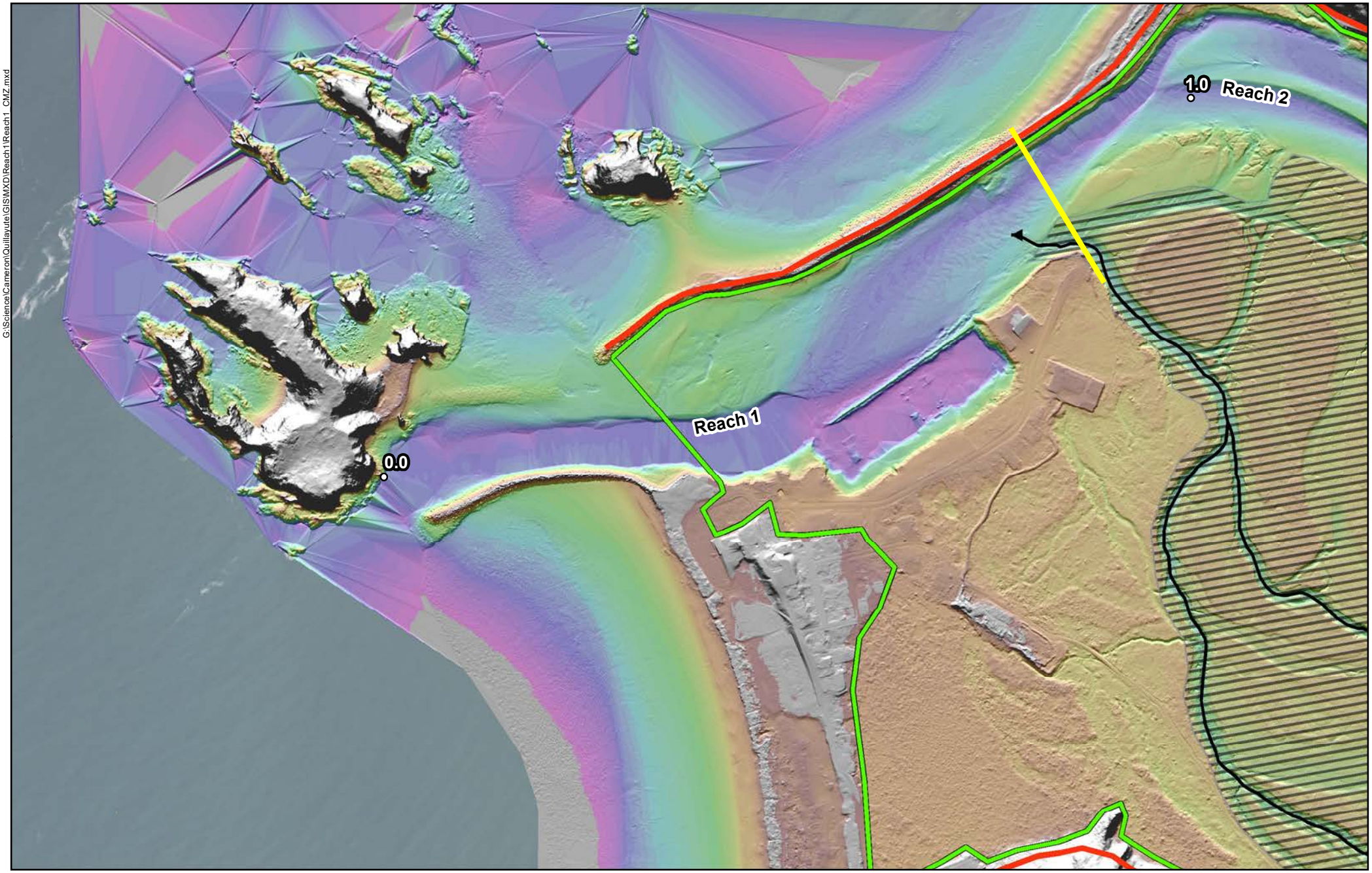

Avulsion Pathways

AHA

MVB

CMZ

Relative Elevation Model

Height Above Channel Bottom (ft)

High : 25

Low : -5

River Miles

Geomorphic Reaches

Quillayute River Geomorphic Assessment

Channel Migration Zone (CMZ) Analysis
Reach 1

Figure H-2

TETRA TECH

N

W

E

S

0 750 1,500

Feet

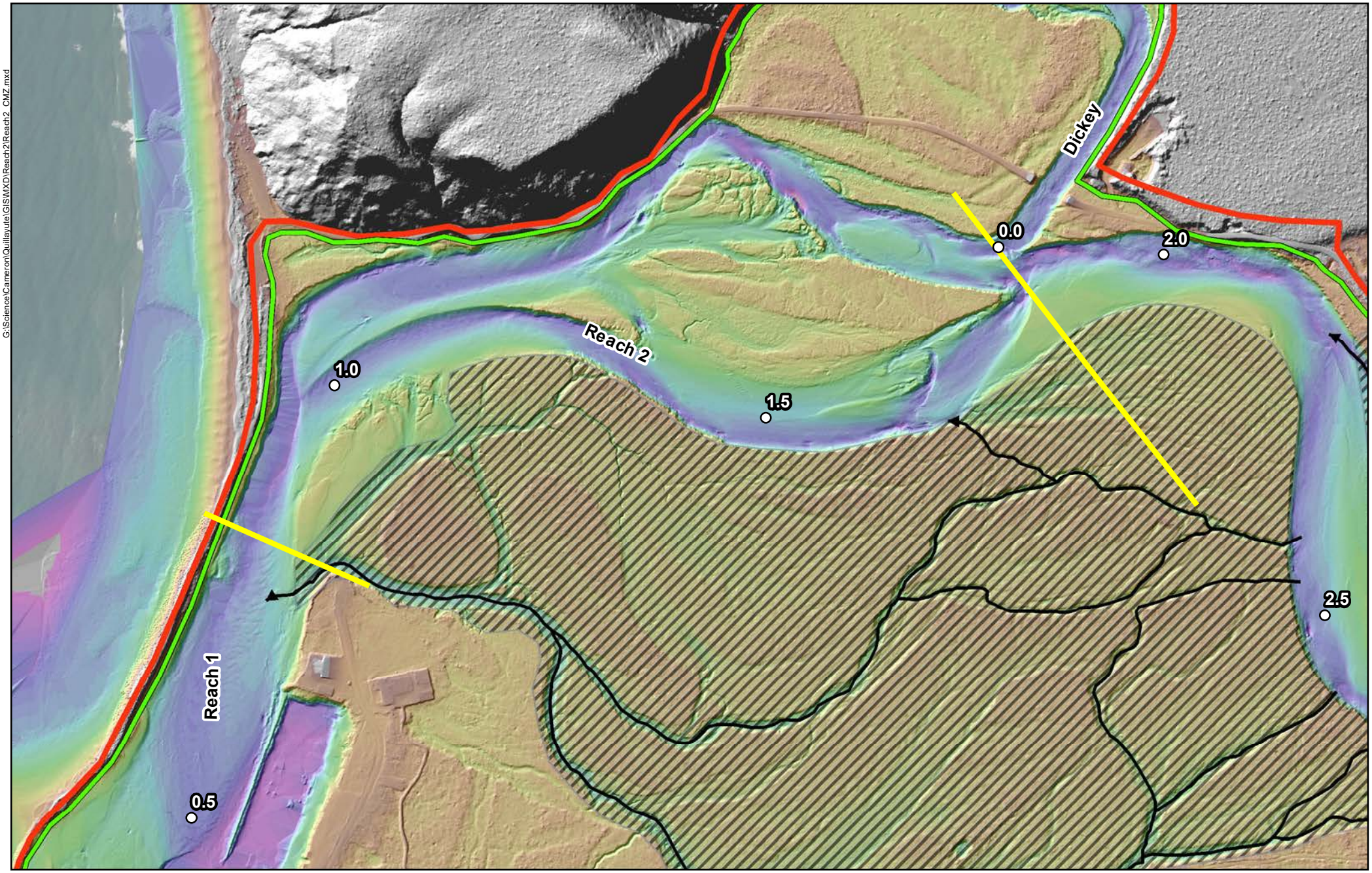

Avulsion Pathways

Relative Elevation Model

Height Above Channel Bottom (ft)

High : 25

Low : -5

AHA

MVB

CMZ

River Miles

Geomorphic Reaches

Quillayute River Geomorphic Assessment

Channel Migration Zone (CMZ) Analysis
Reach 2

Figure H-3

TETRA TECH

N

W E

S

0 750 1,500

Feet

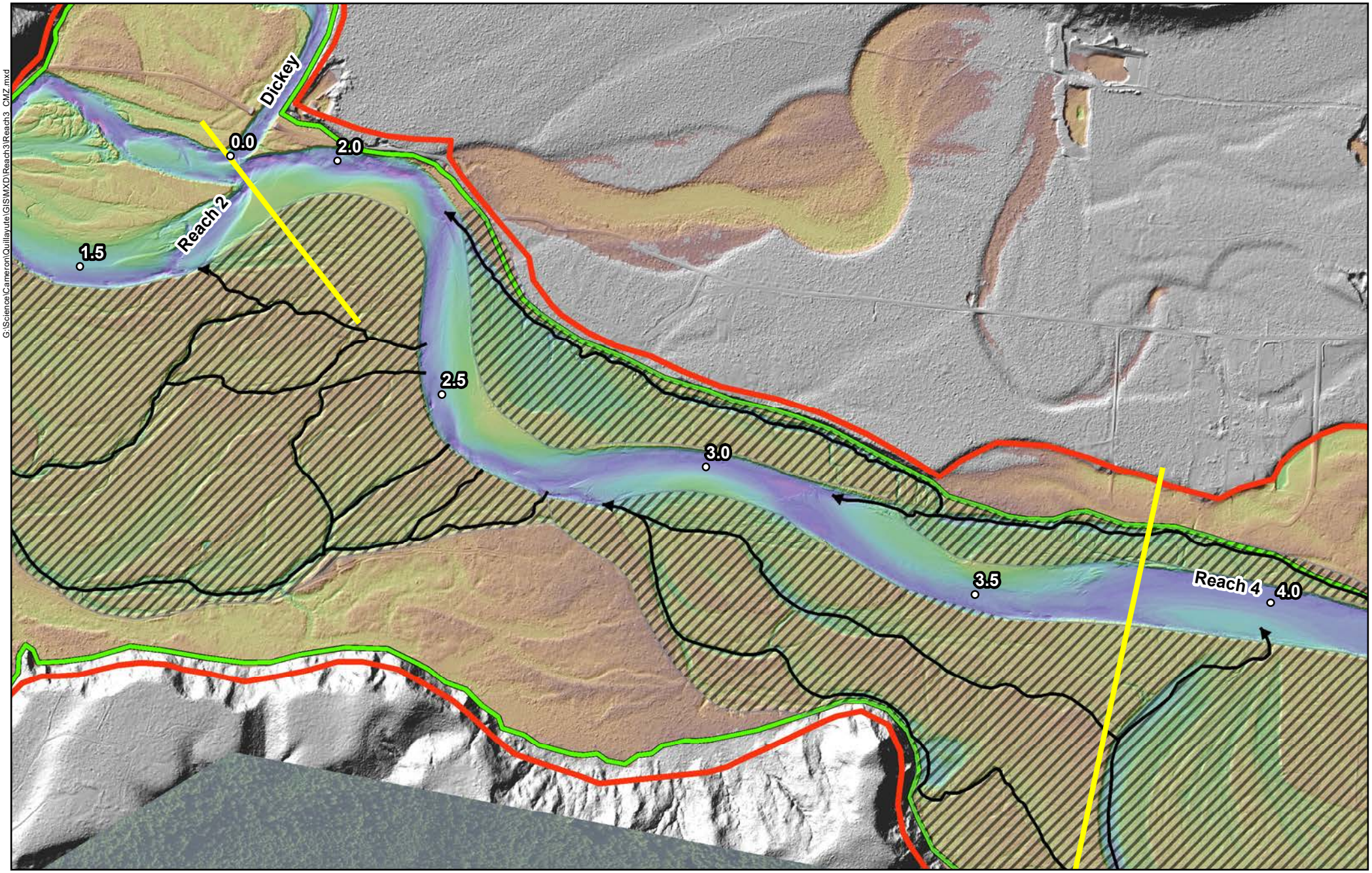

Avulsion Pathways

AHA

MVB

CMZ

Relative Elevation Model

Height Above Channel Bottom (ft)

High : 25

Low : -5

River Miles

Geomorphic Reaches

Quillayute River Geomorphic Assessment

Channel Migration Zone (CMZ) Analysis
Reach 3

Figure H-4

TETRA TECH

N
W E
S

0 1,250 2,500

Feet

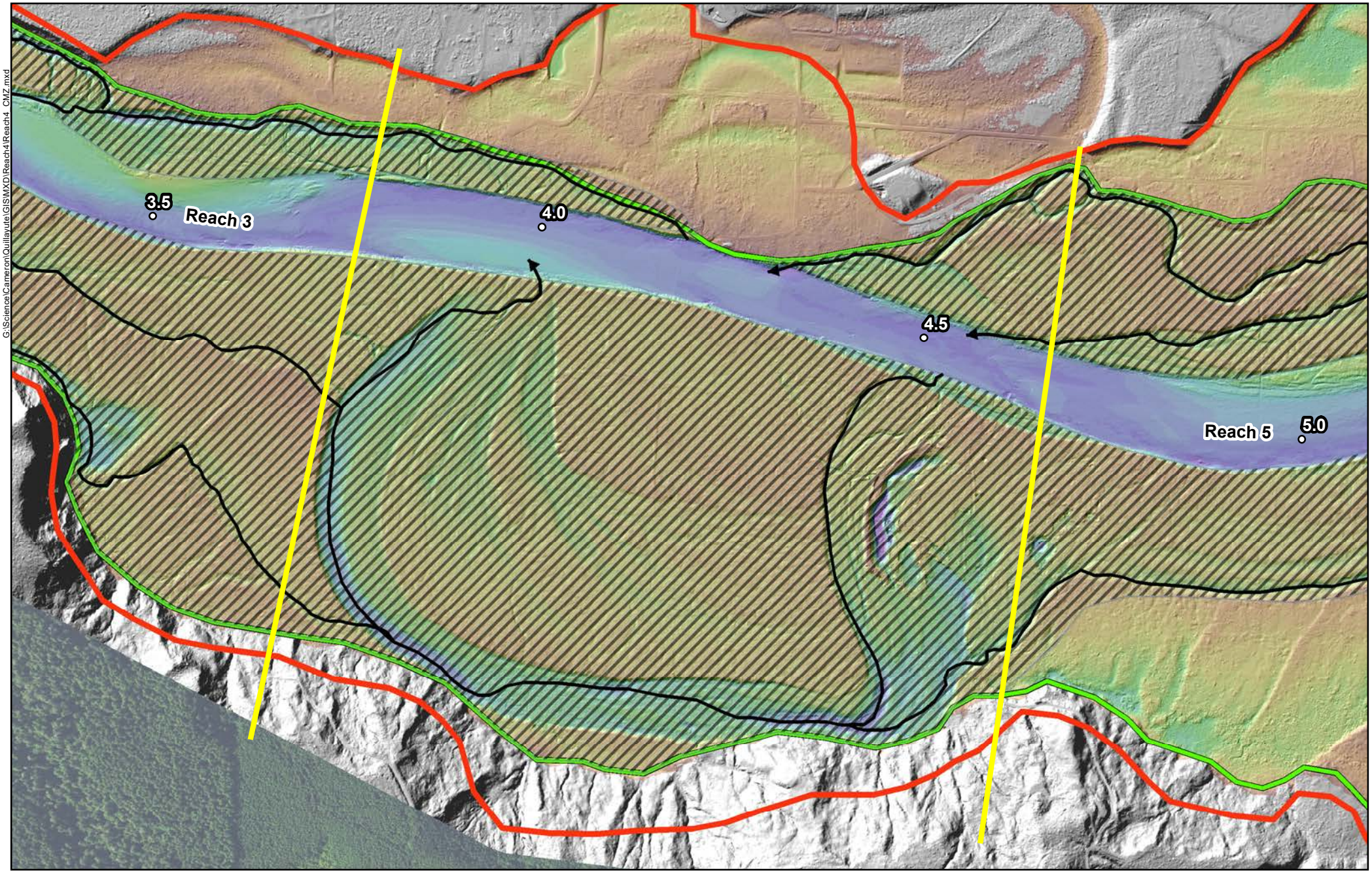

Avulsion Pathways

AHA

MVB

CMZ

Relative Elevation Model

Height Above Channel Bottom (ft)

High : 25

Low : -5

River Miles

Geomorphic Reaches

Quillayute River Geomorphic Assessment

Channel Migration Zone (CMZ) Analysis
Reach 4

Figure H-5

TETRA TECH

N

W E

S

0 1,000 2,000

Feet

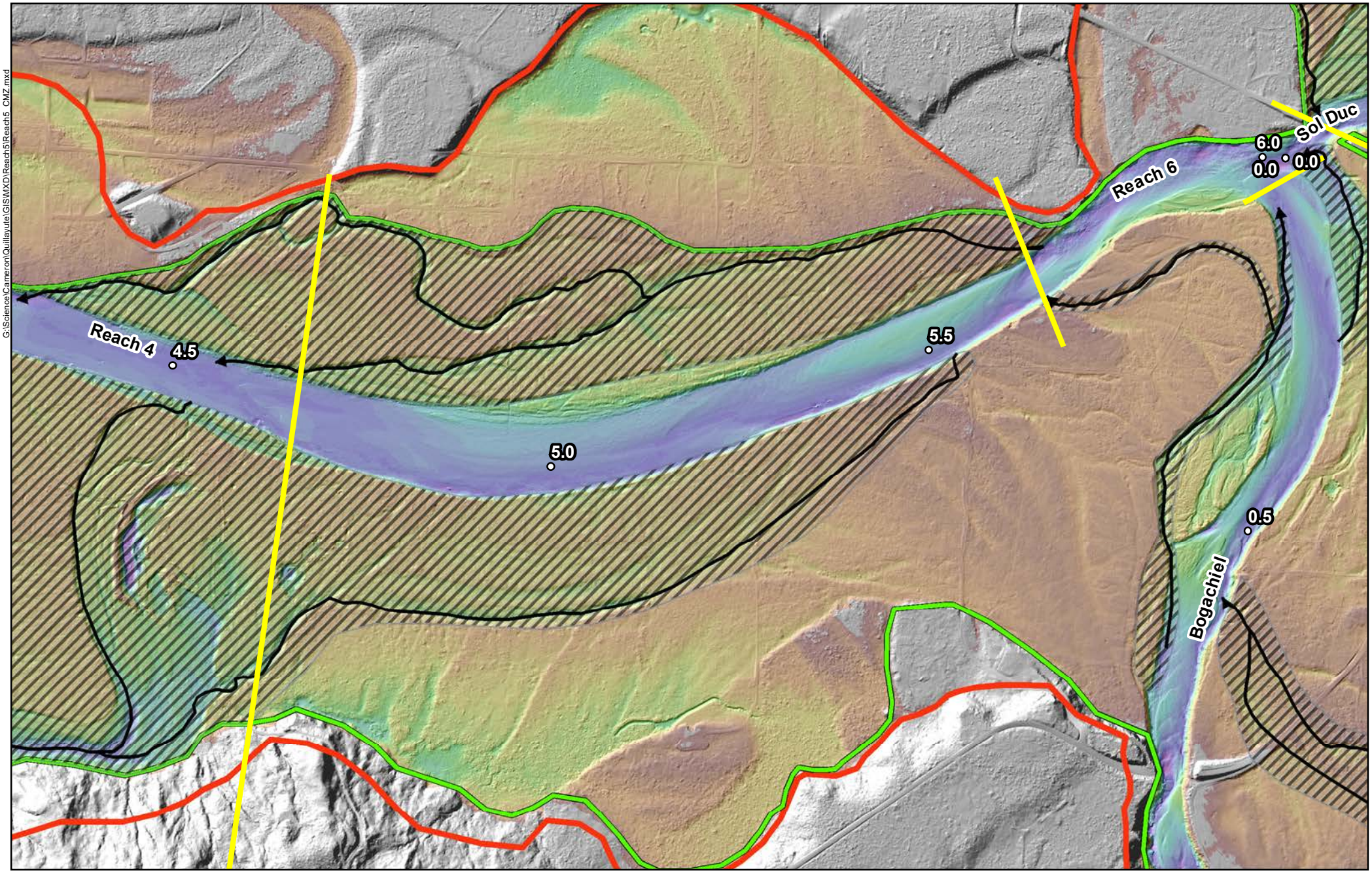

Avulsion Pathways

AHA

MVB

CMZ

Relative Elevation Model

Height Above Channel Bottom (ft)

High : 25

Low : -5

River Miles

Geomorphic Reaches

Quillayute River Geomorphic Assessment

Channel Migration Zone (CMZ) Analysis
Reach 5

Figure H-6

TETRA TECH

N

W E

S

0 1,000 2,000

Feet

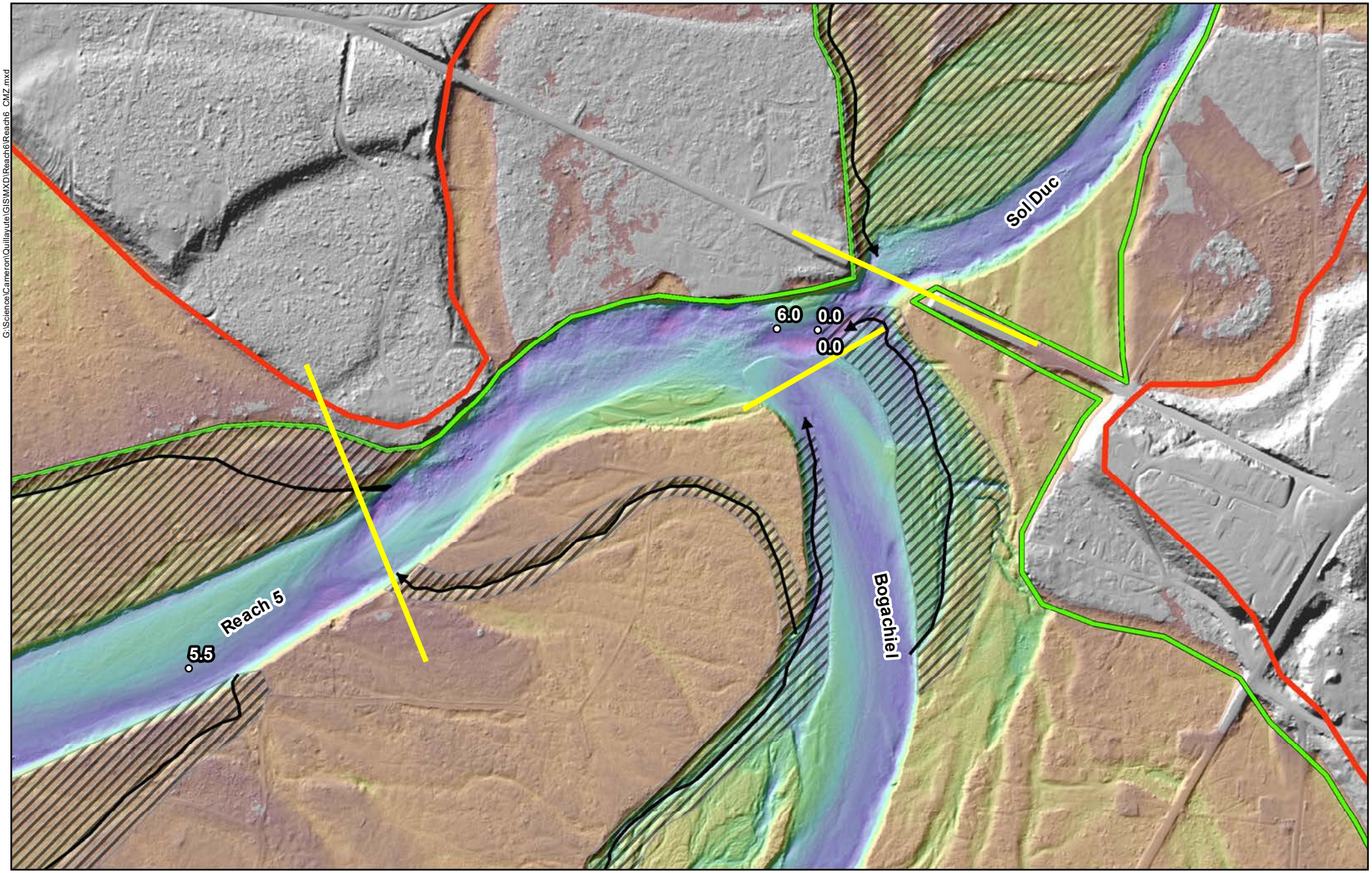

Avulsion Pathways

AHA

MVB

CMZ

Relative Elevation Model

Height Above Channel Bottom (ft)

High : 25

Low : -5

River Miles

Geomorphic Reaches

Quillayute River Geomorphic Assessment

Channel Migration Zone (CMZ) Analysis
Reach 6

Figure H-7

TETRA TECH

N
W E
S

0 500 1,000
Feet

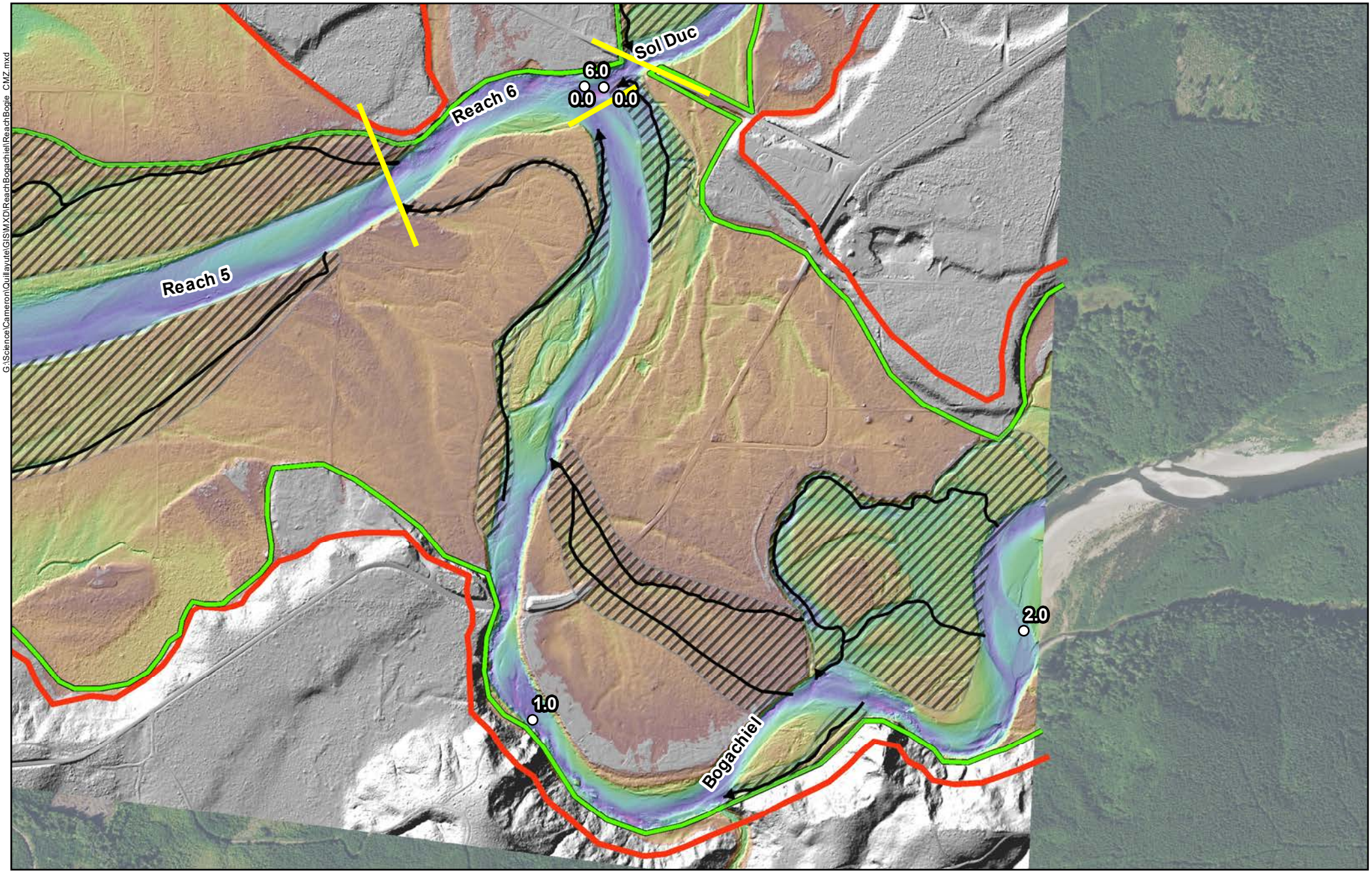

Avulsion Pathways

AHA

MVB

CMZ

Relative Elevation Model

Height Above Channel Bottom (ft)

High : 25

Low : -5

River Miles

Geomorphic Reaches

Quillayute River Geomorphic Assessment

Channel Migration Zone (CMZ) Analysis
Lower Bogachiel River

Figure H-8

TETRA TECH

N

W E

S

0 1,000 2,000

Feet

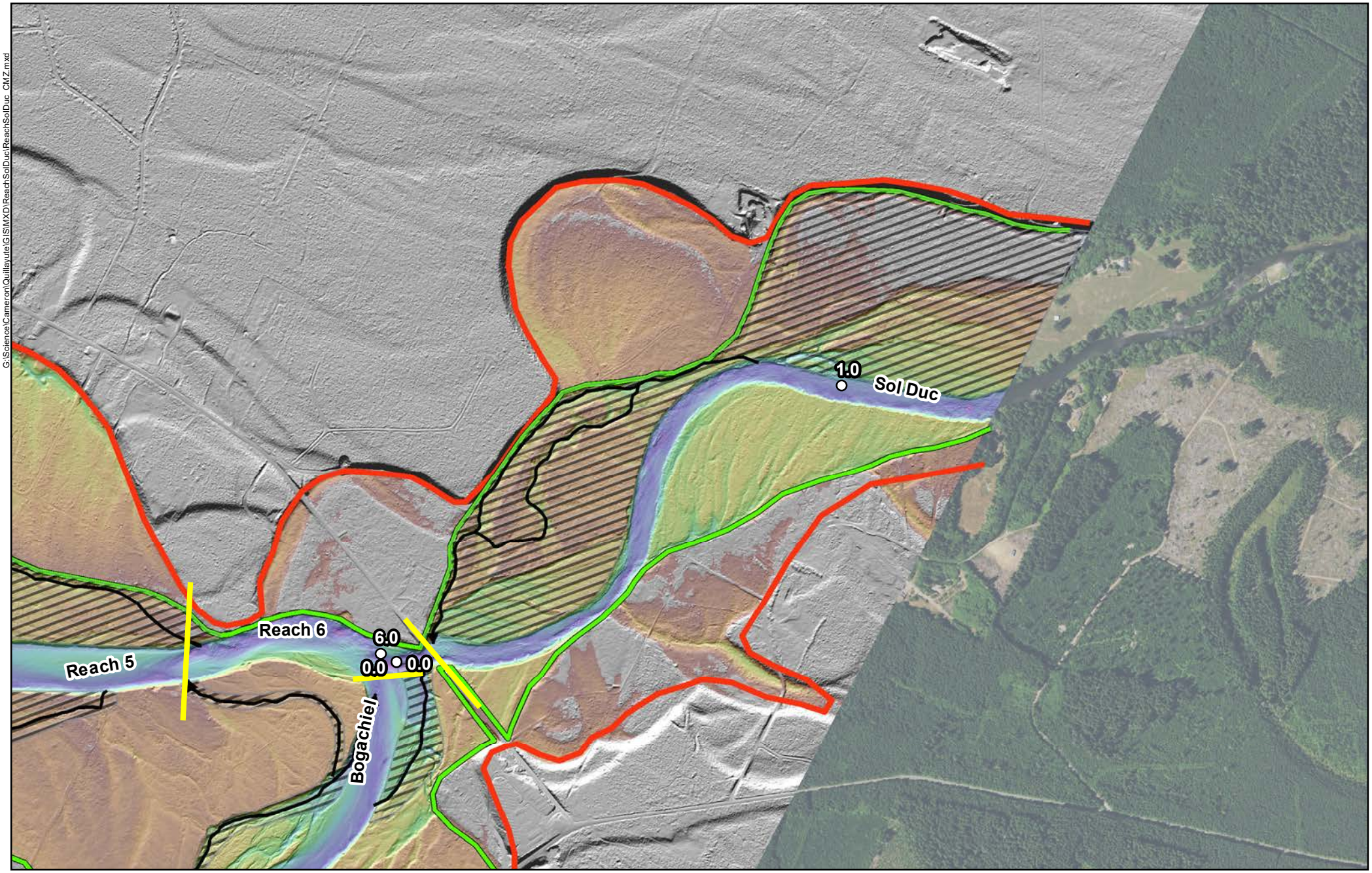

Avulsion Pathways

AHA

MVB

CMZ

Relative Elevation Model

Height Above Channel Bottom (ft)

High : 25

Low : -5

River Miles

Geomorphic Reaches

Quillayute River Geomorphic Assessment

Channel Migration Zone (CMZ) Analysis
Lower Sol Duc River

Figure H-9

TETRA TECH

N

W

E

S

0 1,000 2,000

Feet

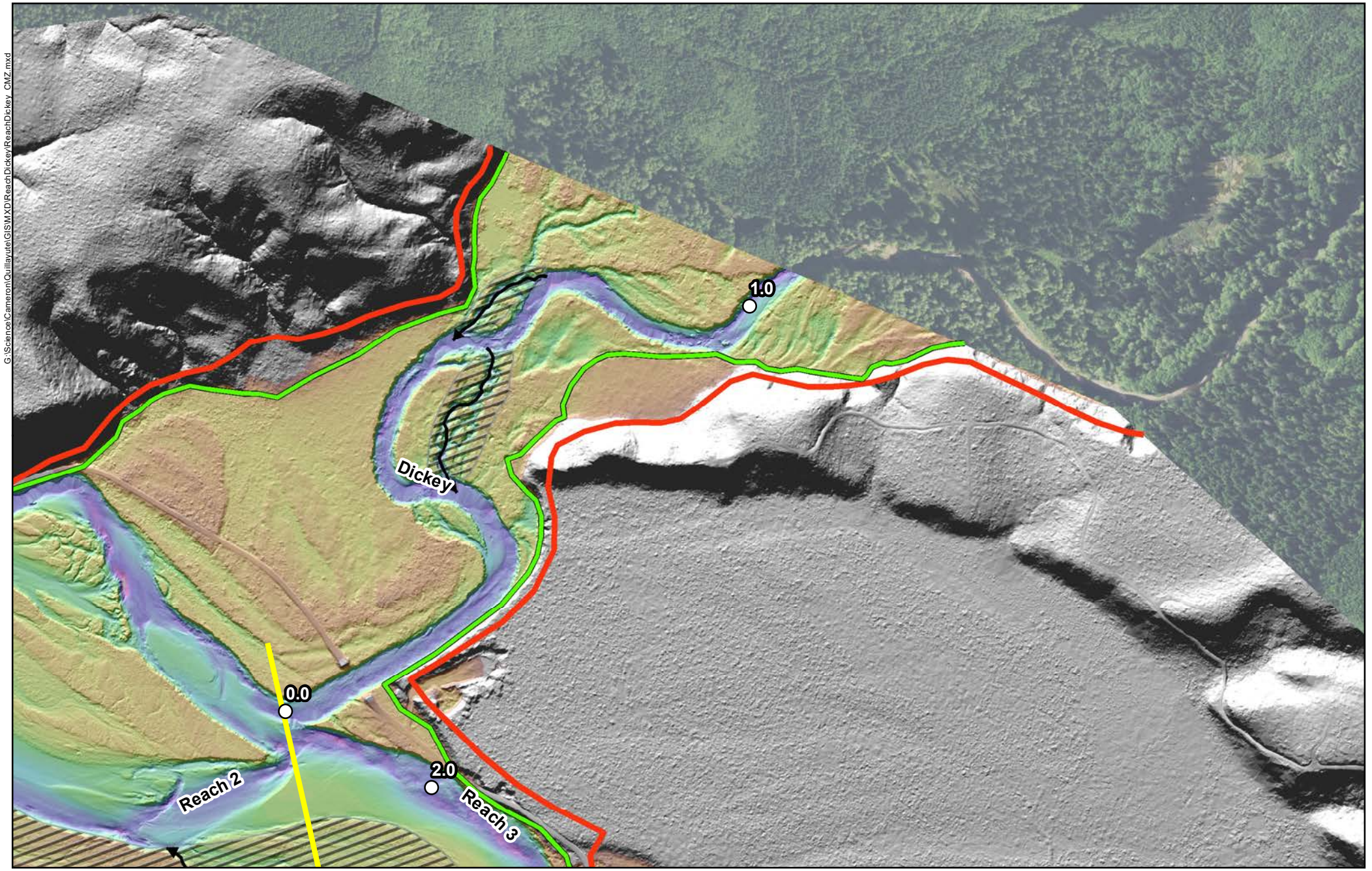

Avulsion Pathways

AHA

MVB

CMZ

Relative Elevation Model

Height Above Channel Bottom (ft)

High : 25

Low : -5

River Miles

Geomorphic Reaches

Quillayute River
Geomorphic Assessment

Channel Migration Zone (CMZ) Analysis
Lower Dickey River

Figure H-10

TETRA TECH

N
W
E
S

0 750 1,500
Feet

APPENDIX I – HABITAT SUITABILITY MODELING RESULTS

Quillayute River Project
Geomorphic Assessment and Action Plan
Habitat Suitability Modeling Results

Appendix I

Submitted to:

Quileute Natural Resources
401 Main Street
La Push, WA 98350

Submitted by:

TETRA TECH

19803 North Creek Parkway
Bothell, WA 98011
Tel 425.482.7600 | Fax 425.482.7652
www.tetratech.com

September 2020

LIST OF FIGURES

Figure I-1. Depth Overview at High Flow and High Tide
Figure I-2. Depth Overview at High Flow and Low Tide
Figure I-3. Depth Overview at Low Flow and High Tide
Figure I-4. Depth Overview at Low Flow and Low Tide
Figure I-5. Velocity Overview at High Flow and High Tide
Figure I-6. Velocity Overview at High Flow and Low Tide
Figure I-7. Velocity Overview at Low Flow and High Tide
Figure I-8. Velocity Overview at Low Flow and Low Tide
Figure I-9. Chinook Rearing Overview at High Flow and High Tide
Figure I-10. Chinook Rearing Overview at High Flow and Low Tide
Figure I-11. Chinook Rearing Overview at Low Flow and High Tide
Figure I-12. Chinook Rearing Overview at Low Flow and Low Tide
Figure I-13. Chinook Spawning Overview at High Flow and High Tide
Figure I-14. Chinook Spawning Overview at High Flow and Low Tide
Figure I-15. Chinook Spawning Overview at Low Flow and High Tide
Figure I-16. Chinook Spawning Overview at Low Flow and Low Tide
Figure I-17. Coho Rearing Overview at High Flow and High Tide
Figure I-18. Coho Rearing Overview at High Flow and Low Tide
Figure I-19. Coho Rearing Overview at Low Flow and High Tide
Figure I-20. Coho Rearing Overview at Low Flow and Low Tide
Figure I-21. Coho Spawning Overview at High Flow and High Tide
Figure I-22. Coho Spawning Overview at High Flow and Low Tide
Figure I-23. Coho Spawning Overview at Low Flow and High Tide
Figure I-24. Coho Spawning Overview at Low Flow and Low Tide
Figure I-25. Steelhead Rearing Overview at High Flow and High Tide
Figure I-26. Steelhead Rearing Overview at High Flow and Low Tide
Figure I-27. Steelhead Rearing Overview at Low Flow and High Tide
Figure I-28. Steelhead Rearing Overview at Low Flow and Low Tide
Figure I-29. Steelhead Spawning Overview at High Flow and High Tide
Figure I-30. Steelhead Spawning Overview at High Flow and Low Tide
Figure I-31. Steelhead Spawning Overview at Low Flow and High Tide
Figure I-32. Steelhead Spawning Overview at Low Flow and Low Tide

Depth (ft)
0
21.6

River Miles

Quillayute River Flow: 2,890 cfs
High Tide: 7.85 ft. (NAVD88)
Low Tide: -0.66 ft. (NAVD88)

Quillayute River
Geomorphic Assessment

Habitat Suitability Modeling
Depth
High Flow/High Tide
Figure I-1

TETRA TECH

N
W E
S

0 0.5 1
Miles

Depth (ft)
0
15.7

River Miles

Quillayute River Flow: 2,890 cfs
High Tide: 7.85 ft. (NAVD88)
Low Tide: -0.66 ft. (NAVD88)

Quillayute River
Geomorphic Assessment

Habitat Suitability Modeling
Depth
High Flow/Low Tide
Figure I-2

TETRA TECH

N
W E
S

0 0.5 1
Miles

Depth (ft)
0
21.6

River Miles

Quillayute River Flow: 423 cfs
High Tide: 7.85 ft. (NAVD88)
Low Tide: -0.66 ft. (NAVD88)

Quillayute River
Geomorphic Assessment

Habitat Suitability Modeling
Depth
Low Flow/High Tide
Figure I-3

TETRA TECH

N
W E
S

0 0.5 1
Miles

Depth (ft)
0
14.6

River Miles

Quillayute River Flow: 423 cfs
High Tide: 7.85 ft. (NAVD88)
Low Tide: -0.66 ft. (NAVD88)

Quillayute River
Geomorphic Assessment

Habitat Suitability Modeling
Depth
Low Flow/Low Tide
Figure I-4

TETRA TECH

N
W E
S

0 0.5 1
Miles

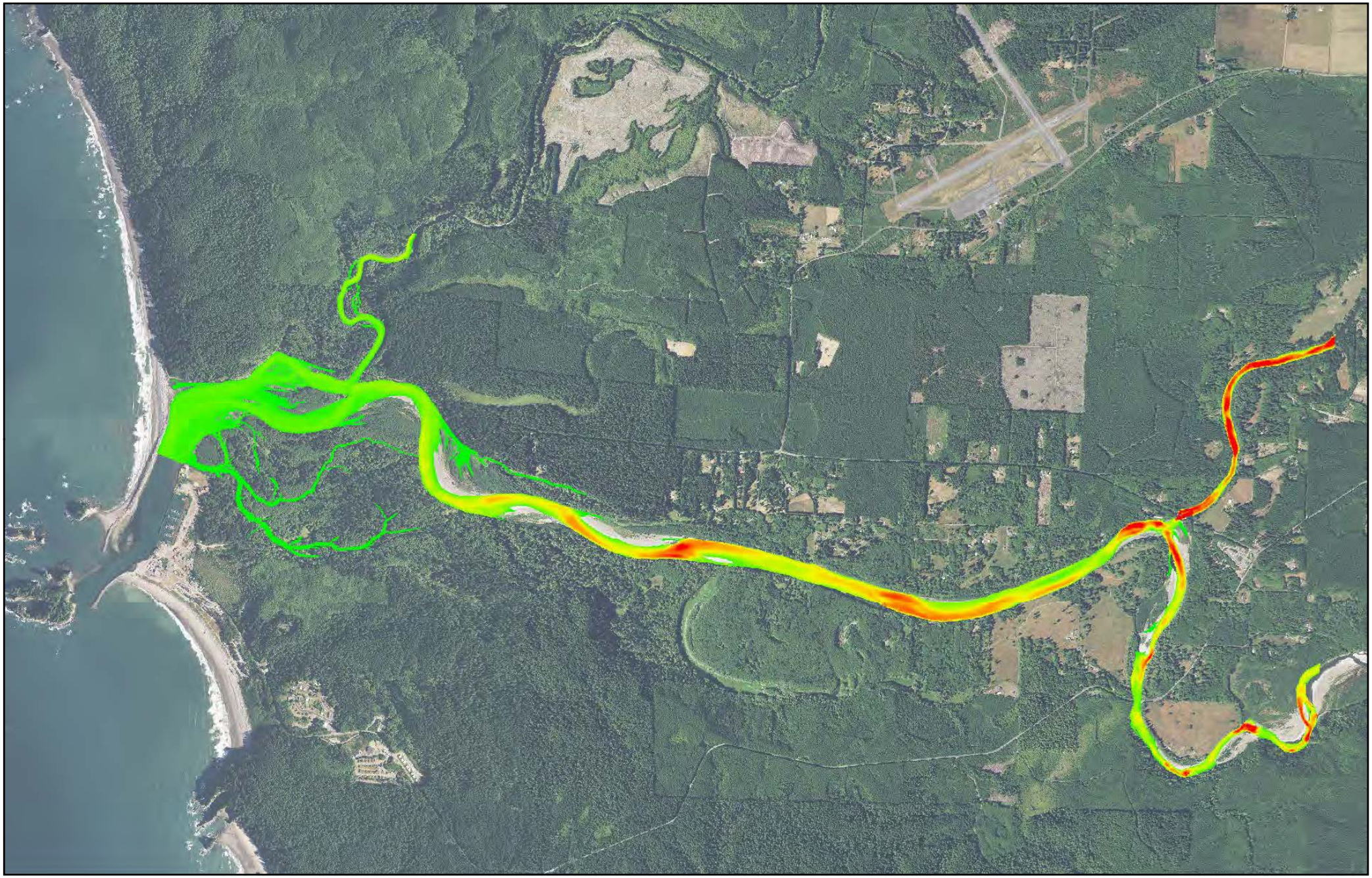

Velocity (ft/s)

0

10.1

River Miles

Quillayute River Flow: 2,890 cfs
High Tide: 7.85 ft. (NAVD88)
Low Tide: -0.66 ft. (NAVD88)

Quillayute River Geomorphic Assessment

Habitat Suitability Modeling
Velocity
High Flow/High Tide
Figure I-5

TETRA TECH

N
W E
S

0 0.5 1
Miles

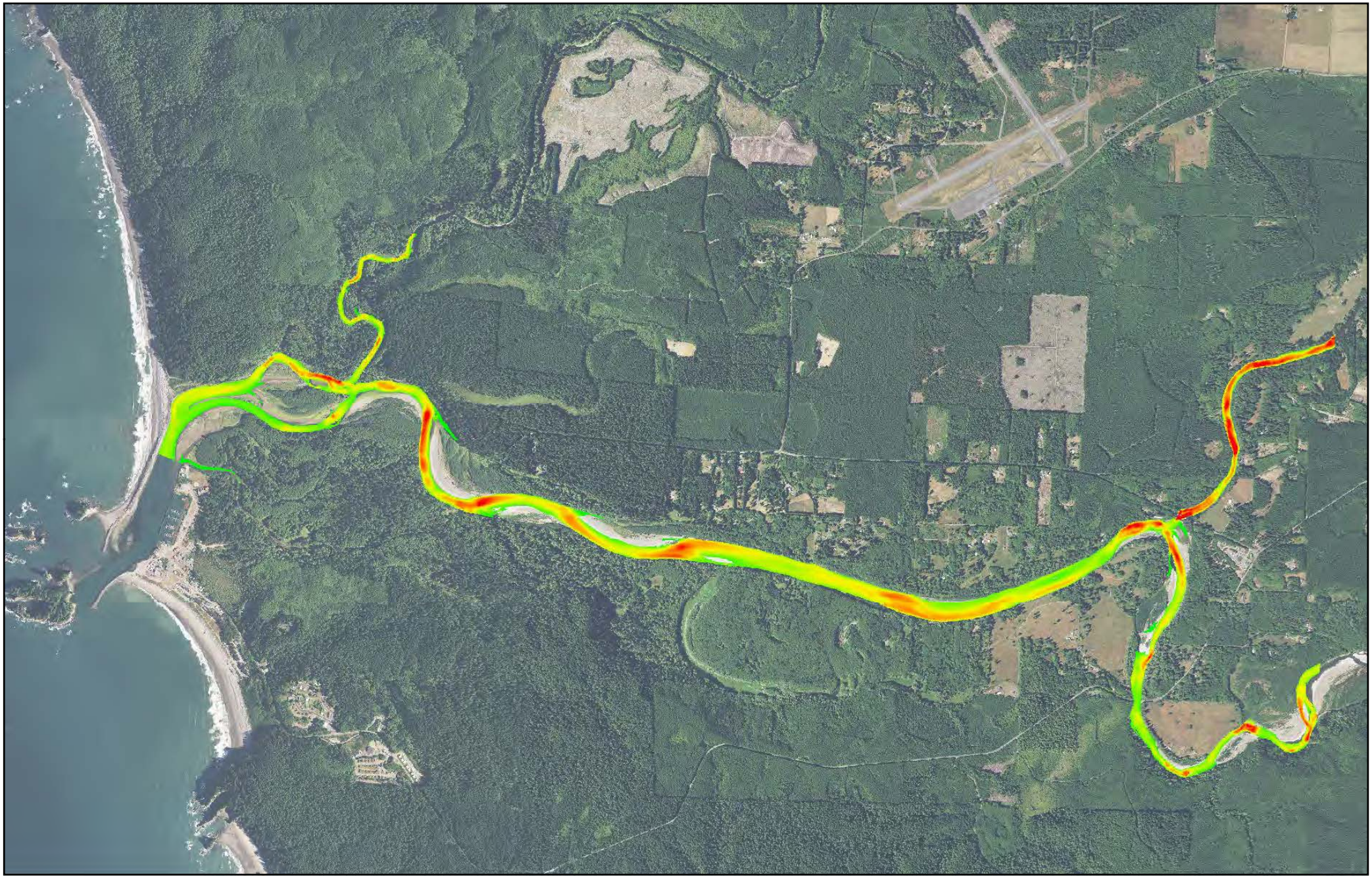

Velocity (ft/s)

0

10.1

River Miles

Quillayute River Flow: 2,890 cfs
High Tide: 7.85 ft. (NAVD88)
Low Tide: -0.66 ft. (NAVD88)

Quillayute River Geomorphic Assessment

Habitat Suitability Modeling
Velocity
High Flow/Low Tide
Figure I-6

TETRA TECH

N
W
E
S

0 0.5 1
Miles

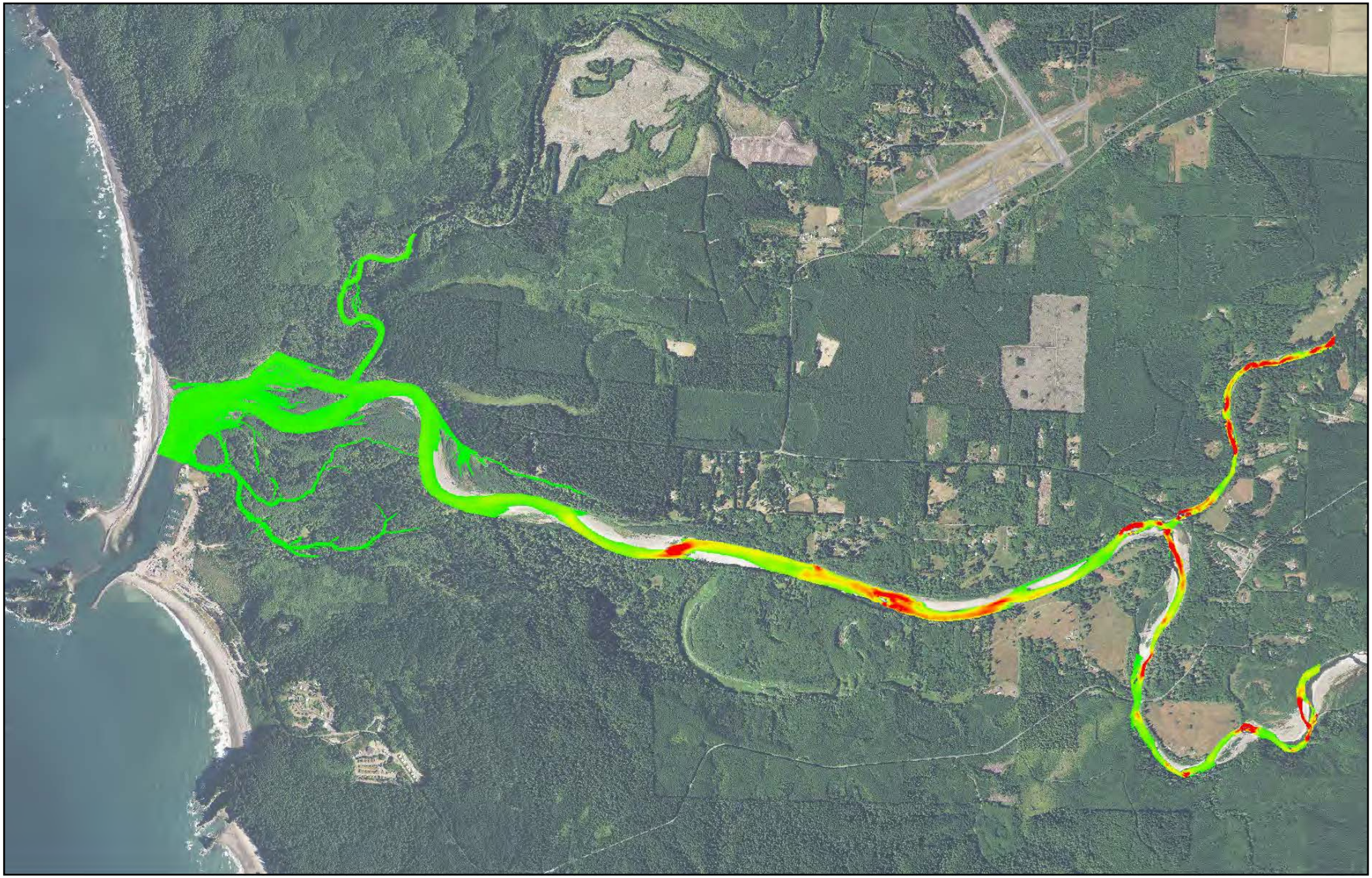

Velocity (ft/s)

0

5.2

River Miles

Quillayute River Flow: 423 cfs
High Tide: 7.85 ft. (NAVD88)
Low Tide: -0.66 ft. (NAVD88)

Quillayute River Geomorphic Assessment

Habitat Suitability Modeling
Velocity
Low Flow/High Tide
Figure I-7

TETRA TECH

N
W
E
S

0 0.5 1
Miles

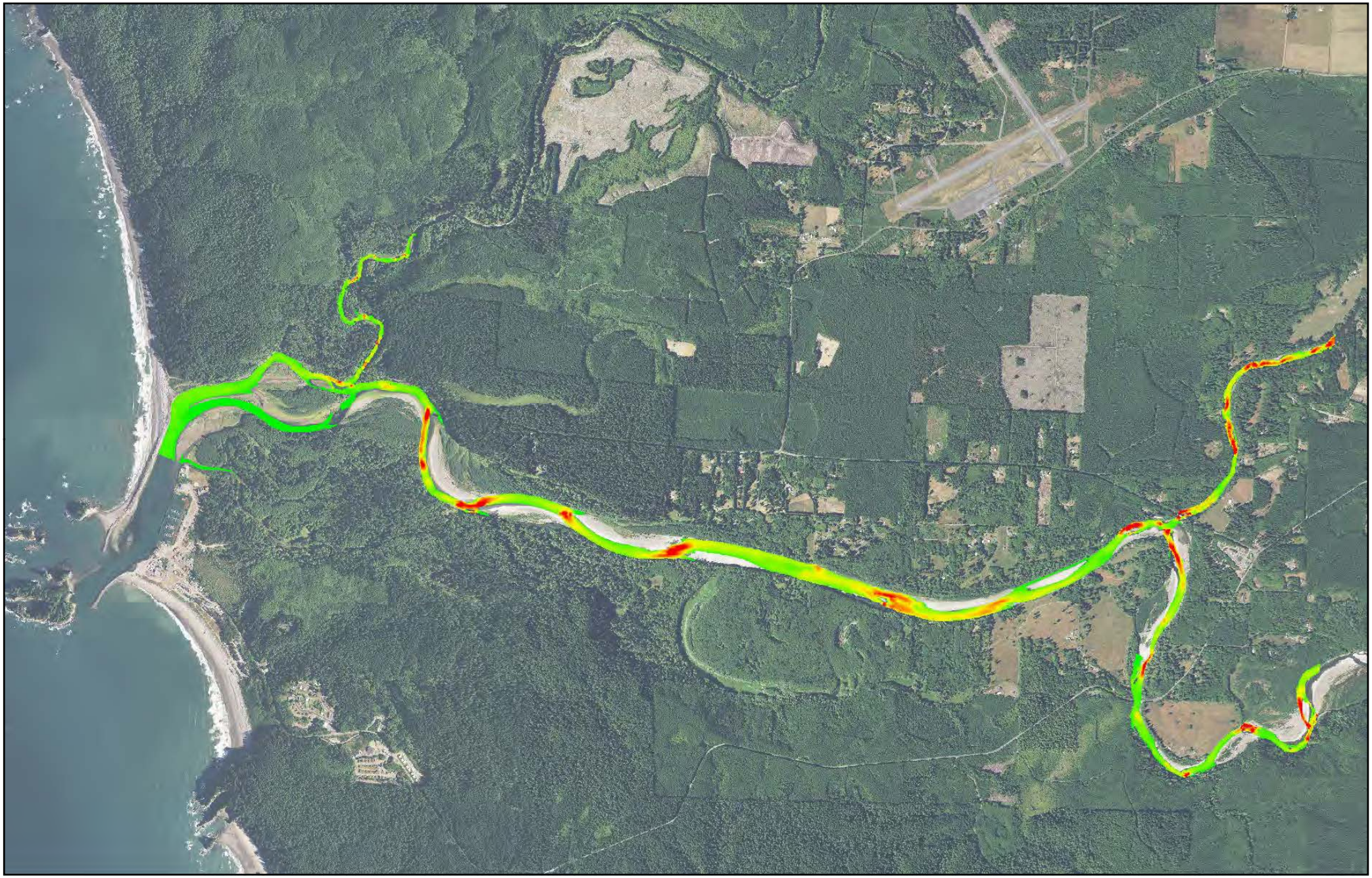

Velocity (ft/s)

0

5.2

River Miles

Quillayute River Flow: 423 cfs
High Tide: 7.85 ft. (NAVD88)
Low Tide: -0.66 ft. (NAVD88)

Quillayute River Geomorphic Assessment

Habitat Suitability Modeling
Velocity
Low Flow/Low Tide
Figure I-8

TETRA TECH

N
W E
S

0 0.5 1
Miles

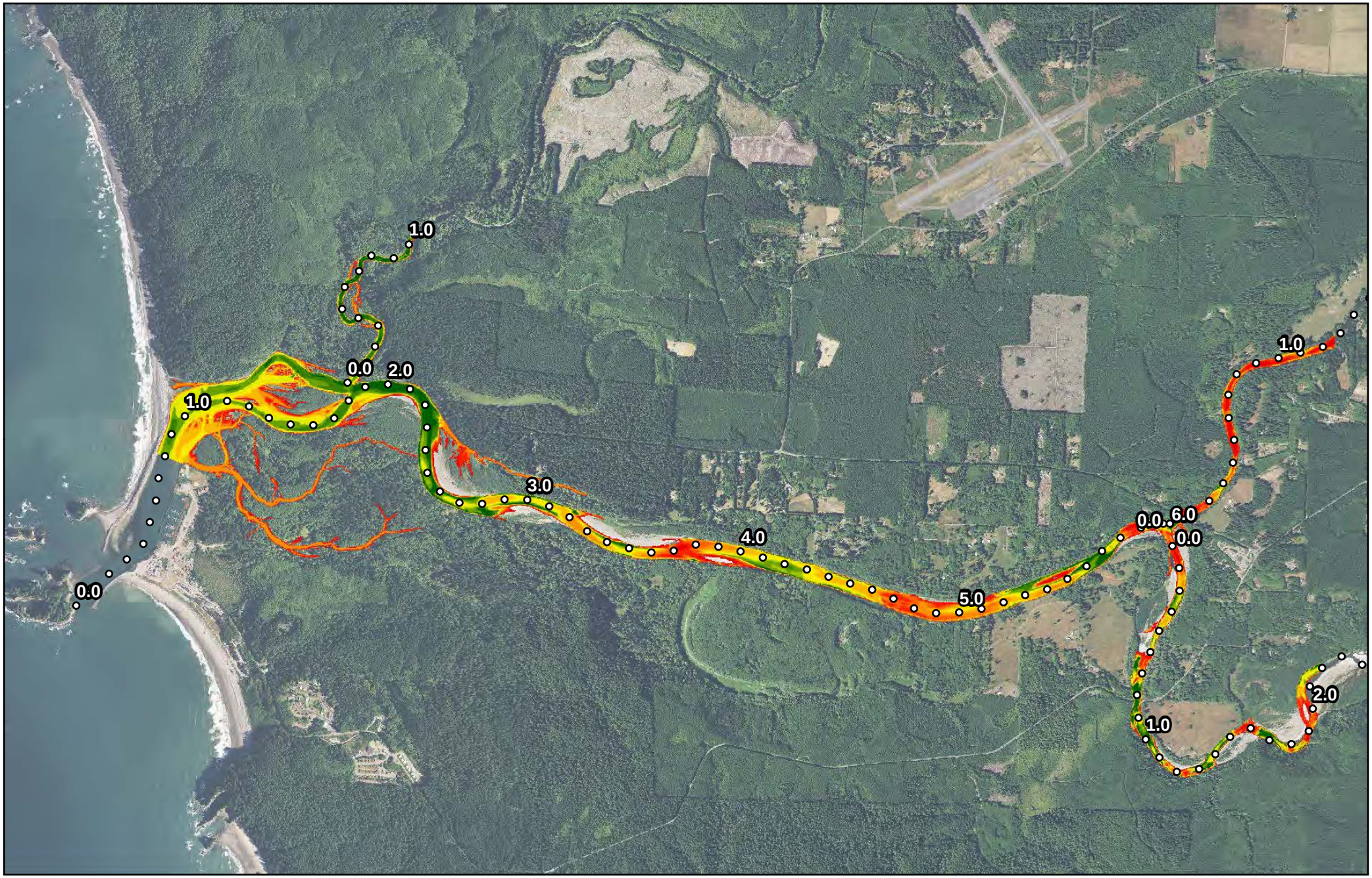

Habitat Suitability Index

High

Low

River Miles

Quillayute River Flow: 2,890 cfs
High Tide: 7.85 ft. (NAVD88)
Low Tide: -0.66 ft. (NAVD88)

Quillayute River Geomorphic Assessment

Habitat Suitability Modeling
Chinook Rearing
High Flow/High Tide
Figure I-9

TETRA TECH

N
W
E
S

0 0.5 1
Miles

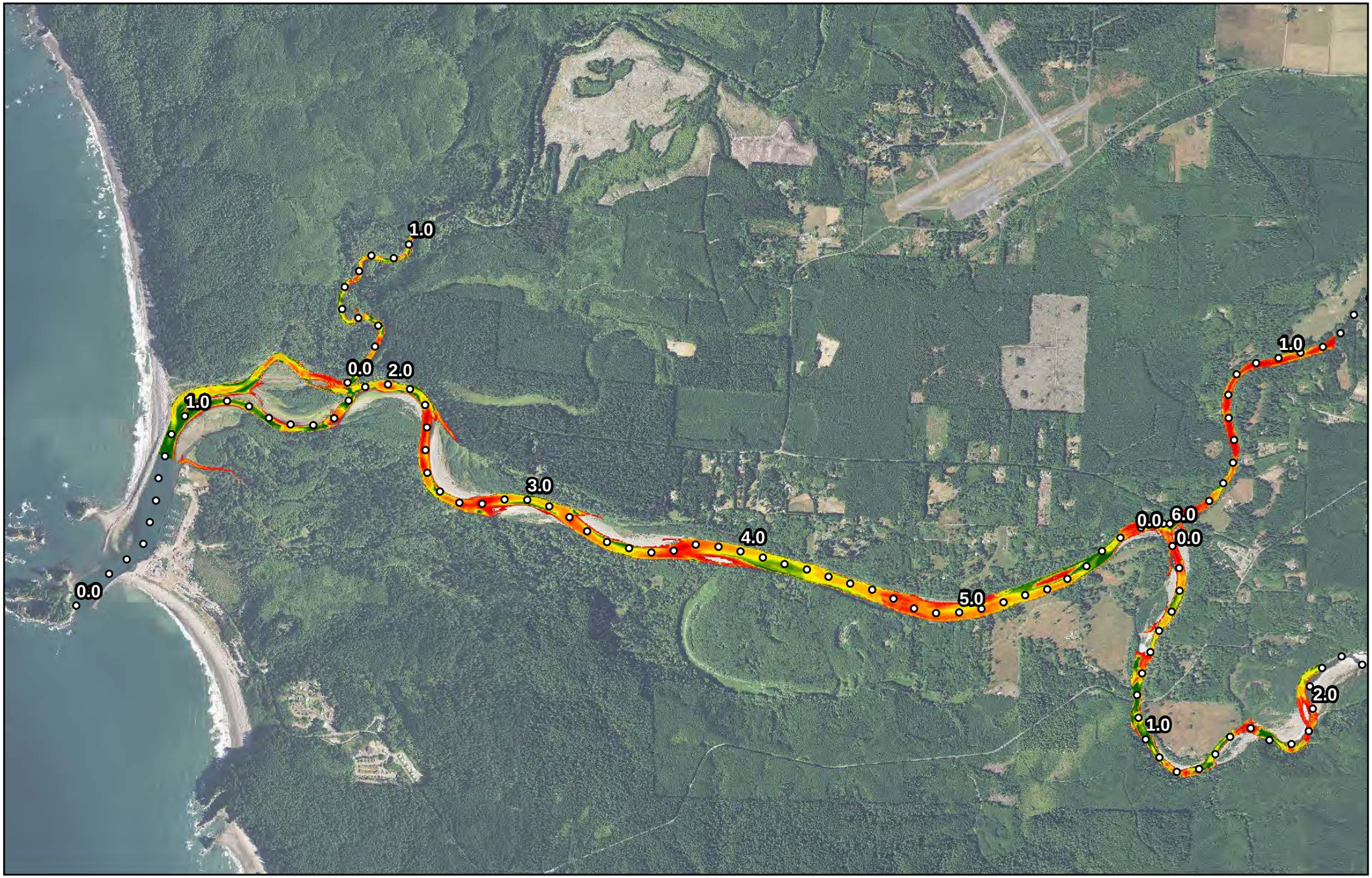

Habitat Suitability Index

High

Low

River Miles

Quillayute River Flow: 2,890 cfs
High Tide: 7.85 ft. (NAVD88)
Low Tide: -0.66 ft. (NAVD88)

Quillayute River Geomorphic Assessment

Habitat Suitability Modeling
Chinook Rearing
High Flow/Low Tide
Figure I-10

TETRA TECH

N
W
E
S

0 0.5 1
Miles

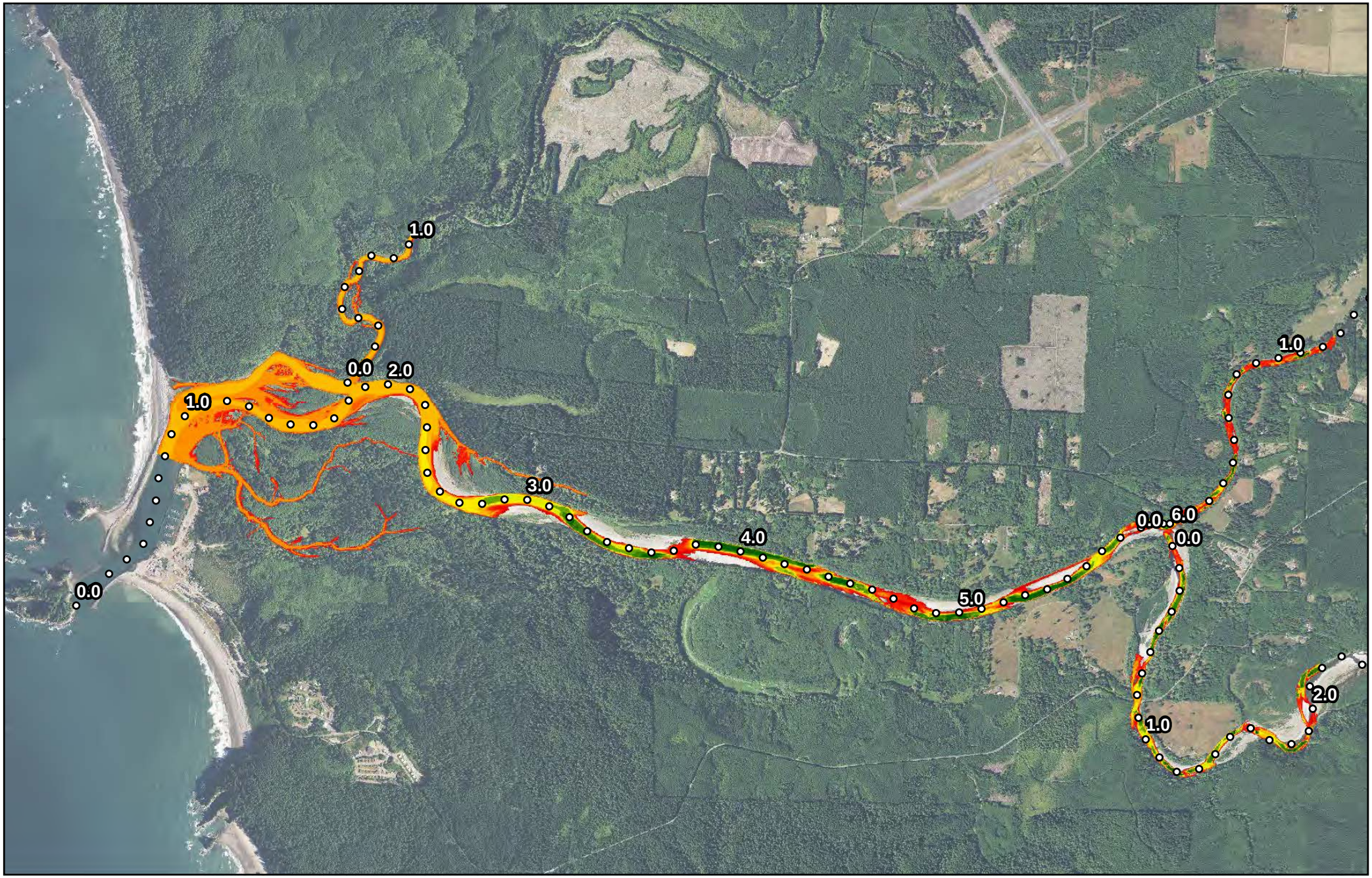

Habitat Suitability Index

High

Low

River Miles

Quillayute River Flow: 423 cfs
High Tide: 7.85 ft. (NAVD88)
Low Tide: -0.66 ft. (NAVD88)

Quillayute River Geomorphic Assessment

Habitat Suitability Modeling
Chinook Rearing
Low Flow/High Tide
Figure I-11

TETRA TECH

N
W
E
S

0 0.5 1
Miles

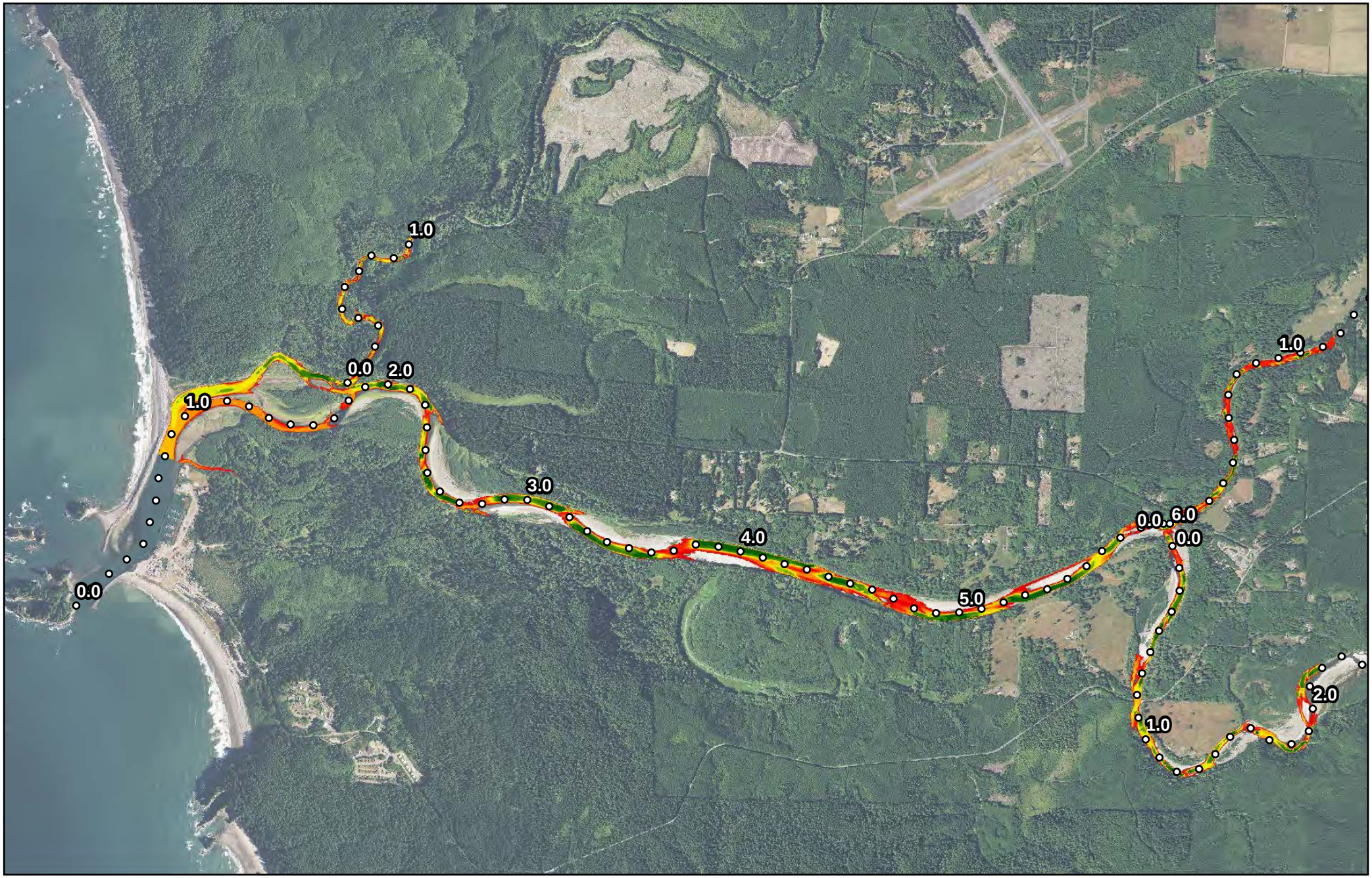

Habitat Suitability Index

High

Low

River Miles

Quillayute River Flow: 423 cfs
High Tide: 7.85 ft. (NAVD88)
Low Tide: -0.66 ft. (NAVD88)

Quillayute River Geomorphic Assessment

Habitat Suitability Modeling
Chinook Rearing
Low Flow/Low Tide
Figure I-12

TETRA TECH

N
W
E
S

0 0.5 1
Miles

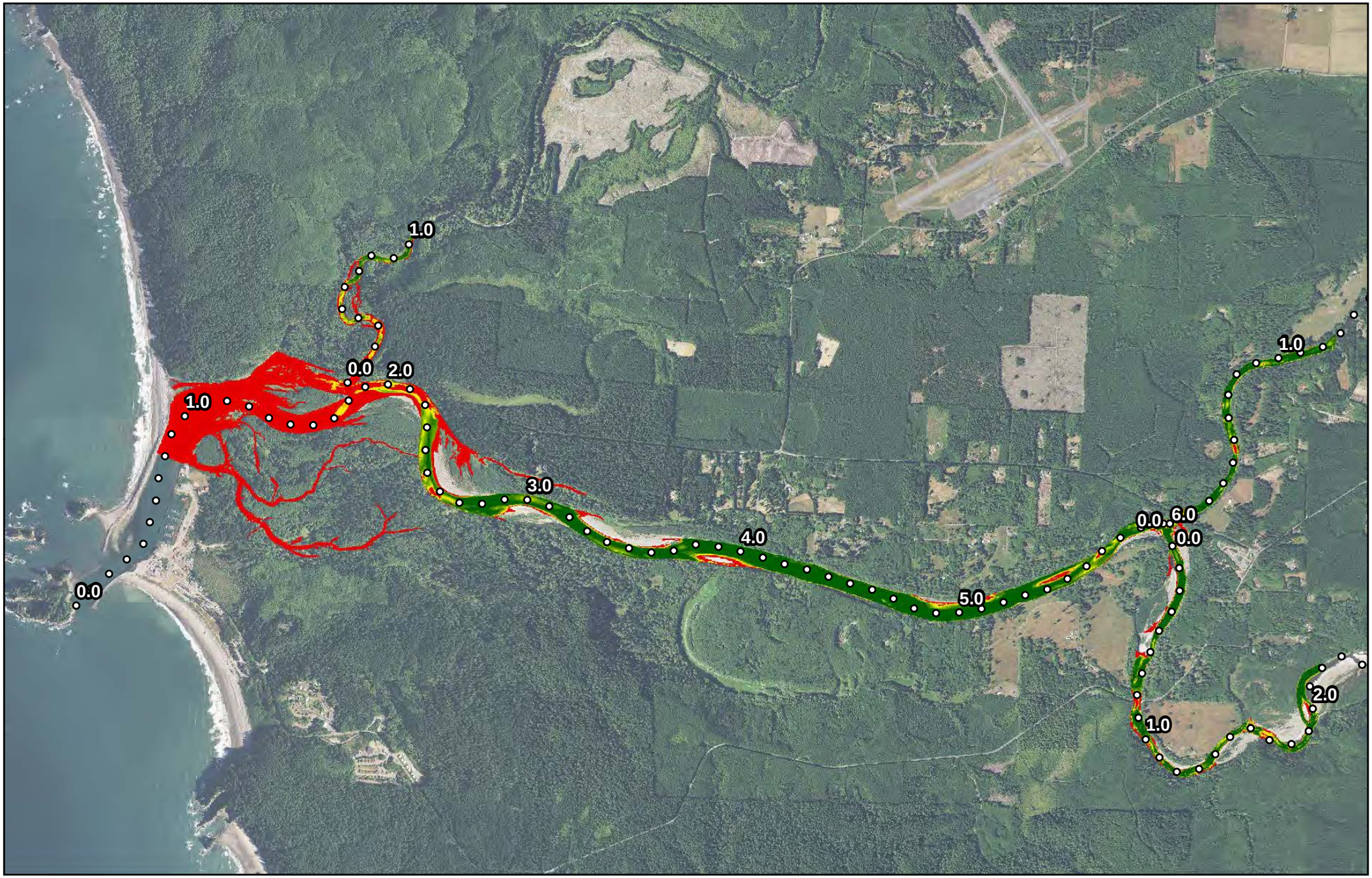

Habitat Suitability Index

High

Low

River Miles

Quillayute River Flow: 2,890 cfs
High Tide: 7.85 ft. (NAVD88)
Low Tide: -0.66 ft. (NAVD88)

Quillayute River Geomorphic Assessment

Habitat Suitability Modeling
Chinook Spawning
High Flow/High Tide
Figure I-13

TETRA TECH

N
W
E
S

0 0.5 1
Miles

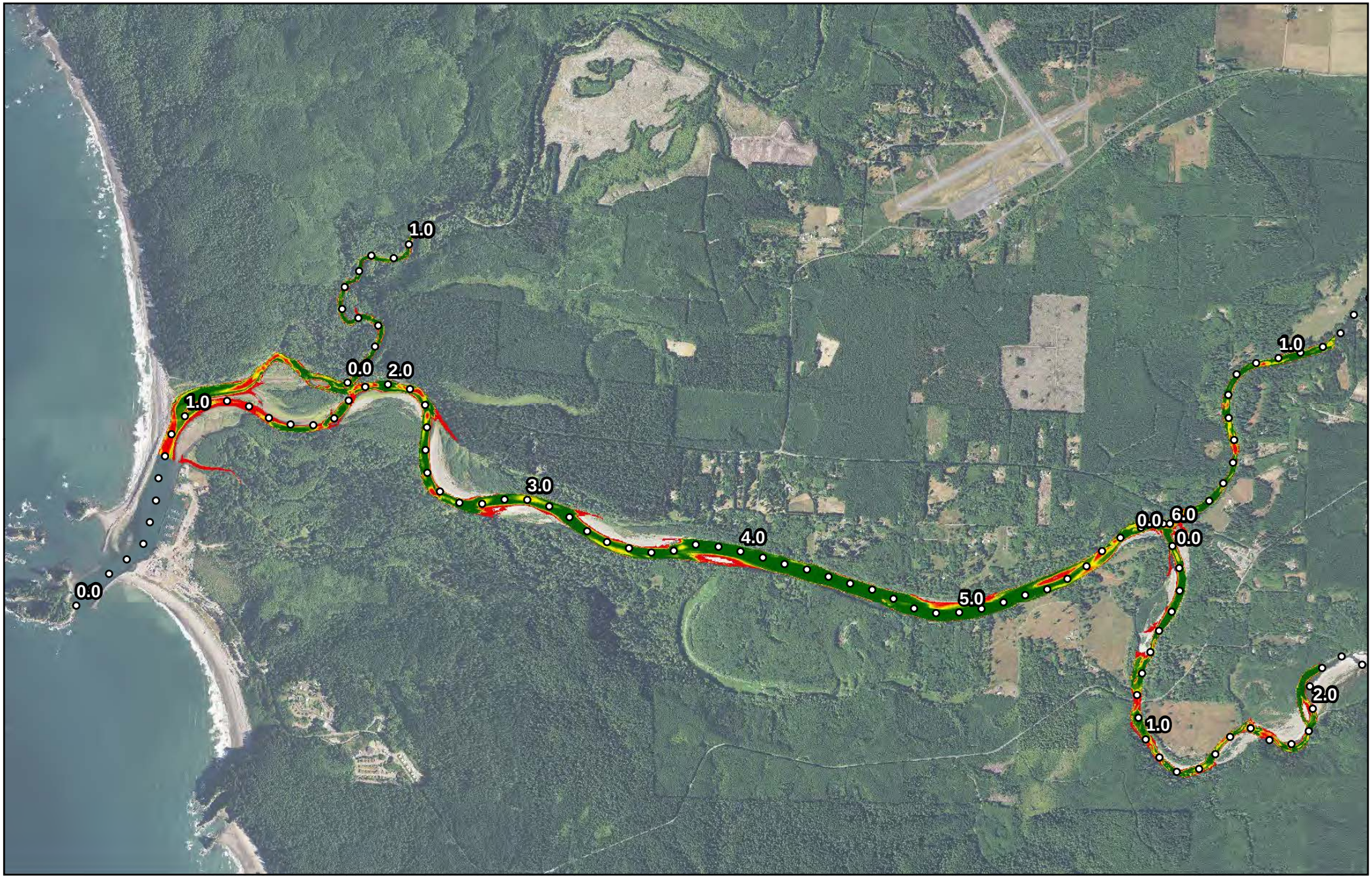

Habitat Suitability Index

High

Low

River Miles

Quillayute River Flow: 2,890 cfs
High Tide: 7.85 ft. (NAVD88)
Low Tide: -0.66 ft. (NAVD88)

Quillayute River Geomorphic Assessment

Habitat Suitability Modeling
Chinook Spawning
High Flow/Low Tide
Figure I-14

TETRA TECH

N
W
E
S

0 0.5 1
Miles

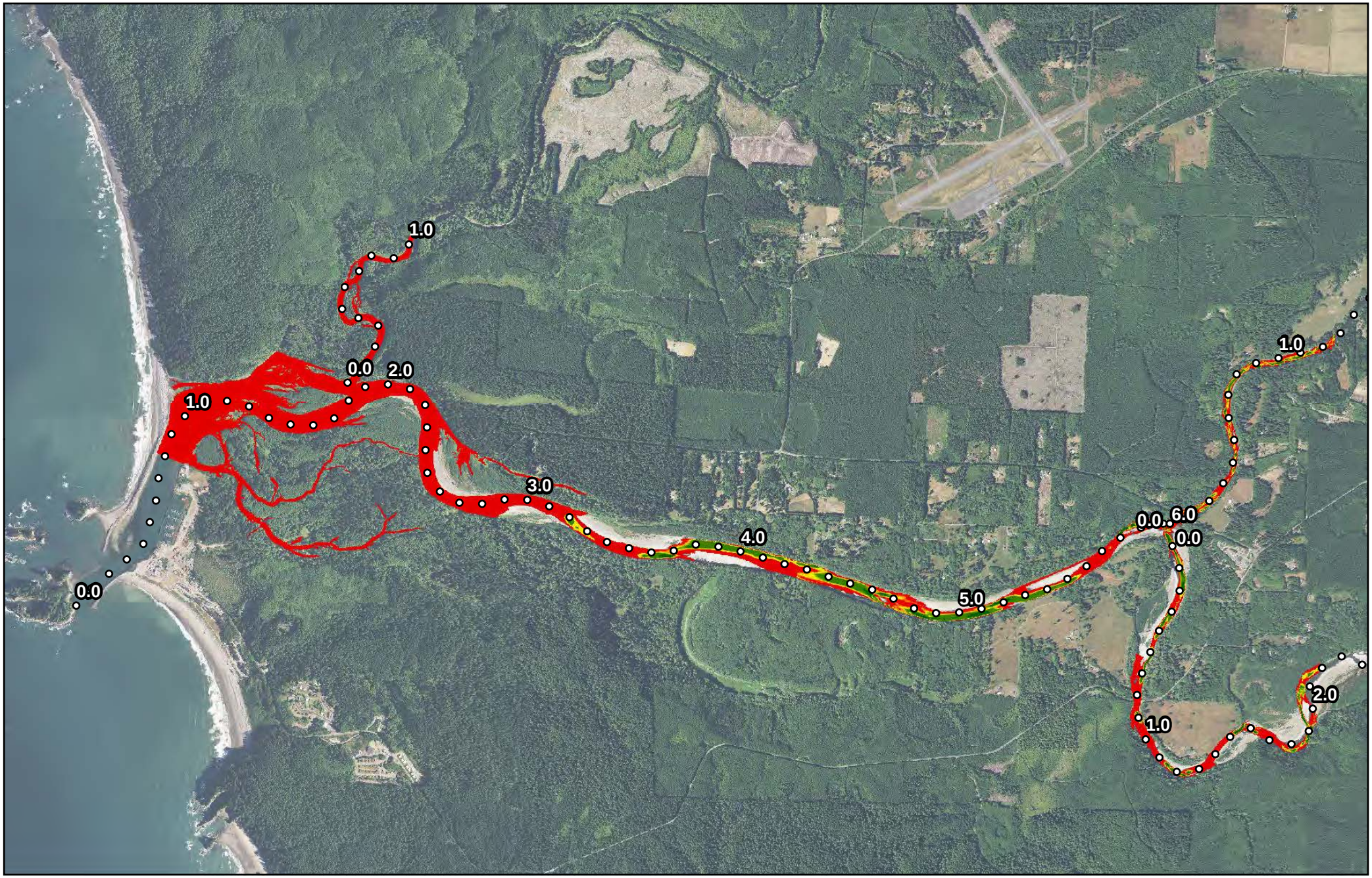

Habitat Suitability Index

High

Low

River Miles

Quillayute River Flow: 423 cfs
High Tide: 7.85 ft. (NAVD88)
Low Tide: -0.66 ft. (NAVD88)

Quillayute River Geomorphic Assessment

Habitat Suitability Modeling
Chinook Spawning
Low Flow/High Tide
Figure I-15

TETRA TECH

N
W
E
S

0 0.5 1
Miles

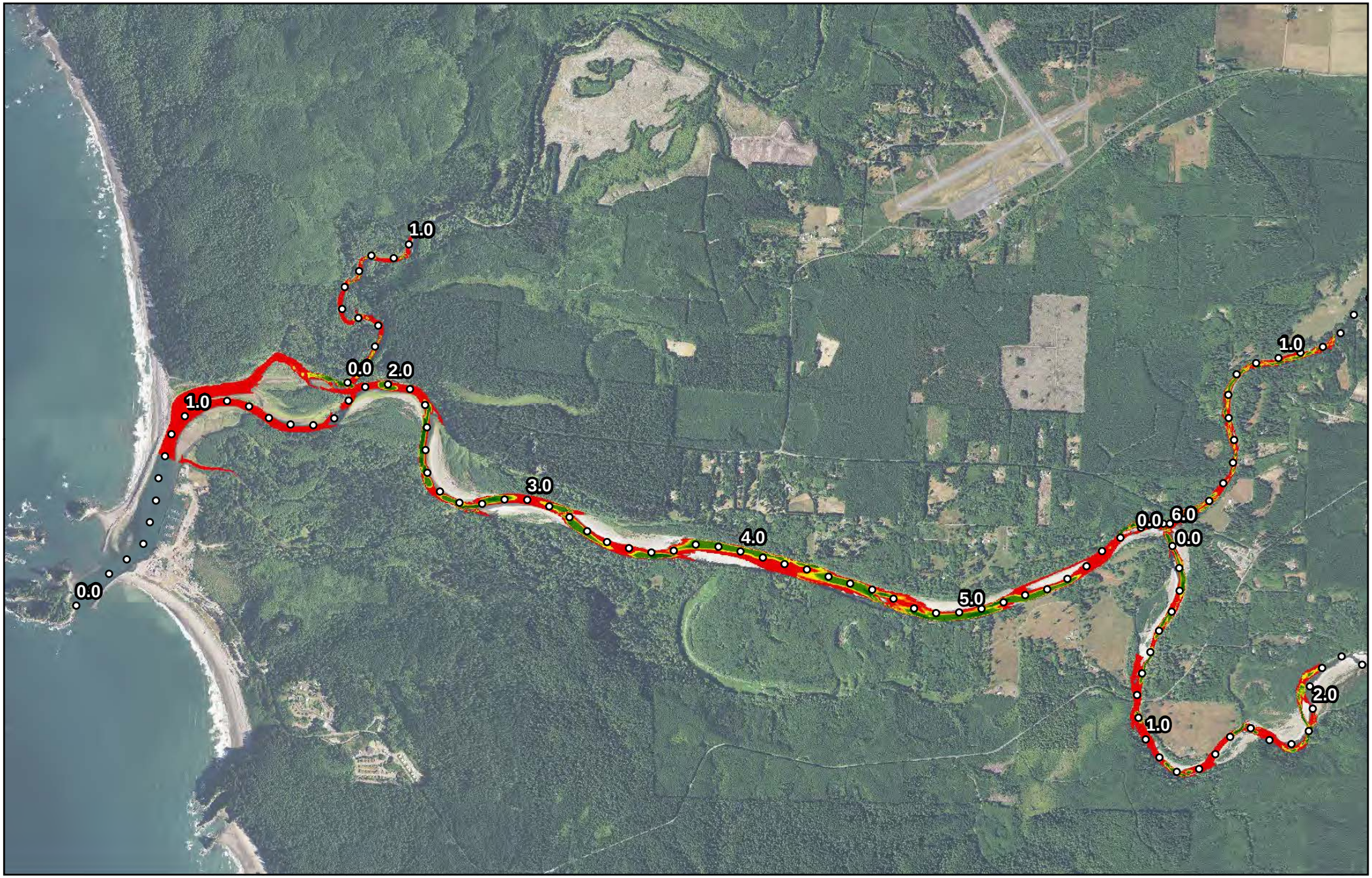

Habitat Suitability Index

High

Low

River Miles

Quillayute River Flow: 423 cfs
High Tide: 7.85 ft. (NAVD88)
Low Tide: -0.66 ft. (NAVD88)

Quillayute River Geomorphic Assessment

Habitat Suitability Modeling
Chinook Spawning
Low Flow/Low Tide
Figure I-16

TETRA TECH

N
W
E
S

0 0.5 1
Miles

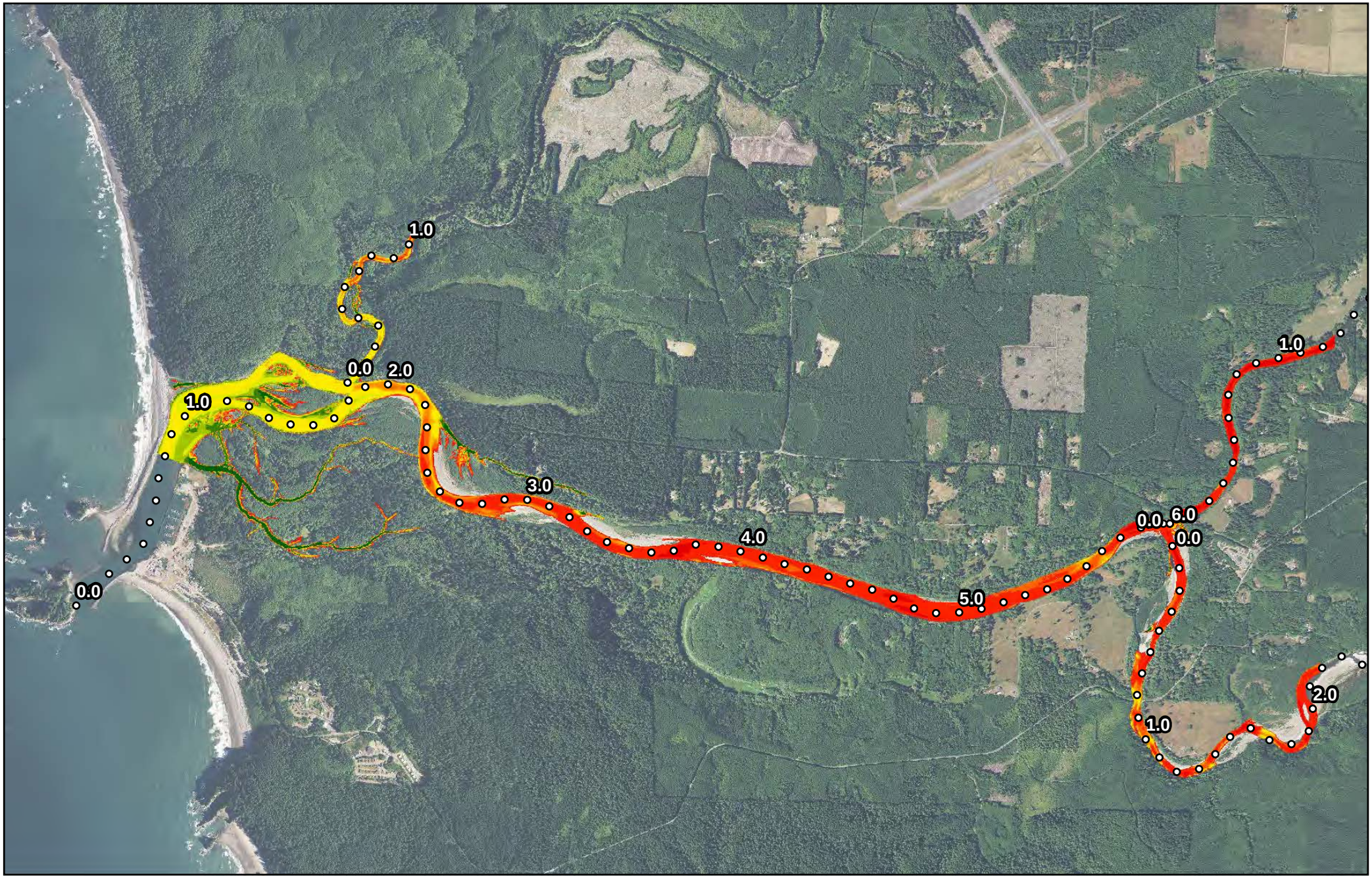

Habitat Suitability Index

High

Low

River Miles

Quillayute River Flow: 2,890 cfs
High Tide: 7.85 ft. (NAVD88)
Low Tide: -0.66 ft. (NAVD88)

Quillayute River Geomorphic Assessment

Habitat Suitability Modeling
Coho Rearing
High Flow/High Tide
Figure I-17

TETRA TECH

N
W
E
S

0 0.5 1
Miles

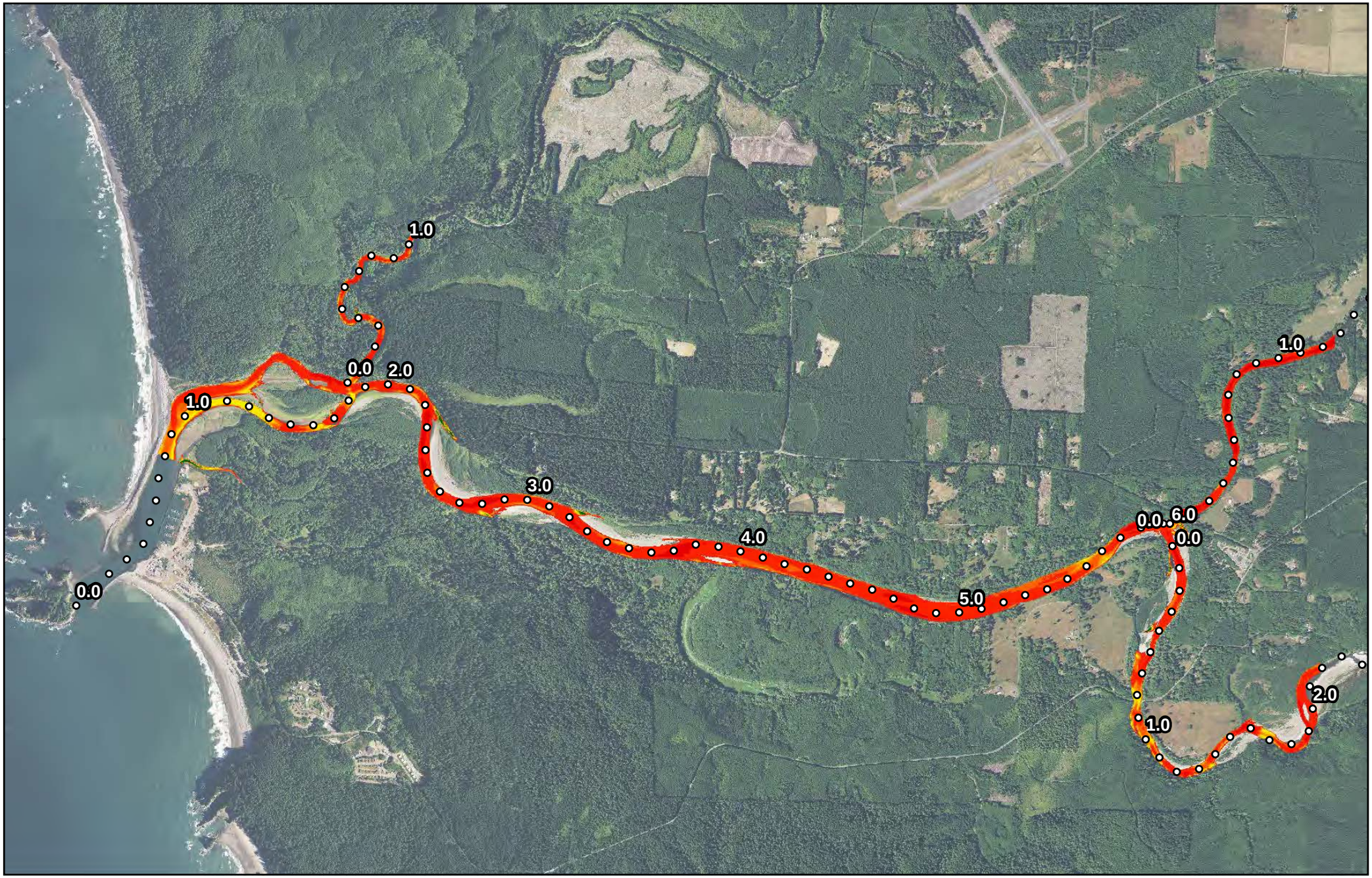

Habitat Suitability Index

High

Low

River Miles

Quillayute River Flow: 2,890 cfs
High Tide: 7.85 ft. (NAVD88)
Low Tide: -0.66 ft. (NAVD88)

Quillayute River
Geomorphic Assessment

Habitat Suitability Modeling
Coho Rearing
High Flow/Low Tide
Figure I-18

TETRA TECH

N
W
E
S

0 0.5 1
Miles

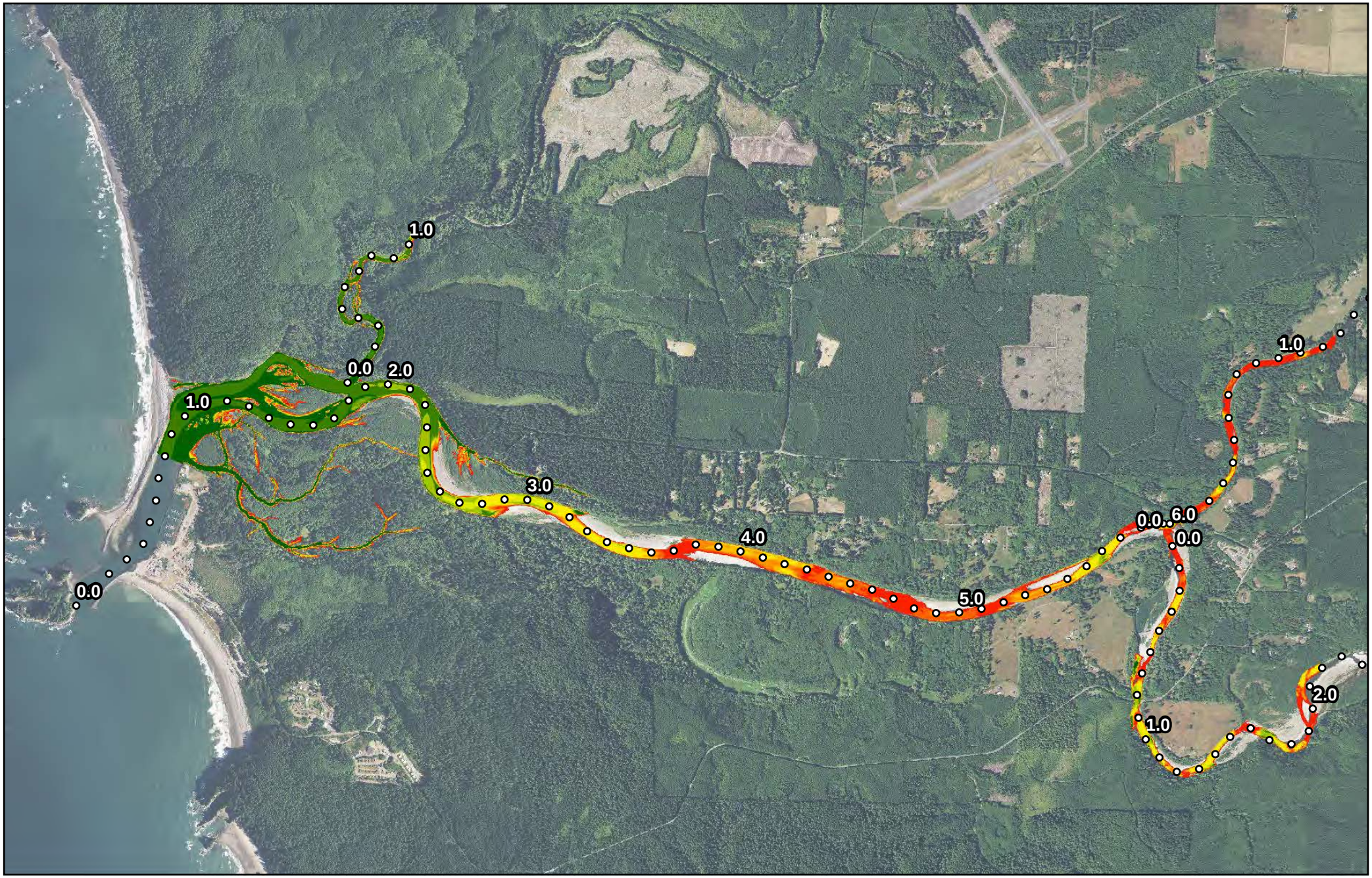

Habitat Suitability Index

High

Low

River Miles

Quillayute River Flow: 423 cfs
High Tide: 7.85 ft. (NAVD88)
Low Tide: -0.66 ft. (NAVD88)

Quillayute River Geomorphic Assessment

Habitat Suitability Modeling
Coho Rearing
Low Flow/High Tide
Figure I-19

TETRA TECH

N
W
E
S

0 0.5 1
Miles

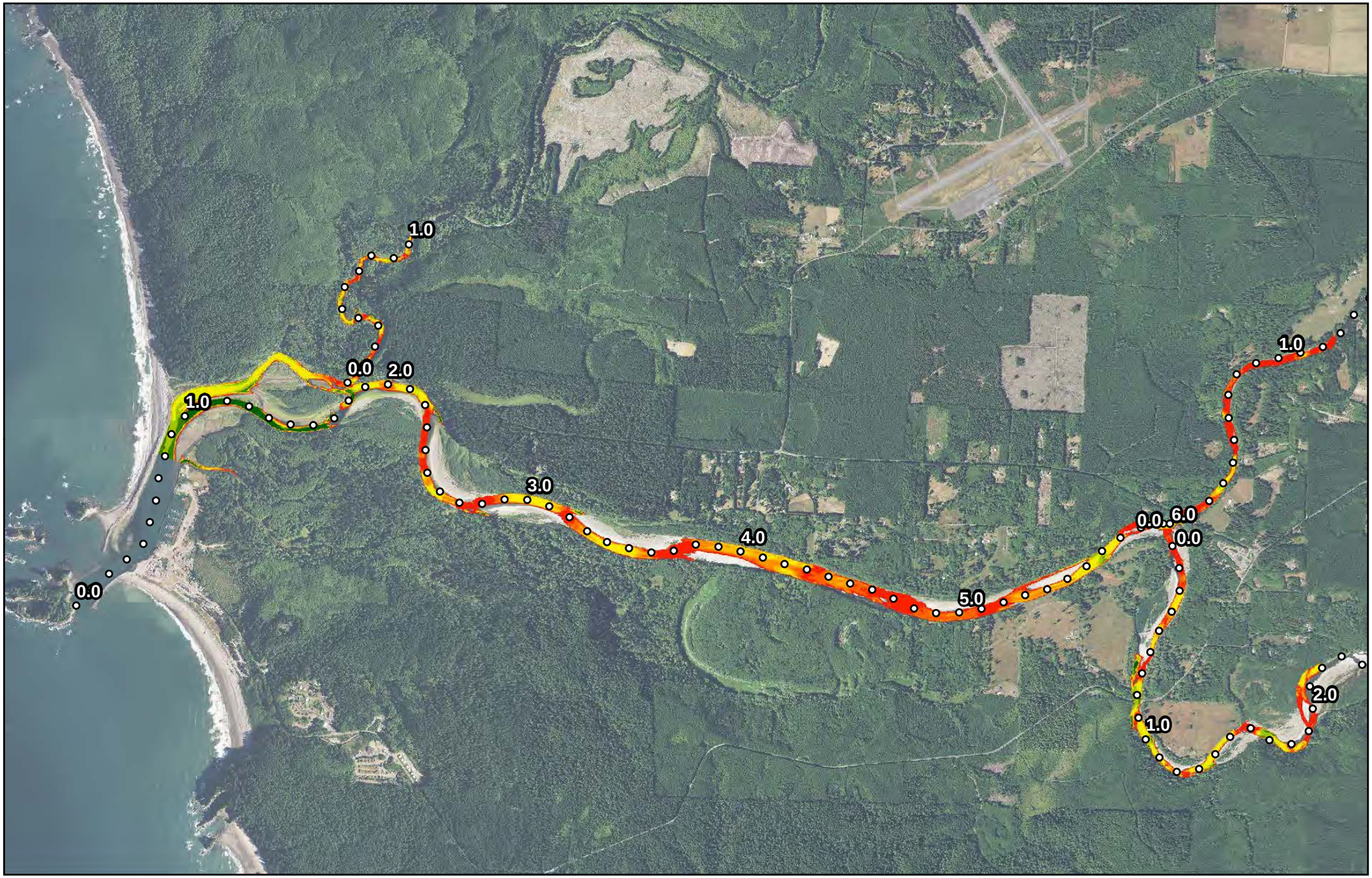

Habitat Suitability Index

High

Low

River Miles

Quillayute River Flow: 423 cfs
High Tide: 7.85 ft. (NAVD88)
Low Tide: -0.66 ft. (NAVD88)

Quillayute River
Geomorphic Assessment

Habitat Suitability Modeling
Coho Rearing
Low Flow/Low Tide
Figure I-20

TETRA TECH

N
W
E
S

0 0.5 1
Miles

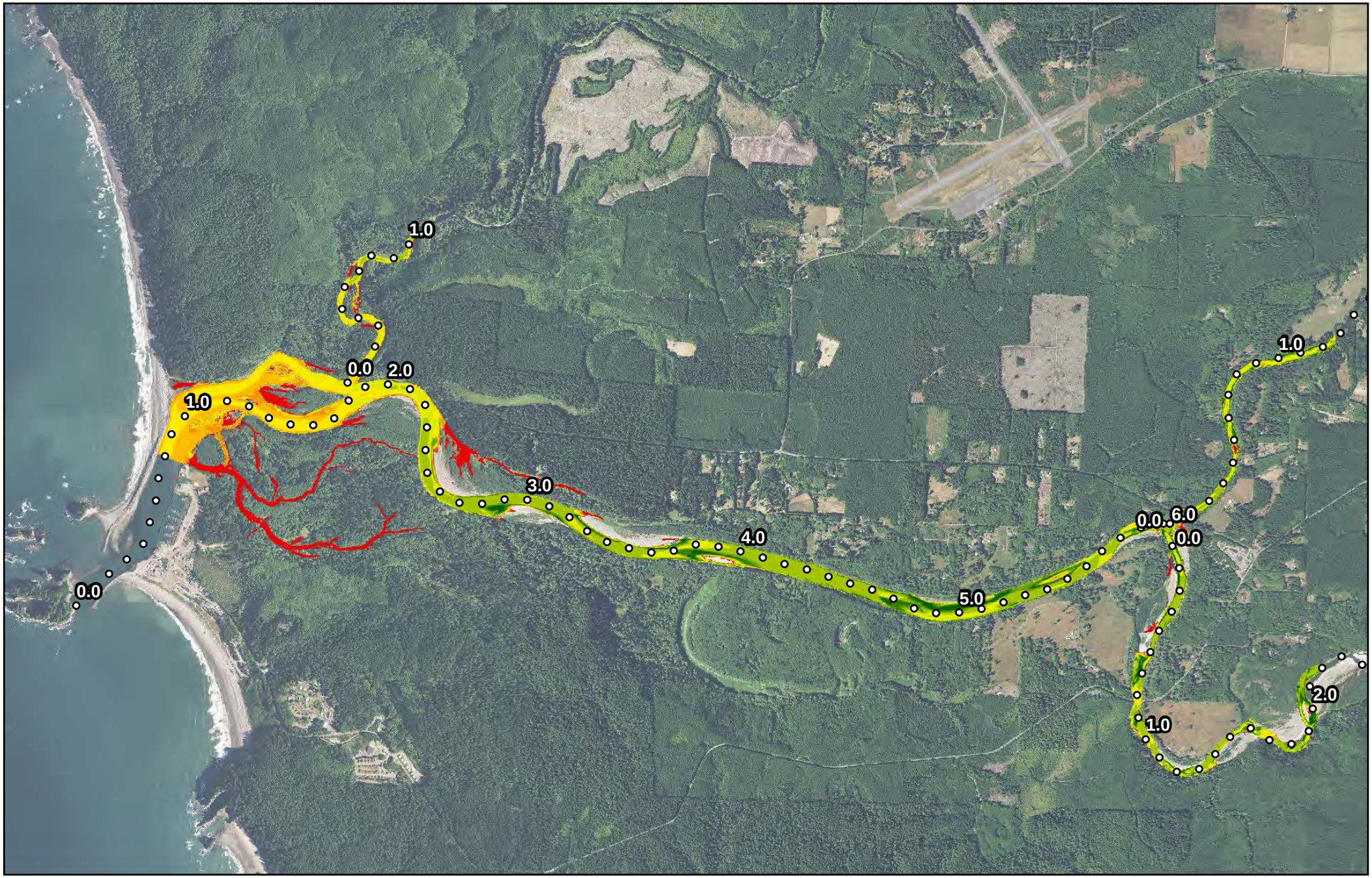

Habitat Suitability Index

High

Low

River Miles

Quillayute River Flow: 2,890 cfs
High Tide: 7.85 ft. (NAVD88)
Low Tide: -0.66 ft. (NAVD88)

Quillayute River Geomorphic Assessment

Habitat Suitability Modeling
Coho Spawning
High Flow/High Tide
Figure I-21

TETRA TECH

N
W
E
S

0 0.5 1
Miles

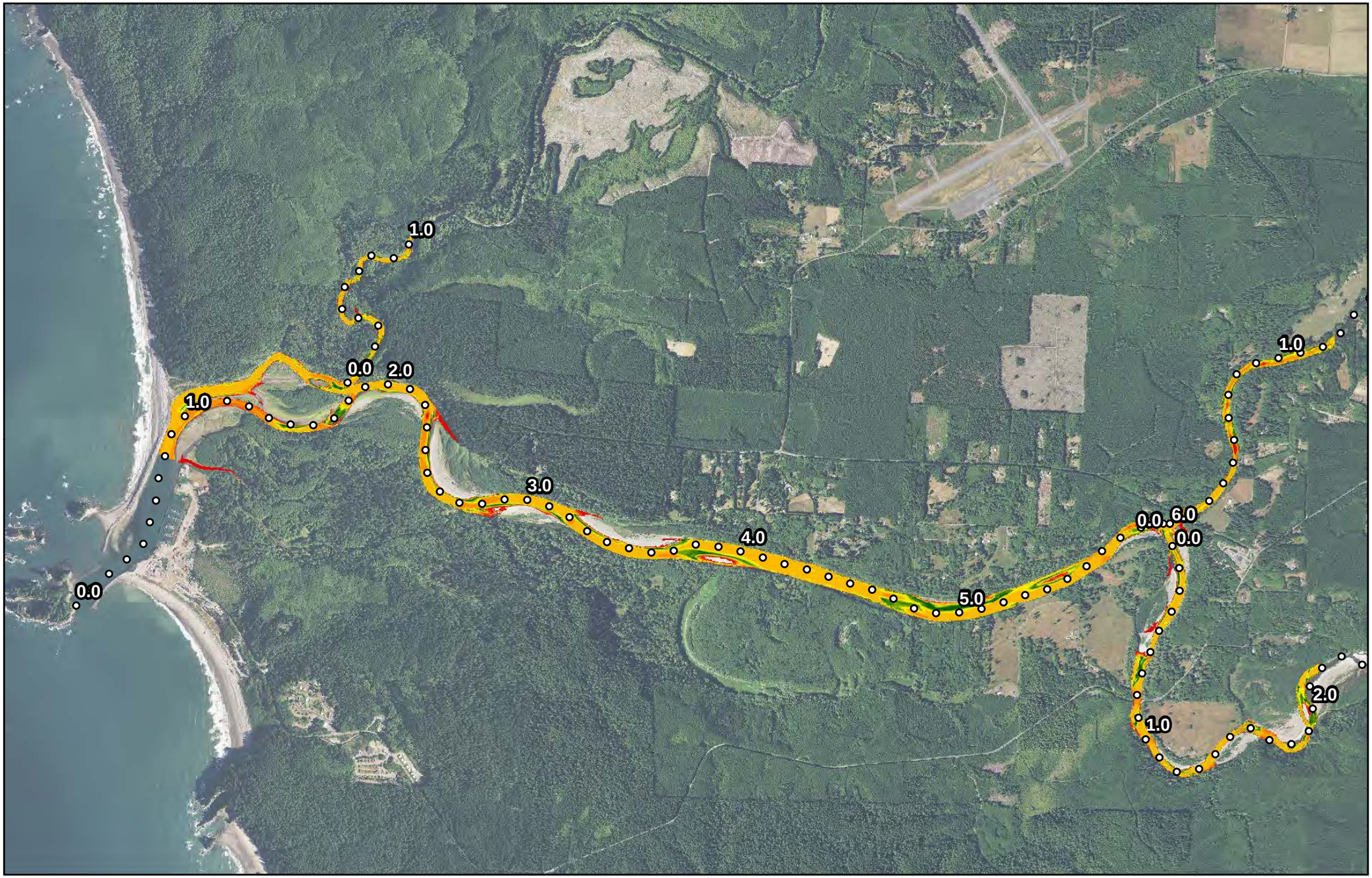

Habitat Suitability Index

High

Low

River Miles

Quillayute River Flow: 2,890 cfs
High Tide: 7.85 ft. (NAVD88)
Low Tide: -0.66 ft. (NAVD88)

Quillayute River Geomorphic Assessment

Habitat Suitability Modeling
Coho Spawning
High Flow/Low Tide
Figure I-22

TETRA TECH

N
W
E
S

0 0.5 1
Miles

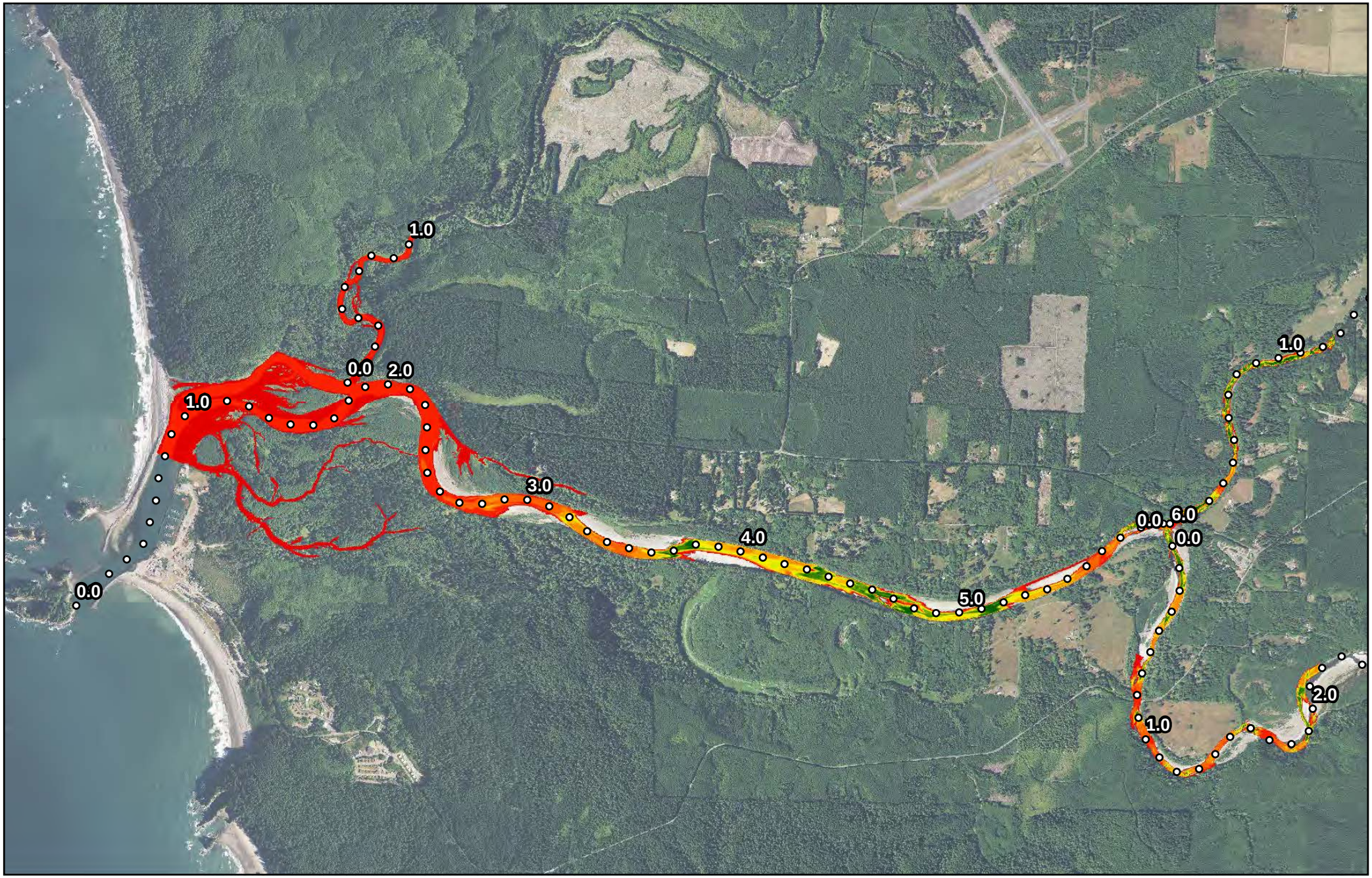

Habitat Suitability Index

High

Low

River Miles

Quillayute River Flow: 423 cfs
High Tide: 7.85 ft. (NAVD88)
Low Tide: -0.66 ft. (NAVD88)

Quillayute River Geomorphic Assessment

Habitat Suitability Modeling
Coho Spawning
Low Flow/High Tide
Figure I-23

TETRA TECH

N
W
E
S

0 0.5 1
Miles

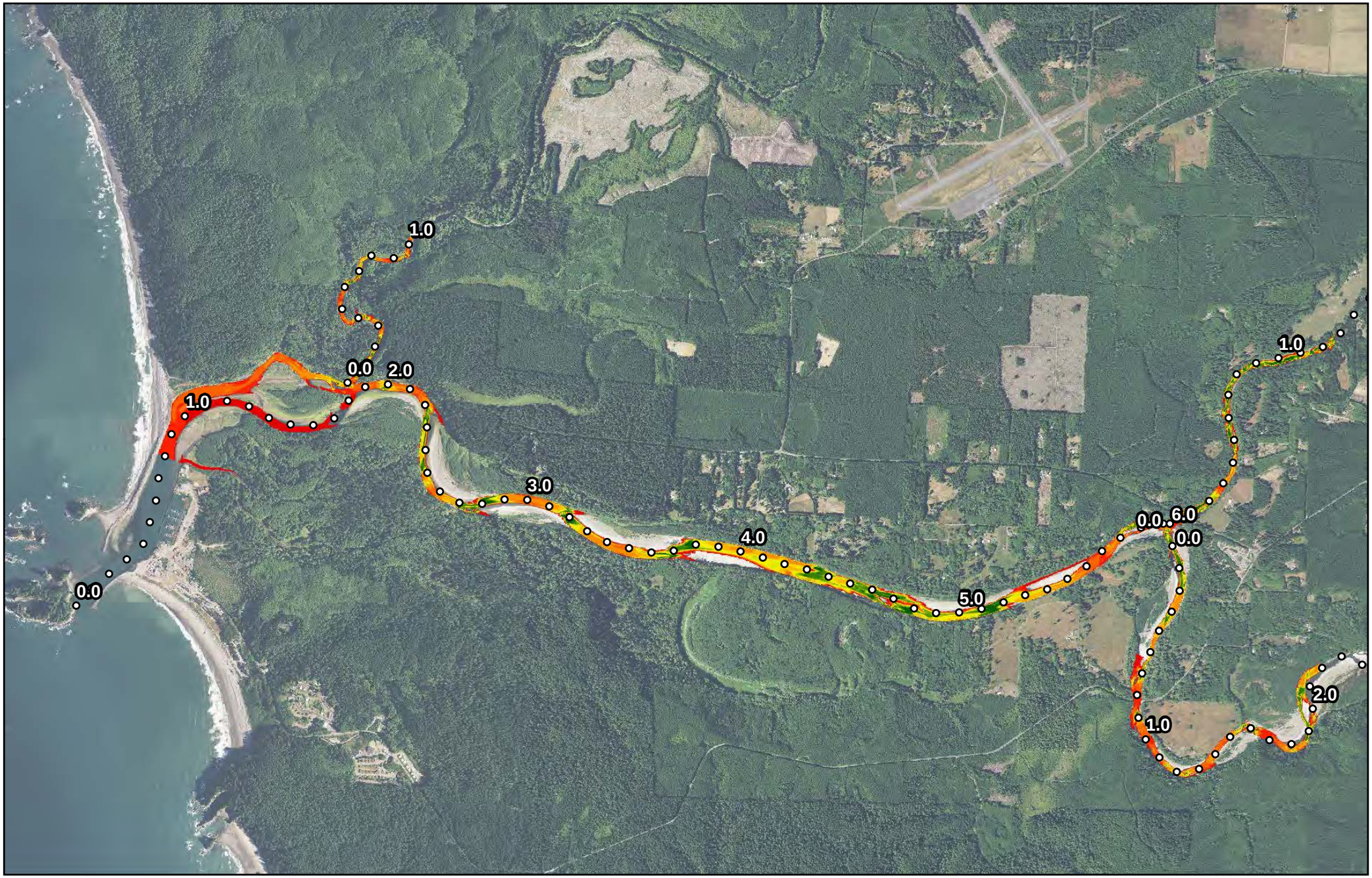

Habitat Suitability Index

High

Low

River Miles

Quillayute River Flow: 423 cfs
High Tide: 7.85 ft. (NAVD88)
Low Tide: -0.66 ft. (NAVD88)

Quillayute River Geomorphic Assessment

Habitat Suitability Modeling
Coho Spawning
Low Flow/Low Tide
Figure I-24

TETRA TECH

N
W
E
S

0 0.5 1
Miles

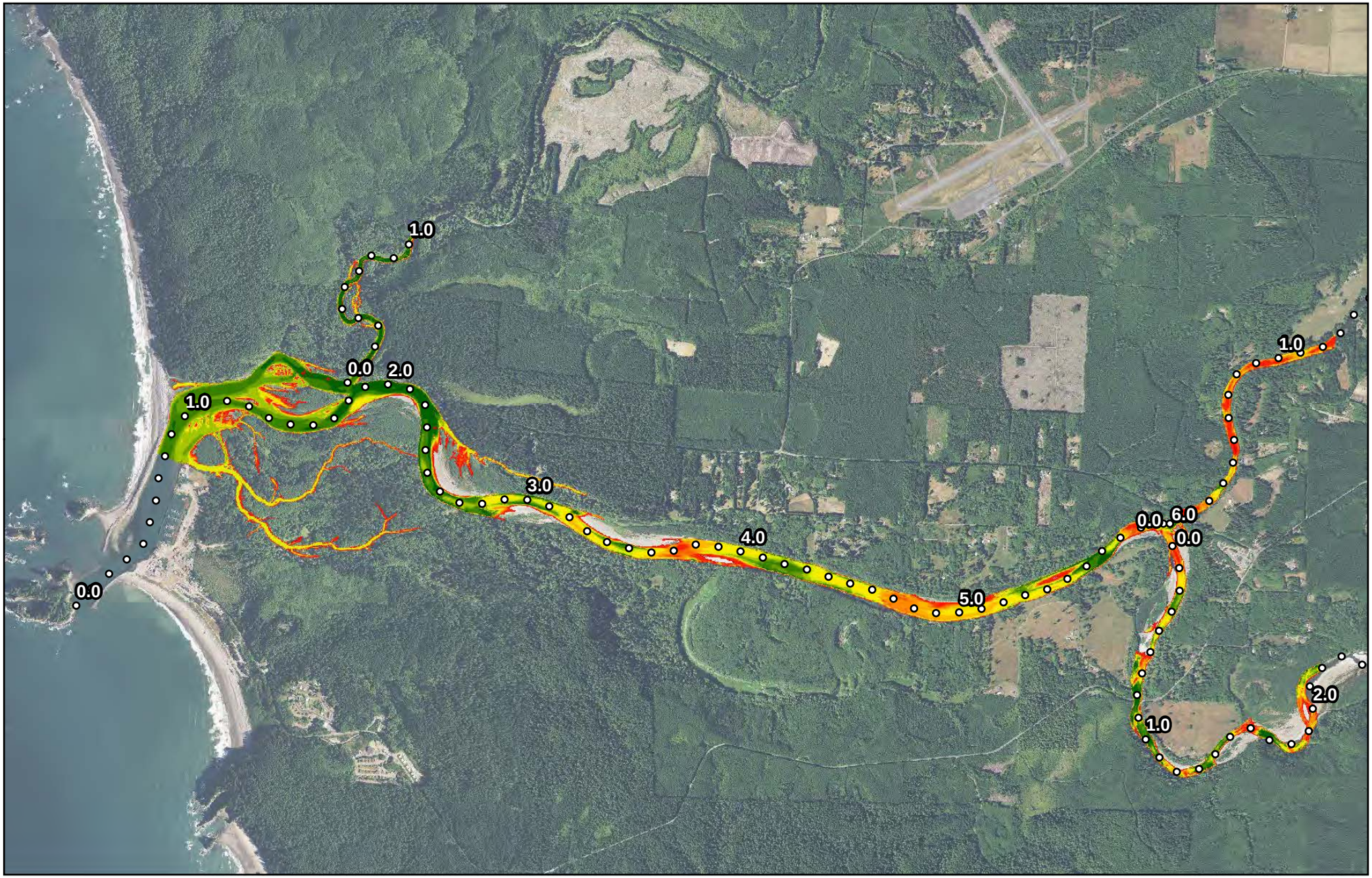

Habitat Suitability Index

High

Low

River Miles

Quillayute River Flow: 2,890 cfs
High Tide: 7.85 ft. (NAVD88)
Low Tide: -0.66 ft. (NAVD88)

Quillayute River Geomorphic Assessment

Habitat Suitability Modeling
Steelhead Rearing
High Flow/High Tide
Figure I-25

TETRA TECH

N
W
E
S

0 0.5 1
Miles

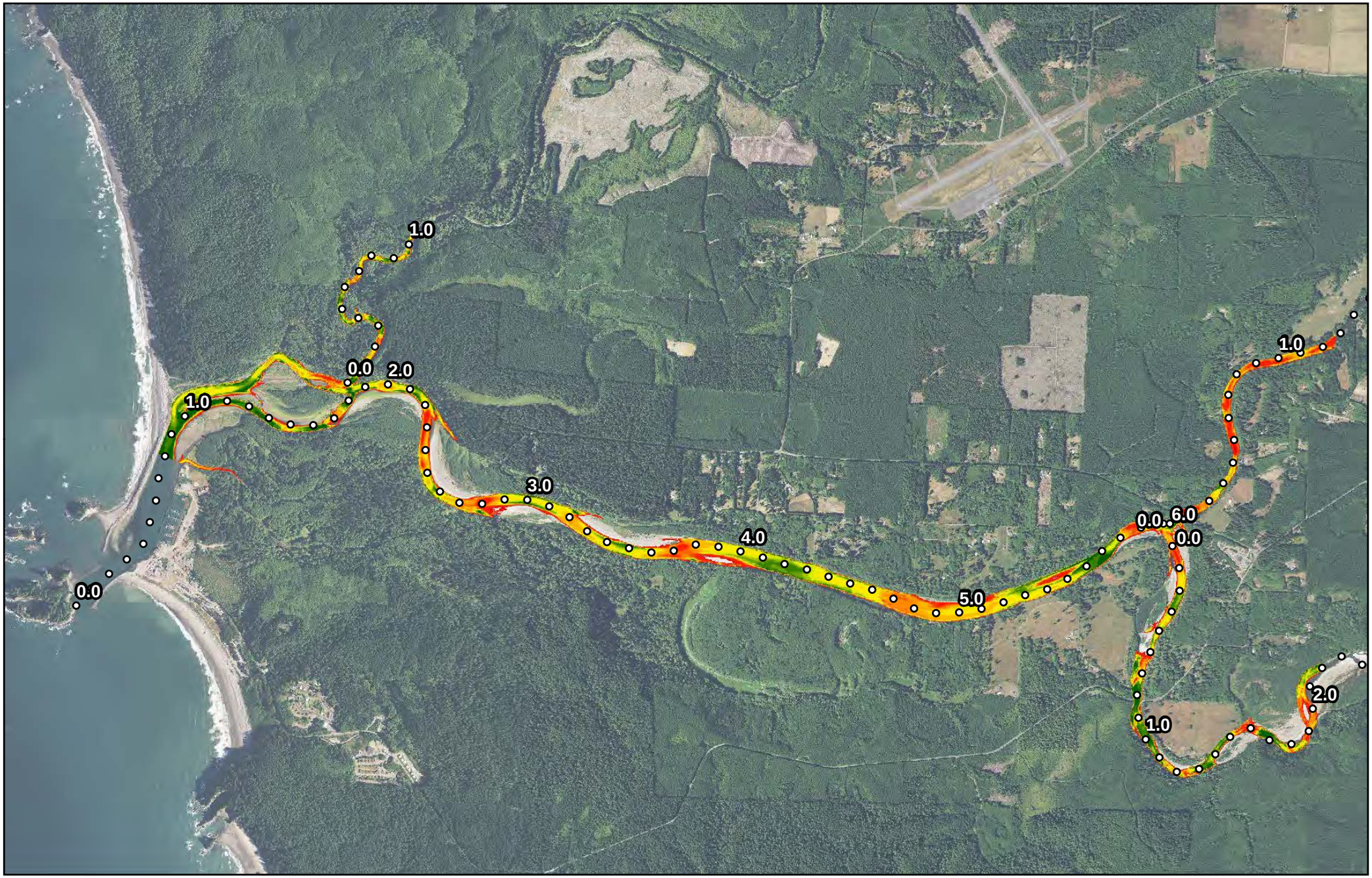

Habitat Suitability Index

High

Low

River Miles

Quillayute River Flow: 2,890 cfs
High Tide: 7.85 ft. (NAVD88)
Low Tide: -0.66 ft. (NAVD88)

Quillayute River Geomorphic Assessment

Habitat Suitability Modeling
Steelhead Rearing
High Flow/Low Tide
Figure I-26

TETRA TECH

N
W
E
S

0 0.5 1
Miles

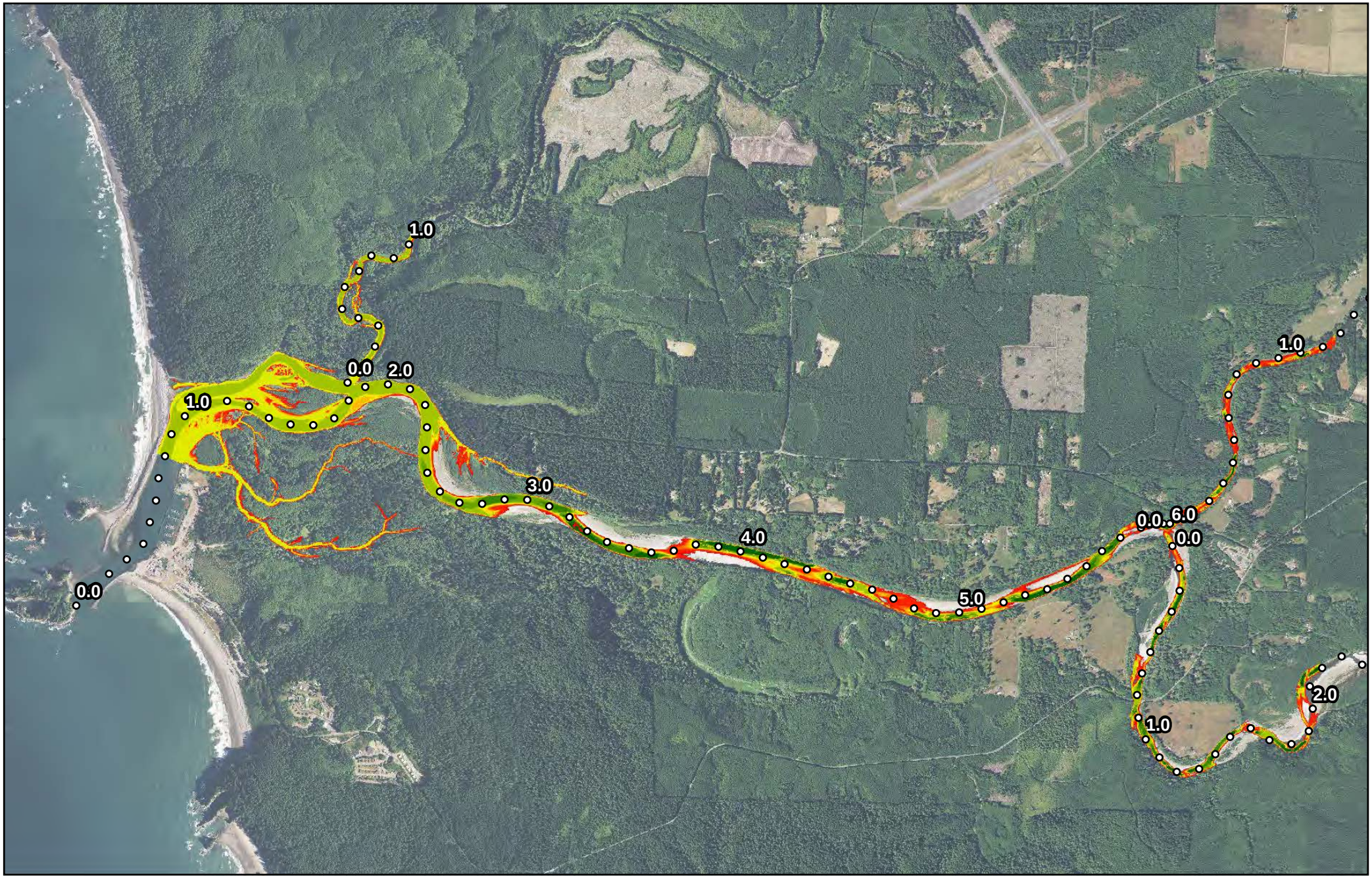

Habitat Suitability Index

High

Low

River Miles

Quillayute River Flow: 423 cfs
High Tide: 7.85 ft. (NAVD88)
Low Tide: -0.66 ft. (NAVD88)

Quillayute River Geomorphic Assessment

Habitat Suitability Modeling
Steelhead Rearing
Low Flow/High Tide
Figure I-27

TETRA TECH

N
W
E
S

0 0.5 1
Miles

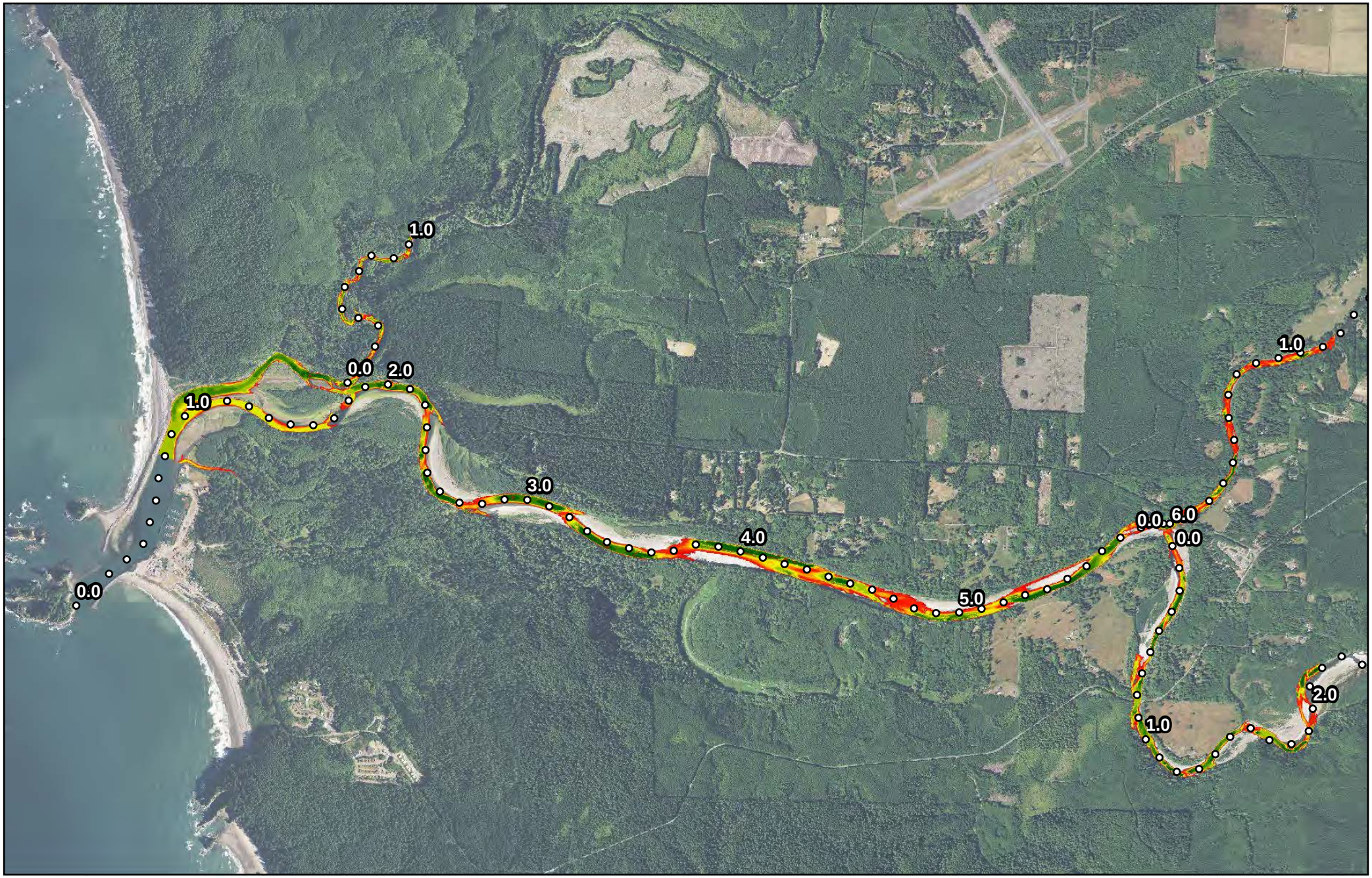

Habitat Suitability Index

High

Low

River Miles

Quillayute River Flow: 423 cfs
High Tide: 7.85 ft. (NAVD88)
Low Tide: -0.66 ft. (NAVD88)

Quillayute River Geomorphic Assessment

Habitat Suitability Modeling
Steelhead Rearing
Low Flow/Low Tide
Figure I-28

TETRA TECH

N
W
E
S

0 0.5 1
Miles

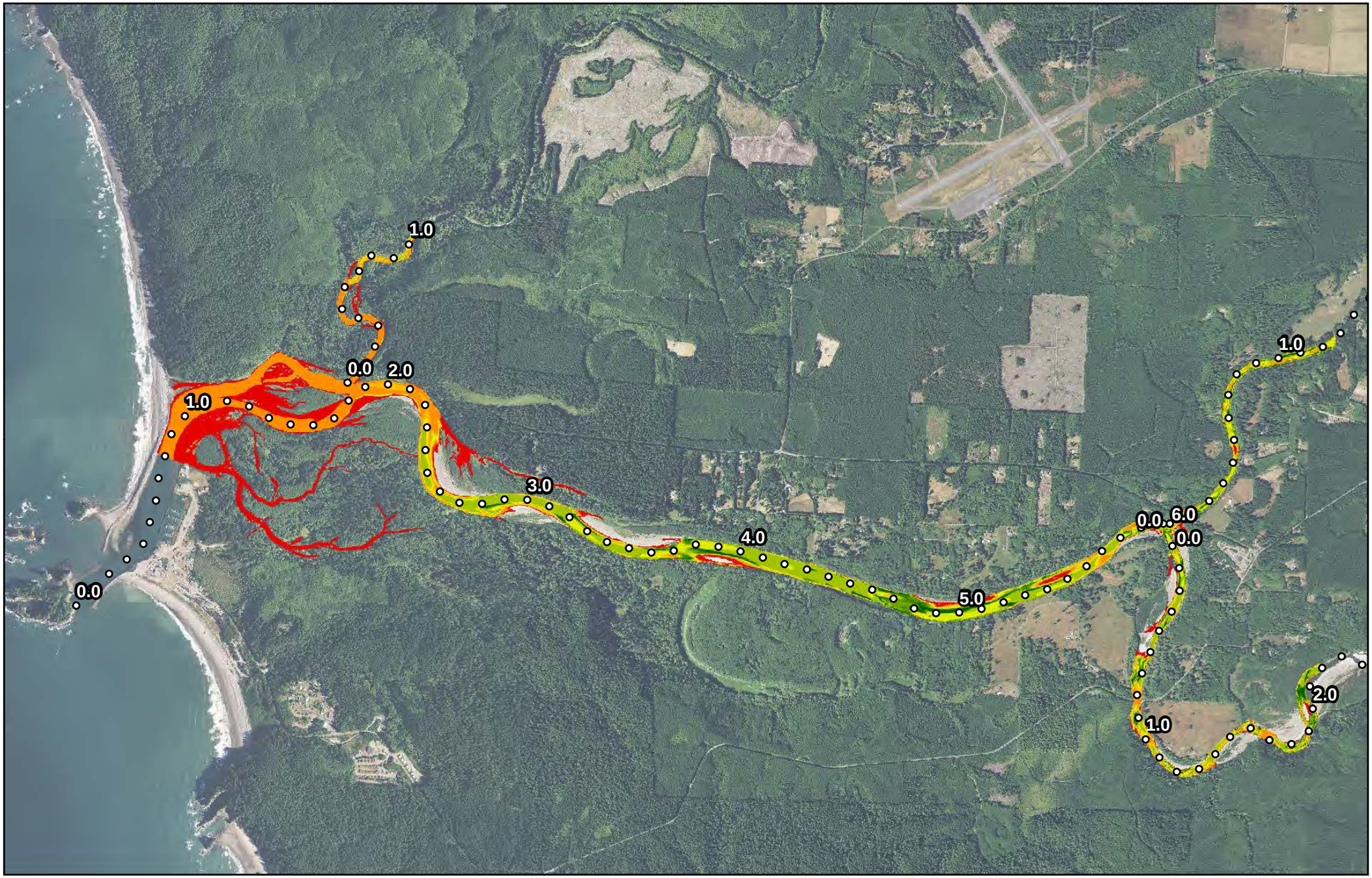

Habitat Suitability Index

High

Low

River Miles

Quillayute River Flow: 2,890 cfs
High Tide: 7.85 ft. (NAVD88)
Low Tide: -0.66 ft. (NAVD88)

Quillayute River Geomorphic Assessment

Habitat Suitability Modeling
Steelhead Spawning
High Flow/High Tide
Figure I-29

TETRA TECH

N
W
E
S

0 0.5 1
Miles

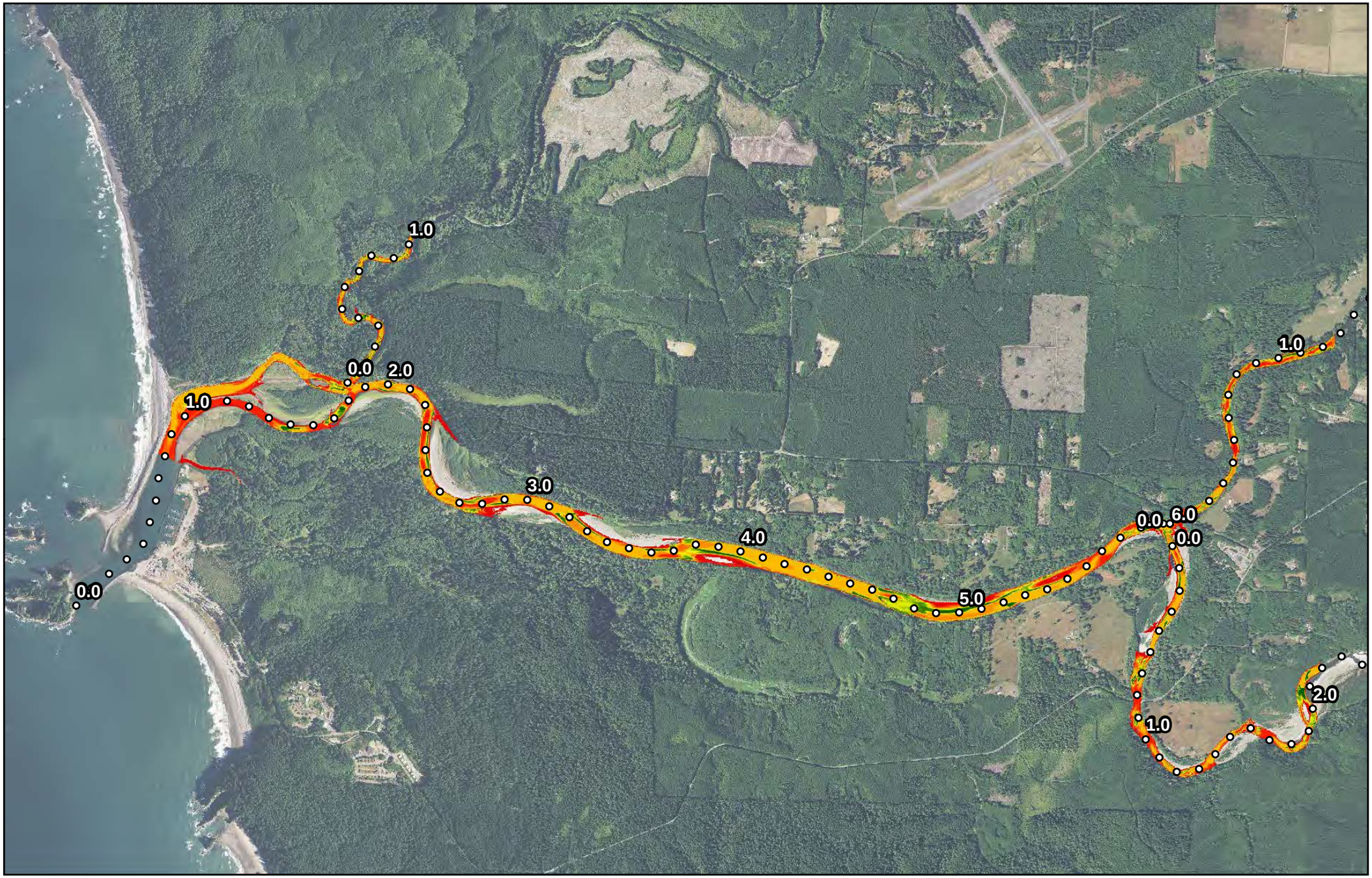

Habitat Suitability Index

High

Low

River Miles

Quillayute River Flow: 2,890 cfs
High Tide: 7.85 ft. (NAVD88)
Low Tide: -0.66 ft. (NAVD88)

Quillayute River Geomorphic Assessment

Habitat Suitability Modeling
Steelhead Spawning
High Flow/Low Tide
Figure I-30

TETRA TECH

N
W
E
S

0 0.5 1
Miles

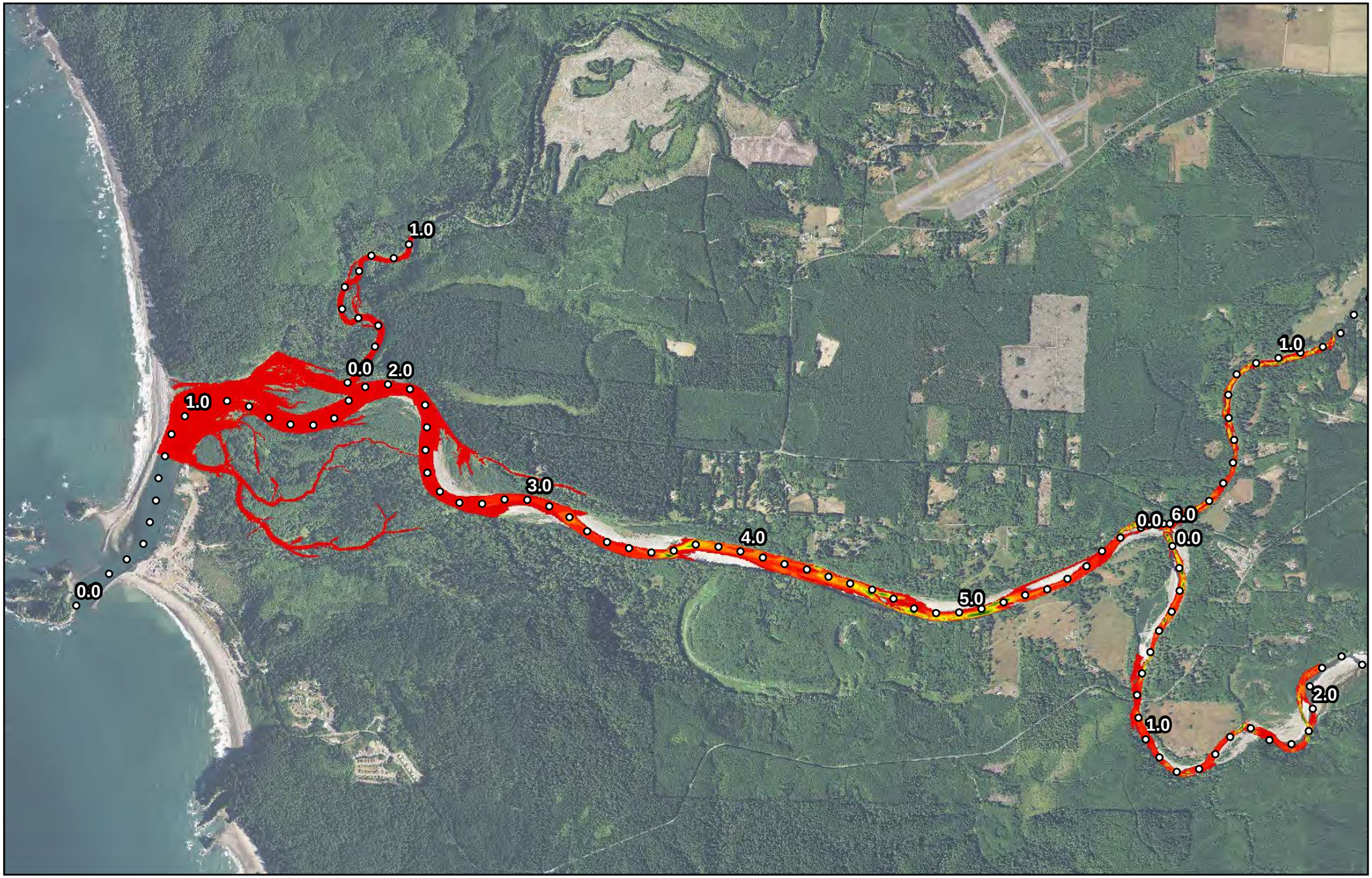

Habitat Suitability Index

High

Low

River Miles

Quillayute River Flow: 423 cfs
High Tide: 7.85 ft. (NAVD88)
Low Tide: -0.66 ft. (NAVD88)

Quillayute River Geomorphic Assessment

Habitat Suitability Modeling
Steelhead Spawning
Low Flow/High Tide
Figure I-31

TETRA TECH

N
W
E
S

0 0.5 1
Miles

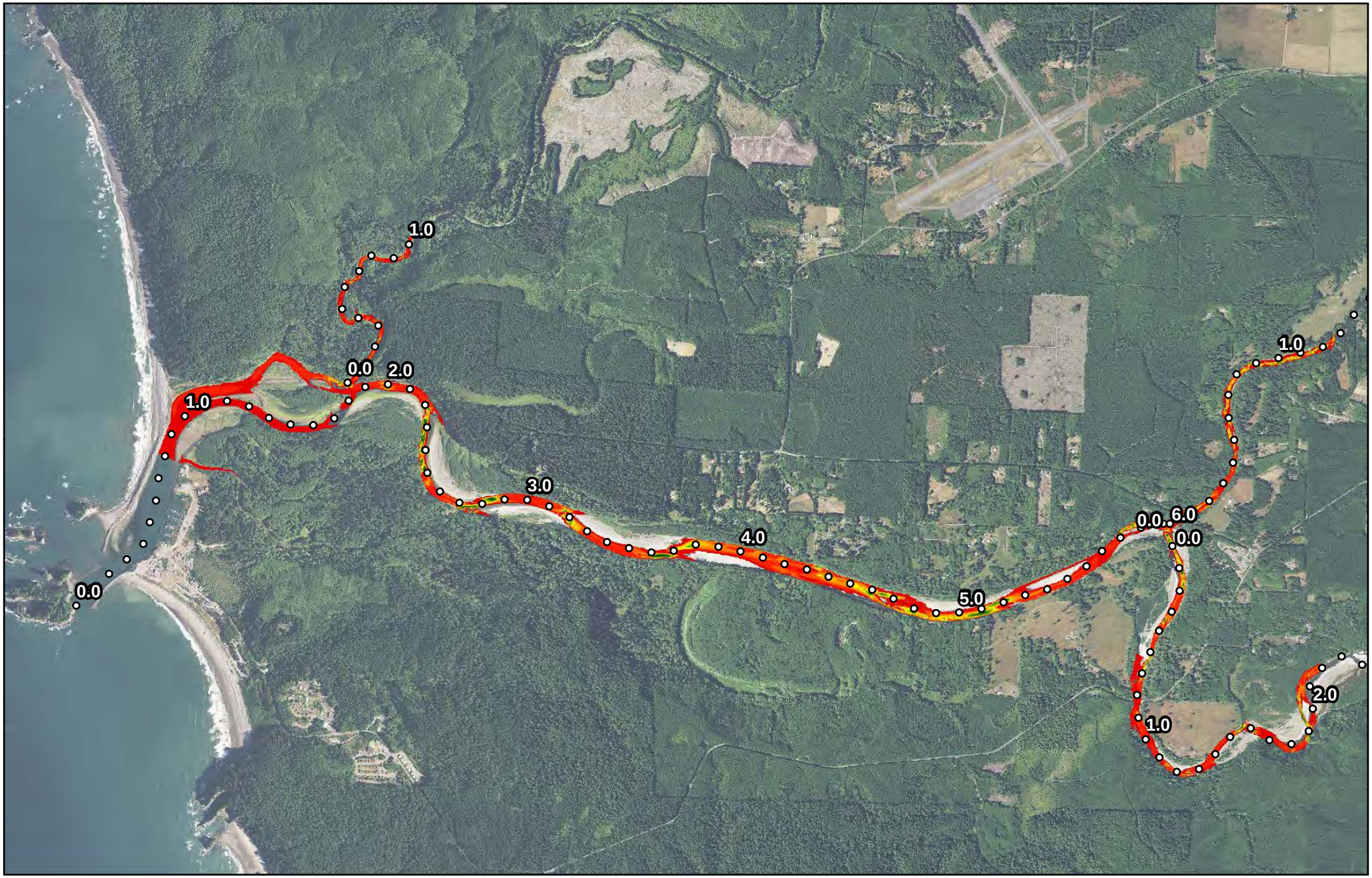

Habitat Suitability Index

High

Low

River Miles

Quillayute River Flow: 423 cfs
High Tide: 7.85 ft. (NAVD88)
Low Tide: -0.66 ft. (NAVD88)

Quillayute River Geomorphic Assessment

Habitat Suitability Modeling
Steelhead Spawning
Low Flow/Low Tide
Figure I-32

TETRA TECH

N
W
E
S

0 0.5 1
Miles

APPENDIX J – REACH-BASED ECOSYSTEM INDICATORS

Quillayute River Project
Geomorphic Assessment and Action Plan
Reach-Based Ecosystem Indicators

Appendix J

Submitted to:

Quileute Natural Resources
401 Main Street
La Push, WA 98350

Submitted by:

TETRA TECH

19803 North Creek Parkway
Bothell, WA 98011
Tel 425.482.7600 | Fax 425.482.7652
www.tetratech.com

September 2020

1. INTRODUCTION

The Reach-based Ecosystem Indicator (REI) assessment provides a well-established and consistent means of evaluating biological and physical conditions in relation to criteria that represent known habitat requirements for aquatic biota. The following REI assessment characterizes the state of geomorphic and ecological processes within the Quillayute River drainage and within each of the project area reaches. The REI pathways and indicators used in this assessment are presented in Table 1.1, and are based on the Matrix of Diagnostics/Pathways and Indicators (US Fish and Wildlife Service (USFWS) 1998) and the National Oceanic and Atmospheric Administration National Marine Fisheries Service (NMFS) Matrix of Pathways and Indicators (1996) as well as more recent work conducted within the region by the Bureau of Reclamation and their adaptation of these indicators (USBR 2012).

Data collected during the 2019 habitat survey, the Quillayute River Geomorphic Assessment (Assessment), and hydraulic analysis informed this REI assessment. Specific assessment results are presented and discussed for each indicator and are used to assign a condition rating of "adequate," "at risk," or "unacceptable." The criteria for rating categories are explained in detail for each indicator below.

Table 1.1. Pathways and Indicators included in the Quillayute River REI assessment

Pathways and Indicators (USFWS 1998, NMFS 1996)		
Pathway	**General Indicator**	**Specific Indicator**
Watershed Condition	Watershed Road Density and Effective Drainage Network	Increase in Drainage Network/ Road Density
	Disturbance Regime	Natural & Human-Caused
	Streamflow	Change in Peak/Base Flows
Reach-Scale Habitat Access	Physical Barriers	Main Channel Barriers
Reach-Scale Habitat Quality	Large Woody Debris (LWD)	Pieces per mile at Bankfull
	Pools	Pool Frequency & Quality
	Off-Channel Habitat	Connectivity with Main Channel
Channel Forms & Processes	Channel Dynamics	Floodplain Connectivity
		Bank Stability/Channel Migration Vertical Channel Stability
Riparian Condition	Disturbance	Human Disturbance

2. PATHWAY: WATERSHED CONDITION

GENERAL INDICATOR: EFFECTIVE DRAINAGE NETWORK AND WATERSHED ROAD DENSITY

Metric Overview

Road density can be a good indicator of watershed condition, as it has been shown that high road density can result in altered drainage networks (Montgomery 1994; Wemple et al. 1996) which in turn often increases fine sediment load to streams and rivers (Reid and Dunne 1984; Goode et al. 2011). In addition, increased road density can result in greater mass wasting events and erosion than in a less disturbed watershed (Montgomery 1994; Wemple et al. 1996). Increased sediment delivery to streams can have significant effects on aquatic systems, such as reducing suitable spawning habitat; smothering salmon eggs (Lisle 1989); clogging hyporheic flow paths (Boulton et al. 1998); reducing substrates for aquatic plants, biofilms, and aquatic invertebrates (Henley et al. 2000); as well as impacting channel morphology and water clarity (Waters 1995; Wood and Armitage 1997).

Criteria: From USFWS (1998), modified by USBR (2012)

Pathway	General Indicators	Specific Indicators	Adequate	At Risk	Unacceptable
Watershed Condition	Effective Drainage network and Watershed Road Density	Increase in Drainage Network/Road Density	Zero or minimum increase in active channel length correlated with human-caused disturbance And Road density <1 miles/mile^2	Low to moderate increase in active channel length correlated with human-caused disturbance And Road density 1 to 2.4 miles/mile^2	Greater than moderate increase in active channel length correlated with human-caused disturbance And Road density >2.4 miles/mile^2

Assessment Results

Road density was calculated using an ArcGIS layer comprised of Clallam County road data as well as Washington Department of Natural Resources (DNR) active roads data. Road density was assessed for the Quillayute River watershed which contained the Hydrologic Unit Code (HUC)-10 basins Dickey River, Sol Duc River-Quillayute River, Calawah River, and Bogachiel River.

Road density for the Quillayute River watershed was 2.95 miles per square mile. Based on the rating criteria, the watershed is functioning at an **unacceptable** condition.

REI Rating

Watershed Rating: **Unacceptable**

INDICATOR: DISTURBANCE REGIME (NATURAL & HUMAN-CAUSED)

Metric Overview

Disturbance is an integral part of natural systems (Ward 1998). Natural disturbance regimes create habitat and biological diversity (Ward 1998; Nakamura et al. 2000) that maintain the larger ecosystem processes. Natural disturbance regimes include events such as landslides, fire, flood, drought, and windstorms. Human activities such as flow regulation, channelization, bank stabilization, road construction, and land-use modifications (conversion to agriculture, development, etc.) can change how systems respond to natural events, frequency of events, and ability to recover (Waples et al. 2009).

Criteria: From USFWS (1998)

Pathway	General Indicators	Specific Indicators	Adequate	At Risk	Unacceptable
Watershed Condition	Disturbance Regime	Natural/Human Caused	Environmental disturbance is short lived; predictable hydrograph; high quality habitat and watershed complexity providing refuge and rearing space for all lifestages or multiple life-history forms. Natural processes are stable.	Scour events, debris torrents, or catastrophic fires are localized events that occur in several minor parts of the watershed. Resiliency of habitat to recover from environmental disturbance is moderate.	Frequent flood or drought producing highly variable and unpredictable flows, scour events, debris torrents, or high probability of catastrophic fire exists throughout a major part of the watershed. The channel is simplified, providing little hydraulic complexity in the form of pools or side channels. Natural processes are unstable.

Assessment Results

This rating was determined based on historical accounts of riparian timber harvest, splash damming, log drives (*The Timberman* 1922; Hashim 2002; HistoryLink 2019), and development in and around the floodplain. Similar alterations in the lower watershed include past human disturbance as well as on-going disturbances that limit the resiliency of habitat to recover from disturbance events. For example, along the Quillayute River, roads and other land use development has constrained river channel migration, disconnected habitat, and decreased woody debris abundance, as observed during 2019 field surveys.

Based on the rating criteria, the watershed is functioning at an **at risk** condition for this indicator.

REI Rating

Watershed Rating: **At Risk**

INDICATOR: STREAMFLOW (CHANGE IN PEAK/BASE FLOWS)

Metric Overview

The magnitude, timing, duration, and frequency of stream flows within a watershed are important drivers within the ecological system (Poff et al. 1997). Stream discharge and channel morphology are directly linked to these processes and largely controlled by climate, vegetation, geology, and human alterations and impacts. Alterations to the natural hydrology of a watershed can affect timing and magnitude of peak flow and low flow events (Kondolf et al. 2001). The frequency of high-flow events can also be dramatically affected by human actions, potentially decreasing due to flow regulation (e.g., dams) and water withdrawals (e.g., for irrigation), or increasing from widespread timber harvest, increased impervious surfaces, or extensive road networks (Anderson et al 2006).

Criteria: From USFWS (1998)

Pathway	General Indicators	Specific Indicators	Adequate	At Risk	Unacceptable
Watershed Condition	Streamflow	Change in Peak/Base flows	Magnitude, timing, duration and frequency of peak flows within a watershed are not altered relative to natural conditions of an undisturbed watershed of similar size, geology, and geography.	Some evidence of altered magnitude, timing, duration and frequency of peak flows relative to natural conditions of an undisturbed watershed of similar size, geology, and geography.	Pronounced evidence of altered magnitude, timing, duration and frequency of peak flows relative to natural conditions of an undisturbed watershed of similar size, geology, and geography.

Assessment Results

In the Quillayute River watershed, there is substantial precipitation, and streamflow primarily comes from storm-derived rainfall in the winter, and snowmelt in the spring and summer (WRCC 2020). Rainfall in the basin averages 120 inches a year, among the highest in Washington state (Quileute Tribe 2016). The Quillayute River forms where the Sol Duc and Bogachiel Rivers meet, and most of the flow in the Quillayute comes from these tributaries, as well as the Calawah River, a tributary of the Bogachiel, and the Dickey River, a tributary of the Quillayute near its mouth. In winter, flow from the Sol Duc River is about 1.5 times that of the Bogachiel or the Calawah Rivers. For most streams in the basin, the highest monthly flows during the winter are about 10 times greater than the lowest monthly flows during the summer, except for the Dickey River where winter flows are about 20 times greater than summer flows (Nelson 1982).

Flooding is common in the Quillayute watershed, especially during the high flows of the winter months. Severe floods in western Clallam County occurred in 1935, 1955 (the most severe in recent history), 1956, 1968, 1979, and 1990. The estimated peak discharge of the Quillayute River based on hydrologic analysis is 131,500 cubic feet per second (cfs), which exceeds the estimated 100-year flood

discharge of 119,000 cfs calculated by Leonard (1982). Over the past 17 years alone, the Quillayute River and its tributaries have frequently flooded their banks, and there have been 42 breaches on the Bogachiel River near its mouth to the Quillayute (NWS 2020). Table 2.1 below shows the top ten of these high-water crests.

Since 2010, streamflows for the Calawah River, which ultimately flows into the Quillayute River, have followed the same overall trends as the previous 35 years, exhibiting increasing peak flows and decreasing low flows (Quileute Tribe 2016). This change in peak and low flows is likely a result of climate change, which impacts rainfall, as well as the magnitude, timing, duration, and frequency of streamflows. On the Olympic Peninsula, climate change is expected to decrease stream flow (OCCRI 2017), while raising ocean water levels (OCCRI 2019), both of which will affect the Quillayute watershed. Hydraulic modeling further confirms descriptions of fish passage issues in the lower Quillayute River at low flows (see Pathway 3 below and Sections 2, 3, and 4 of the Assessment). Climate change may further affect stream flows by generating more severe and more frequent storm surges from an increase in wave energy, leading to more flooding and erosion (Ruggiero et al. 2010; MacLennan et al. 2013).

Therefore, based on the altered magnitude and frequency in peak flows in the recent past, as well as expected effects of climate change on criteria for watershed hydrology, this indicator is rated **at risk**.

REI Rating

Watershed Rating: **At Risk**

Table 2.1. Top 10 High Water Crests on the Bogachiel River near the Quillayute since 2003 (Flood height is 37 ft) (NWS 2020)

Event Rank	Water Year	Feet
1	2006	42.64
2	2003	42.54
3	2009	41.63
4	2007	41.34
5	2010	41.32
6	2015	40.73
7	2017	40.73
8	2015	39.91
9	2007	39.19
10	2016	38.86

3. PATHWAY: REACH-SCALE HABITAT ACCESS

INDICATOR: PHYSICAL BARRIERS (MAIN CHANNEL BARRIERS)

Metric Overview

Physical barriers restrict movement of aquatic species throughout a watershed. This can result in reduced genetic diversity within populations and reduced distribution of marine derived nutrients throughout the system and may also impact transport of woody debris material downstream from source areas. This indicator evaluates the presence or absence of fish passage barriers in both the mainstem Quillayute River and associated off-channel habitat.

Criteria: From USFWS (1998), modified by USBR (2012)

Pathway	General Indicators	Specific Indicators	Adequate	At Risk	Unacceptable
Reach-Scale Habitat Access	Physical Barriers	Main Channel Barriers	No barriers present that limit upstream or downstream fish passage at any flows	Barriers present that prevent upstream or downstream migration at some flows that are biologically significant	Barriers present that prevent upstream or downstream migration at multiple or all flows

Assessment Results

Fish passage barriers are present on the Quillayute River, as assessed during 2019 field surveys. Barriers were not identified in Quillayute River reaches 1, 5, 6 or in Lower Bogachiel, Lower Sol Duc, or Lower Dickey reaches and are considered **adequate**. Quillayute River Reach 2 includes two culverts along Mora Road on the right bank of the Quillayute River that precludes fish passage at lower flows and at lower tidal levels. Reach 3 also includes culverts that connect James Pond to the Quillayute River riparian area along the right bank. These culverts also preclude fish passage at lower flows and at lower tidal levels. Furthermore, hydraulic modeling confirms identification of fish passage issues in Quillayute River reaches 3 and 4 at low flows late in the summer. Therefore, these reaches are considered **at risk**.

Main Channel Barriers REI Rating

Reach 1	Reach 2	Reach 3	Reach 4	Reach 5	Reach 6	Lower Bogachiel	Lower Sol Duc	Lower Dickey
adequate	at risk	at risk	at risk	adequate	adequate	adequate	adequate	adequate

4. PATHWAY: REACH-SCALE HABITAT QUALITY

INDICATOR: LARGE WOODY DEBRIS (LWD) (PIECES PER MILE AT BANKFULL)

Metric Overview

Large woody debris (LWD) in streams impacts sediment distribution, stream morphology, and processes such as floodplain connectivity, benefitting streams by creating and sustaining channel complexity through space and time (Montgomery et al 2003). Large pieces of wood and log jams create critical habitat features including pools, cover and velocity refugia for fish (Dolloff and Warren 2003). LWD also creates habitat for invertebrates, a primary source of food for fish (Benke and Wallace 2003; Dolloff and Warren 2003).

This indicator evaluates the quantity of LWD in pieces per mile. There is some disagreement on appropriate LWD targets including frequencies, size requirements, and whether bankfull channel width should be considered in setting targets. NMFS (1996) and USFWS (1998) state that functioning coastal streams should have more than 80 pieces of LWD per mile. As described by Fitzgerald (2004), others propose much higher targets for LWD per mile for coastal streams, varying size definitions for LWD, and recommend varying targets based on a stream's bankfull width. NMFS (1996) and USFWS (1998) targets have been used for this assessment to remain consistent with sources for all other indicators and due to data availability.

Criteria: NMFS (1996), USFWS (1998)

Pathway	General Indicators	Specific Indicators	Adequate	At Risk	Unacceptable
Reach-Scale Habitat Quality	Large Woody Debris (LWD)	Pieces per mile at bankfull	>80 pieces/mile >12" dbh > 35' length; and adequate sources of woody debris available for both long- and short-term recruitment.	Current levels meet piece frequency standard for **Adequate** but lacks potential sources from riparian areas for wood debris recruitment to maintain that standard.	Does not meet standards for **Adequate** and lacks potential large woody material recruitment.

Assessment Results

The quantity of LWD historically present in the mainstem Quillayute River is uncertain. Previous studies have found that the abundance of instream LWD does decrease with basin area in large rivers as a result of increased transport potential. However, the current conditions in most large rivers of the Pacific Northwest do not accurately represent historical conditions due to widespread modification, riparian clearing, and snag removal (Collins et al. 2002). Qualitative historical records indicate that extensive log jams sometimes miles in length and channel-spanning were historically

present on many large rivers across North America (Wohl 2013). LWD throughout each reach was inventoried during the 2019 field surveys. Eight of the nine reaches are considered **unacceptable** due to a general lack of LWD. Future LWD recruitment is also limited in most reaches by restricted access to the floodplain due to bank hardening and incision. Quillayute River Reach 2 is considered **at risk**; while it meets the piece frequency standard, bank hardening features reduce the potential to recruit large wood.

Large Woody Debris Pieces per Mile (data collected during 2019 field survey)

Large Woody Debris (LWD)	Reach 1	Reach 2	Reach 3	Reach 4	Reach 5	Reach 6	Lower Bogachiel	Lower Sol Duc	Lower Dickey
Pieces/mile	0	100	17	3	4	2	40	4	3

LWD REI Rating

Reach 1	Reach 2	Reach 3	Reach 4	Reach 5	Reach 6	Lower Bogachiel	Lower Sol Duc	Lower Dickey
unacceptable	at risk	unacceptable	unacceptable	unacceptable	unacceptable	unacceptable	unacceptable	unacceptable

INDICATOR: POOLS (POOL FREQUENCY & QUALITY)

Metric Overview

Along with large woody debris, pools create important habitat and refuge for fish. This criterion focuses on the number and quality of pools per mile of stream. The largest bankfull channel width provided in the NMFS matrix is 65 to 100 feet, and 4 pools per mile is the standard for this width.

Criteria: Adapted from NMFS (1996)

Pathway	General Indicators	Specific Indicators	Adequate	At Risk	Unacceptable
Reach-Scale Habitat Quality	Pools	Pool Frequency and Quality	Pools have good cover and cool water and only minor reduction of pool volume by fine sediment; each reach has many large pools > 1m deep with good cover	Meets pool quality standards, but does not meet LWD standards, so unable to maintain pools over time; reaches have few deep pools (>1m) present with good fish cover	Lacking pools, pool quality is inadequate and there has been a major reduction of pool volume by fine sediment; reaches have no deep pools (> 1m) with good fish cover

Assessment Results

The Quillayute River is wide and for the most part is dominated by riffles and runs. During 2019 field surveys, reaches were evaluated by channel units and whether there were pools present. Quillayute River Reach 1 to the mouth, is effectively a navigation channel and does not have natural channel features. The rest of the Quillayute River is comprised of riffles and runs, with a few pools scattered throughout. All reaches were rated **unacceptable** due to the overall lack of pools throughout the system, failure to meet the LWD standards, and lack of sufficient fish cover (see Section 4 of the Assessment).

Pool Characteristics by Reach

Pool Characteristics	Reach 1	Reach 2	Reach 3	Reach 4	Reach 5	Reach 6	Lower Bogachiel	Lower Sol Duc	Lower Dickey
Pool percentage	0%	0%	2%	0%	0%	5%	few pools present (percent not available)	0%	few pools present (percent not available)

Pool Frequency and Quality REI Rating

Reach 1	Reach 2	Reach 3	Reach 4	Reach 5	Reach 6	Lower Bogachiel	Lower Sol Duc	Lower Dickey
Unacceptable	Unacceptable	Unacceptable	Unacceptable	Unacceptable	Unacceptable	Unacceptable	Unacceptable	Unacceptable

INDICATOR: OFF-CHANNEL HABITAT (CONNECTIVITY WITH MAIN CHANNEL)

Metric Overview

Off-channel habitats, sloughs, wetlands, oxbow lakes, backwaters, floodplain channels, and blind and flow-through side-channels can provide important rearing habitat for juvenile salmonids (Roni et al. 2002). These areas can provide velocity refugia, temperature refugia, and cover, as well as productive feeding areas.

Criteria: Modified from USFWS (1998) and USBR (2012)

Pathway	General Indicators	Specific Indicators	Adequate	At Risk	Unacceptable
Reach-Scale Habitat Quality	Off-Channel Habitat	Connectivity with main channel	Reach has ponds, oxbows, backwaters, and other low-energy off-channel areas with cover; similar to conditions that would be expected in the absence of human disturbance	Reach has some ponds, oxbows, backwaters, and other low-energy off-channel areas with cover; but availability or access is less than what would be expected in the absence of human disturbance	Reach has few or no ponds, oxbows, backwaters, or other off-channel areas relative to what would be expected in the absence of human disturbance.

Assessment Results

The Quillayute River generally lacks adequate off-channel habitat, as inventoried during the 2019 field surveys. Quillayute River reaches 1 and 6 are considered **unacceptable** due to limited side-channels and other off-channel areas. In Quillayute River Reaches 2, 3, 4, 5, Lower Dickey, Lower Bogachiel, and Lower Sol Duc, the abundance of off-channel habitat is considered **at risk**, with some off-channel habitat present (more in Quillayute River Reach 2) but less than would be expected prior to human development. Quillayute River Reach 2 has relatively abundant off-channel habitat in the distributary channels and a slough on the left bank, but this is still less than expected in the absence of human disturbance due to the presence of a road on the right bank.

Channel Type Distribution

	Reach 1	Reach 2	Reach 3	Reach 4	Reach 5	Reach 6	Lower Bogachiel	Lower Sol Duc	Lower Dickey
Off Channel Habitat Types	none	Estuarine, backwater alcoves, side channels	Side channel, backwater alcoves	Alcoves, side channels, wetlands	Alcoves, side channels	Alcoves	Alcoves, side channels, tributaries, wetlands	Alcoves, side channels	Estuarine, wetlands, side channels, alcoves

Off-Channel Habitat REI Rating

Reach 1	Reach 2	Reach 3	Reach 4	Reach 5	Reach 6	Lower Bogachiel	Lower Sol Duc	Lower Dickey
Unacceptable	At risk	At risk	At risk	At risk	Unacceptable	At risk	At risk	At risk

5. PATHWAY: CHANNEL FORMS & PROCESSES

INDICATOR: CHANNEL DYNAMICS (FLOODPLAIN CONNECTIVITY)

Metric Overview

Floodplains serve a number of significant geomorphic and ecological functions including conveyance of flood waters, sediment source and storage, supply of large wood, and development of diverse habitat for aquatic and terrestrial species (e.g., Allen 1970; Nanson and Croke 1992; Zwolinski 1992).

Criteria: Modified from USFWS (1998)

Pathway	General Indicators	Specific Indicators	Adequate	At Risk	Unacceptable
Channel Forms & Processes	Channel Dynamics	Floodplain Connectivity	Floodplain areas are frequently hydrologically linked to main channel; overbank flows occur and maintain wetland functions, riparian vegetation and succession	Reduced linkage of wetlands, floodplains, and riparian areas to main channel; overbank flows are reduced relative to historic frequency, as evidenced by moderate degradation of wetland function, riparian vegetation/succession	Severe reduction in hydrologic connectivity between off-channel wetland, floodplain, and riparian areas; wetland extent drastically reduced and riparian vegetation/succession altered significantly

Assessment Results

Floodplain connectivity was evaluated based on the results from the hydraulic modeling, floodplain inundation and geomorphic mapping. For this analysis, connected floodplain was defined as the area that would be inundated with over-bank flows under a 100-year flood given current conditions. Disconnected floodplain was defined as the area that would likely be inundated under a 100-year-flood event in the absence of human alterations such as levees, roads, bridges, agriculture and other development that restrict floodplain connectivity.

In Quillayute River reaches 1 through 4, 6, and the Lower Bogachiel and Lower Dickey reaches, floodplain connectivity is considered **adequate**. Quillayute River Reach 5 and the Lower Sol Duc Reach are considered **at risk** due to more substantial alteration to geomorphic conditions that limit connectivity.

Percent Disconnected Floodplain

Floodplain Connectivity	Reach 1	Reach 2	Reach 3	Reach 4	Reach 5	Reach 6	Lower Bogachiel	Lower Sol Duc	Lower Dickey
Percent Disconnected	0%	0%	15%	19%	30%	0%	5%	50%	3%

Floodplain Connectivity REI Rating

Reach 1	Reach 2	Reach 3	Reach 4	Reach 5	Reach 6	Lower Bogachiel	Lower Sol Duc	Lower Dickey
Adequate	Adequate	Adequate	Adequate	At risk	Adequate	Adequate	At risk	Adequate

INDICATOR: CHANNEL DYNAMICS (BANK STABILITY/CHANNEL MIGRATION)

Metric Overview

Channel migration and bank erosion are natural processes that maintain river habitats by recruiting substrate, LWD, and introduction of new channel dynamics (Ecology 2014). Low gradient alluvial channels, such as much of the Quillayute River, adjust laterally via bank erosion and channel avulsions (rapid shifting of channel location). Natural channel migration rates are a result of numerous physical and biological processes including hydrologic regime, underlying geology, sediment supply, streambank vegetation, and floodplain hydraulic roughness (Ecology 2014). Human actions can affect these processes, which subsequently can alter channel migration rates and erosion locations. Bank armoring, levee construction, and channelization restrict flow to generally more straightened paths as well as limiting where erosion can occur; water withdrawals and dams can alter the hydrologic regime, affecting when and how much water interacts with the channel margins; and changes in riparian vegetation such as removal of streambank vegetation and development within the floodplain can affect erosion rates and how a river interacts with the channel margins (Collins et al. 2012; Ecology 2014).

Criteria: From USFWS (1998)

Pathway	General Indicators	Specific Indicators	Adequate	At Risk	Unacceptable
Channel Forms & Processes	Channel Dynamics	Bank Stability/ Channel Migration	Channel is migrating at or near natural rates and has stable banks.	Limited amount of channel migration is occurring at a faster/slower rate relative to natural rates, but significant change in channel width or planform is not detectable; large woody debris is still being recruited.	Little or no channel migration is occurring because of human actions preventing reworking of the floodplain and large woody debris recruitment; or channel migration is occurring at an accelerated rate such that channel width has a least doubled, possibly resulting in a channel planform change, and sediment supply has noticeably increased from bank erosion.

Assessment Results

The Quillayute River is a dynamic system that historically shifted and migrated significantly, making full use of its floodplain and side channels. The course of the river has changed substantially over time and has become more altered by human development preventing natural channel migration. In the Puget Sound ecoregion, channel migration is the primary floodplain geomorphic process that creates habitat patches of different ages within the river corridor and allows for the resetting of vegetation communities and aquatic habitats (Ecology 2013).

There has been significant human alteration to the Quillayute River and armoring of streambanks that has reduced the ability of the river to migrate laterally. Bank armoring in the form of riprap, embankment structures steel piles, steel sheets, bridge abutments, and levees were mapped as part of the Assessment. The total length of bank armoring was calculated as a percentage of reach length. This does not include areas of channel upstream and downstream of bridges where channel migration might be affected by the bridge. Reaches with greater degrees of bank armoring were considered more impaired than those with less armoring. For this analysis, reaches with less than 5 percent armoring were assumed **adequate**, between 5 and 10 percent **at risk**, and more than 10 percent **unacceptable**.

Bank Characteristics by Reach

Bank Characteristics	Reach 1	Reach 2	Reach 3	Reach 4	Reach 5	Reach 6	Lower Bogachiel	Lower Sol Duc	Lower Dickey
Armored Banks	69.8%	14.8%	2.9%	0.0%	0.0%	25.3%	4.7%	3.3%	7.6%
Eroding Banks	0.0%	0.0%	61.2%	51.2%	90.9%	71.5%	3.2%	0.0%	0.0%

Bank Stability/ Channel Migration REI Rating

Reach 1	Reach 2	Reach 3	Reach 4	Reach 5	Reach 6	Lower Bogachiel	Lower Sol Duc	Lower Dickey
Unacceptable	Unacceptable	Unacceptable	Unacceptable	Unacceptable	Unacceptable	At risk	Adequate	At risk

INDICATOR: CHANNEL DYNAMICS (VERTICAL CHANNEL STABILITY)

Metric Overview

Under natural conditions, alluvial river systems tend toward a balanced state in which some erosion and deposition occurs during sediment transporting events but no net change in dimension, pattern and profile over the course of years. These systems are frequently referred to as regime channels and are in a state of dynamic equilibrium in which there is a continuous inflow and output water and sediment (Lane 1954; Ecology 2014). Changes in the conditions including sediment supply, channel form modification, flow, or bank strength can upset the balance leading to higher rates and a trend of aggradation or incision. This can result in disconnection from the floodplain due to incision (Cluer and Thorne 2014). Channel form modification can be the result of human actions including bank armoring, removal of riparian vegetation, levee building, channel straightening, and channelization which can reduce vertical channel stability (Constantine et al. 2009; Dunne et al. 2010).

Criteria: From USBR (2012)

Pathway	General Indicators	Specific Indicators	Adequate	At Risk	Unacceptable
Channel Forms & Processes	Channel Dynamics	Vertical Channel Stability	No measurable trend of aggradation or incision and no visible change in channel planform.	Measurable trend of aggradation or incision that has the potential to but not yet caused disconnection of the floodplain or a visible change in channel planform (e.g., single thread to braided).	Enough incision that the floodplain and off-channel habitat areas have been disconnected; or, enough aggradation that a visible change in channel planform has occurred (e.g., single thread to braided).

Assessment Results

Field surveys and hydraulic modeling found that overall, the Quillayute River is vertically stable, as the river can meander horizontally. However, an increase in armored banks and rip rap causes a decrease in vertical stability, as the river is forced one way or another. All reaches are considered to be **at risk,** because of observed channel modification which could lead to aggradation, incision, or a change in channel planform.

Vertical Channel Stability REI Rating

Reach 1	Reach 2	Reach 3	Reach 4	Reach 5	Reach 6	Lower Bogachiel	Lower Sol Duc	Lower Dickey
At risk	At risk	At risk	At risk	At risk	At risk	At risk	At risk	At risk

6. PATHWAY: RIPARIAN CONDITION

INDICATOR: DISTURBANCE (HUMAN)

Metric Overview

Riparian areas have many important geomorphic and ecological roles within the river system. Intact riparian corridors help maintain streambank stability, provide large wood, water filtration processes, organic input, streamside habitat and cover, hydraulic regulation, and temperature fluctuation modification (Gregory et al., 1991).

Human disturbance changes how a river interacts with its floodplain and riparian areas. Often human disturbance in the floodplain results in reduced occurrence of mature seral stages of vegetation and riparian structure, and limits channel migration and erosion processes (UCSRB 2017). This can reduce the riparian functions identified by Gregory et al (1991).

Criteria: From USBR (2012) and NMFS (1996)

Pathway	General Indicators	Specific Indicators	Adequate	At Risk	Unacceptable
Riparian Condition	Disturbance	Disturbance (human)	>80 percent mature trees (medium-large) in the riparian buffer zone (defined as a 30 m belt along each bank) that are available for recruitment by the river via channel migration; <20 percent disturbance in the floodplain (e.g., agriculture, residential, roads, etc.); <2 mi/mi^2 road density in the floodplain.	50-80 percent mature trees (medium-large) in the riparian buffer zone (defined as a 30 m belt along each bank) that are available for recruitment by the river via channel migration; 20-50 percent disturbance in the floodplain (e.g., agriculture, residential, roads, etc.); 2-3 mi/mi^2 road density in the floodplain.	<50 percent mature trees (medium-large) in the riparian buffer zone (defined as a 30 m belt along each bank) that are available for recruitment by the river via channel migration; >50 percent disturbance in the floodplain (e.g., agriculture, residential, roads, etc.); >3 mi/mi^2 road density in the floodplain.

Assessment Results

Human disturbance on riparian areas was documented during 2019 field surveys and included bank hardening, buildings, pavement, roads, and pastures or fields. Vegetation data were collected as part of the field and LiDAR surveys. Percent canopy cover varies by reach, ranging from 20 percent to 88 percent canopy cover. Most of the canopy is less than 5 feet high with heights averaging 38 feet. Road density was calculated as 2.95 miles/square mile of road density.

Based on the above criteria, Quillayute River reaches 1, 2, and 5 are rated as **unacceptable** due to the amount of canopy cover being less than 50 percent mature trees in the riparian buffer zone as well as having greater than 50 percent disturbance in the floodplain. Quillayute River reaches 3, 4, 6 as well as the Lower Bogachiel, Lower Sol Duc, and Lower Dickey rivers were rated as **at risk** because the

canopy cover is between 50 – 80 percent (or greater than 80 percent on the Lower Dickey Reach) and the road density falls between 2 – 3 miles per square mile .

Riparian Characteristics by Reach

Riparian Characteristics	Reach 1	Reach 2	Reach 3	Reach 4	Reach 5	Reach 6	Lower Bogachiel	Lower Sol Duc	Lower Dickey
Percent Canopy Cover > 5 ft	20%	50%	75%	77%	46%	56%	72%	80%	88%
Average Height	15 ft	44 ft	50 ft	41 ft	39 ft	39 ft	43 ft	54 ft	69 ft

Disturbance (Human) REI Rating

Reach 1	Reach 2	Reach 3	Reach 4	Reach 5	Reach 6	Lower Bogachiel	Lower Sol Duc	Lower Dickey
Unacceptable	Unacceptable	At risk	At risk	Unacceptable	At risk	At risk	At risk	At risk

7. REFERENCES

Allen, J.R.L. 1970. Physical Processes of Sedimentation: An Introduction. American Elsevier Company. New York, NY.

Anderson, B.G., I.D. Rutherfurd, I., and A. Western. 2006. An analysis of the influence of riparian vegetation on the propagation of flood waves. Environmental Modelling and Software 21,1290-1296.

Benke, A.C. and J.B. Wallace. 2003. Influence of Wood in Invertebrate Communities in Streams and Rivers. American Fisheries Society Symposium 37: 149-177.Boulton, A.J., S. Findlay, P. Marmonier, E.H. Stanley, and M. Valett. 1998. The functional significance of the hyporheic zone in streams and rivers. Annual Review of Ecological Systems 29: 59–81.

Clallam County 911 Road Layer GIS Data. 2020. Accessed: September 2019. Available online at: http://www.clallam.net/Maps/mapdata.html

Cluer, B.L., and C. R. Thorne. 2014. A Stream Evolution Model Integrating Habitat and Ecosystem Benefits. River Research and Applications 30: 135-154.

Collins, B.D., D.R. Montgomery, K. L. Fetherston, K., and T. B. Abbe. 2012. The Floodplain Large-Wood Cycle Hypothesis: A Mechanism for the Physical and Biotic Structuring of Temperate Forested Alluvial Valleys in the North Pacific Coastal Ecoregion. Geomorphology 139-140, 460-470.

Collins, B.D., D.R. Montgomery, and A.D. Haas. 2002. Historical changes in the distribution and functions of large wood in Puget Lowland rivers. Canadian Journal of Fisheries and Aquatic Sciences 59: 66–76.

Constantine, J.A., S.R. McLean, and T. Dunne. 2009. A mechanism of chute cutoff along large meandering rivers with uniform floodplain topography. *Geological Society of America Bulletin*, v. 122, p. 855–869.

Dolloff, C.A. and M.L. Warren. 2003. Fish Relationships with Large Wood in Small Streams. American Fisheries Society Symposium 37: 179-193.

DNR (Washington State Department of Natural Resources) Active Roads GIS Data Layer. 2020. Accessed: September 2019. Available online at: http://data-wadnr.opendata.arcgis.com/datasets/wadnr-active-roads

Dunne, T., J.A. Constantine, and M.B. Singer. 2010. The Role of Sediment Transport and Sediment Supply in the Evolution of River Channel and Floodplain Complexity. Transactions, Japanese Geomorphological Union. v. 31, p. 155–170.

Ecology (Washington State Department of Ecology). 2013. Draft Channel Migration Assessment Clallam County. Retrieved February 2020 from: http://www.clallam.net/landuse/documents/CMZ_study_WRIA_20.pdf

Ecology. 2014. Channel Migration Processes and Patterns in Western Washington: A synthesis of Floodplain Management and Restoration. Shorelands and Environmental Assistance Program. Olympia, Washington. Publication no.14-06-028.

Fitzgerald, R. 2004. Salmonid Freshwater Habitat Targets for Sediment-Related Parameters. State of California North Coast Regional Water Quality Control Board. Retrieved February 2020 from: https://www.waterboards.ca.gov/northcoast/water_issues/programs/basin_plan/110504/110504-targets.pdf

Goode, J.R., C.H. Luce, and J.M Buffington. 2011. Enhanced sediment delivery in a changing climate in semi-arid mountain basins: Implications for water resource management and aquatic habitat in the northern Rocky Mountains. Geomorphology doi:10.1016/j.geomorph.2011.06.021.

Gregory, S.V., F.J. Swanson, A.K. McKee, and K.W. Cummins. 1991. An ecosystem perspective of riparian zones. Bioscience 41(8):540–551.

Hashim, W.A. 2002. Water quality summaries for the 62 Water Resource Inventory Areas of Washington State. Department of Ecology, Olympia, Washington. 185 pp.

Henley, W.F., M.A. Patterson, R.J. Neves, and D.A. Lemly. 2000. Effects of sedimentation and turbitity on lotic food webs: A concise review for natural resource managers. Reviews in Fisheries Science 2:125–139.

HistoryLink. 2019. HistoryLink File #8397, Forks - -Thumbnail History. The State of Washington, Washington Department of Archaeology and Historic Preservation. Accessed online September 26, 2019 at: http://www.historylink.org

Kondolf, G.M., M.W. Smeltzer, S.F. Railsback. 2001. Design and performance of a channel reconstruction project in a coastal California gravel-bed stream. Environmental Management 28, 761-776.

Lane, E. 1954. The Importance of Fluvial Morphology in Hydraulic Engineering: U.S. Department of the Interior, Bureau of Reclamation, Commissioner's Office.

Leonard, N.M. 1982. Streamflow and Sediment Transport in the Quillayute River Basin, Washington, USGS Open File Report 82-627, Tacoma, WA. URL: https://pubs.er.usgs.gov/publication/ofr82627. Accessed 16 October 2019.

Lisle, T.E. 1989. Sediment transport and resulting deposition in spawning gravels, north coastal California. Water Resources Research 25(6):1303–1319.

MacLennan, A.J., J.F. Waggoner, J.W. Johannessen, and S.A. Williams. 2013. Sea level rise vulnerability in San Juan County, Washington. Prepared by Coastal Geologic Services, Inc.

Montgomery, D.R. 1994. Road surface drainage, channel initiation, and slope instability. 1994. Water Resources Research 30(6).

Montgomery, D.R., B.D. Collins, J.M. Buffington, T.B. Abbe. 2003. Geomorphic Effects of Wood in Rivers. American Fisheries Society Symposium 37:21-47.

Nakamura, F., F.J. Swanson, and S.M. Wondzell. 2000. Disturbance regimes of stream and riparian systems – a disturbance-cascade perspective. Hydrological Processes 14:2849-2860.

Nanson, G.C., and J.C. Croke. 1992. A genetic classification of floodplains. Geomorphology 4:459-486.

Nelson. 1982. Streamflow and Sediment Transport in the Quillayute River Basin, Washington. US Geological Survey. Tacoma, WA. Retrieved February 2020 from: https://pubs.usgs.gov/of/1982/0627/report.pdf

NMFS (National Marine Fisheries Service). 1996. Making Endangered Species Act determinations of effect for individual or grouped actions at the watershed scale. Lacey, Washington, National Marine Fisheries Service, Environmental and Technical Services Division, Habitat Conservation Branch.

NWS. 2020. Bogachiel River Near La Push, WA Stream Gage. National Weather Service. Retrieved February 2020 from: https://water.weather.gov/ahps2/hydrograph.php?wfo=sew&gage=bogw1

OCCRI (Oregon Climate Change Research Institute). 2017. Climate Change Vulnerability Assessment for the Treaty of Olympia Tribes: A Report to the Quinault Indian Nation, Hoh Tribe, and Quileute Tribe. Oregon Climate Change Research Institute, Corvallis, OR.

OCCRI. 2019. Assessing the Impacts of Coastal Flooding on Treaty of Olympia Infrastructure: A Report to the Quinault Indian Nation, Hoh Tribe, and Quileute Tribe. Oregon Climate Change Research Institute, Corvallis, OR.

Poff, N.L., J.D. Allan, M.B. Bain, J.R. Karr, K.L. Prestegaard, B.D. Richter, R.E. Sparks, R., and J.C. Stromberg. 1997. The Natural Flow Regime: A Paradigm for River Conservation and Restoration. BioScience 47, 769-784.

Quileute Tribe. 2016. State of Our Watersheds Report Quillayute River Basin. Retrieved February 2020 from: http://geo.nwifc.org/sow/SOW2016_Report/Quileute.pdf

Reid, L. M., and T. Dunne. 1984. Sediment production from forest road surfaces. Water Resources Research 20(11):1753–1761; doi:10.1029/WR020i011p01753.

Roni, P., T.J. Beechie, R.E. Bilby, F.E. Leoneti, M.M. Pollock, and G.R. Pess. 2002. A review of stream restoration techniques and a hierarchical strategy for prioritizing restoration in Pacific Northwest watersheds. North American Journal of Fisheries Management 22:1-20.

Ruggiero, P., P.D. Komar, and J.C. Allan. 2010. Increasing wave heights and extreme value projections: The wave climate of the U.S. Pacific Northwest. Coastal Engineering, 57(5), 529-552.

The Timberman. 1922. "Ocean Log Towing on the Pacific". *The Timberman*. August 1922.

USBR (U.S. Bureau of Reclamation). 2012. Lower Entiat Reach Assessment. U.S. Bureau of Reclamation Pacific Northwest Region, Boise, ID, U.S. Department of the Interior.

USFWS (U.S. Fish and Wildlife Service). 1998. A Framework to assist in making Endangered Species Act determinations of effect for individual or grouped actions at the Bull Trout subpopulation watershed scale. USFWS, Department of the Interior.

Waples, R., T. Beechie, G.R. Pess. 2009. Evolutionary history, habitat disturbance regimes, and anthropogenic changes: what do these mean for resilience of Pacific Salmon populations? Ecology and Society 14(1):3.

Ward, J.V. 1998. Riverine landscapes: biodiversity patterns, disturbance regimes, and aquatic conservation. Biological Conservation 83(3): 269–278.

Waters, T.F. 1995. Sediment in Streams: sources, biological effects, and control. American Fisheries Society, Monograph 7. Bethesda, MD.

Wemple, B.C., J.A. Jones, and G.E. Grant. 1996. Channel network extension by logging roads in two basins, western Cascades, Oregon. Water Resources Bulletin 32(6).

Wohl, E. 2013. Floodplains and wood. Earth-Science Reviews 123:194–212.

Wood, P.J., and P.D. Armitage. 1997. Biological effects of fine sediment in the lotic environment. Environmental Management 21(2):203–217.

WRCC. 2020. Western Regional Climate Center Climate of Washington. Retrieved February 2020 from: https://wrcc.dri.edu/Climate/narrative_wa.php

Zwolinski, Z. 1992. Sedimentology and geomorphology of overbank flows on meandering river floodplains. Geomorphology 4(6):367–379.

APPENDIX K – CONCEPTUAL ALTERNATIVE PLAN DRAWINGS

Quillayute River Project
Geomorphic Assessment and Action Plan
Conceptual Alternative Plan Drawings

Appendix K

Submitted to:

Quileute Natural Resources
401 Main Street
La Push, WA 98350

Submitted by:

19803 North Creek Parkway
Bothell, WA 98011
Tel 425.482.7600 | Fax 425.482.7652
www.tetratech.com

September 2020

LIST OF FIGURES

Figure K-1. ..... Conceptual Alternative 1 Overview
Figure K-2. ..... Conceptual Alternative 1 Thunder Field Overview and Cross Sections
Figure K-3. ..... Conceptual Alternative 2 Overivew
Figure K-4. ..... Conceptual Alternative 2 Thunder Field Overview and Cross Sections
Figure K-5. ..... Conceptual Alternative 3 Overview
Figure K-6. ..... Conceptual Alternative 3 Thunder Field Overview and Cross Sections
Figure K-7. ..... Conceptual Alternative 1A Overview
Figure K-8. ..... Conceptual Alternative 1A Thunder Field Overview and Cross Sections
Figure K-9. ..... Conceptual Alternative 1B Overview
Figure K-10. ..... Conceptual Alternative 1B Thunder Field Overview and Cross Sections

Quillayute River Restoration Project

PROJECT OVERVIEW

ALTERNATIVE 1

Lowered Jetty for High Flow and Tide Flood Relief

Remove Culvert to Create Backwater Alcove

New Berm/Levee

Decompact Surface

High Flow Channel with Helicopter Log Placement

Backwater Alcove

Wetland

Helicopter Log Placement

Log Jam

Improved Fishing Access

Thunder Field Road Improvement

Mora Road Relocation

Mora Road Connection Options

Lay Back Banks and Install Fish-friendly Large Wood Structures

Install Fish-friendly Bank Protection via Bioengineering with Log Jams

Walking Path

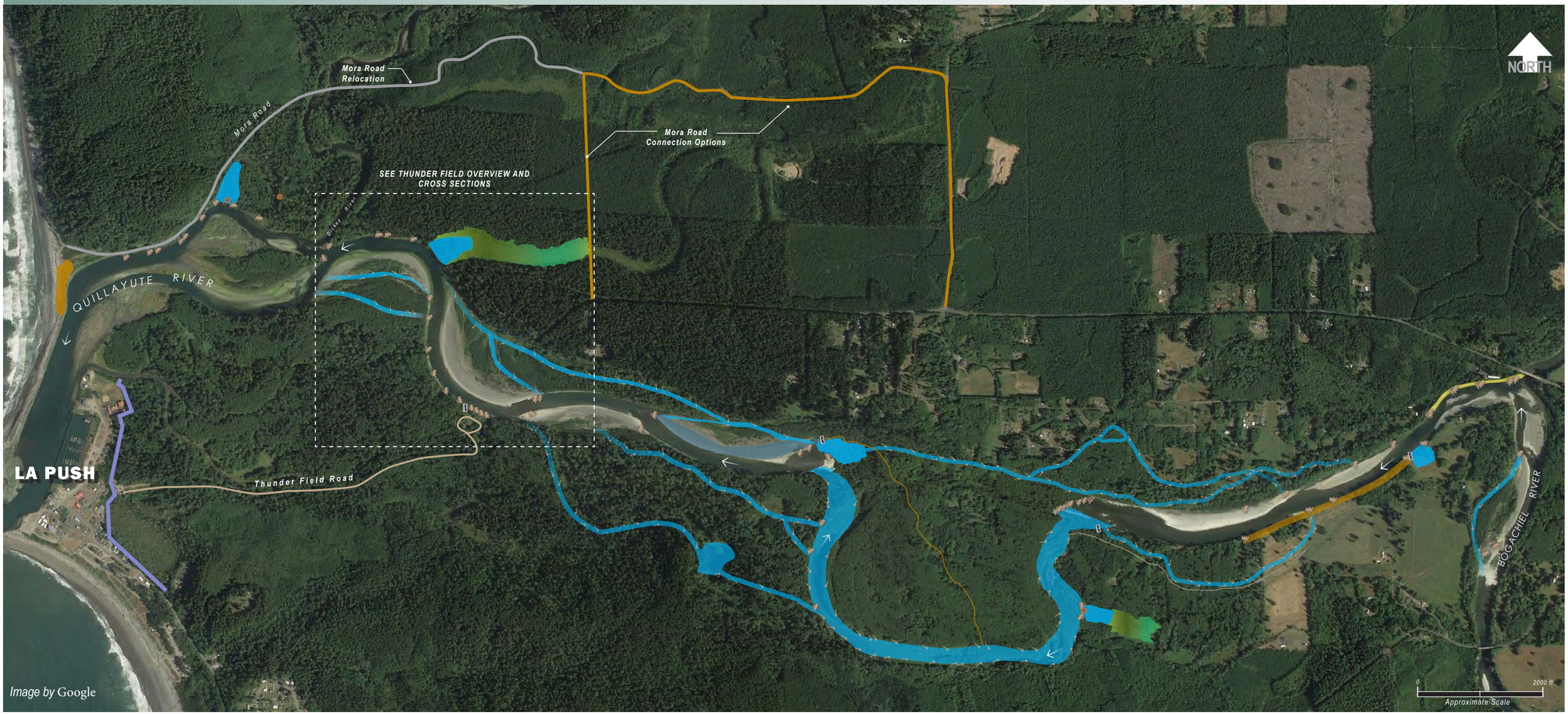

ALT#1 Revised version 2-13-2020

Appendix K

Figure K-1

ALTERNATIVE 1: THUNDER FIELD OVERVIEW AND CROSS SECTIONS

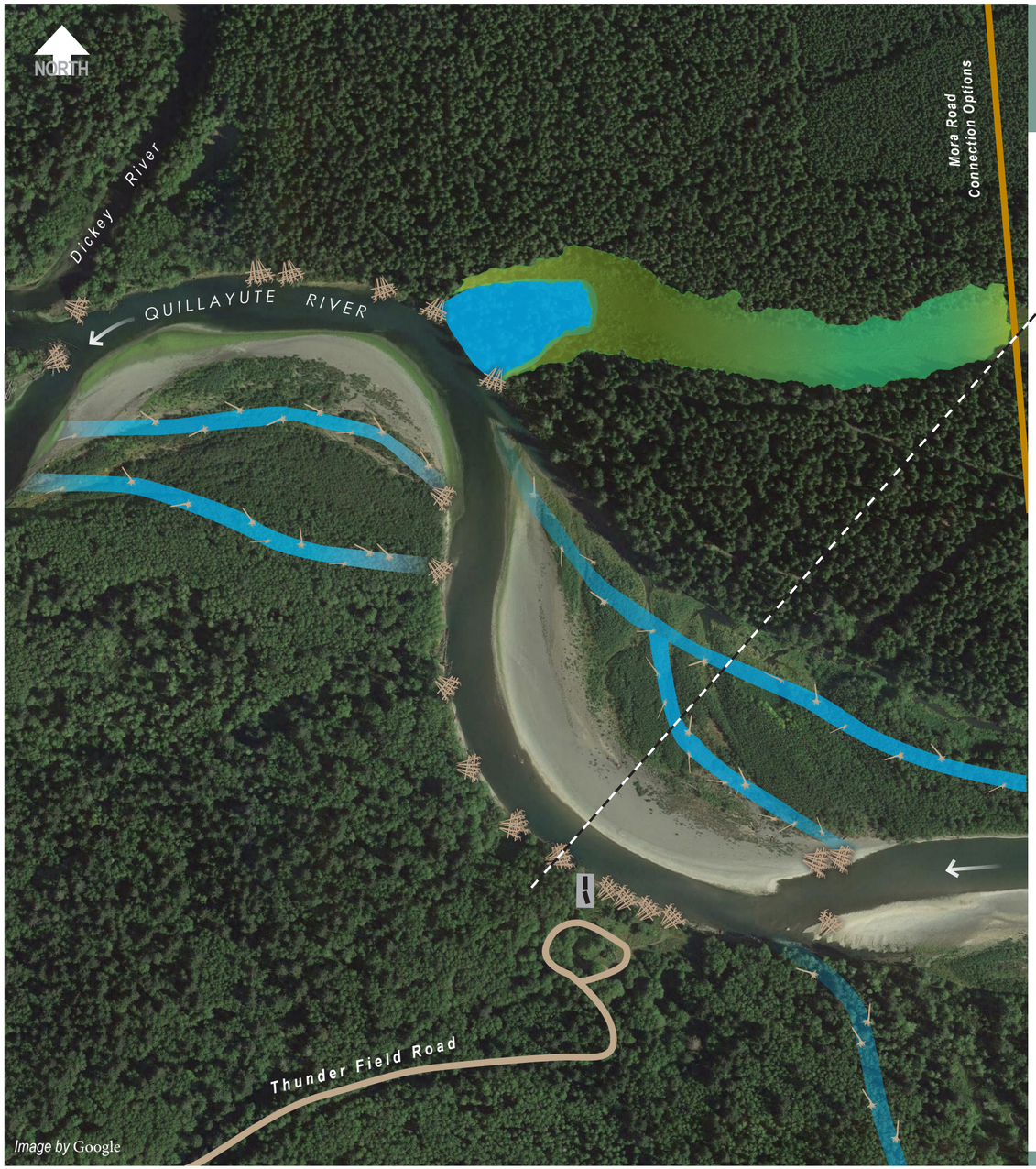

A LOG JAM CROSS SECTION

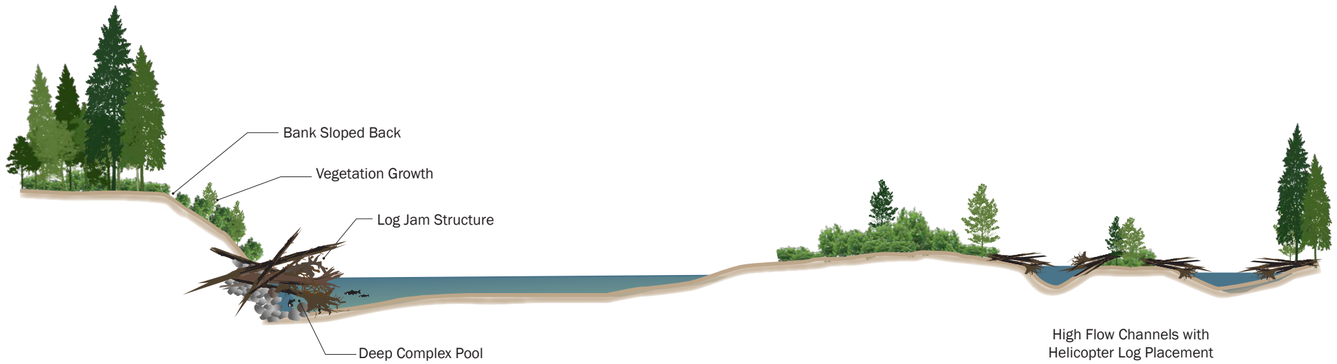

High Flow Channel with Helicopter Log Placement | Backwater Alcove | Wetland | Log Jam | Helicopter Log Placement | Improved Fishing Access | Thunder Field Road Improvement | Mora Road Connection Options

Not to Scale | Illustration Purpose Only

Quillayute River Restoration Project

ALT#1 - LWR 2-13F-2020

Appendix K

Figure K-2

Quillayute River Restoration Project

PROJECT OVERVIEW

ALTERNATIVE 2

Improve Existing Berm

Replace Culvert with Fish-friendly Structures to Reconnect Habitat

Decompact Surface

High Flow Channel with Large Wood Structures

Backwater Alcove

Large Wood Structure

Log Jam

Improved Fishing Access

Thunder Field Road Improvement

Log Revetment

Lay Back Banks and Install Fish-friendly Large Wood Structures

SEE THUNDER FIELD OVERVIEW AND CROSS SECTIONS

Dickey River

QUILLAYUTE RIVER

Thunder Field Road

LA PUSH

BOGACHIEL RIVER

NORTH

Image by Google

0 2000 ft

Approximate Scale

ALT#2 Revised version 2-13-2020

Appendix K

Figure K-3

ALTERNATIVE 2: THUNDER FIELD OVERVIEW AND CROSS SECTIONS

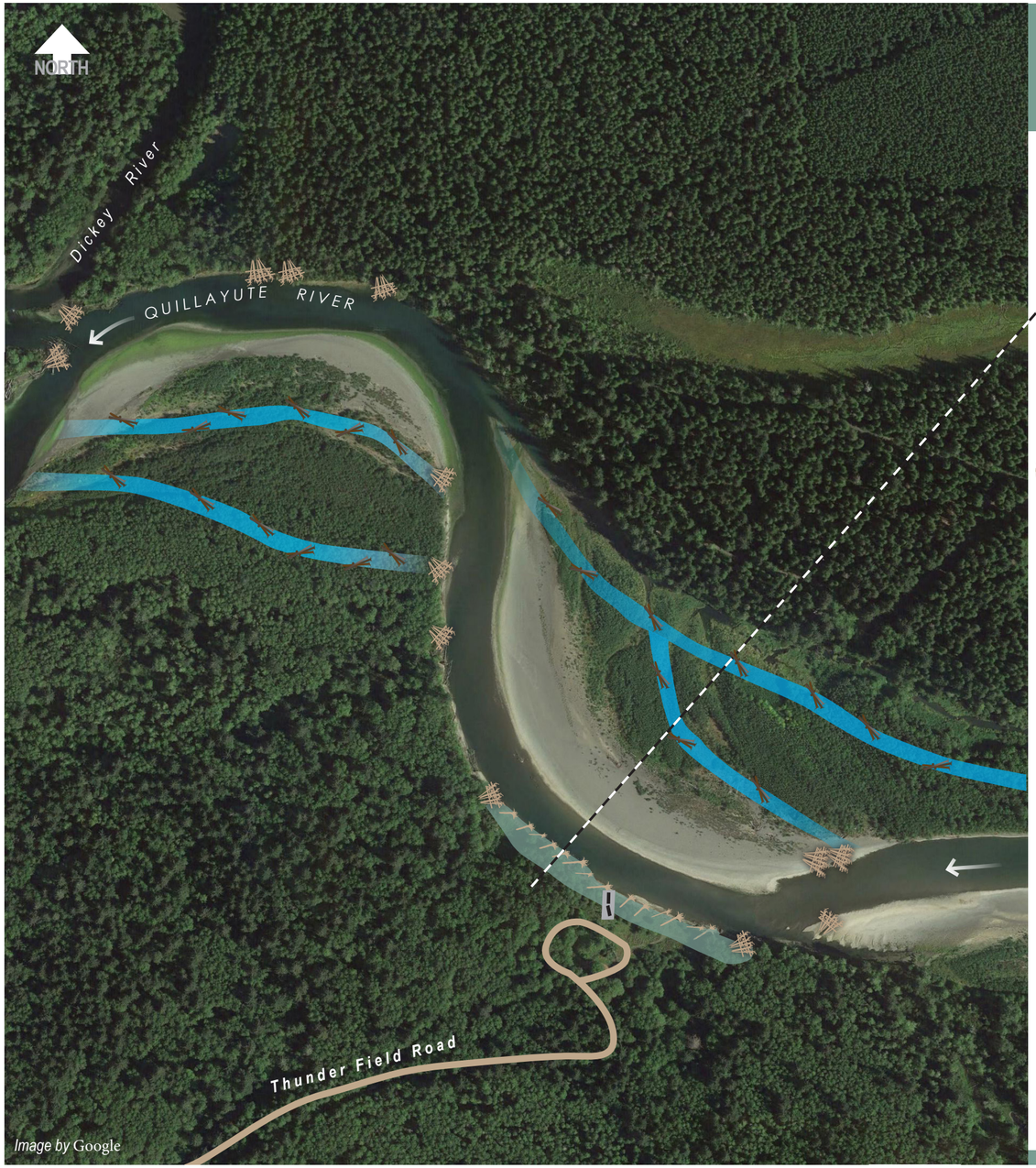

LARGE WOOD REVETMENT ALTERNATIVE CROSS SECTION

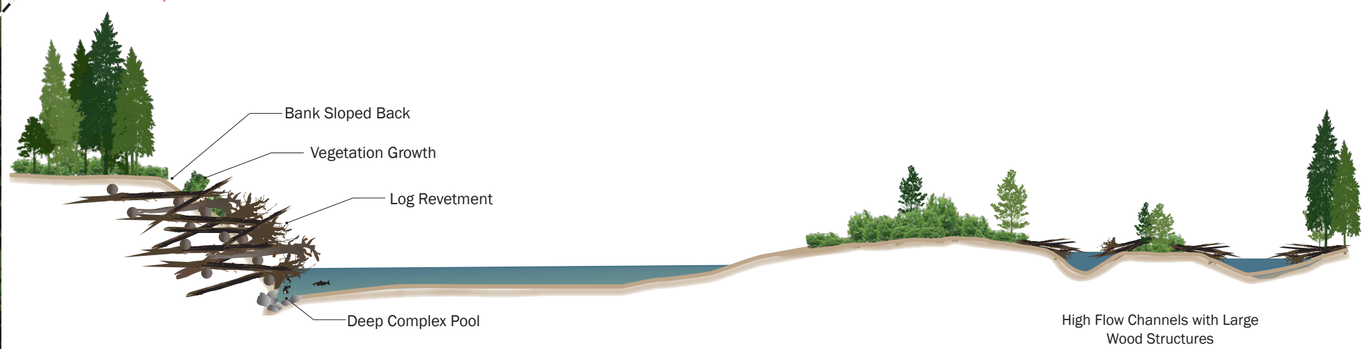

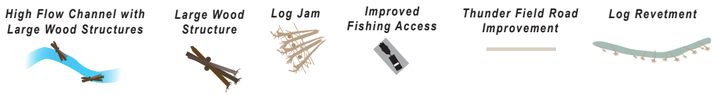

Not to Scale | Illustration Purpose Only

Quillayute River Restoration Project

Quillayute River Restoration Project

PROJECT OVERVIEW
ALTERNATIVE 3

New Levee

Replace Culvert with Fish-friendly Structures to Reconnect Habitat

Launchable Rock

Improved Fishing Access

Thunder Field Road Improvement

Log Revetment

ALT# 3 2-13F-2020

Appendix K

Figure K-5

ALTERNATIVE 3: THUNDER FIELD OVERVIEW AND CROSS SECTIONS

A LAUNCHABLE ROCK ALTERNATIVE PHASE ONE CROSS SECTION

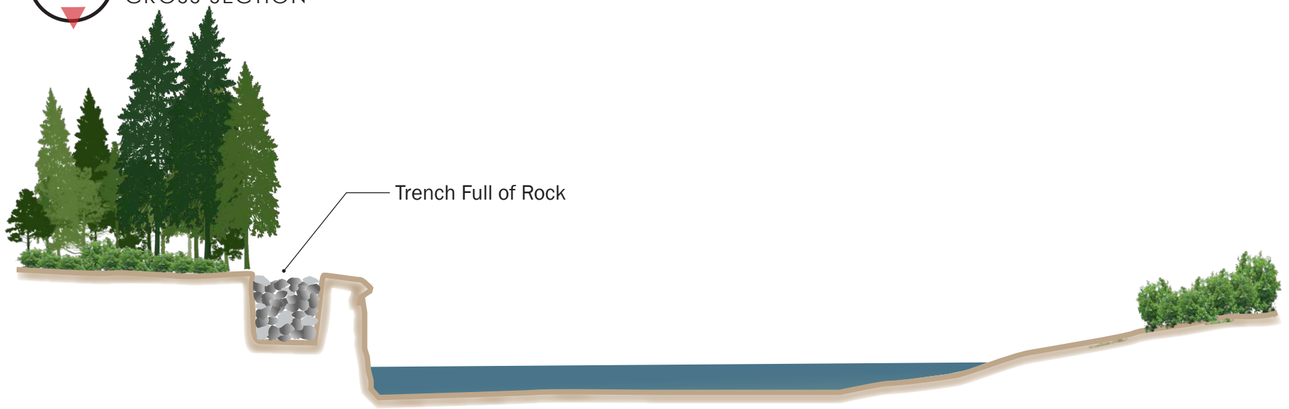

B LAUNCHABLE ROCK ALTERNATIVE PHASE TWO CROSS SECTION

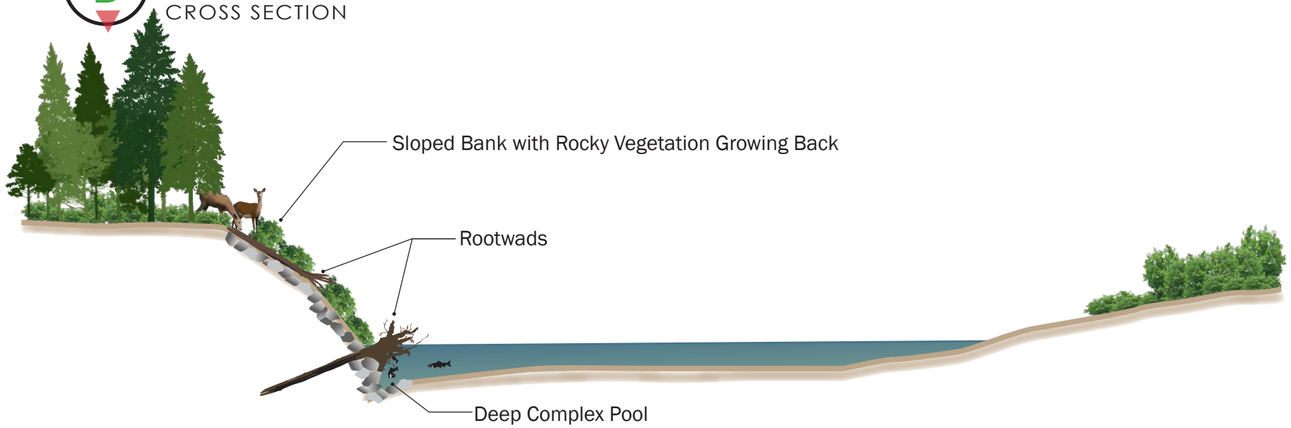

Launchable Rock *Improved Fishing Access* *Thunder Field Road Improvement*

Quillayute River Restoration Project

ALT#1 - LRock 2-12-2020

Not to Scale | Illustration Purpose Only

Quillayute River Restoration Project

PROJECT OVERVIEW

ALTERNATIVE 1A

Remove Culvert to Create Backwater Alcove

Improved Berm/ Levee

Decompact Surface

High Flow Channel with Large Wood Structures

Backwater Alcove

Wetland

Large Wood Structure

Log Jam

Improved Fishing Access

Thunder Field Road Improvement

Mora Road Relocation

Mora Road Connection Options

Lay Back Banks and Install Fish-friendly Large Wood Structures

Install Fish-friendly Bank Protection via Bioengineering with Log Jams

Log Revetment

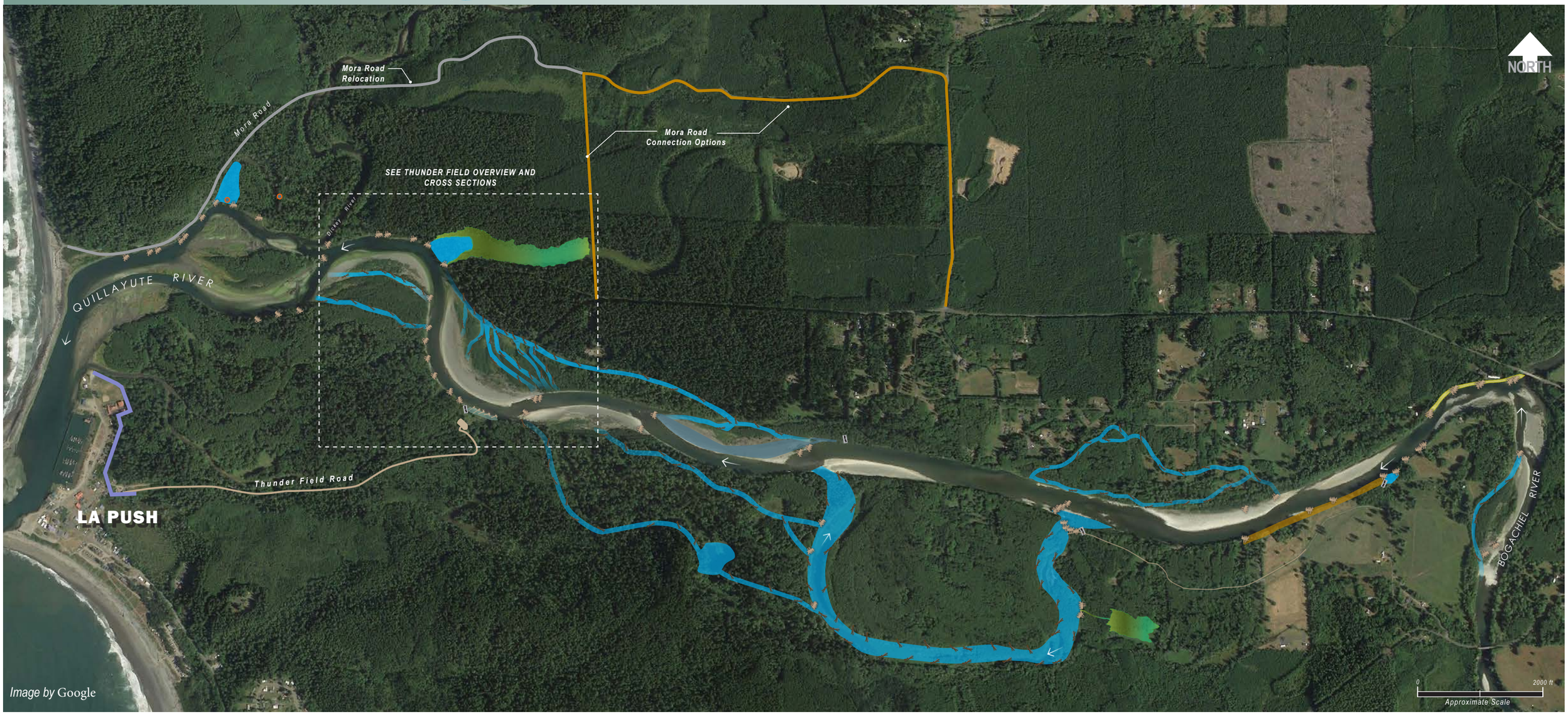

ALT#1A 2-13-2020

Appendix K

Figure K-7

ALTERNATIVE 1A: THUNDER FIELD OVERVIEW AND CROSS SECTIONS

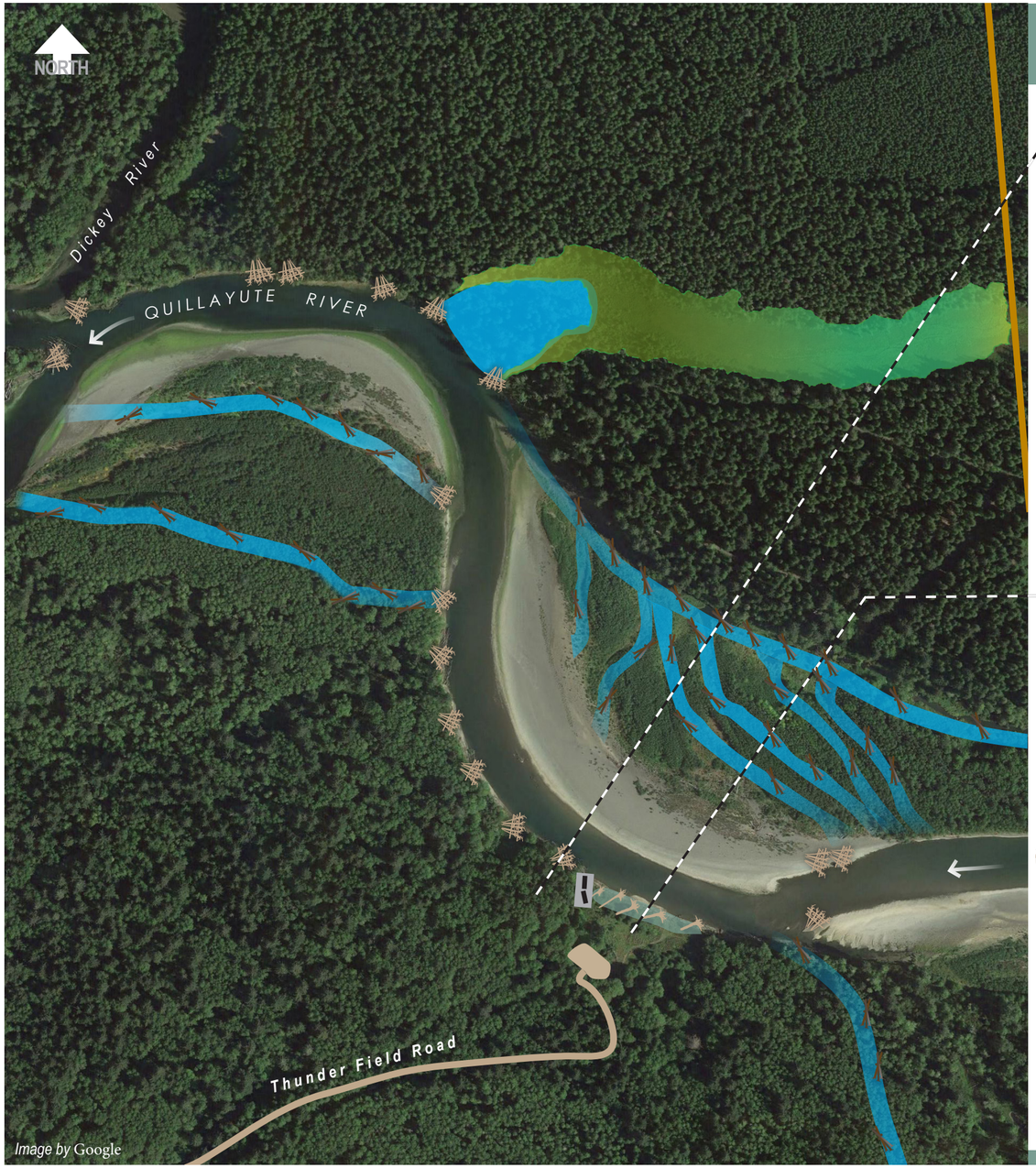

A

LOG JAM
CROSS SECTION

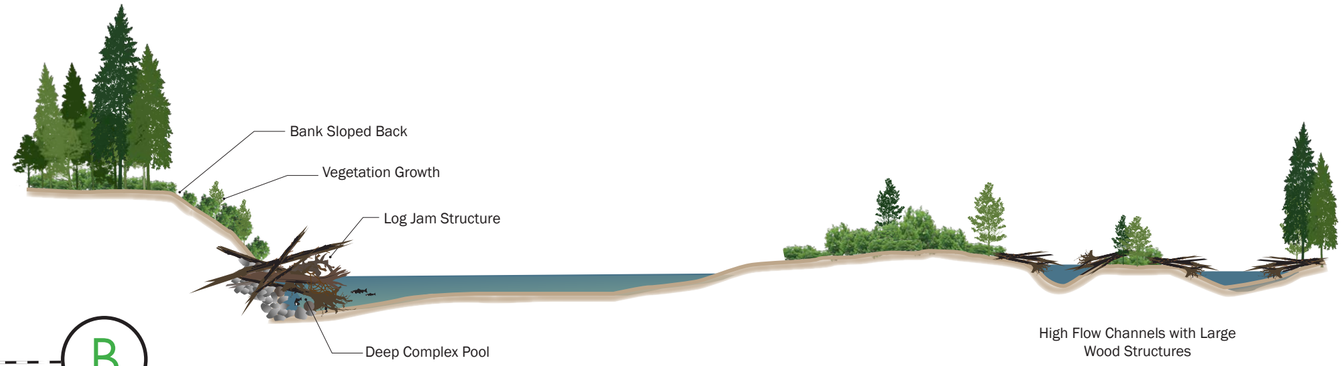

B

LOG REVETMENT
CROSS SECTION

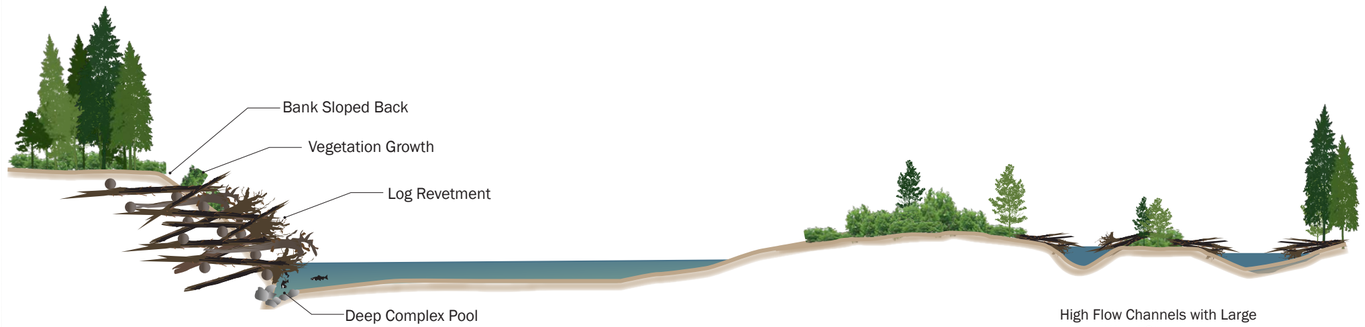

Not to Scale | Illustration Purpose Only

Quillayute River Restoration Project

ALT#1A - CrossSec 2-13-2020

Appendix K

Figure K-8

Quillayute River Restoration Project

PROJECT OVERVIEW

ALTERNATIVE 1B

Install Fish-friendly Structure

Improved Berm/ Levee

Decompact Surface

High Flow Channel with Large Wood Structures

Backwater Alcove

Wetland

Large Wood Structure

Log Jam

Improved Fishing Access

Thunder Field Road Improvement

Lay Back Banks and Install Fish-friendly Large Wood Structures

Install Fish-friendly Bank Protection via Bioengineering with Log Jams

Log Revetment

SEE THUNDER FIELD OVERVIEW AND CROSS SECTIONS

NORTH

Dickey River

QUILLAYUTE RIVER

Thunder Field Road

LA PUSH

BOGACHIEL RIVER

Image by Google

0 2000 ft

Approximate Scale

ALT#1A 2-14-2020

Appendix K

Figure K-9

ALTERNATIVE 1B: THUNDER FIELD OVERVIEW AND CROSS SECTIONS

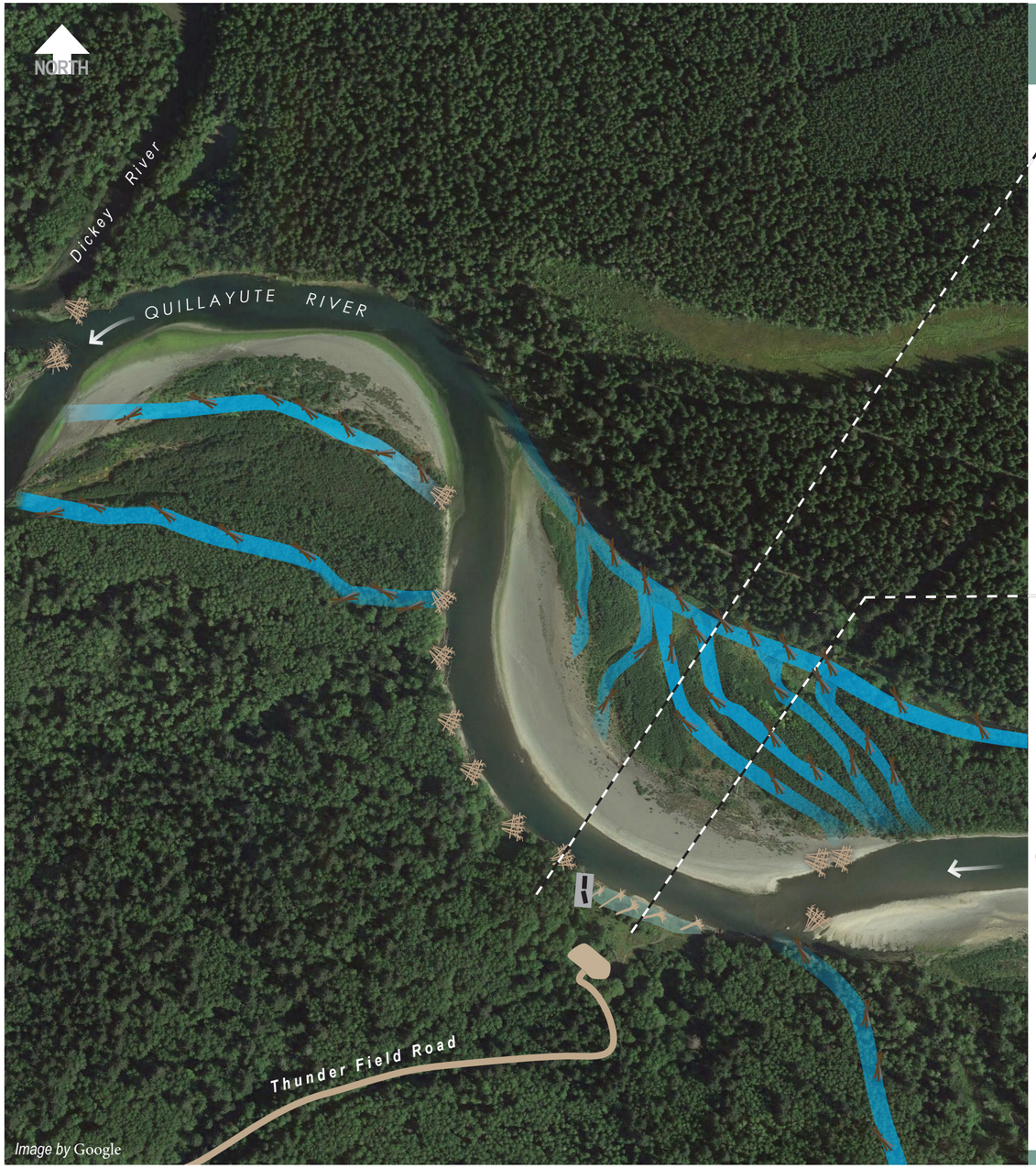

A

LOG JAM
CROSS SECTION

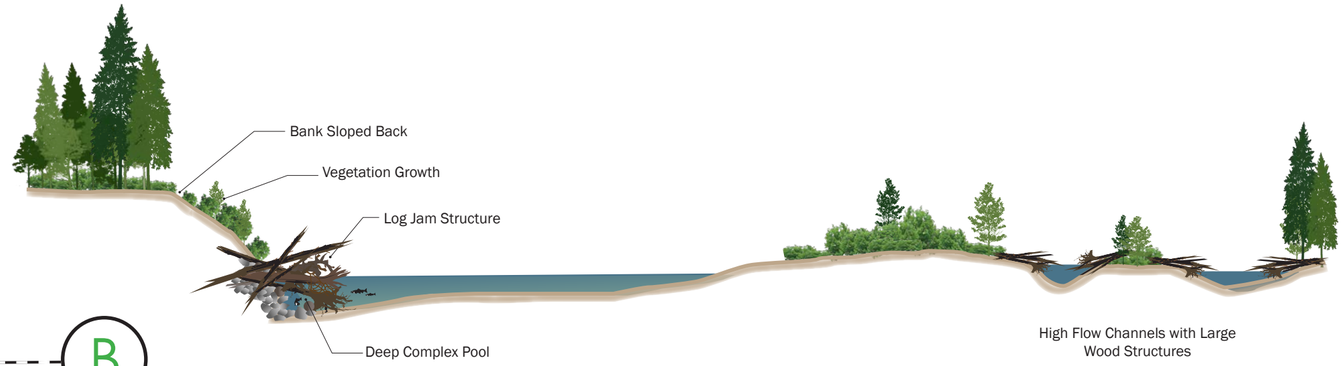

B

LOG REVETMENT
CROSS SECTION

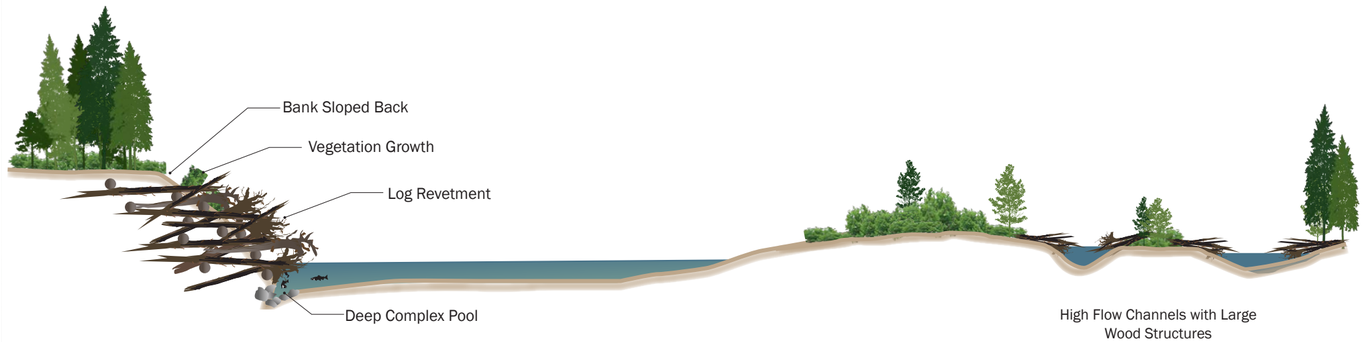

Not to Scale | Illustration Purpose Only

Quillayute River
Restoration Project

ALT#1B - CrossSec 2-14-2020

Appendix K

Figure K-10

APPENDIX L – STAKEHOLDER OUTREACH ANALYSIS

Quillayute River Project
Geomorphic Assessment and Action Plan
Stakeholder Outreach Analysis

Appendix L

Submitted to:

Quileute Natural Resources
401 Main Street
La Push, WA 98350

Submitted by:

TETRA TECH

19803 North Creek Parkway
Bothell, WA 98011
Tel 425.482.7600 | Fax 425.482.7652
www.tetratech.com

September 2020

1 STAKEHOLDER OUTREACH ANALYSIS

As identified under preliminary next steps for the Quillayute River Assessment and Action Plan, stakeholder outreach and communication related to the Assessment and Action Plan is needed. This is because stakeholder involvement will be critical as a next step in the process of implementing projects on the Quillayute River. Stakeholder involvement will involve public outreach to various federal, state, and local agencies, private landowners, and Quileute Tribal community. Public meetings will need to be held to gain input to advance designs within the reservation, including at Thunder Field, as well as to inform on the status of upcoming project activities. To aid in this process, stakeholder tracking of involvement will be completed by the Quileute Tribe. A tool called the Stakeholder Tracker and Analysis Tool has been developed to assist in implementing tracking of stakeholders. The tool will allow the Quileute Tribe to track stakeholder participation in the project, including meetings attended, financial support provided, and whether the stakeholder is a project advocate, a critic of the project, or neutral. In addition to tracking stakeholder participation, the tool has been designed to document stakeholder interest and influence on projects. An example of Quillayute River Project stakeholders and an output of a stakeholder matrix tool is shown on Figure 1-1.

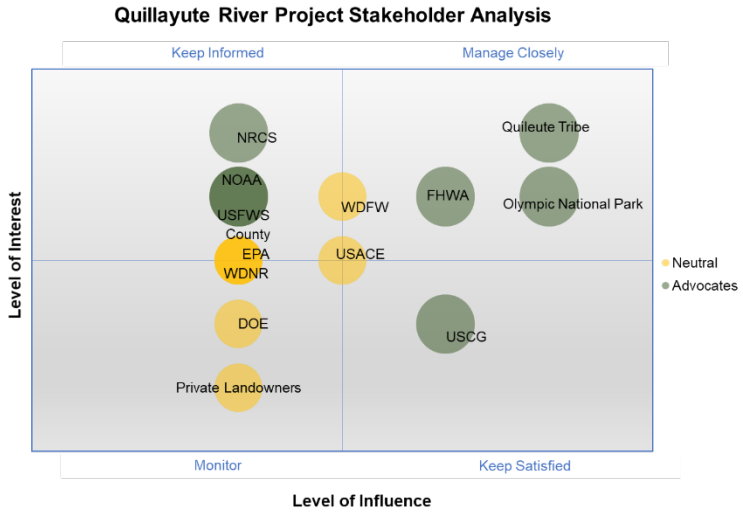

Figure 1-1. Example Quillayute River Project Stakeholder Matrix

The intended user of the tool is the Quileute Tribe. While some metrics of the tool are objective, such as stakeholder attendance in meetings and level of financial support, other metrics such as level of interest, influence, and support are more subjective. Particularly for the more subjective metrics, it will be important to update the tool with input from the project management team.

Stakeholder engagement will be valuable for any projects undertaken by the Quileute Tribe. Stakeholder involvement, influence, or support of projects may change through time and stakeholders may change during projects. As stakeholder engagement needs are better understood, the Stakeholder Tracker and Analysis Tool should be updated and, if needed, adapted to accommodate those needs. At a minimum, the tool should be updated following each stakeholder meeting.

TETRA TECH